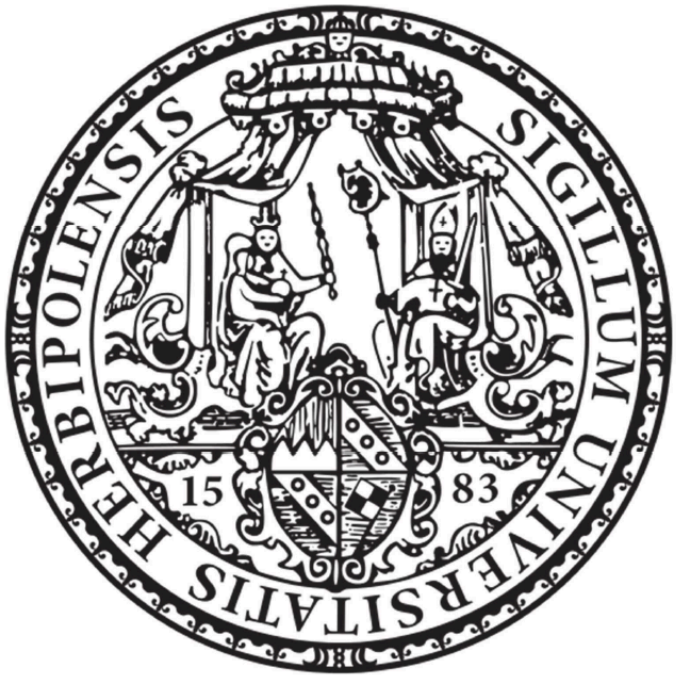

The role of cancer cell-expressed PD-1 in tumorigenesis and tumor immune evasion.

Funktionelle Charakterisierung von Tumorzell-exprimiertem PD-1 in der Karzinogenese und antitumoralen Immunabwehr.

Doctoral thesis for a doctoral degree
at the Graduate School of Life Sciences,
Julius-Maximilians-Universität Würzburg,
Section Biomedicine

submitted by

Sonja Beate Kleffel

from

Leverkusen

Würzburg 2017

Submitted on: _____

Members of the Promotionskomitee:

Chairperson: _____

Primary Supervisor: Professor Dr. Ana Maria Waaga-Gasser

Supervisor (Second): Professor Dr. Manfred Schartl

Supervisor (Third): Professor Dr. Tobias Schatton

Supervisor (Fourth): Professor Dr. Markus Frank

Date of Public Defence: _____

Date of Receipt of Certificates: _____

Affidavit

I hereby confirm that my thesis entitled “The role of cancer cell-expressed PD-1 in tumorigenesis and tumor immune evasion” is the result of my own work. I did not receive any help or support from commercial consultants. All sources and/or materials applied are listed and specified in the thesis.

Furthermore, I confirm that this thesis has not yet been submitted as part of another examination process neither in identical nor in similar form.

Würzburg, January 14th 2017 _____

Eidesstattliche Erklärung

Hiermit erkläre ich an Eides statt, die Dissertation “Funktionelle Charakterisierung von Tumorzell-exprimiertem PD-1 in der Karzinogenese und antitumoralen Immunabwehr” eigenständig, d.h. insbesondere selbstständig und ohne Hilfe eines kommerziellen Promotionsberaters, angefertigt und keine anderen als die von mir angegebenen Quellen und Hilfsmittel verwendet zu haben.

Ich erkläre außerdem, dass die Dissertation weder in gleicher noch in ähnlicher Form bereits in einem Prüfungsverfahren vorgelegen hat.

Würzburg, den 14. Januar 2017 _____

You'll never find a rainbow if you are looking down.

Charlie Chaplin

Table of Contents

List of abbreviations

7-AAD	7-amino-actinomycin D
Ab (Abs)	Antibody (antibodies)
ABC	ATP binding cassette
ABCB1	ATP-binding cassette member B1
ABCB5	ATP-binding cassette member B5
ABCC1	ATP-binding cassette member C1
ABCC3	ATP-binding cassette member C3
ABCG2	ATP-binding cassette member G2
ACT	adoptive T cell transfer
ADCC	antibody-dependent cellular cytotoxicity
AO	acridine orange
APCs	antigen presenting cells
BSA	bovine serum albumin
CAR	chimeric antigen receptors
CC3	cleaved caspase 3
CDK	cyclin-dependent kinases
CDK4	cyclin-dependent kinase 4
CDKN2A	cyclin-dependent kinase inhibitor 2A
CDS	coding sequence
CK20	cytokeratin 20
CRI	Cancer Research Institute
CSC	cancer stem cell
CTLA-4	cytotoxic T lymphocyte antigen-4
CTLs	cytotoxic T lymphocytes
DAB	3,3'-diaminobenzidine
DAPI	4',6-Diamidino-2-Phenylindole
DCs	dendritic cells
DKO	double knockout
dLNs	draining lymph nodes
DMSO	dimethylsulfoxide
DNA	deoxyribonucleic acid
DTT	dithiothreitol
EBNA-1	Epstein Barr Virus Nuclear Antigen-1
ECM	extracellular matrix
EDTA	ethylenediaminetetraacetic acid
eIF-4B	eukaryotic translation initiation factor 4B
Elisa	enzyme-linked immunosorbent assay
EtBr	ethidium bromide
FACS	fluorescence-activated cell sorting
FDA	U.S. Food and Drug Administration
FMO	Fluorescence minus one
FRET	fluorescence resonance energy transfer
Gal-1	galectin-1
GITR	glucocorticoid-induced tumor necrosis factor receptor-related protein
GM-CSF	granulocyte macrophage colony-stimulating factor
H&E	hematoxylin and Eosin
Hi-FBS	heat inactivated fetal bovine serum
HRP	horseradish peroxidase

i.p.	intraperitoneal
ICS	intracellular cytokine staining
IDO	indoleamine 2,3-dioxygenase
IF	immunofluorescence
IFN-α	interferon- α
IFN-γ	interferon-γ
IHC	immunohistochemistry
IL-10	interleukin-10
IL-2	interleukin-2
IL-2R	interleukin-2 receptor
irAEs	immune related adverse events
IRBs	Institutional Review Boards
IRDye	infrared fluorescent dye
ITIM	immunoreceptor-tyrosine-based inhibitory motif
ITSM	immunoreceptor-tyrosine-based switch motif
KD	knockdown
KO	knockout
LAG-3	lymphocyte-activation gene 3
LB	Luria-Bertani
LT	large T
MAAs	melanoma-associated antigens
mAb	monoclonal antibody
MAP3K	MAP kinase kinase kinase
MAPK	mitogen-activated protein kinase
MART-1	melanoma antigen recognized by T cells-1
MCC	Merkel cell carcinoma
MCPyV	Merkel cell polyomavirus
MDR	multidrug resistance
MDSCs	Myeloid-derived suppressor cells
MgCl2	magnesium chloride
MHC-1	major histocompatibility complex-1
Mitf	microphthalmia-associated transcription factor
MMICs	malignant melanoma-initiating cells
MMP	matrix metalloproteinases
MSAs	melanoma-specific antigens
mTOR	mechanistic target of rapamycin
MTT	3-(4,5-dimethylthiazol-2-yl)-2,5-diphenyltetrazolium bromide
MZK	Merkelzellkarzinom
NCI	National Cancer Institute
NGFR	nerve growth factor receptor
NK	natural killer
NOD/SCID	non-obese diabetic/severe combined immunodeficiency
NSCLC	non-small cell lung cancer
NSG	NOD/SCID IL-2R γ-chain(-/-) null
OE	overexpressing/ overexpression
oriP	origin of plasmid replication
ORR	objective response rates
OVA	ovalbumin
p	phosphorylated
PBMCs	peripheral blood mononuclear cells

PBS	phosphate-buffered saline
P_{CMV}	Cytomegalovirus immediate early promoter
PCR	polymerase chain reaction
PD-1	programmed cell death-1 (PDCD1)
PD-L1	programmed cell death-1 ligand 1 (PDCD1lg1)
PD-L2	programmed cell death-1 ligand 2 (PDCD1lg2)
PFS	progression-free survival
PI	propidium iodide
PI3K	phosphatidylinositol-4,5-bisphosphate 3-kinase
PMA	phorbol 12-myristate 13-acetate
PTEN	phosphatase and tensin homolog
RB	retinoblastoma protein
RCC	renal cell carcinoma
Rh123	Rhodamine 123
RIPA	Radio-immunoprecipitation
RNA	ribonucleic acid
ROS	reactive oxygen species
RT-PCR	reverse transcriptase-polymerase chain reactions
s.c.	subcutaneous
S6K1	ribosomal protein S6 kinase beta-1
SD	standard deviation
SDS/page	sodium dodecyl sulfate polyacrylamide gel electrophoresis
SEM	standard error of the mean
shRNA	short hairpin RNA
ST	small T
TAg	tumor antigen
TBS	tris-buffered saline
TCR	T cell receptor
TGF-β	transforming growth factor beta
Th1	type 1 T helper cell
TIC	tumor-initiating cells
TILs	tumor-infiltrating lymphocytes
TIM-3	T cell immunoglobulin mucin domain receptor-3
TME	tumor microenvironment
TNF-α	tumor necrosis factor-α
Tregs	regulatory T cells
TSAP	thermosensitive alkaline phosphatase
UV	ultraviolet
V600E	valine to glutamic acid substitution at the 600 amino acid position
VEGF	vascular endothelial growth factor
VEGFR-1	vascular endothelial growth factor receptor-1

Abstract

Melanoma and Merkel cell carcinoma (MCC) are highly aggressive cancers of the skin that frequently escape immune recognition and acquire resistance to chemotherapeutic agents, which poses a major obstacle to successful cancer treatment. Recently, a new class of therapeutics targeting the programmed cell death-1 (PD-1) immune checkpoint receptor has shown remarkable efficacy in the treatment of both cancers. Blockade of PD-1 on T cells activates cancer-specific immune responses that can mediate tumor regression. The data presented in this Ph.D. thesis demonstrates that PD-1 is also expressed by subsets of cancer cells in melanoma and MCC. Moreover, this work identifies PD-1 as a novel tumor cell-intrinsic growth receptor, even in the absence of T cell immunity. PD-1 is expressed by tumorigenic cell subsets in melanoma patient samples and established human and murine cell lines that also co-express ABCB5, a marker of immunoregulatory tumor-initiating cells in melanoma. Consistently, melanoma-expressed PD-1 downmodulates T effector cell functions and increases the intratumoral frequency of tolerogenic myeloid-derived suppressor cells. PD-1 inhibition on melanoma cells by RNA interference, blocking antibodies, or mutagenesis of melanoma-PD-1 signaling motifs suppresses tumor growth in immunocompetent, immunocompromised, and PD-1-deficient tumor graft recipient mice. Conversely, melanoma-specific PD-1 overexpression enhances tumorigenicity, including in mice lacking adaptive immunity. Engagement of melanoma-PD-1 by its ligand PD-L1 promotes tumor growth, whereas melanoma-PD-L1 inhibition or knockout of host-PD-L1 attenuates growth of PD-1-positive melanomas. Mechanistically, the melanoma-PD-1 receptor activates mTOR signaling mediators, including ribosomal protein S6. In a proof-of-concept study, tumoral expression of phospho-S6 in pretreatment tumor biopsies correlated with clinical responses to anti-PD-1 therapy in melanoma patients. In MCC, PD-1 is similarly co-expressed by $ABCB5^{+}$ cancer cell subsets in clinical tumor specimens and established human cell lines. ABCB5 renders MCC cells

resistant to the standard-of-care chemotherapeutic agents, carboplatin and etoposide. Antibody-mediated ABCB5 blockade reverses chemotherapy resistance and inhibits tumor xenograft growth by enhancing chemotherapy-induced tumor cell killing. Furthermore, engagement of MCC-expressed PD-1 by its ligands, PD-L1 and PD-L2, promotes proliferation and activates MCC-intrinsic mTOR signaling. Consistently, antibody-mediated PD-1 blockade inhibits MCC tumor xenograft growth and phosphorylation of mTOR effectors in immunocompromised mice. In summary, these findings identify cancer cell-intrinsic functions of the PD-1 pathway in tumorigenesis and suggest that blocking melanoma- and MCC-expressed PD-1 might contribute to the striking clinical efficacy of anti-PD-1 therapy. Additionally, these results establish ABCB5 as a previously unrecognized chemoresistance mechanism in MCC.

Zusammenfassung in deutscher Sprache

Das Melanom und das Merkelzellkarzinom (MZK) sind Hauttumoren neuroendokrinen Ursprungs, die sich durch ein besonders aggressives Wachstum auszeichnen. Melanome und MZK entgehen häufig der antitumoralen Immunabwehr und erwerben Resistenzen gegen Chemotherapeutika, was eine erfolgreiche Behandlung der betroffenen Patienten erschwert. In klinischen Studien hat eine neue Klasse von therapeutischen Antikörpern, die den Immun-Checkpoint Rezeptor PD-1 (Programmed Cell Death-1) inhibieren, hohe Ansprechraten und dauerhafte Remissionen bei Melanom- und MZK-Patienten erzielt. Die Blockade des PD-1 Rezeptors auf T-Zellen reaktiviert autologe Immunreaktionen gegen Tumorzellen, die zur Reduktion des Tumors führen können. Die vorgelegte Dissertation zeigt, dass Subpopulationen von Melanom- und MZK-Zellen PD-1 exprimieren, und dass die Aktivierung von Tumorzell-intrinsischem PD-1 einen pro-tumorigenen Mechanismus darstellt, einschliesslich in T-Zell-defizienten Mäusen. In Biopsien von Melanom-Patienten, sowie in humanen und murinen Melanom-Zelllinien wird PD-1 präferentiell von tumorigenen, immunregulatorischen, $ABCB5^{+}$ Melanom-Stammzellen exprimiert. $PD\text{-}1^{+}$ Melanomzellen hemmen die Aktivität von Effektor-T-Zellen und erhöhen die Anzahl der tolerogenen myeloiden Suppressorzellen im Tumor. Die Inhibierung des PD-1 Rezeptors auf Melanomzellen durch RNA-Interferenz, blockierende Antikörper oder Mutagenese der intrazellulären Signalmotive des PD-1 Proteins unterdrückt das Melanom-Wachstum in immunkompetenten, immunsupprimierten und PD-1-defizienten Mäusen. Umgekehrt führt die Melanom-spezifische Überexpression von PD-1 zu einem signifikant erhöhtem Tumorwachstum, sogar in immunsupprimierten Mäusen. Die Aktivierung des PD-1 Rezeptors auf Melanomzellen durch die Bindung seines Liganden, PD-L1, fördert das Tumorwachstum, während das protumorigene Potential von PD-1-positiven Melanomzellen durch die Inhibierung von PD-L1 auf Melanomzellen, sowie in PD-L1-defizienten Mäusen, gehemmt wird. In Melanomzellen aktiviert der PD-1 Rezeptor den

mTOR Signaltransduktionsweg, einschließlich des Effektormoleküls ribosomales Protein S6. In einer Teststudie korrelierte die Expression des Phospho-S6 Proteins in Melanomzellen aus Biopsien, die vor Gabe der Immuntherapie entnommen wurden, mit den Ansprechraten der Melanom Patienten auf die Behandlung mit PD-1-Antikörpern. Auch in Biopsien von MZK-Patienten und in etablierten humanen MZK-Zelllinien wird PD-1 präferentiell von $ABCB5^{+}$ Subpopulationen exprimiert. Im MZK vermittelt der ABCB5-Membrantransporter Resistenzen gegenüber den Zytostatika Carboplatin und Etoposid. Die Antikörper-vermittelte Blockade des ABCB5-Transporters sensibilisiert MZK-Zellen für die Carboplatin- und Etoposid-vermittelte Apoptose, was zu einer signifikanten Reduktion des experimentellen Tumorwachstums führt. Ähnlich wie im Melanom fördert die Bindung des PD-1 Rezeptors auf MZK Zellen durch seine Liganden, PD-L1 und PD-L2, deren Proliferation und die intrazelluläre Aktivierung der mTOR-Signalkaskade. Entsprechend führt die antikörper-vermittelte Blockade von PD-1 zur Inhibierung des MZK-Tumorwachstums in immunsupprimierten Mäusen und zu einer reduzierten Phosphorylierung von mTOR Effektormolekülen. Zusammenfassend konnte in der vorliegenden Dissertation gezeigt werden, dass Subpopulationen von Melanom- und MZK-Zellen PD-1 exprimieren, und dass Tumorzell-intrinsische PD-1-Funktionen das Krebswachstum fördern. Diese Ergebnisse deuten darauf hin, dass die Blockade des PD-1-Rezeptors auf Tumorzellen zu der klinischen Wirksamkeit der anti-PD-1 Therapie beitragen könnte. Darüber hinaus konnte ABCB5 als neuer Chemoresistenz-Mechanismus in MZK identifiziert werden.

Preface

Portions of this thesis have been previously published in peer-reviewed scientific journals. Specifically, sections of the Introduction chapter 1.5 “The cancer stem or tumor-initiating cell hypothesis“ were published in *Kleffel S. & Schatton T. Tumor dormancy and cancer stem cells: two sides of the same coin? Adv Exp Med Biol. 2013; 734:145-79.* Data presented in Results chapters 4.1 “The immune checkpoint receptor PD-1 is expressed by tumorigenic melanoma subpopulations“, 4.2 “Melanoma-expressed PD-1 modulates antitumor immune responses“, and 4.3 “Melanoma cell-intrinsic PD-1 receptor functions promote tumor growth“, have been published in *Kleffel S. et al. Melanoma Cell-Intrinsic PD-1 Receptor Functions Promote Tumor Growth. Cell 2015;162(6):1242-56*. The findings in Results chapter 4.4 “ABCB5 marks therapy-refractory cell populations in Merkel cell carcinoma“ have been published in *Kleffel S. et al. ABCB5-targeted chemoresistance reversal inhibits Merkel cell carcinoma growth. J Invest Dermatol. 2016;136(4):838-46.* Contributions of co-authors are listed in chapter 2 “Materials and methods“, Chapter 9 “Credits“, and can be found in each publication. Authors’ rights for each journal allow for full publications or parts thereof to be included in this dissertation.

1 Introduction

Skin cancers are the most common type of cancer in the United States according to the National Cancer Institute (NCI) (Howlader, 2016). There are many different types of cutaneous cancers that arise from abnormal growth of skin cells. Although melanoma and Merkel cell carcinoma (MCC) account for less than 5% of all skin cancers, they are responsible for the vast majority of deaths (Howlader, 2016), and will be the focus of this thesis.

Cancer cells acquire hallmark features to maintain neoplastic progression, including genetic instability, sustained proliferative signaling, insensitivity to growth suppressors, resistance to apoptosis, unlimited replication potential, deregulated cellular metabolism, sustained angiogenesis, tissue invasion and metastasis, and modulation of antitumor immunity (Hanahan and Weinberg, 2011). The current understanding of genetic alterations that drive cancer growth, functional tumor cell heterogeneity, resistance to therapy, modulation of antitumor immune responses, the complex interplay of molecular and cellular networks that drive melanoma and MCC pathogenesis, and treatment options for the respective cancers are discussed in this chapter.

1.1 Melanoma

Melanomas arise from malignantly transformed pigment-producing melanocytes. Cutaneous melanomas, which develop from activated and/or genetically altered melanocytes at the epidermal-dermal junction of the human skin, represent the most common form of melanoma skin cancers (Slominski et al., 2001) and will be the focus of this thesis work. Non-cutaneous melanomas arise from melanocytes within mucosal surfaces and the uveal tract of the eye, albeit at low frequencies (Tas et al., 2011).

According to the NCI, melanoma is the sixth most common form of cancer, and incidences are higher among Caucasian, male and elderly populations. While the lifetime risk and overall mortality of patients diagnosed with cutaneous melanoma escalates yearly, the survival rate has improved considerably over the past decades (Beddingfield, 2003, Thompson et al., 2005). Currently, the 5-year survival rate for patients with melanoma localized to the skin is 98%, but drops to only 17% in patients with metastatic disease (Soengas and Lowe, 2003).

Early diagnosed melanoma lesions that are localized to the skin can be cured by surgical excision (Eggermont et al., 2014). However, disease frequently progresses and transformed cells start metastasizing (Slominski et al., 2001, Thompson et al., 2005). Metastatic melanomas exploit various strategies to bypass or become resistant to systemic treatment with chemotherapeutic agents, including decreased intracellular build up of the drug, reprogramming of proliferation and survival pathways, inhibition of pro-apoptotic pathways, and activation of DNA repair mechanisms (discussed in chapter 1.4) (Bradbury and Middleton, 2004, Helmbach et al., 2003, Soengas and Lowe, 2003). Accordingly, systemic treatment with chemotherapeutic agents has failed to demonstrate a significant clinical benefit in patients with advanced melanoma, highlighting the need for novel therapies to treat disseminated disease (Eggermont et al., 2014).

Exposure to ultraviolet (UV) radiation, particularly during childhood, represents a major risk factor for developing cutaneous melanoma (Gandini et al., 2005b, Shtivelman et al., 2014). In addition, genetic determinants that control pigmentary traits such as skin and hair color, and the number of benign or dysplastic nevi are associated with an increased risk for melanoma (Gandini et al., 2005a, Gandini et al., 2005c, Kabbarah and Chin, 2006). Patients with a strong family history of melanoma account for 8-12% of all cases (Kabbarah and Chin, 2006). Familial melanoma has been linked to two key susceptibility genes: the cyclin-dependent kinase inhibitor 2A (CDKN2A), and the cyclin-dependent

kinase 4 (CDK4), which induce and stabilize tumor suppressor genes, including the retinoblastoma protein (RB) and the tumor protein p53. Inactivating germline mutations or deletions are commonly found in both genes, and predispose patients to the development of melanoma (Kabbarah and Chin, 2006).

In recent years, the mutational landscape of various cancers has been analyzed using next-generation sequencing and large-scale expression analysis. On average, the mutational burden observed in melanomas exceeds that reported for other aggressive tumors (Zhang et al., 2016a), which has been linked to increased exposure to UV radiation during melanoma pathogenesis (Shtivelman et al., 2014). Studies of human melanomas and derivative cell lines have identified multiple genes and related cellular pathways that are commonly altered in cancer cells, and their relevance to melanoma pathogenesis has been validated on a functional level. The vast majority of melanomas are defined by driver mutations in BRAF and NRAS genes. These activating mutations deregulate various pathways including the mitogen-activated protein kinase (MAPK) signaling cascade RAS/RAF/MEK/ERK, which is involved in cell survival, differentiation and proliferation (Shtivelman et al., 2014).

Approximately 50-60% of melanomas contain activating mutations in the proto-oncogene encoding for the MAP kinase kinase kinase (MAP3K) BRAF (Flaherty et al., 2012, Shtivelman et al., 2014). The vast majority of these BRAF mutations result in a single valine to glutamic acid substitution at the 600 amino acid position (V600E). This mutation yields a constitutively active kinase that hyperstimulates the MAPK pathway by inducing MEK independent of upstream signals, including RAS (Flaherty and Fisher, 2011, Kumar et al., 2003). Selective inhibitors for mutant BRAF and its downstream effector, MEK, have been approved by the U.S. Food and Drug Administration (FDA) based on their clinical activity in up to 60% of patients with metastatic melanoma (Flaherty and Fisher, 2011, Shtivelman et al., 2014, Tsao et al., 2012). However, melanomas

frequently develop resistance to these inhibitors within a short period of time, as evidenced by a median progression-free survival (PFS) of only 6-7 months (Flaherty and Fisher, 2011, Shtivelman et al., 2014, Tsao et al., 2012).

Approximately 20-25% of melanomas carry mutations that permanently activate the GTPase, NRAS (Flaherty et al., 2012, Shtivelman et al., 2014). Sequencing studies suggest that mutations in NRAS and BRAF are almost always mutually exclusive (Flaherty et al., 2012). Under normal conditions, NRAS functions as a molecular switch that cycles between active "GTP-bound" and inactive "GDP-bound" states, and activates several downstream pathways including MAPK and phosphatidylinositol-4,5-bisphosphate 3-kinase (PI3K)/AKT/mechanistic target of rapamycin (mTOR). Point mutations that disable GTP hydrolysis result in constitutively active GTP-bound NRAS. Therapeutic approaches to either displace GTP or restore GTPase activity are inherently challenging and have not yet been successful (Flaherty and Fisher, 2011, Shtivelman et al., 2014, Tsao et al., 2012).

The PI3K/AKT/mTOR pathway is another important regulator of cell survival, growth, metabolism, differentiation, and migration. This pathway is aberrantly activated in melanoma, although PI3K itself is rarely mutated (Flaherty et al., 2012, Shtivelman et al., 2014). The tumor suppressor protein phosphatase and tensin homolog (PTEN) inhibits this pathway, and is a major negative regulator of cell proliferation and survival. The PTEN gene is inactivated in 40-60% of melanoma cases via allelic deletion or missense mutations, resulting in increased PI3K/AKT/mTOR signaling activity (Flaherty et al., 2012, Shtivelman et al., 2014). In human melanomas, loss of PTEN is often associated with activating BRAF but not NRAS mutations, perhaps because the latter can directly activate the PI3K pathway, even without PTEN deficiency (Shtivelman et al., 2014). Although mTOR inhibitors as single agents are not effective in patients with metastatic melanoma, clinical trials of combined mTOR and MAPK, PI3K, or AKT inhibitors are currently underway (Flaherty and Fisher, 2011, Shtivelman et al., 2014, Tsao et al., 2012).

Because melanomas frequently develop resistance to these inhibitors, there is a need for novel targets that may work synergistically with existing therapies, to produce long-term clinical activity in melanoma patients.

Recent studies have highlighted the importance of epigenetic mechanisms in the pathogenesis of melanoma. New technologies facilitate not only the identification of micro, non-coding, and competing-endogenous RNAs, chromatin remodeling, DNA methylation and histone modifications that are differentially regulated between normal and malignant cells, but also help explain their functional contributions to melanoma progression and maintenance (Kabbarah and Chin, 2006, Shtivelman et al., 2014). This is a first step towards identifying epigenetic mechanisms as potential drugable targets to inhibit melanoma initiation and growth.

Although numerous genetic and epigenetic alterations with implications for melanoma pathogenesis have been identified over the past decades, the complex crosstalk between heterogeneous tumor lesions and the tumor microenvironment (TME), particularly its immune components, that play important roles in melanomagenesis are only beginning to be unraveled (discussed in chapters 1.6 and 1.7). Melanoma has historically been considered an immunogenic cancer. Melanoma cells are characterized by the aberrant expression of cellular antigens termed melanoma-associated antigens (MAAs) and melanoma-specific antigens (MSAs), that can be recognized by the immune system as foreign and elicit tumor-specific immune responses (Kawakami et al., 1996, Lee et al., 2016b). Primary tumors, metastatic lesions, and their surrounding stroma are commonly infiltrated by lymphocytes. Most epidemiologic studies correlate the frequency of tumor-infiltrating lymphocytes (TILs) with improved survival and decreased melanoma metastasis (Azimi et al., 2012, Clark et al., 1989, Clemente et al., 1996, Day et al., 1981, Hillen et al., 2008, Kruper et al., 2006, Ladanyi et al., 2004, Larsen and Grude, 1978, Lee et al., 2016b, Mihm et al., 1996, Taylor et al., 2007, van Houdt et al., 2008). In particular,

high frequencies of melanoma antigen-specific cytotoxic T lymphocytes (CTLs) and antibodies (Abs) are linked to a good prognosis (Boon et al., 2006). Spontaneous regression of metastatic melanomas has been associated with the re-activation of tumor-specific immunity (Kalialis et al., 2009). However, the underlying mechanism require further analysis. On the contrary, patients with clinical immunodeficiencies have an increased risk for developing melanoma and show poorer clinical outcomes compared with the general population (Dahlke et al., 2014, Grulich et al., 2007). Indeed, withdrawal of immunosuppression has previously resulted in melanoma regression (Dillon et al., 2010). Taken together, these observations suggest that adaptive host-anti-tumor immune responses play a crucial role in regulating melanomagenesis. However, disease progression can be observed in the majority of patients, despite the existence of melanoma-specific humoral and cellular immune responses (Lee et al., 2016b). This is, at least in part, due to the fact that melanoma cells exploit various mechanisms to evade and suppress antitumor immunity in order to thrive (discussed in chapter 1.8). Improved understanding of these immune escape mechanisms has led to the development of cancer immunotherapies aimed at enhancing CTL responses against tumor cells (Redman et al., 2016). Clinical trials to assess the therapeutic efficacy of cancer immunotherapies, including proinflammatory cytokines, cancer cell vaccines, adoptive transfer of autologous T cells, and immune checkpoint blockade provide proof-of-principle that adaptive immunity can produce complete and durable responses in a subset of patients with metastatic melanoma (discussed in chapter 1.10) (Baumeister et al., 2016, Hodi et al., 2010, Rosenberg et al., 2004, Rosenberg et al., 2011).

1.2 Human tumor xenograft and murine syngeneic B16 melanoma models

Experimental mouse models have provided a unique framework to dissect mechanisms underlying human melanoma pathogenesis, identify novel targets for cancer therapy, evaluate the efficacy of therapeutics and help identify biomarkers of response in longitudinal studies. Although mice rarely develop melanomas spontaneously, a variety of *in vivo* models are available, including UV radiation- or carcinogen-induced models, genetically engineered models, and syngeneic or xenogeneic transplantation models (Khavari, 2006). Each of these mouse models has specific advantages and limitations, and provides distinct opportunities to analyze intrinsic genetic, epigenetic or extrinisic environmental factors involved in neoplastic progression. However, the differences in the anatomy and physiology between mice and humans should be considered when analyzing the results from animal studies and assessing their relevance to human disease (Frese and Tuveson, 2007, Hidalgo et al., 2014). The human melanoma xenograft model used in this thesis employs the subcutaneous (s.c.) implantation of human-derived primary tumor cells or established melanoma cell lines into immmunodeficient mice, typically non-obese diabetic/severe combined immunodeficiency (NOD/SCID) or NOD/SCID interleukin-2 receptor (IL-2R) γ-chain(-/-) null (NSG) mice. Upon s.c. injection, melanoma cells form a network with the host's lymphatic system and blood vessels, which yields highly reproducible tumors with similar growth kinetics that can spontaneously metastasize to distant sites in mice, thereby simulating the aggressive nature of human melanomas. The genetic, molecular, and histological properties of the resulting tumor xenografts also closely preserve the characteristics of the original patient tumor (Frese and Tuveson, 2007, Hidalgo et al., 2014, Khavari, 2006). Contrary to patient-derived cells, established cell lines are maintained under non-physiological conditions, which can result in a selection of

clones that may not necessarily represent the cellular make up of the original patient tumor. However, established cell lines can be genetically manipulated to study the effects of distinct genes on melanomagenesis in a well-defined experimental context.

In humans, melanomas develop in the context of a stroma, which is comprised of extracellular matrix (ECM) and cellular components, including immune cells. The crosstalk between arising melanoma cells and the stromal compartment plays an important role in regulating melanomagenesis (discussed in chapters 1.6 and 1.7). However, the tumor xenograft model does not fully recapitulate the intricate interplay between TME, environmental factors, and cancer cells that govern neoplastic progression in human disease, because already transformed cancer cells are injected into normal tissue of murine hosts (Frese and Tuveson, 2007, Khavari, 2006, Le Magnen et al., 2016). Hence, the lack of stromal involvement during melanomagenesis may limit studies designed to examine the impact of the TME on tumor initiation and growth, and should be considered when interpreting results from this model.

Studies aimed at dissecting the role of tumor-specific immune responses in melanomagenesis are limited in the tumor xenograft model, because tumors form in mice that lack adaptive immunity. Thus, animal models that accurately recapitulate the crosstalk between immune and cancer cells in the TME are needed to examine the role of adaptive immunity in tumorigenesis. Mice that harbor a human immune system may be able to overcome these limitations, however, patient-matched melanomas and peripheral blood mononuclear cells (PBMCs) are scarce, and it is inherently challenging to fully recapitulate the human immune system in mice (Rongvaux et al., 2014).

In syngeneic models, melanoma cells are transplanted into mice with the same genetic background that have a functional immune system, thereby allowing the study of melanoma growth and metastasis in the context of immunity. The most widely used syngeneic melanoma model is the B16 model, which is derived from a murine melanoma

that spontaneously originated in a C57BL/6 mouse over six decades ago (Fidler and Nicolson, 1976). Since then, multiple B16 subclones have been generated, each with distinct proliferative, invasive, and metastatic capacities. The two variants used in this thesis are the original B16-F0 clone that has low metastatic potential, and the B16-F10 clone that was derived through ten *in vivo* passages in C57BL/6 mice and has higher metastatic potential (Fidler and Nicolson, 1976). Since all B16 melanoma subclones originated from one melanoma lesion of an inbred mouse strain, this model fails to fully recapitulate the genetic heterogeneity of human melanomas. Sequence analysis revealed that murine B16 melanoma cell lines, unlike the majority of human melanomas, do not carry activating mutations in the BRAF oncogene or deletions of the PTEN tumor suppressor gene (Melnikova et al., 2004). Nonetheless, the MAPK and PI3K/AKT/mTOR pathways are aberrantly activated in B16 melanomas (Melnikova et al., 2004), consistent with human disease. Genetic deletions of the region encoding for the tumor suppressor protein CDKN2A, the key susceptibility gene for familial human melanoma, are also present in B16 melanoma cell lines (Melnikova et al., 2004).

B16 melanoma cells express low major histocompatibility complex-1 (MHC-I) levels, which results in poor recognition of melanoma cells by cytotoxic T cells (Becker et al., 2010). Thus B16 tumors, in contrast to human melanomas, have been historically defined as low immunogenic cancers (Celik et al., 1983, Schatton et al., 2010). However, B16 tumors do express MAAs and neoantigens and respond to immunotherapies, including proinflammatory cytokines, cancer vaccines, adoptive T cell transfer (ACT) and immunomodulatory Abs (Becker et al., 2010). These studies imply that B16 melanomas may be more immunogenic than initially presumed, and suggest that B16 may be a valid model to predict the efficacy of novel immunotherapeutic regimens against human melanomas. Nonetheless, the study of melanoma-specific immunity, and particularly T cell responses in the B16 model, remains inherently difficult. The use of transgenic models, in

which all T cells are committed to one specific unique antigen and thus elicit reproducible immune responses, may provide a framework to dissect the effects of melanoma-expressed molecules on T cell immunity. In the B16-OVA melanoma model, B16 melanoma cells that stably express chicken ovalbumin (OVA) as a surrogate tumor antigen are transplanted into transgenic OT-1 mice. Since all cytotoxic T cells from the OT-1 mice are genetically engineered to express a single, MHC class I-restricted T cell receptor (TCR) specific for the foreign OVA antigen, engraftment of B16-OVA cells to OT-1 mice provides a well-defined, antigen-specific T cell mediated immune response (Hogquist et al., 1994). To study the effects of distinct melanoma-expressed genes or pathways in the context of well-defined cytotoxic T cell responses, B16-OVA melanoma cells can be genetically engineered to express or repress any gene of interest and transplanted into OT-1 transgenic animals.

1.3 Merkel cell carcinoma (MCC)

Merkel cell carcinoma (MCC) is a rare but highly aggressive neuroendocrine cancer, which arises from Merkel cells that reside at the epidermal-dermal junction of the skin (Thakuria et al., 2014). Merkel cells are commonly located in complexes with nerve axons, and compelling evidence suggests they function as mechanoreceptors and chemoreceptors of the skin (Morrison et al., 2009). There are only approximately 1500 new cases per year in the United States, however the reported MCC lifetime risk and overall mortality has tripled over the past 20 years and continues to rise (Bhatia et al., 2011). MCC incidence increases with age and is higher in male and Caucasian populations (Agelli and Clegg, 2003). The overall mortality rate for MCC is three-times higher than melanoma, making MCC the most aggressive form of skin cancer (Lemos et al., 2010). Although surgical resection followed by adjuvant radiation therapy can be curative for some patients with

local disease, relapses are frequent and often fatal (Bhatia et al., 2011). Patients with locally advanced and metastatic disease are commonly treated with systemic chemotherapy (Bhatia et al., 2011). However, responses are typically of limited duration as tumors become chemoresistant after approximately 8 months, and ten-year overall survival has been unchanged over decades (discussed in chapter 1.4) (Bhatia et al., 2011, Fitzgerald et al., 2015). There are currently no established second-line treatment options for patients that progress, highlighting the need for novel treatment modalities (Bhatia et al., 2011).

Epidemiologic studies suggest a strong link between the development of MCC and T cell immune suppression, prolonged UV exposure, and advanced age (Moshiri and Nghiem, 2014, Poulsen, 2004). These early observations supported the possibility that MCC may have an infectious etiology, which led to the discovery of the Merkel cell polyomavirus (MCPyV) by Feng and colleagues in 2008 (Feng et al., 2008). Recent studies report that the human MCPy virus is clonally integrated into the host genome of at least 80% of MCC tumors tested (Bhatia et al., 2011, Feng et al., 2008, Rodig et al., 2012a), and suggest that genomic integration and mutation of the MCPy virus are early events in MCC carcinogenesis (Cheng et al., 2013, Goh et al., 2015, Tothill et al., 2015). The majority of these MCC tumors express the viral oncoproteins MCPyV small T (ST) antigen and large T (LT) antigen (Cheng et al., 2013, Rodig et al., 2012a), which appear to be required for malignant transformation, tumor maintenance, and progression of virus-positive MCCs (Cheng et al., 2013, Houben et al., 2010, Shuda et al., 2011). Sequencing of the viral genome in clinical MCC tumors and established cell lines revealed that the gene encoding the LT antigen undergoes truncating mutations, rendering it unable to initiate viral replication and subsequent cell death, while the ST antigen gene remains intact (Cheng et al., 2013, Shuda et al., 2008). Truncated LT antigen has been shown to bind and inactivate the cell cycle regulator and tumor suppressor RB to promote cellular growth (Cheng et al., 2013). ST antigen acts as an independent oncoprotein downstream of the

mTOR pathway and inhibits the translational repressor protein 4E-BP1, thereby activating cap-dependent mRNA translation (Shuda et al., 2011). Interestingly, the ST antigen gene contains an UV-inducible promotor (Mogha et al., 2010), linking UV-radiation to the expression of the oncoprotein ST antigen and mTOR activation during MCC development. Exposure to UV radiation and aging increase the mutational burden of Merkel cells undergoing neoplastic progression, and has been suggested to play a key role in MCC pathogenesis, particularly in MCPyV-negative tumors (Goh et al., 2015). Accordingly, virus-negative MCCs have significantly higher mutational frequencies, particularly in regions encoding for tumor suppressor genes like RB and TP53, and chromosomal alterations that result in increased levels of neoantigens compared to MCPyV-positive MCCs (Goh et al., 2015, Harms et al., 2015, Wong et al., 2015). Thus, emerging evidence suggests that two distinct etiologies, one driven by MCPyV infection and the other one caused by UV radiation, may lead to the development of MCC.

Several studies have identified genes and pathways that are commonly deregulated in MCC tumors and may serve as potential targets for novel MCC therapies. For examples, MCC tumors express high levels of the receptor tyrosine kinase c-KIT, matrix metalloproteinases (MMPs), and vascular endothelial growth factor (VEGF), and commonly contain deletions or inactivating mutations of the tumor suppressor proteins, RB and TP53 (Thakuria et al., 2014). Furthermore, MCC tumors frequently show aberrant activation of the oncogenic PI3K/AKT/mTOR, NF-κB, and hedgehog signaling pathways (Nardi et al., 2012, Thakuria et al., 2014).

While MCPyV infections and UV radiation are potent drivers of malignant transformation in Merkel cells, the immune system plays a critical role in regulating MCC pathogenesis (Paulson et al., 2013). Patients with clinical immunodeficiency are at higher risk for developing MCC, and have poorer clinical outcomes compared to immunocompetent individuals (Heath et al., 2008). However, the vast majority of MCC

patients have a functional immune system (Heath et al., 2008). Persistent expression of viral T antigens and neoantigens by MCC tumors elicit robust cellular and humoral immune responses in MCC patients (Goh et al., 2015, Harms et al., 2015, Iyer et al., 2011, Paulson et al., 2010, Wong et al., 2015). Lymphocytic infiltration of the TME, particularly by $CD8^+$ T cells, and presence of MCPyV-specific Abs correlate with improved patient survival (Ibrani, 2015, Paulson et al., 2010, Paulson et al., 2011, Touze et al., 2011). In addition, the few documented cases of spontaneous regression of primary and metastatic MCCs report dense inflammatory infiltrates of mainly T cells and macrophages in tissue biopsies of residual disease (Pang et al., 2015). Taken together, these observations suggest that the host immune system can elicit immune responses against MCC cells that express immunogenic viral antigens and/or neoantigens. The lack of a syngeneic MCC animal model and the inherent challenges of conducting longitudinal studies in at-risk patients make it difficult to further elucidate the effects of tumor-specific immunity on MCC pathogenesis. To overcome these limitations, humanized mouse models have to be developed to dissect the complex crosstalk between immune cells and MCC cells during neoplastic progression.

MCC tumors, like melanomas, are able to evade antitumor immune responses in order to thrive (Thakuria et al., 2014). Recent advances in understanding the molecular mechanisms underlying MCC pathogenesis and the potential role of the immune system in regulating tumorigenesis suggest that immunotherapies aimed at restoring tumor-specific T cell immunity may be effective for the treatment of patients with recurrent metastatic disease. In this regard, vaccines targeting viral T antigens or MCC-specific neoantigens, adoptive transfer of MCPyV or neoantigen specific $CD8^+$ T cells, immunostimulatory cytokines and immune checkpoint inhibitors are of particular interest, and will be discussed in chapter 1.10.

1.4 Mechanisms of cancer therapeutic resistance

Melanoma and MCC are both highly aggressive cutaneous malignancies. Until recently, standard-of-care treatment for advanced disease was cytotoxic chemotherapy. Chemotherapy preferentially targets cancer cells to induce apoptosis by virtue of their increased proliferation compared to most physiologic tissue. Because this mechanism of action is not specific and treatment affects all rapidly dividing cells, chemotherapy is often associated with severe adverse events that can be prohibitive in treating elderly patients, which are commonly afflicted with these malignancies (Malhotra and Perry, 2003). Chemotherapies currently in use to treat patients with metastatic melanoma include the alkylating agents dacarbazine and temozolomide that covalently link an alkyl-group to nucleic acids and proteins (Bradbury and Middleton, 2004, Malhotra and Perry, 2003). Cytotoxic agents used for MCC treatment include platinum-based drugs like carboplatin, that bind and cross-link DNA, and the topoisomerase inhibitor etoposide, which inhibits DNA replication (Malhotra and Perry, 2003, Thakuria et al., 2014). Even within the same lesion, cancer cells exhibit a high degree of heterogeneity due to differences in genetic and epigenetic make-up and crosstalk with the TME, all of which may predispose cancer cells to intrinsic and/or acquired drug resistance (Gottesman et al., 2002, Gottesman et al., 2016). Tumor cells frequently develop resistance to multiple, structurally and mechanistically unrelated drugs, a phenomenon termed multidrug resistance (MDR) (Gottesman et al., 2002). Due to MDR, complete eradication of local or advanced disease is rare, and chemotherapy typically fails to improve overall survival of both melanoma and MCC patients (Bradbury and Middleton, 2004, Thakuria et al., 2014).

Cancer cells commonly modify DNA damage responses to become resistant to multiple classes of drugs. For example, they overexpress enzymes that are involved in nucleotide excision and mismatch repair to remove alkyl- and platinum-DNA adducts and arrest the cell cycle prior to entering mitosis, which facilitates the repair of damaged DNA

(Bradbury and Middleton, 2004, Housman et al., 2014). In addition, cancer cells can become resistant to chemotherapies that target proliferative cells by altering cell cycle checkpoints to prolong cell cycle arrest or induce cellular quiescence (Bradbury and Middleton, 2004, Housman et al., 2014). It is well established that DNA damage induced by cytotoxic drugs activates apoptotic cell death (Housman et al., 2014, Pommier et al., 2004). Thus, inactivation of apoptotic pathways, for example by inhibiting pro-apoptotic signals such as p53 transcriptional targets and the Fas/Fas-ligand axis, or activation of survival pathways, for example via induction of anti-apoptotic proteins, such as Bcl-2 and Bcl-x_L, are additional mechanisms that cancer cells commonly employ to resist therapy (Pommier et al., 2004).

Another MDR mechanism that is particularly relevant to this thesis work is drug efflux via energy-dependent ATP binding cassette (ABC) transporters, which causes decreased intracellular accumulation of chemotherapeutic agents. The family of ABC transporters can be divided into seven subfamilies (ABC-A through ABC-G) with several members each, on the basis of sequence and structural homology (Dean et al., 2001, Gottesman et al., 2002). Multiple studies have demonstrated that ABC transporters, including ABCB1, ABCC1, ABCC3, ABCG2 and ABCB5, efflux a variety of low molecular weight compounds in non-malignant and malignant cells in an ATP-dependent fashion (Gottesman et al., 2002). ABCB5 is a clinically relevant MDR mediator in human melanoma (Chartrain et al., 2012, Frank et al., 2005, Wilson et al., 2014), colorectal cancer (Wilson et al., 2011), hepatocellular carcinoma (Cheung et al., 2011b), and osteosarcoma (Wang and Teng, 2016). Because ABCB5 marks therapy-refractory cancer cells, $ABCB5^+$ cancer cell subsets may be a potential cause for disease relapse following chemotherapy. Notably, inhibition of the ABCB5 transporter can sensitize tumor cells to chemotherapy-induced apoptosis (Cheung et al., 2011a, Frank et al., 2005, Wilson et al., 2011).

Moreover, ABCB5 also mediates alternative, efflux-independent mechanisms of resistance. For example, ABCB5 has previously been shown to regulate the maintenance of slow-cycling melanoma subpopulations (Wilson et al., 2014) and limbal stem cells (Ksander et al., 2014), which may mediate MDR against chemotherapeutic regimens that target rapidly dividing cells. ABCB5 also confers anti-apoptotic functions in limbal stem cells (Ksander et al., 2014). In addition, ABCB5 regulates the glycolysis pathway in cancer cells, providing a growth advantage in the commonly hypoxic tumor niches (Lutz et al., 2016). Thus, ABCB5 might further promote resistance of cancer cells to chemotherapeutic drugs by inducing cellular quiescence and inhibiting cellular apoptosis, in addition to mediating the efflux of cytotoxic agents. Together, these findings provide a rationale for targeting cancer cell-expressed ABCB5 to sensitize tumor cells to various chemotherapeutic drugs, thereby enhancing clinical benefits.

1.5 The cancer stem or tumor-initiating cell hypothesis

Parts of this chapter have been previously published in *Kleffel S. & Schatton T. Tumor dormancy and cancer stem cells: two sides of the same coin? Adv Exp Med Biol. 2013; 734:145-79.*

Tumors, like physiologic tissues, are complex structures composed of genetically, phenotypically, and functionally heterogeneous cell populations that differ in their ability to initiate and maintain tumor growth (Hanahan and Weinberg, 2011). The prevailing stochastic model of neoplastic progression postulates that the accumulation of genetic mutations followed by clonal selection induces tumor heterogeneity (Michor et al., 2004). According to this theory, all cancer cells, regardless of their phenotype, possess equivalent intrinsic capacities to proliferate, initiate tumor growth, and cause relapse (Nowell, 1976).

However, phenotypic and functional differences of cancer cells can be explained only in part by sequential acquisition of genetic variations. This has led to the development of the cancer stem cell (CSC) hypothesis of tumor growth (Bruce and Van Der Gaag, 1963, Hamburger and Salmon, 1977). The CSC model postulates that tumors are organized as defined hierarchies with CSCs at their apex, and suggests that only CSCs can proliferate extensively and give rise to morphologically and functionally diverse cancer cell progeny that comprises the malignant lesion (Reya et al., 2001). It should be noted, however, that the stochastic and CSC models of tumorigenicity are not mutually exclusive, and stochastic processes may occur within the CSC population (Dirks, 2010).

CSCs have been operationally defined by their (i) preferential ability to initiate tumor growth, (ii) capacity to self-renew, and (iii) competence to differentiate into various non-self renewing tumor bulk populations (Clarke et al., 2006), thereby providing an explanation for functional differences between tumor subpopulations (Reya et al., 2001). Experimental verification of these defining CSC traits requires serial xenotransplantation at limiting dilution of marker-defined clinical cancer subpopulations into an orthotopic site of immunocompromised animals (typically NOD/SCID mice) (Clarke et al., 2006, Schatton et al., 2009). Using this approach, the preferential ability to initiate and maintain tumor growth is ascribed to the putative CSC population. Importantly, the CSCs' capacity to self-renew and differentiate also requires experimental confirmation in serial *in vivo* passaging studies. This can be demonstrated through re-establishment of the original patient's tumor heterogeneity in primary and secondary cancer xenografts upon serial inoculation of immunocompromised hosts with purified CSCs (Clarke et al., 2006). Some studies have demonstrated the selective ability of CSC subsets to undergo cell divisions that expand the CSC pool and generate differentiated cancer cell progeny, whereas non-CSC subsets exclusively give rise to differentiated tumor populations (Lathia et al., 2011, Schatton et al., 2009, Schatton et al., 2008, Vlashi et al., 2009). However, other reports

suggest a more dynamic regulation of CSC phenotype and function, allowing for a bidirectional interconversion between the CSC compartment and non-stem cancer cells in response to signals from the TME (Chaffer et al., 2011, Quintana et al., 2010). Such findings of CSC plasticity highlight the critical importance of the stromal microenvironment and the host immune system in governing tumorigenesis, as well as CSC and non-tumor-initiating cell fate (discussed in chapters 1.6 and 1.7) (Scadden, 2006, Schatton and Frank, 2009). Thus, variations in the methodologies and experimental model systems used to assess cancer "stemness" require careful scrutiny, as they might influence experimental outcomes (Dirks, 2010).

Although CSC studies have fundamentally advanced current understanding of functional tumor heterogeneity, the CSC concept remains controversial (Gupta et al., 2009, Jordan, 2009). Disagreements mainly result from three presumptions. First, physiological stem cells are commonly regarded to be the cellular origin of CSCs. However, while some experimental tumor model systems have identified adult tissue stem cells as the source of malignant transformation (Barker et al., 2009, Zhu et al., 2009), other models propose that transiently amplifying cells (Jamieson et al., 2004, Krivtsov et al., 2006) or even terminally differentiated cells (Sun et al., 2005) could acquire CSC-like properties through a series of mutagenic events. The term CSC should therefore refer to the functional traits of the cancer cell, rather than to its cellular origin and biological properties within normal tissues (Gupta et al., 2009). Second, the notion that CSCs should represent only a small fraction of cancer cells (Quintana et al., 2008, Shackleton et al., 2009), paralleling low frequencies of physiologic stem cells in normal tissues (Simons and Clevers, 2011) has yielded further dissonance regarding the CSC model. However, "rareness" is not a defining trait of CSCs (Reya et al., 2001), and relative CSC frequencies, analogous to physiologic stem cell systems (Morrison and Kimble, 2006), likely rely on the dynamic crosstalk between CSCs, tumor bulk populations and the microenvironment. Third, multiple studies suggest that

CSCs may not be a distinct, unchangeable subpopulation that resides at the apex of a hierarchically organized tumor. Rather, the majority of cancer cells may be in a constant state of flux with regard to CSC phenotype and function, depending on the composition and configuration of the surrounding niche environment (Chaffer et al., 2011, Quintana et al., 2010). This observed CSC plasticity does not undermine the CSC hypothesis, because distinct tumor populations can be distinguished phenotypically and functionally at any given time point within a tumor (Gupta et al., 2009). Given these potential misconceptions associated with the term "CSC", many investigators in the field are now referring to these cell subsets as tumor-initiating cells (TICs) (Clarke et al., 2006).

In human melanoma, TICs can be identified and prospectively isolated based on their selective expression of ABCB5 (Schatton et al., 2008). Moreover, ABCB5 expression by cancer cells correlates with neoplastic progression of melanomas and hepatocellular carcinomas (Cheung et al., 2011a, Gambichler et al., 2016, Schatton et al., 2008). The nerve growth factor receptor (NGFR, also known as CD271) is a second marker for melanoma-initiating cells (MMICs) (Boiko et al., 2010), and expression of both markers overlaps (Civenni et al., 2011, Frank et al., 2011). Mechanisms underlying the tumorigenic potential of $ABCB5^+$ MMICs result in part from their preferential ability to resist standard-of-care chemotherapeutic regimens. ABCB5 decreases the intracellular buildup of multiple chemotherapeutic drugs (Chartrain et al., 2012, Frank et al., 2005) and also regulates the maintenance of slow-cycling MMICs (Wilson et al., 2014), among other potential mechanisms discussed in chapter 1.4. Creation of a vascular system is crucially important for tumor initiation, growth, and metastasis, because it provides tumor cells with nutrients and oxygen, while removing metabolic waste and carbon dioxide (Folkman, 2002, Kerbel, 2008). Interestingly, $ABCB5^+$ MMICs preferentially express the vascular endothelial growth factor receptor-1 (VEGFR-1) to induce the formation of vasculogenic networks and efficient tumor xenograft growth *in vivo* (Frank et al., 2011), suggesting that angiogenesis

may be another contributing mechanism through which ABCB5 promotes tumor growth. Finally, the immune system plays a critical role in regulating every step of cancer development (discussed in chapters 1.6-1.8). $ABCB5^+$ MMICs have low to absent expression of MAAs and MHC-1 molecules and preferentially express coinhibitory immune checkpoint receptors, thereby reducing their immunogenicity (Schatton et al., 2010). In addition, $ABCB5^+$ MMICs inhibit cytotoxic T cell responses and activate tolerogenic regulatory T cells (Tregs) (Schatton et al., 2010). This ability of $ABCB5^+$ MMICs to modulate antitumor immune responses may confer selective growth advantages to these virulent cancer subsets.

In summary, TICs are likely causing disease relapse due to their ability to survive cytotoxic therapies, induce angiogenic responses, overcome hostile microenvironments and evade immunological clearance. Novel treatment strategies designed to target TICs should consider the mechanisms underlying TIC virulence to achieve more durable responses in tumor patients.

1.6 Chronic inflammation and cancer progression

The observation that immune cells commonly infiltrate tumor tissues dates back to 1863, when Rudolf Virchow first hypothesized a functional link between chronic inflammation and cancer development (Balkwill and Mantovani, 2001). Since then, studies have aimed to dissect the inflammatory infiltrates of tumors, and the mechanisms by which immune cells regulate each stage of tumor development and progression are beginning to be unraveled. Current data suggests that the immune system plays a dual role during cancer pathogenesis. While activated lymphocytes of the adaptive immune system can recognize and eradicate malignantly transformed cells, immune cells can also directly promote tumor progression by selecting for poorly immunogenic cancer cells and by chronically activating

innate proinflammatory immune responses in the TME (de Visser et al., 2006, Zou, 2005). Under normal conditions, complex and dynamic networks of immune and non-immune cells defend the host against foreign pathogens, while maintaining self-tolerance. In the context of cancer, however, malignantly transformed cells can express high levels of proinflammatory cytokines and chemokines that recruit and activate innate immune cells, including dendritic cells (DCs), natural killer (NK) cells, macrophages, neutrophils, mast cells, and myeloid-derived suppressor cells (MDSCs) (de Visser et al., 2006, Zou, 2005). Chronically activated innate immune cells, in turn, secrete various bioactive factors, such as matrix remodeling proteases, growth factors, cytokines, and chemokines, to actively induce proliferation and survival of neoplastic cells, stimulate angiogenesis and remodeling of the ECM and basement membrane of the stromal environment. These changes in the TME foster tumor growth and facilitate the progression from pre-malignant to a malignant phenotype with metastatic ability (de Visser et al., 2006, Mueller and Fusenig, 2004). By releasing reactive oxygen species (ROS), innate immune cells not only directly induce DNA mutagenesis, but also promote T cell hyporesponsiveness or apoptosis and modulate T effector cell differentiation, thereby further contributing to neoplastic transformation (Belikov et al., 2015, de Visser et al., 2006, Hildeman et al., 2003). In summary, increasing evidence suggests that chronic inflammation directly facilitates cellular transformation and promotes cancer progression. Accordingly, infiltration of malignant tissues by innate immune cells, including macrophages, neutrophils and mast cells, often correlates with poor clinical outcomes (de Visser et al., 2006). Epidemiologic studies also suggest a link between chronic inflammatory diseases and an increased risk for developing cancer (de Visser et al., 2006, Zou, 2005).

1.7 The cancer immunoediting hypothesis

The immune surveillance theory, originally proposed by Burnet and Thomas in 1957, hypothesized that the immune system can recognize and eliminate transformed cells in immunocompetent hosts, thereby protecting against cancer development (Burnet, 1957). This concept was based on the demonstration that genetic and epigenetic alterations, which occur during malignant transformation, endow tumor cells with a unique set of tumor antigens (TAgs) that can be detected by the immune system as foreign. For example, cancer cells commonly express increased levels of normal cellular antigens, viral antigens, differentiation antigens, neoantigens that are products of mutated cellular genes, and antigens that are expressed in germ cells but are silent in normal somatic cells (Cheever et al., 2009, Schumacher and Schreiber, 2015).

Since this first proposal of the immunosurveillance hypothesis, additional molecular and cellular mechanisms that mediate the crosstalk between the immune system and the evolving tumor have been described. The discovery that a functional immune system not only protects the host against cancer initiation and growth, but also directly sculpts the immunogenicity of emerging tumor cells, prompted a major revision of the original immunosurveillance hypothesis (Shankaran et al., 2001). To more accurately describe the paradoxical protective versus tumor-promoting roles of the immune system, the old concept was refined and extended to the cancer immunoediting hypothesis, which describes three distinct phases: elimination, equilibrium and escape (Mittal et al., 2014, Schreiber et al., 2011). During neoplastic progression, tumors may proceed through these phases sequentially, however, various factors within the TME can influence the directionality of the process. The elimination phase is an updated version of the old immunosurveillance concept, which proposes that the immune system detects and eradicates transformed cells before cancer lesions become clinically apparent (Mittal et al., 2014, Schreiber et al., 2011). The immune system can identify developing malignant

lesions via several mechanisms, including the expression of proinflammatory cytokines and stress ligands by viable tumor cells, and the release of damage-associated molecular pattern molecules from dying tumor cells or damaged tissues (Schreiber et al., 2011). These mechanisms activate innate immune responses, which propagate the expansion of TAg-specific effector $CD4^+$ and $CD8^+$ T cells, and further establish a TME that facilitates tumor-specific adaptive immune response (Schreiber et al., 2011). The inherent problem of studying the elimination phase in humans is that the readout is the absence of tumors. Thus, experimental validation of the elimination phase largely depends on mouse models (Mittal et al., 2014). In experimental models, successful elimination relies mainly on T lymphocytes, NK cells, macrophages, and effector molecules, such as interferon-γ (IFN-γ), perforin, and the FAS/FAS-ligand axis (Mittal et al., 2014, Vesely et al., 2011). If malignant cells are successfully eradicated by the host's immune system, the elimination phase presents the endpoint of the cancer immmunoediting process.

However, subsets of tumor cells may survive the elimination phase to enter the equilibrium state. During equilibrium, the adaptive immune system prevents tumor cell outgrowth by maintaining residual cancer cells in a functional state of dormancy (Mittal et al., 2014, Schreiber et al., 2011). The molecular mechanisms underlying immune-mediated tumor dormancy are poorly understood, because the equilibrium phase is inherently difficult to model in animals, and only anecdotal evidence describes this state in humans. In a mouse model, the immune-mediated equilibrium state was associated with high frequencies of $CD8^+$ T cells and low frequencies of tolerogenic Tregs and MDSCs in the TME (Wu et al., 2013). Notably, many of the mechanisms that regulate tumor cell dormancy also play key roles in governing the behavior of $ABCB5^+$ MMICs (discussed in chapter 1.5), suggesting a potential overlap between both cancer populations in the equilibrium phase.

Due to the constant selective pressure of the immune system on genetically unstable tumor cells that are kept in the equilibrium state, edited tumor cell variants emerge that are poorly immunogenic (Schreiber et al., 2011). Tumor cells can escape the immune system through many different mechanisms, including (i) reduced immune recognition (e.g. by losing the expression of TAgs, MHC proteins, and/or costimulatory molecules), (ii) inhibition of immune effector mechanisms (e.g. by activation of negative immune checkpoints including cytotoxic T lymphocyte antigen-4 (CTLA-4), programmed death-1 (PD-1), T cell immunoglobulin mucin domain receptor-3 (TIM-3), and lymphocyte-activation gene 3 (LAG-3), (iii) increased resistance to apoptosis (e.g. by expressing anti-apoptotic molecules), and (iv) differential expression of chemokines and downregulation of adhesion molecules in the tumor vasculature to regulate lymphocyte trafficking in the TME (Schreiber et al., 2011, Spranger et al., 2013). In addition, cancer cells induce an immunosuppressive TME to limit tumor-specific immune responses by producing immunosuppressive cytokines and soluble factors, including interleukin-10 (IL-10), VEGF, transforming growth factor beta (TGF-β), galectin-1 (Gal-1), indoleamine 2,3-dioxygenase (IDO), and by recruiting and/or maintaining tolerogenic Tregs and MDSCs (Highfill et al., 2014, Jacobs et al., 2012, Schreiber et al., 2011, Spranger et al., 2013). Under physiologic conditions, Tregs and MDSCs play a critical role in maintaining immune homeostasis by regulating immunological self-tolerance, thereby protecting the host from autoimmune and chronic inflammatory diseases (Nagaraj et al., 2013, Vignali et al., 2008). $CD4^+CD25^+FoxP3^+$ Tregs mediate immune suppression via multiple mechanisms, including the secretion of inhibitory cytokines like IL-10 and TGF-β. Tregs can also promote cytolysis via secretion of granzymes and perforin, deplete nutrients required for T cell function by releasing IDO, induce pro-apoptotic metabolites, and inhibit the maturation and function of DCs (Vignali et al., 2008).

MDSCs comprise a heterogeneous group of myeloid cells, including $CD11b^+Ly6C^+$ monocytic MDSCs and $CD11b^+Ly6G^+$ granulocytic MDSCs that can be induced from progenitor cells by various factors, including granulocyte macrophage colony-stimulating factor (GM-CSF) and VEGF in the TME (Kumar et al., 2016, Nagaraj et al., 2013). The suppressive capacity of MDSCs is mediated through several independent mechanisms that modulate both innate and adaptive immunity, for example by producing inhibitory cytokines such as IL-10 and TGF-β, and by inducing and expanding Treg populations. MDSCs also inhibit T cell functions via generation of oxidative stress, depletion of nutrients required by effector T cells, nitration and inactivation of the TCR, and alteration of lymphocyte trafficking (Kumar et al., 2016, Nagaraj et al., 2013). Moreover, MDSCs can directly support tumor growth by secreting factors like VEGF to promote angiogenesis and MMPs to remodel the ECM, thereby further driving tumor invasion and metastasis (Condamine et al., 2015). As a consequence of this immune selection process, edited cancer cell variants emerge that have acquired the ability to escape immune recognition and destruction, which allows them to grow. Thus, progression from equilibrium to immune escape can occur because the selective pressure from the immune system changes the tumor cells to become less immunogenic, and/or because the tumor cells induce an immunosuppressive TME.

Similarly to edited low immunogenic cancers, $ABCB5^+$ MMICs downmodulate the expression of MAAs and MHC-1 molecules, while preferentially expressing coinhibitory receptors including PD-1, LAG-3, and TIM-3. Moreover, $ABCB5^+$ MMICs are capable of inhibiting T effector cell functions and inducing Tregs ((Schatton et al., 2010) and unpublished data by S. Kleffel, S. Barthel and T. Schatton). This suggests that the immune system may possibly select for virulent MMICs with reduced immunogenicity, that can escape immune eradication and promote tumor outgrowth.

Although the cancer immunoediting hypothesis was mainly deduced from experimental tumor models, studies of human cancers suggest that the immune system can alter the course of tumorigenesis in cancer patients. As discussed in chapters 1.1 and 1.3, clinical immune deficiency is associated with an increased risk for developing melanoma and MCC (Dahlke et al., 2014, Grulich et al., 2007, Heath et al., 2008). Conversely, infiltration of the TME by activated T cells, the presence of effector cytokines, and low frequencies of intratumoral Tregs and MDSCs are often correlated with improved prognosis in patients with melanoma or MCC (Bhatia et al., 2011, Lee et al., 2016b). In addition, tumor-reactive Abs and CTLs can be detected in the blood, primary tumors, lymph nodes and visceral metastases of cancer patients, suggesting that the immune system can develop responses against malignantly transformed cells (Bhatia et al., 2011, Huang et al., 1998, Lee et al., 2016b). Albeit rare, spontaneous eliminations of established tumors have been reported in cancer patients and have been linked to the re-activation of cancer-specific immune responses (Kalialis et al., 2009, Pang et al., 2015). However, immune recognition of malignant cells rarely results in eradication, as humoral and adaptive immune responses are commonly observed in patients with progressive disease (Schreiber et al., 2011). Support for the notion that immunoediting takes place in cancer patients also stems from cancer vaccine trials. For example, a melanoma patient whose pre-treatment lesion tested positive for the MAA NY-ESO-1 received a vaccine targeting this antigen. Upon tumor progression, the outgrown cancer cells lacked NY-ESO-1 expression (von Boehmer et al., 2013), supporting the possibility that immunoediting occurs as a consequence of T cell immunity in human cancer patients. In addition, a case report described a melanoma being transferred to an immunosuppressed organ recipient from an organ donor that had been disease-free for over a decade (MacKie et al., 2003). This suggests that pressure from the organ donor's intact immune system was able to maintain the malignant cells in a state of equilibrium, while transfer of these dormant cancer cells to

the immunosuppressed recipient allowed the cancer cells to escape and grow into a clinically apparent lesion.

Together, this suggests that the adaptive immune system not only elicits a response against tumor cells, but also plays a critical role in regulating malignant transformation and cancer outgrowth. The tumor-promoting effects of chronic inflammation (discussed in chapter 1.6) and the effects of cancer immunoediting are dynamically interconnected processes that can co-exist within the same tumor model. Similar to the dual role of the immune system during cancer development, cytokines, such as INF-γ and tumor necrosis factor-α (TNF-α), can have either pro-oncogenic activity or induce antitumor immune responses, depending on cues from the TME (Schreiber et al., 2011). The discovery that the immune system not only recognizes and destroys malignantly transformed cells, but also edits the immunogenicity of cancer cells that progress, may help guide the development of novel immunotherapeutic approaches. To achieve clinical efficacy against cancer, immunotherapies have to overcome the plasticity of cells within the TME, to increase the quality and quantity of immune effector cells and eliminate cancer-induced immunosuppressive mechanisms. Multiple forms of immunotherapy, including combinatorial approaches, are currently being explored and will be discussed in detail in chapter 1.10.

1.8 Mechanisms of immune evasion in melanoma and MCC pathogenesis

Melanomas and MCCs employ several different mechanisms to evade tumor-specific immunity (discussed in chapter 1.7). For example, melanoma and MCC cells downregulate the expression of TAgs and MHC-1 molecules, both of which are critical for the

recognition by tumor-specific CTLs (Khong et al., 2004, Maeurer et al., 1996, Paulson et al., 2014, Schatton et al., 2010). As discussed, melanoma and MCC cells commonly mediate immunosuppression of the TME by recruiting and/or inducing Tregs and MDSCs, and increased frequencies of these tolerogenic cell subsets correlate with melanoma progression (Dowlatshahi et al., 2013, Jacobs et al., 2012, Jandus et al., 2008, Jordan et al., 2013, Vence et al., 2007, Weide et al., 2014). In addition, melanomas and MCCs commonly exploit immune checkpoints to escape immune-mediated rejection. Under physiologic conditions, immune checkpoints are crucial regulators of immune homeostasis, thereby inhibiting potentially pathogenic immune effector cell responses (Francisco et al., 2010). In response to prolonged antigen exposure, for example in the context of cancer, antigen-specific T cells upregulate immune inhibitory checkpoint receptors like PD-1. Various cancers, including melanoma and MCC, express PD-1 ligands, PD-L1 and PD-L2, in the tumor stroma to induce immune resistance by inhibiting T cell responses. Indeed, the frequency of melanoma-infiltrating T cells expressing the inhibitory checkpoint receptor PD-1 is significantly higher in metastatic melanoma lesions compared to normal tissue and blood from both patient-matched and healthy donors. Moreover, PD-1 expression by TILs versus circulating lymphocytes correlated with impaired effector functions and cytokine production in these studies, indicative of an exhausted T cell phenotype specific to the TME (Ahmadzadeh et al., 2009, Baitsch et al., 2011b). Consistently, PD-1 expression by lymphocytes in metastatic melanoma lesions is negatively correlated with survival (Kakavand et al., 2015). Similarly, MCC-infiltrating and circulating $CD8^+$ T cells express reduced levels of T cell activation markers, CD25 and CD69, and high levels of the PD-1 checkpoint receptor, particularly in patients with progressive lesions (Afanasiev et al., 2013, Dowlatshahi et al., 2013). Conversely, frequencies of PD-1-positive TILs were significantly decreased in MCC tumors that spontaneously regressed after biopsy, compared to MCCs that did not regress (Afanasiev et al., 2013, Dowlatshahi et al., 2013,

Fujimoto et al., 2015). In addition, cancer cells and TILs commonly express the PD-1 ligand, PD-L1, thereby further maintaining an immunosuppressive TME. And PD-L1 expression by the tumor and surrounding stroma has been linked to an unfavorable prognosis (Afanasiev et al., 2013, Dong et al., 2002b, Dowlatshahi et al., 2013, Herbst et al., 2014, Kakavand et al., 2015, Lipson et al., 2013, Massi et al., 2014).

In summary, these observations suggest that both melanoma and MCC are immunogenic cancers that nevertheless frequently evade antitumor immunity. The PD-1 pathway plays a critical role in maintaining an immunosuppressive TME in melanoma and MCC patients. Thus, cancer immunotherapies aimed at enhancing endogenous T cell responses to eradicate tumor cells may be particularly effective in generating durable responses in patients with melanoma and MCC.

1.9 The two-signal paradigm of T cell activation

Activation of T cells requires two distinct signals. Signal 1 occurs when antigenic peptide/MHC complexes bind to the TCR. A second, antigen-independent signal is mediated by costimulatory or coinhibitory checkpoint molecules, and integrates with the primary TCR-signal to regulate the extent and quality of T cell activation and clonal expansion (Figure 1) (Okazaki et al., 2013). Lack of a signal 2 induces a state of non-responsiveness in TCR-activated T cells termed anergy (Schwartz, 2003). Ligation of costimulatory receptors, such as CD28, CD40 ligand, glucocorticoid-induced tumor necrosis factor receptor-related protein (GITR), 4-1BB or OX40 on T cells enhances TCR signaling and promotes proliferation, metabolism, survival and production of immunostimulatory cytokines including interleukin-2 (IL-2) (Chen and Flies, 2013). Signaling through coinhibitory receptors, like CTLA-4, PD-1, TIM-3, and LAG-3, limits the expansion and effector functions of T cells, while modulating suppressive capacity of

Tregs, for example by outcompeting costimulatory signals, inactivating TCR-associated signaling mediators, or inducing immunosuppressive factors. These coinhibitory receptors have overlapping, as well as unique roles in T cell tolerance induction (Baumeister et al., 2016, Chen and Flies, 2013). T cell responses are tightly regulated by concurrent activation of multiple costimulatory and coinhibitory pathways, which can further be controlled by dynamic expression of respective ligands within various tissues. Under physiologic conditions, immune checkpoint proteins are critically important for sustained immune homeostasis. As discussed, cancer cells often exploit coinhibitory pathways to evade tumor-specific immune responses by expressing the ligands of these coinhibitory receptors. Thus, blockade of coinhibitory pathways to reactivate pre-existing antitumor immune responses has emerged as a promising target for cancer therapy, and will be discussed in chapters 1.10.4 and 1.10.5.

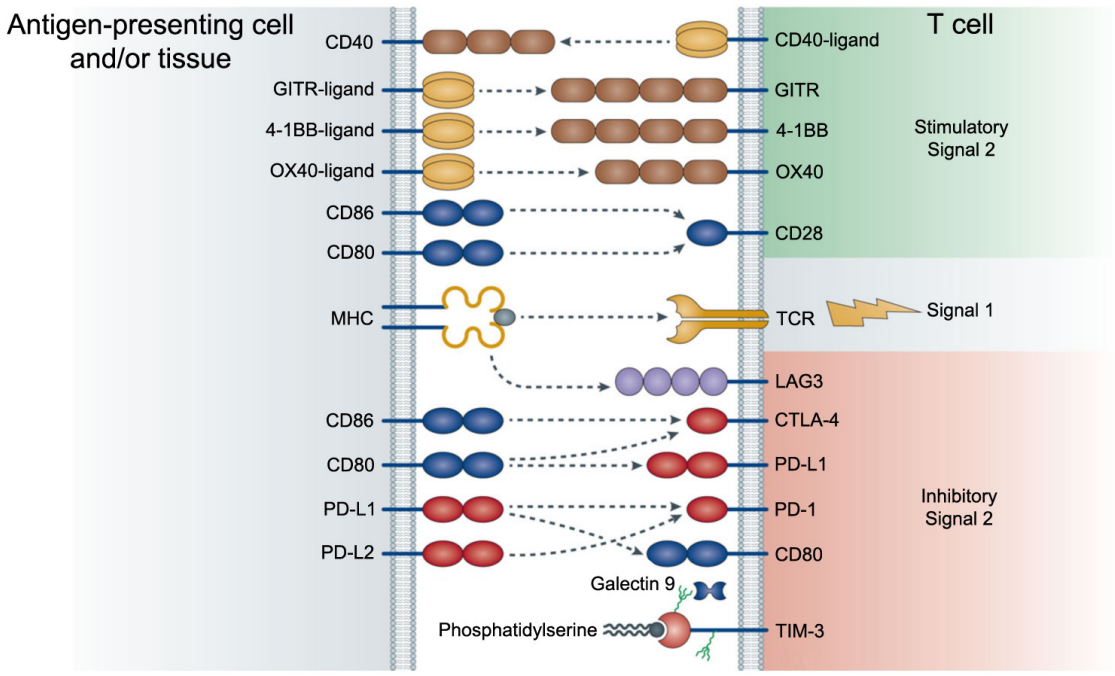

Figure 1. T cell function is regulated by costimulatory and coinhibitory signals. *Adapted from Mahoney et al., Nature Reviews Drug Discovery 14, 61-584 (2015)* (Mahoney et al., 2015). T cell activation requires two distinct signals. Signal 1 is mediated when the TCR binds a specific antigen/ MHC complex. Signal 2 is mediated via

costimulatory or coinhibitory interactions that are required to further regulate T cell function. Activation of costimulatory pathways, including CD28:CD80/CD86, CD40-ligand:CD40, GITR:GITR-ligand, 4-1BB:4-1BB-ligand, and OX-40:OX40-ligand promote T cell function. Signaling via coinhibitory pathways, such as LAG-3:MHC class II, CTLA-4:CD80/CD86, PD-1:PD-1-ligand 1(PD-L1)/-ligand 2 (PD-L2) and TIM-3:Galectin 9, on the other hand, induces T cell tolerance.

1.10 Cancer immunotherapy

Improved understanding of the mechanisms that govern the crosstalk between malignantly transformed cells and the patient's immune system, and its critical role in tumor progression, has paved the way for new therapeutic approaches. This chapter will focus on the use of proinflammatory cytokines, cancer vaccines, ACT and immune checkpoint inhibitors, which have proven successful therapeutic strategies in generating lasting responses in patients with a broad spectrum of tumors, including melanoma and MCC.

1.10.1 Immunostimulatory cytokines

The cytokine IL-2 is important for the activation, proliferation, and differentiation of immune cells, particularly $CD4^+$ and $CD8^+$ T cells (Boyman and Sprent, 2012). Early attempts to fuel patient's immune responses to eradicate tumors exploited this immunostimulatory capacity of IL-2. Although high-dose recombinant IL-2 therapy yielded tumor regression in less than 10% of patients with metastatic melanoma, responses were typically durable compared to chemo-, radiation-, or targeted therapy, which failed to improve long-term survival (Atkins et al., 1999, Rosenberg et al., 1998). This led to the FDA-approval of IL-2 immunotherapy for the treatment of metastatic melanoma in 1998. Interestingly, response to IL-2 therapy was associated with increased intratumoral

frequencies of both T cells and macrophages in melanoma patients (Rubin et al., 1989). The failure of IL-2 therapy to produce responses in the majority of patients may, at least in part, be due to the ability of IL-2 to potently induce the differentiation of $CD4^+$ T cells into tolerogenic $CD4^+CD25^{hi}FoxP3^+$ Tregs, in addition to other immunosuppressive mechanisms that are commonly active in the TME (Ahmadzadeh and Rosenberg, 2006, Shtivelman et al., 2014) (discussed in chapters 1.7 and 1.8). Although response rates to IL-2 therapy were low, these early studies serve as proof-of-principle to demonstrate that a patient's immune system can be manipulated to successfully eradicate established disease and prevent recurrence. A second immunostimulatory cytokine, interferon-alpha (IFN-α), was approved by the FDA as adjuvant treatment for patients with advanced melanoma. However, IFN-α therapy only improved relapse-free survival, but did not impact overall survival (Shtivelman et al., 2014). According to the Cancer Research Institute (CRI), two clinical trials aimed at assessing the efficacy of recombinant interleukin-12 and interleukin-15 in stimulating anti-tumor immunity are currently recruiting patients with advanced melanoma.

1.10.2 Cancer vaccines

Melanoma and MCC express a wide variety of TAgs that can be recognized by the immune system as foreign and trigger autologous antitumor immune responses. Thus, active immunization with distinct TAgs to stimulate immune responses against cancer cells presents an opportunity to develop new cancer immunotherapies. Cancer vaccines are frequently based on peptides derived from TAgs, or inactivated antigen-rich whole tumor cells that may be engineered to also express co-stimulatory receptors, and are commonly co-administered with adjuvants and immune-stimulatory cytokines (Engelstein et al., 2016, Ribas et al., 2003, Rosenberg et al., 2004). Another approach utilizes *ex vivo* peptide-

pulsed DCs to generate cancer antigen-specific cytotoxic T cell responses and eliminate established melanomas, taking advantage of DCs' ability to effectively migrate to lymphoid organs to prime and activate effector T cells (Ridgway, 2003, Rosenberg et al., 2004). Clinical trials have explored numerous vaccines strategies using different melanoma antigens or whole cell lysates as the peptide source, diverse immune stimulatory cytokines, DC subsets and maturation protocols, and viral systems, to treat patients with metastatic melanoma. However, the overall objective response rates (ORR) to cancer vaccines in melanoma patients was below 5%, independent of the peptides, cytokines, adjuvants, DCs or virus selected for the study (Rosenberg et al., 2004). Nonetheless, the CRI lists twelve currently ongoing clinical trials that test the efficacy of various vaccine strategies alone, or in combination with other immunotherapeutic regimens, in the treatment of patients with advanced melanoma. Recent studies have also assessed the efficacy of recombinant oncolytic viruses engineered to express TAgs and/or immunogenic cytokines to stimulate cellular immune responses against established melanomas (Rosenberg et al., 2004). For example, Talimogene Laherparepvec, a genetically modified herpes simplex virus type 1 that lyses cancer cells to release TAgs and also expresses GMC-SF to promote anti-tumor immune responses gained FDA approval for the treatment of advanced melanoma based on a phase 3 clinical trial that reported durable responses in 16% of patients compared to 2% among melanoma patients treated with GM-CSF alone (Andtbacka et al., 2015). Failure of cancer vaccines and oncolytic virus therapies to produce clinical benefits in the majority of patients has been attributed to their inability to (i) generate sufficient numbers of CTLs with a high avidity for the TAgs *in vivo*, (ii) traffic to and efficiently infiltrate the TME, and (iii) overcome the systemic immune suppression within the TME (Ribas et al., 2003, Rosenberg et al., 2004). In addition, the genetic instability of cancer cells coupled with the immune system's ability to create low immunogenic cancer cells that lack expression of distinct TAgs and MHC-1 molecules (discussed in chapter 1.7) may further explain why

cancer vaccine strategies are not successful in eradicating tumors in the majority of patients.

1.10.3 Adoptive T cell transfer

Adoptive transfer of *ex vivo* generated, expanded, and activated tumor-specific autologous T cells back into the patient is one strategy to overcome shortcomings of cancer vaccines. Adoptive T cell transfer (ACT) in combination with high dose IL-2 has been quite successful in achieving objective cancer regression in about 50% of lymphodepleted patients with metastatic melanoma, with durable complete responses observed in 20% of patients (Dudley et al., 2002, Rosenberg et al., 2011). T cells that are used for ACT therapy are typically generated from TILs or PBMCs of cancer patients *ex vivo* by first selecting clones with a high avidity for TAgs, then activating and expanding these cells *in vitro,* and depleting immunosuppressive Tregs. The final product is then re-infused into lymphodepleted patients (Dudley et al., 2002). Another approach utilizes tumor-reactive T cell populations engineered to express chimeric antigen receptors (CAR) that do not depend on MHC-mediated presentation of TAgs, a process often impaired in cancer cells, and clinical trials are currently underway (Kershaw et al., 2013).

However, manufacturing large numbers of T cells for ACT therapy is labor intensive and requires complex methodologies and highly specialized equipment. Moreover, to further improve upon the clinical efficacy of ACT, long-term engraftment of infused T cells has to be achieved, for example by transferring memory T cell populations, increased numbers of $CD8^+$ T cells, and/or younger cells with longer telomeres. In addition, transfer of $CD4^+$ Th1 and Th2 type T cells has resulted in encouraging anti-cancer effects in pre-clinical modes, however the potential use of $CD4^+$ T cell subsets and the effects of various cytokines secreted by these cells on cancer erradication in humans requires further scrutiny

(Braumuller et al., 2013, Busch et al., 2016, Lorvik et al., 2016, Rosenberg et al., 2004). Failure of *ex vivo* generated T cells to eradicate established tumors in all patients may be due to loss or mutation of the targeted TAgs and MHC-1 proteins, induction of an immunosuppressive TME (e.g. by recruiting and/or expanding tolerogenic Tregs and MDSCs), and activation of inhibitory immune checkpoint pathways. This has opened a new field for immunotherapies, including antibody-mediated blockade of inhibitory checkpoint receptors, agonistic Abs to activate costimulatory receptors, and agents that deplete or neutralize tolerogenic immune cells, and may thus work synergistically with ACT to improve its clinical efficacy.

1.10.4 Antibody-mediated inhibition of the immune checkpoint receptor CTLA-4

The CTLA-4 (CD152) receptor is expressed upon activation of native $CD4^+$ and $CD8^+$ T cells, and plays an important role in inducing T cell tolerance. In addition, CTLA-4 is constitutively expressed by $FoxP3^+$ Treg cells and controls their suppressive functions (Baumeister et al., 2016, Ott et al., 2013). CTLA-4 and its structural homolog, the costimulatory receptor CD28, share the same ligands B7-1 (CD80) and B7-2 (CD86), both of which are commonly expressed by antigen presenting cells (APCs) among other cells (Greenwald et al., 2005). CTLA-4 inhibits T cell functions by (i) binding the B7 ligands with a higher affinity than the costimulatory receptor CD28, (ii) recruiting phosphatases to its intracellular domain to inhibit TCR-mediated signaling, (iii) downmodulating the expression of B7 ligands on APCs, and (iv) inducing IDO secretion to indirectly impair T cell function (Baumeister et al., 2016, Ott et al., 2013). Because activation of CTLA-4 inhibits T effector cell functions while concurrently promoting maintenance and

immunosuppressive activity of Tregs, blockade of the CTLA-4 pathway emerged as a promising strategy for cancer treatment. In clinical trials for ipilimumab (Yervoy®), a fully humanized monoclonal Ab (mAb) that blocks CTLA-4, response rates averaged between 10 to 15% among patients with advanced melanoma (Hodi et al., 2010, Ott et al., 2013, Robert et al., 2011). Importantly, the majority of these responses to CTLA-4 blockade were durable and often resulted in complete regression (Schadendorf et al., 2015). Based on these studies, the anti-CTLA-4 Ab ipilimumab was the first immune checkpoint inhibitor to gain FDA approval for the treatment of metastatic melanoma in 2011. Because CTLA-4 plays a critical role in maintaining T cell tolerance, significant immune related adverse events (irAEs) were reported in approximately 60% of patients treated with ipilimumab. Both, the expression of immunogenic neoantigens by the tumor cells and irAEs correlated with clinical response in melanoma patients (Flaherty et al., 2012, Snyder et al., 2014b, Van Allen et al., 2015). Increased intratumoral frequencies of activated CTLs and decreased levels of Tregs were commonly found in post-treatment biopsies of residual disease (Hodi et al., 2008, Wang et al., 2012). Moreover, ipilimumab treatment induced TAg-specific cellular and humoral immunity in melanoma patients (Kitano et al., 2013, Weber et al., 2012). Together, this suggests that therapeutic CTLA-4 blockade works by re-activating and expanding endogenous tumor-reactive T cells. In addition, the therapeutic benefit of CTLA-4 blockade may also result from depleting Tregs via antibody-dependent cellular cytotoxicity (ADCC) (Baumeister et al., 2016, Peggs et al., 2009).

The clinical experience with CTLA-4 blockade has initiated a new era of cancer immunotherapy. The immune system is highly dynamic and not only recognizes a wide range of TAgs on highly heterogeneous cancer cell populations, but also adapts to target novel antigens on cancer cells as they acquire mutations. This plasticity of endogenous immune responses may explain why immune checkpoint blockade aimed at re-activating pre-existing endogenous T cell immunity can achieve durable responses, while tumors may

become more easily resistant to cancer vaccines and ACT strategies due to mutation of the targeted antigens. However, to date only a small subset of patients with advanced cancers respond to CTLA-4 inhibition, highlighting the need for novel immunotherapies to improve clinical efficacy.

Interestingly, studies have demonstrated that CTLA-4 is not only expressed by immune cells, but also by subpopulations of tumor cells in established cancer cell lines and patient-derived melanomas (Contardi et al., 2005, Shah et al., 2008). Activation of tumor cell-expressed CTLA-4 by recombinant B7 ligands induces cancer cell apoptosis *in vitro*, which can be reversed via Ab-mediated CTLA-4 blockade (Contardi et al., 2005). Thus, this finding suggests that therapeutic CTLA-4 blockade may also have pro-tumorigenic effects, by protecting cancer cells from apoptotic cell death.

1.10.5 Therapeutic blockade of the immune checkpoint receptor PD-1

PD-1 (CD279) is a coinhibitory receptor expressed by antigen-stimulated T cells and functions as a major negative regulator of T cell immunity, to control peripheral tissue tolerance and immune homeostasis (Okazaki et al., 2013). PD-1 has two known ligands, PD-L1 (B7-H1, also known as CD274) and PD-L2 (B7-DC, also known as CD273) (Freeman et al., 2000, Keir et al., 2008, Latchman et al., 2001). PD-L1 is widely expressed by hematopoietic and non-hematopoietic cells, including APCs, epithelial, stromal and cancer cells, and expression is stimulated by proinflammatory cytokines such as IFN-γ, TNF-α, and VEGF. Expression of PD-L2, on the other hand, is mainly restricted to APCs, including DCs, macrophages, and B cells, and is induced by proinflammatory cytokines such as IL-4 and GM-CSF (Baumeister et al., 2016, Francisco et al., 2010). Although the PD-1 receptor itself has no known enzymatic function, its intracellular domain contains an

immunoreceptor-tyrosine-based inhibitory motif (ITIM) and an immunoreceptor-tyrosine-based switch motif (ITSM) (Chemnitz et al., 2004). Engagement by either ligand, PD-L1 or PD-L2, crosslinks the PD-1 receptor with the TCR complex, which results in tyrosine phosphorylation of the ITIM and/or ITSM domains and recruitment of phosphatases SHP-1 and SHP-2 (Chemnitz et al., 2004, Okazaki et al., 2013). Subsequently, activated SHP-1 and/or SHP-2 enzymes dephosphorylate key signaling mediators downstream of the TCR complex, thereby inhibiting PI3K/AKT/mTOR and MAPK signaling pathways, expression of transcription factors, and IL-2 production, all of which are important for T cell activation, proliferation and effector functions (Okazaki et al., 2013, Patsoukis et al., 2012, Sheppard et al., 2004). In addition, the activated PD-1 receptor sequesters TCR signaling mediators (Chemnitz et al., 2004), induces expression of pro-apoptotic factors and alters T cell motility and metabolism (Baumeister et al., 2016). In summary, the PD-1 pathway impairs T cell activation and attenuates T cell effector functions and proliferation, thereby promoting T cell exhaustion (Baumeister et al., 2016, Wherry, 2011). Dynamic changes in the expression of PD-1 ligands by peripheral tissues, for example in response to proinflammatory cytokines, may further contribute to the fine-tuning of T cell functions to regulate peripheral tolerance and immune homeostasis.

PD-1 is also expressed by Tregs, and recent studies suggest that engagement by PD-L1 promotes the differentiation, maintenance and suppressive function of Tregs, thereby further inducing T cell tolerance (Francisco et al., 2009). B cells also express PD-1 upon antigen stimulation, and PD-1 signaling impairs humoral immunity by inhibiting B cell expansion, plasma cell differentiation, and B cell effector functions (Okazaki et al., 2013). NK cells express PD-1 in response to chronic inflammation, and PD-1 signaling has been shown to impair NK cell migration, cytokine secretion, and cytotoxic activity (Benson et al., 2010). An inflammatory milieu also triggers PD-1 expression by DCs, monocytes, and macrophages. PD-1 activation has been shown to suppress their capacity to present

antigen, shift the balance from proinflammatory to immunosuppressive cytokine secretion, induce apoptosis, and suppress phagocytic activity (Huang et al., 2009, Karyampudi et al., 2016, Park et al., 2014, Said et al., 2010, Zhang et al., 2011). Together, PD-1 expression by B cells and innate immune cells further inhibits T cell immunity. Although studies have mainly focused on the effects of PD-1 ligands as activators of PD-1 receptor signaling on T cells, recent findings suggest that receptor-ligand interactions can also be bidirectional (Azuma et al., 2008, Keir et al., 2008). Moreover, a recent study proposes that both PD-1 ligands, PD-L1 and PD-L2, may directly bind each other, adding to the complexity of PD-1 pathway interactions (Lee et al., 2016a). However, further work is needed to identify the molecular mechanisms underlying reverse signaling through PD-1 ligands and their effects on cellular functions.

The PD-1 pathway has been suggested to play a pivotal role in dampening antitumor immunity. T cells that are chronically stimulated by antigen, for example in the context of cancer, maintain high levels of PD-1 expression (Okazaki et al., 2013). The tumor and its surrounding stroma are commonly characterized by chronic inflammation, which also upregulates the expression of PD-1 by Tregs, B cells, NK cells, DCs, monocytes and macrophages, to further promote immune tolerance (Baumeister et al., 2016, Krempski et al., 2011, Okazaki et al., 2013). In addition, the proinflammatory milieu of the TME also upregulates the expression of PD-L1 and PD-L2 by tumor, immune, and stromal cells (Baumeister et al., 2016). Interactions between PD-1 and its ligands may attenuate antitumor immune responses to protect cancer cells from CTLs. In preclinical models, blockade of PD-1:PD-L1 interactions has been linked to increased proliferation, cytolytic activity, and secretion of proinflammatory cytokines by $CD8^+$ T cells, providing a rationale for evaluating the clinical activity of PD-1 pathway interference in cancer patients (Baumeister et al., 2016, Okazaki et al., 2013).

In recent clinical trials, antibody-based therapeutics targeting the PD-1 pathway have demonstrated unprecedented response rates and encouraging toxicity profiles in patients with advanced-stage cancers of various etiology, including melanoma and MCC (Ansell et al., 2015, Borghaei et al., 2015, Brahmer et al., 2015, Garon et al., 2015, Hamid et al., 2013, Kaufman et al., 2016, Larkin et al., 2015, Motzer et al., 2015, Nghiem, 2015, Pai et al., 2016, Postow et al., 2015a, Ribas et al., 2015, Robert et al., 2015a, Robert et al., 2015b, Rosenberg et al., 2016, Topalian et al., 2012b, Topalian et al., 2014, Weber et al., 2015, Wolchok et al., 2013). This has led to FDA approval of two monoclonal Abs that block PD-1, nivolumab (Opdivo®) for the treatment of metastatic melanoma in 2014, advanced non-small cell lung cancer (NSCLC) and renal cell carcinoma (RCC) in 2015, and Hodgkin Lymphoma in 2016, and pembrolizumab (Keytruda®) for the treatment of metastatic melanoma in 2014, advanced NSCLC in 2015, and metastatic head and neck squamous cell carcinoma in 2016. In addition, an Ab inhibiting PD-L1, atezolizumab (Tecentriq®), received FDA approval for the treatment of urothelial carcinoma in 2016.

An early clinical trial designed to evaluate the activity of the anti-PD-1 Ab, nivolumab, as a single agent reported ORR of 28% among patients with advanced melanoma. The majority of these responses were durable, and immune related toxicities were tolerable (Topalian et al., 2012b, Topalian et al., 2014). Another trial tested the clinical efficacy of nivolumab versus standard-of-care chemotherapy as an up-front therapeutic option for previously untreated melanoma patients without BRAF mutation. In this study, the ORR was 40% in patients treated with nivolumab versus 14% in patients that received chemotherapy. Importantly, nivolumab treatment resulted in significantly higher overall survival and fewer toxicities compared to chemotherapy (Robert et al., 2015a). A small phase 2 clinical trial tested the efficacy of the second anti-PD-1 monoclonal Ab, pembrolizumab, in previously untreated patients with metastatic MCC and reported responses in 62% among patients with MCPyV-positive tumors compared to 44%

in patients with virus-negative tumors, the majority of which were durable (Nghiem et al., 2016). Subsequent studies testing the efficacy of pembrolizumab for the treatment of advanced melanoma confirmed long-lasting clinical activity in 52% of responders. Interestingly, in this study no significant differences in response rates were observed in patients who had previously received ipilimumab treatment compared to those who had not (Hamid et al., 2013). To expand upon this finding, melanoma patients that were refractory to treatment with ipilimumab and, when BRAF V600E mutant-positive, resistant to BRAF or MEK inhibitors, were subsequently treated with anti-PD-1 Ab, which resulted in significantly increased progression-free survival (PFS), ORRs, and fewer toxicities compared to treatment with standard-of-care chemotherapy (Ribas et al., 2015, Weber et al., 2015). These studies established that PD-1 pathway blockade has a clinical benefit, even in patients with ipilimumab-refractory melanomas. Moreover, based on outcomes reported from these clinical trials, both anti-PD-1 Abs had significantly higher response rates and survival benefits and fewer irAE in patients with metastatic melanoma compared to CTLA-4 inhibitors (Hodi et al., 2010, Ott et al., 2013, Robert et al., 2011). These results were confirmed in a randomized clinical trial that directly compared the clinical efficacy of pembrolizumab to ipilimumab in patients with metastatic melanoma. The clinical activity and safety profile of anti-PD-1 Ab was superior compared to anti-CTLA-4 Ab, with ORR of 30% for pembrolizumab treatment versus 10% for ipilimumab treatment (Robert et al., 2015b). Another clinical trial determined a significantly prolonged median PFS in previously untreated patients with metastatic melanoma that received a combination of anti-PD1 plus anti-CTLA4 Ab (11.5 months), or anti-PD-1 Ab (6.9 months) versus anti-CTLA-4 Ab (2.9 months) alone (Larkin et al., 2015). Therapeutic inhibition of the PD-1 pathway using the monoclonal anti-PD-L1 Ab atezolizumab also yielded durable responses in 17% of patients with advanced melanoma (Brahmer et al., 2012). In another clinical trial, 32% of patients with chemotherapy-refractory MCC showed objective, durable

responses to PD-L1 blockade (Kaufman et al., 2016). The overall inferior clinical activity of anti-PD-L1 versus anti-PD-1 Abs may, at least in part, be due to the fact that PD-L1 inhibition does not block interactions between PD-1 and its second ligand, PD-L2.

Although PD-1 pathway inhibitors have yielded unprecedented response rates in patients with advanced cancers, the majority of melanoma patients still do not respond to therapy. The two coinhibitory pathways, CTLA-4 and PD-1, regulate different phases of T cell tolerance (Baumeister et al., 2016). In addition, blockade of CTLA-4 has been suggested to work by driving re-activated tumor-reactive T cells from secondary lymphoid organs to the TME while concurrently depleting $FoxP3^+$ Tregs, whereas PD-1 blockade is thought to function by restoring T effector cell functions within peripheral tissue, including in the TME (Baumeister et al., 2016, Okazaki et al., 2013). Combination of PD-1- and CTLA-4-targeted therapies was therefore hypothesized to act synergistically to improve outcomes. Indeed, a clinical trial that evaluated the combination of nivolumab with ipilimumab in patients with advanced melanoma yielded ORR in 53% in patients with advanced melanoma (Wolchok et al., 2013). In a second study, in which previously untreated melanoma patients received ipilimumab either in combination with nivolumab or placebo, ORRs were 61% among patients that received both ipilimumab and nivolumab versus 11% in the group that received ipilimumab and placebo, further demonstrating the superior clinical efficacy of combinatorial treatment (Postow et al., 2015b). Importantly, both studies reported long-lasting clinical activity and acceptable levels of adverse events.

Lastly, a retrospective review of the clinical activity of PD-1 pathway blockade in patients with advanced melanoma reported response rates of 33% among individuals with pre-existing autoimmune disorders and 40% among patients that suffered major irAE requiring systemic immunosuppresion after treatment with ipilimumab (Menzies et al., 2016).

The clinical success of combining anti-PD-1 and anti-CTLA-4 blocking Abs to treat patients with metastatic melanoma has paved the way for combinatorial approaches targeting additional coinhibitory or costimulatory pathways. Improved understanding of the temporal and spatial expression of inhibitory and stimulatory co-receptors and ligands by immune cells and the TME, and of their unique roles in regulating the cytotoxic capacity of tumor-reactive T cells, has provided a strong foundation to explore combinations of additional immune checkpoint modulators in cancer patients. For example, T cells in the TME also express the coinhibitory receptors TIM-3 and LAG-3, and expression levels have been linked to functional unresponsiveness of CTLs, suggesting that respective blocking Abs may be effective in re-activating antitumor immunity (Baumeister et al., 2016, Sakuishi et al., 2010). In addition, agonistic Abs capable of activating costimulatory receptors, including GITR, 4-1BB, CD40, and OX40, represent another approach to re-activate cancer-specific immunity and eliminate cancer cells (Mahoney et al., 2015). According to the CRI, over 20 clinical trials are currently testing the efficacy of PD-1/PD-L1 checkpoint inhibitors alone, or in combination with Abs targeting additional coinhibitory or costimulatory receptors, as outlined above, in patients with advanced melanoma.

Combination of immune checkpoint inhibitors with other cancer immunotherapies that either unspecifically activate immunity, such as immunostimulatory cytokines and oncolytic viruses, or therapies that generate tumor specific T cell responses, such as cancer vaccines and ACT, may also work synergistically to produce effective antitumor immunity in cancer patients. Moreover, studies suggest that cytotoxic chemo- and radiation therapies promote the release of immunostimulatory factors and TAgs by inducing cancer cell apoptosis, thereby inducing a proinflammatory milieu that promotes tumor-specific immunity. Various chemotherapies also decrease the frequencies of tolerogenic Tregs and MDSC populations directly without affecting T effector cell functions, thereby altering the

immunosuppressive TME (Eriksson et al., 2016, Mahoney et al., 2015). Hence, chemotherapy may synergize with immune checkpoint blockade to improve clinical responses in cancer patients. Finally, treatment of BRAF V600E mutant melanomas with BRAF inhibitors has been associated with increased expression of melanoma antigens and intratumoral $CD8^+$ T cell infiltration, which was reversed in progressive lesions (Cooper et al., 2014, Frederick et al., 2013). In addition, resistance to BRAF inhibitors has also been linked to upregulation of the immunosuppressive PD-1 ligand, PD-L1, by melanoma cells (Frederick et al., 2013, Jiang et al., 2013a, Mahoney et al., 2015), providing a clear rationale for combining BRAF inhibition with anti-PD-1 Ab treatment.

1.10.6 Biomarkers predicting clinical responses to PD-1 checkpoint blockade

Recent studies have been geared towards elucidating the molecular and cellular networks that regulate tumor immune escape, to understand the mechanisms that underlie effective PD-1 therapy. These efforts have identified a variety of tumor- and microenvironment-specific alterations as well as immune modulators that may function as biomarkers to reliably predict responses to PD-1 therapy in individual cancer patients.

Initial studies suggested that PD-L1 expression by tumor cells and TILs may predict clinical responses to PD-1 pathway interference (Herbst et al., 2014, Postow et al., 2015b, Taube et al., 2014, Topalian et al., 2012b, Tumeh et al., 2014), consistent with the predicted mechanism of action. However, recent clinical trials did not observe significant differences in response rates to PD-1 pathway inhibitors between melanoma patients whose pre-treatment tumors were defined as PD-L1-positive versus PD-L1-negative (Hugo et al., 2016, Kakavand et al., 2015, Larkin et al., 2015, Postow et al., 2015b). In these

correlative studies of clinical trial samples, PD-L1 expression by tumor cells and TILs was analyzed in patient biopsies using immunohistochemical (IHC) analysis, and inconsistencies may be assay-related, as IHC-methodologies, Abs for PD-L1 detection, and thresholds for assaying PD-L1 positivity varied between studies. PD-L1 expression by tumor cells and cells of the TME is highly dynamic and can fluctuate over the course of the disease and in response to changes in the TME resulting from inflammatory mediators, modulation of glycosylation and/or ubiquitination pathways, as well as previous treatment regimens (Fusi et al., 2015, Li et al., 2016, Schalper et al., 2016). These discrepancies between PD-L1 expression and clinical responses caution against the use of tumor cell- or TIL-expressed PD-L1 as a biomarker to select patients for treatment and highlight the need for additional research (Kakavand et al., 2015).

Studies suggest that effective PD-1 blockade requires the presence of pre-existing tumor-reactive CTLs in the TME, that are functionally exhausted due to PD-1 pathway activation (Tumeh et al., 2014). Hence, the status of tumor-infiltrating immune cells, particularly $CD8^+$ CTLs, may be associated with responses to therapeutic PD-1 Abs. For example, increased density and proliferation of intra-tumoral $CD8^+$ T cells and clonally expanded TCR repertoires in pretreatment biopsies were associated with response to therapy (Tumeh et al., 2014). Moreover, expression of Th1 cell cytokines (e.g. IFN-γ), and markers of an inhibitory TME, including CTLA-4 and PD-1, in baseline tumor biospecimens may be linked to positive outcomes (Herbst et al., 2014, Postow et al., 2015b, Tumeh et al., 2014). Emerging evidence also suggests that transcriptional analysis of tumor biopsies to assess the mutational load, expression of immunogenic neoantigen transcripts or inflammatory gene signatures may be of predictive value (Gubin et al., 2014, Johnson et al., 2016b, Rizvi et al., 2015, Yadav et al., 2014). However, additional studies with larger patient cohorts are required to validate the reliability of these emerging biomarkers, since patients whose tumors do not express the aforementioned markers can

still respond to therapeutic PD-1 Abs. Biomarkers based on immune status of TILs and gene profiling often rely on the combination of markers and highly specialized sequencing and bioinformatics methodologies to predict responses to PD-1 therapy. Because the majority of patients currently do not respond to PD-1 pathway blockade, novel biomarkers that reliably and independently allow for treatment selection of cancer patients are urgently needed.

2 Rationale and specific aims of the thesis

Dr. Markus Frank and Dr.Tobias Schatton previously demonstrated that PD-1 is not only expressed by immune cells, but also by subpopulations of normal skin cells (Schatton et al., 2015) and tumorigenic melanoma cells (Schatton et al., 2010). Specifically, $ABCB5^+$ dermal cells inhibit T cell activation and maintain Tregs, at least in part, via dermal cell-expressed PD-1 (Schatton et al., 2015). In addition, PD-1-expressing $ABCB5^+$ MMICs attenuate T effector cell functions and induce Tregs (Schatton et al., 2010). Moreover, isolated $PD\text{-}1^+$ melanoma cell subsets demonstrated significantly increased tumorigenicity compared to $PD\text{-}1^-$ tumor cells in immunocompromised mice that lack adaptive immunity (Schatton et al., 2010). Together, these findings raise the possibility that melanoma-expressed PD-1 may both suppress tumor-specific T cell immunity and promote tumor growth via immune-independent mechanisms.

While the presence of neo-antigens and an immune-active TME are associated with favorable outcomes in melanoma patients treated with either PD-1- (Gubin et al., 2014, Rizvi et al., 2015, Yadav et al., 2014) or CTLA-4-directed checkpoint blockade (Snyder et al., 2014a), current evidence suggests that PD-1 inhibitors produce greater anticancer activity and fewer irAE compared to the anti-CTLA-4 Ab ipilimumab (Larkin et al., 2015, Postow et al., 2015a, Robert et al., 2015b). Moreover, PD-1 pathway interference also

produces meaningful clinical responses in melanoma patients that do not benefit from anti-CTLA-4 therapy (Hamid et al., 2013, Menzies et al., 2016, Ribas et al., 2015, Weber et al., 2013). Finally, PD-1 pathway blockade has also yielded durable clinical responses in patients with lesser immunogenic cancers that do not typically respond to conventional immunotherapies (Borghaei et al., 2015, Herbst et al., 2014, Topalian et al., 2012b). Together, these observations raise the possibility that anti-PD-1 therapy may also inhibit complementary, pro-tumorigenic mechanisms, in addition to re-activating T cell specific antitumor immunity, thereby contributing to its superior clinical efficacy compared to CTLA-4 blockade.

Therefore, it was hypothesized that cancer cell-expressed PD-1 serves as a protumorigenic mechanism, even in the absence of immunity. The following specific aims were addressed in the thesis in order to test this hypothesis:

Aim 1: To characterize the expression of the PD-1 receptor by melanoma and MCC cells in established cell lines, experimental tumor xenografts and patient biopsies.

Aim 2: To determine the effects of melanoma-expressed PD-1 on antitumor immunity. Particularly, to define the cellular and molecular mechanisms that melanoma-PD-1 utilizes to regulate T cell functions.

Aim 3: To dissect tumor cell-intrinsic protumorigenic functions of melanoma- and MCC-expressed PD-1, including in the absence of adaptive immunity. Specifically, cancer cell-PD-1 was hypothesized to drive tumor growth and activate oncogenic MAPK and/or PI3K/AKT/mTOR signaling pathways that are critically important for melanoma and MCC survival and proliferation (Flaherty et al., 2012, Nardi et al., 2012, Thakuria et al., 2014). In support of this possibility, T cell-expressed PD-1 has been previously demonstrated to control MAPK and PI3K/AKT/mTOR signaling pathways downstream of the TCR (Francisco et al., 2010).

Aim 4: To evaluate the significance of melanoma-expressed PD-1, its interaction partners

and downstream mediators as potential biomarkers of response to PD-1 therapy. Because the majority of cancer patients currently do not benefit from PD-1 inhibition, biomarkers for predicting responses are urgently needed to guide treatment selection and improve clinical outcomes.

Aim 5: To dissect the role of ABCB5 in mediating resistance to the standard-of-care chemotherapic agents, carboplatin and etoposide, in MCC. ABCB5 mediates chemotherapeutic refractoriness, including to platinum-based drugs, in melanoma (Elliott and Al-Hajj, 2009, Frank et al., 2005, Huang et al., 2004), and other solid cancers (Cheung et al., 2011a, Cheung et al., 2011b, Wang and Teng, 2016, Wilson et al., 2011). Similar to melanoma, MCC is highly aggressive and frequently develops resistance to chemotherapy (Serrone and Hersey, 1999, Thakuria et al., 2014), suggesting that ABCB5 may also confer resistance to carboplatin and etoposide in MCC.

As of yet, the role of cancer cell-expressed PD-1 in tumor development and growth is poorly characterized. Dissecting the molecular and cellular mechanisms underlying the immunomodulatory and protumorigenic effects of cancer cell-expressed PD-1 may not only further current understanding of melanoma and MCC tumorigenesis, but also identify potential novel targets and strategies that could improve the clinical efficacy of anti-PD-1 therapies. In addition, the herein presented research aims to establish MCC-expressed ABCB5 as a novel chemoresistance mediator that may be targeted to enhance chemotherapy-induced MCC killing to improve patient outcomes.

3 Materials and methods

3.1 Cell culture and cell isolation techniques

3.1.1 Cultivation of melanoma and Merkel cell carcinoma cell lines

Authenticated human A375, C8161, G3361, FEMX, LOX, MeWo, SK-MEL-28 and UACC-257 and murine B16-F0 and B16-F10 melanoma cell lines were obtained from the American Type Culture Collection (ATCC, Manassas, VA, USA), or were provided by Dr. E. Frei (Dana-Farber Cancer Institute, Boston, MA, USA), Dr. M. Hendrix (Children's Memorial Research Center, Chicago, IL, USA), or Dr. U. Schumacher (University Hospital Hamburg-Eppendorf, Hamburg, Germany). Cells were cultured in RPMI-1640 medium supplemented with 10% (v/v) heat inactivated fetal bovine serum (Hi-FBS) and 1% (v/v) penicillin/streptomycin (Gibco, Waltham, MA, USA) in tissue culture treated flasks (Falcon®, Fisher Scientific, Waltham, MA, USA) at 37 °C and 5% CO_2 in a humidified incubator using aseptic techniques, as described previously (Schatton et al., 2008). Adherent melanoma cells were subcultured every 2-4 days before reaching confluence to maintain exponential growth. To detach melanoma cells from the surface of the culture vessels, spent media was removed, cells were washed with calcium- and magnesium-free phosphate-buffered saline (PBS, Gibco) and incubated in Versene solution (Gibco) for 10-15 min at 37 °C and 5% CO_2. Once the cells were detached, Versene solution was neutralized by addition of complete growth medium, and 1/4 to 1/10 of the cell suspension was transferred into a new culture flask containing fresh growth medium.

Authenticated human MKL-1, MKL-2, MS-1 and WaGa MCC cell lines were obtained from Dr. James DeCaprio (Dana-Farber Cancer Institute, Boston, MA, USA) (Rodig et al., 2012b), and cells grew in suspension in RPMI-1640 medium supplemented with 20% (v/v) Hi-FBS and 1% (v/v) penicillin/streptomycin (Gibco) in tissue culture

treated flasks as described above. MCC cultures were subcultured every 4-6 days before reaching confluence by transferring 1/2 to 1/6 of the cell suspension to a new culture flask containing fresh growth medium, thereby allowing for exponential growth.

For cryopreservation, cells were harvested and counted (described below), resuspended in freezing medium containing 10% of the cryoprotective agent dimethylsulfoxide (DMSO, Fisher Scientific) in Hi-FBS at a density of 5×10^5-2×10^6 cells/mL, and subsequently aliquoted into cryogenic vials (Fisher Scientific). Cryogenic vials were then placed into isopropanol containing freezing containers, placed at -80 °C overnight, before transferring frozen cells to liquid nitrogen tanks for long-term storage. To recover cryopreserved cells, vials were thawed quickly in a 37 °C water bath, cells were washed in 10 mL growth media to remove DMSO, transferred to a tissue culture flask containing fresh growth medium and placed in a 37 °C incubator as described above.

3.1.2 Determination of cell numbers

Numbers of viable cells were determined using an Improved Neubauer hemocytometer (Reichert, Buffalo, NY, USA) and the trypan blue exclusion assay. Specifically, cell suspensions were mixed with 0.4% trypan blue solution (Gibco), and loaded into the hemocytometer chamber. Live (unstained) and dead (blue) cells were counted manually using a light microscope (ECLIPSE T*i*-S, Nikon, Melville, NY, USA) and cell numbers were calculated as follows:

$$Total\ cell\ no. = \frac{No.of\ cells\ counted}{No.of\ quadrants\ counted} \times Sample\ Vol. \times Dil.factor \times 10\text{^}4$$

To enumerate live and dead cells using an automated cell counter, cell suspensions were thoroughly mixed with 1 volume of the dual-fluorescence ViaStain™ AOPI staining

solution (Nexcelom Bioscience, Lawrence, MA, USA) containing the green-fluorescent nucleic acid stain acridine orange (AO), and the red-fluorescent nucleic acid stain propidium iodide (PI). While AO is permeable to both live and dead cells, PI can only enter dead cells with compromised membranes. When both dyes are present in a nucleus, the PI causes a reduction in the AO fluorescence by fluorescence resonance energy transfer (FRET), which results in live nucleated cells staining green, while dead nucleated cells fluoresce red. Stained samples were loaded into a disposable Cellometer Imaging chamber (Nexcelom Bioscience), and cells were automatically counted on brightfield and combined fluorescent images based on cell size, shape and fluorescent signal using the Cellometer® Auto-2000 (Nexcelom Bioscience).

3.1.3 Isolation of tumor cells from patient biopsies and tumor xenografts

Single cell suspensions were generated from clinical melanoma samples (n = 8 patients) that were obtained in accordance with the Institutional Review Boards (IRBs) of Partners Health Care Research Management, the Dana-Farber Cancer Institute, and the University of Bern, Switzerland, upon surgical dissection of tumors from patients, as described (Schatton et al., 2008). Informed consent was obtained from all subjects. Briefly, each tumor specimen was cut into small pieces using a surgical scalpel, and tissue fragments were incubated for 2-4 hours in a shaking incubator at 37 °C and 200 rpm in digestion buffer containing 5mg/ml collagenase type IV (Worthington Biochemical Corp., Lakewood, NJ, USA) in PBS with calcium and magnesium chloride (Gibco) to generate single cell suspensions. Next, samples were filtered through a cell strainer with a 70 μm nylon mesh (Fisher Scientific) to dissociate and remove the remaining cellular aggregates. Cells were washed twice with calcium- and magnesium-free PBS to inactivate and remove the collagenase. Upon determination of the total number of viable cells, tumor single cell

suspensions were subjected to flow cytometric analysis and xenotransplantation to immunodeficient mice (see below).

3.1.4 Isolation of human peripheral blood mononuclear cells

Human peripheral blood mononuclear cells (PBMCs) were isolated from whole blood samples by Ficoll-Paque density gradient centrifugation, as described (Schatton et al., 2010). Briefly, whole blood was collected in sealed glass tubes containing the anti-coagulant sodium citrate (BD Biosciences, San Jose, CA, USA), transferred to a 50 mL polystyrene centrifuge tube (Falcon®, Fisher Scientific) and diluted with 1 volume of calcium- and magnesium-free PBS (Gibco). Ficoll (GE Healthcare, Sigma-Aldrich, St. Louis, MO, USA) was added to a fresh 50 mL tube, carefully overlaid with 1 volume of diluted blood and centrifuged at 400×g for 30 min at room temperature with the brake-mechanism turned off. Next, lymphocytes were collected from the plasma-Ficoll interface, transferred to a fresh 50 mL tube, and washed twice with PBS. To lyse residual erythrocytes, cells were incubated in 1-3 mL of ACK lysing buffer (Lonza, Walkersville, MD, USA) for 3 min at room temperature, before the reaction was stopped by addition of 9 mL media. Cells were washed in PBS, filtered through a 70 μm nylon mesh cell strainer, counted and subsequently subjected to RNA extraction or protein lysis for further analysis (see below).

3.1.5 Isolation of tumor-infiltrating lymphocytes from syngeneic B16 melanoma grafts

Tumor infiltrating lymphocytes (TILs) were isolated from B16 melanoma grafts 14 days post cancer cell inoculation (see below) by density gradient centrifugation. Briefly, viable tumor tissue was excised using a surgical scalpel, and mechanically disaggregated into a single cell suspension by mincing and serial filtration through a 70 μm nylon mesh cell strainer (Fisher Scientific) placed on a 50 mL polystyrene centrifuge tube (Falcon®, Fisher Scientific) to generate single cell suspensions. Cells were washed twice with ice cold PBS (Gibco), resuspended in 4 mL of 40% Percoll solution (GE Healthcare), gently underlaid with 4 mL of 70% Percoll solution and centrifuged at 325×g for 20 min at room temperature with the brake-mechanism turned off. Next, cells were collected from the interface and washed in RPMI-1640 medium supplemented with 10% (v/v) Hi-FBS and 1% (v/v) penicillin/streptomycin (Gibco). To lyse residual erythrocytes, cells were incubated in 1 mL of ACK lysing buffer (Lonza) for 3 min at room temperature, before the reaction was stopped by addition of 9 mL media. Cells were washed in PBS, filtered through a 70 μm nylon mesh cell strainer, counted and subsequently subjected to flow cytometric analysis (see below).

3.1.6 Isolation of lymphocytes from murine tumor-draining lymph nodes and spleens

To isolate murine lymphocytes from the spleens and tumor-draining lymph nodes, mice were euthanized, spleens and lymph nodes dissected and transferred to petri dishes containing RPMI-1640 medium supplemented with 10% (v/v) Hi-FBS and 1% (v/v)

penicillin/streptomycin (Gibco) and placed on ice. Next, tissues were mechanically disaggregated into a single cell suspension by mincing and serial filtration through a 70 µm nylon mesh cell strainer (Fisher Scientific) placed on a 50 mL polystyrene centrifuge tube (Falcon®, Fisher Scientific), and washed with PBS. To lyse the residual erythrocytes in cell preparations isolated from spleens, samples were incubated in 2 mL of ACK lysing buffer (Lonza) for 3 min at room temperature, before the reaction was stopped by addition of 9 mL media. Splenic and lymph node-derived cells were washed in PBS, counted and subsequently subjected to RNA extraction, protein lysis or flow cytometric analysis (see below).

3.1.7 Generation of drug-resistant MCC cells

To render MCC cells drug resistant *in vitro*, 1×10^6 wildtype cells were seeded in T25 tissue culture flasks (Falcon®, Fisher Scientific) and incubated in MCC growth media containing either 5 µM carboplatin or 100 nM etoposide (Sigma-Aldrich). Once per week, cells were harvested, spent media was removed, and cell viability was assessed using the trypan blue exclusion assay as described. Next, cells were suspended in fresh MCC growth media containing either equal or up to four times higher doses of carboplatin or etoposide. Drug concentrations were chosen per cell line based on the calculated cell viability post drug exposure. Over the course of 2 months, carboplatin doses were increased up to 150 µM and etoposide doses up to 3 µM, respectively. Resistant cells were maintained *in vitro*, and new growth media containing fresh drugs was added every 7 days as described. Cells were subjected to ABCB1, ABCB5, ABCC3 and ABCG2 mRNA expression analysis, flow-cytometric viability and ABCB5 expression analysis and proliferation assays (see below). For short-term exposure of MCC cells to cytotoxic concentrations of carboplatin or

etoposide, 1×10^6 wildtype cells were seeded in T25 flasks and incubated in MCC growth media containing either 250 μM carboplatin or 5 μM etoposide for 72 hours, after which the cells were analyzed for viability and ABCB5 surface expression by dual-color flow cytometry (described below).

3.1.8 Three-dimensional melanoma cultures

Melanoma tumor sphere cultures were established as described previously (Aceto et al., 2012, Civenni et al., 2011), in standard culture medium, as above, without exogenous growth factors. Briefly, native, PD-1 (PDCD1/Pdcd1) knockdown (KD), wildtype or mutant PDCD1/Pdcd1-overexpressing (OE) murine B16, human A375, C8161, or G3361 melanoma cell line variants were plated in the presence or absence of monocolonal anti-mouse PD-1 (clone 29F.1A12, Biolegend, San Diego, CA, USA), anti-human PD-1 (clone J116, BioXCell, West Lebanon, NH, USA), or isotype control Abs (clones RTK2758, Biolegend or MOPC-21, BioXCell) (50μg/ml, respectively), recombinant mouse PD-L1 Ig, human PD-L1 Ig (R&D Systems, Minneapolis, MN, USA), or control Ig (R&D Systems and Bethyl Laboratories, Montgomery, TX, USA) (5μg/ml, respectively) in 6-well ultra-low attachment plates (Corning Costar, Fisher Scientific) at a density of 2,000-10,000 viable cells per well in culture medium, supplemented with 0.5% (wt/v) methyl cellulose (Sigma-Aldrich), and cultured for 7-14 days at 37 °C and 5% CO_2. To ensure plating of single, viable cells, melanoma cultures were harvested with Versene solution (Gibco) as above, passed through a 40 μm nylon mesh cell strainer (Fisher Scientific), followed by AO/PI (Nexcelom) counterstaining and automated live/dead nucleated cell counting on a Cellometer Auto 2000 cell viability counter (Nexcelom). Tumor spheroid cultures were fed every three days with 0.5 ml of fresh medium with or without anti-PD-1 or isotype control mAbs, recombinant PD-L1 or control Ig in concentrations as above.

Spheres were stained with 180 µl of 0.4% (wt/v) p-iodonitrotetrazolium violet solution (Sigma-Aldrich) overnight at 37 °C, 5% CO2, and photographed using a Canon T1i camera (Canon USA Inc., Melville, NY, USA) and a 50mm/f2.8 macro lens (Sigma, Ronkonkoma, NY, USA). Subsequently, numbers of tumor spheres per well from n≥3 independent experiments were quantified digitally using the ImageJ software (National Institutes of Health, Bethesda, Maryland, USA).

3.1.9 MTT cytotoxicity and proliferation assays

To confirm the preferential chemosensitivity of wildtype versus drug-resistant MCC lines, and to determine the effects of ABCB5 mAb blockade on carboplatin- or etoposide-induced cell killing, MCC cells were seeded at 5×10^4 cells per well in 100 µL growth medium in round-bottomed 96-well plates (6 replicate points) and exposed to a range of concentrations of carboplatin (0.06-32 µmol/L) or etoposide (1-2500 nmol/L) in the presence or absence of anti-ABCB5 mAb (3C2-1D12, kindly provided by Dr. M. Frank) (Frank et al., 2003) or isotype control mAb (MOPC-21, BioXCell) (20 µg/mL, respectively), and cells were cultured for 7 days at 37 °C and 5% CO_2. *In vitro* growth kinetics of cells were assayed using the TACS 3-(4,5-dimethylthiazol-2-yl)-2,5-diphenyltetrazolium bromide (MTT) cell proliferation assay kit (Trevigen, Gaithersburg, MD, USA) according to the manufacturer's protocol. Briefly, 10 µL of MTT reagent was added to each well, and cells were incubated for 4 hours at 37 °C to allow for intracellular reduction of the soluble yellow MTT reagent to an insoluble purple formazan dye. Subsequently, 90 µL of MTT detergent was added to each well, incubated overnight at 37 °C to lyse the cells and solubilize the formazan precipitate prior to spectrophotometric quantification of the reduced MTT reagent at a wavelength of 595 nm on a Model 680 microplate reader (Bio-Rad, Hercules, CA, USA) at time t_0 (immediately prior to drug

exposure) and at t_7 (after 7-day exposure). Surviving cell fractions were determined from t_7/t_0 absorbance ratios with blanks subtracted. The concentration of drug resulting in 50% cell death (LD50) was calculated using the CalcuSyn software (version 2.1, Biosoft, Cambridge, UK).

3.2 Molecular biology methods

3.2.1 RNA extraction

Total ribonucleic acid (RNA) was isolated from established native and ABCB5-sorted human and murine melanoma and MCC cell lines, PD-1 KD, wildtype or mutant PD-1 OE melanoma cell lines, carboplatin- and etoposide-resistant MCC cell lines, patient-derived clinical MCCs, human melanoma and MCC xenografts, murine melanomas, healthy human skin, human PBMCs and murine spleens using the RNeasy® Plus Mini Kit (Qiagen, Hilden, Germany), following the manufacturer's protocol. Briefly, for total RNA purification from single cell suspensions, cells were washed twice with ice-cold PBS and lysed by addition of RLT buffer containing chaotrophic salts like guanidine-thiocyanate, detergents and 1% (v/v) of the reducing agent β-mercaptoethanol to ensure disruption of cell membranes, linearization of nucleic acids and destabilization of RNAses. To isolate total RNA from fresh tissues, up to 30mg of samples were directly placed in RLT buffer containing β-mercaptoethanol as above and disrupted manually using a rotor-stator homogenizer (Tissue Ruptor, Qiagen). Subsequently, lysed cells and tissues were transferred to a QIAshredder spin column (Qiagen) to allow for complete homogenization of the sample, before applying it to a gDNA eliminator column (Qiagen) for removal of genomic deoxyribonucleic acid (DNA) contamination. Next, 1 volume of 70% ethanol was added to the lysate to ensure binding of the RNA to the silica membrane of the RNeasy

spin column. To remove residual salt, protein and polysaccharide impurities, membranes were washed with buffer RW1, followed by two consecutive washes with the ethanol-containing buffer RPE. Finally, upon thorough centrifugation of the column to remove residual ethanol and dry the membrane, RNA was rehydrated by addition of RNase-free water (Ambion®, Fisher Scientific), and eluated into RNase-free microcentrifuge tubes. The purified total RNA was quantified by spectrophotometric analysis prior to cDNA synthesis (see below). RNA derived from formalin-fixed, paraffin-embedded clinical MCC biospecimens was provided by the Broad Institute (Cambridge, MA, USA) upon patient consent, and in accordance with IRBs of the Dana-Farber Cancer Institute (Boston, MA, USA).

3.2.2 Spectrophotometric measurement of nucleic acid concentration

Absorbance measurements at 260 nm were used to calculate the concentration of nucleic acid preparations using the Beer-Lambert law, which relates absorbance to concentration using the following equation:

$$Nucleic\ Acid\ Conc. = \frac{A260}{Pathlength} \times Standard\ Coefficient \times Sample\ Dilution$$

with 1 cm pathlength standard coefficients of 50 µg/mL for double stranded DNA, 40 µg/mL for single stranded RNA, and 33 µg/mL for single stranded DNA. UV absorbance measured at 280 nm and 230 nm was used to estimate purities of nucleic acid preparations. Proteins containing aromatic acids have an absorbance peak at 280 nm, while carbohydrates, phenol and guanidine contaminants have a characteristic absorbance at 230 nm. Ratios of absorbance at these wavelengths were used as a measure of purity, with A260/A280 absorption ratios between 1.8 and 2.0, and A260/A230 absorption ratios between 2.0-2.2 being generally accepted as pure DNA and RNA, respectively. All nucleic

acid concentration and purity measurements were performed on a BioDrop μLITE spectrophotometer (BioDrop Ltd, Cambridge, UK).

3.2.3 Reverse transcriptase-polymerase chain reaction

Reverse Transcriptase-Polymerase Chain Reactions (RT-PCRs, also referred to as cDNA synthesis reactions) from purified total RNA were carried out using the Superscript® III First-Strand Synthesis System for RT-PCR, the SuperScript VILO cDNA Synthesis Kit (Invitrogen, Carlsbad, CA, USA) or the Advantaged RT-for-PCR Kit (Clontech, Mountainview, CA, USA) as per manufacturer's instructions. Briefly, for cDNA synthesis using the Superscript® III First-Strand Synthesis System for RT-PCR, up to 5μg of total RNA, 0.5μL of 25μM of Oligo(dT) and random hexamer primers each, 1μL of dNTPs and DEPC-treated water were combined in a total volume of 10μL, incubated at 65 °C for 5 min to denature the RNA and placed on ice for 1 min. Thereafter, 10μL of the cDNA Synthesis Mix containing 2μL of the 10× reaction buffer RT, 4 μL of 25mM magnesium chloride ($MgCl_2$), 2 μL of 0.1M dithiothreitol (DTT), 40 units of the recombinant RNase Inhibitor (RNaseOUT™) and 200 units of the Superscript® III reverse transcriptase enzyme was added to the RNA/primer/dNTP mix, and incubated at 25 °C for 10 min to allow primers to anneal. cDNA synthesis was carried out at 50 °C for 50 min, followed by a 5 min incubation at 85 °C to terminate the reaction. RNA templates were digested by addition of RNase H and incubation at 37 °C for 20 min.

For cDNA synthesis using the SuperScript VILO cDNA Synthesis Kit, up to 2.5 μg of total RNA was combined with the 4μL of 5×Reaction Mix containing random hexamer primers, $MgCl_2$ and dNTPs in a buffer formulation and 2μL of 10×Superscript Enzyme Mix containing the Superscript® III reverse transcriptase enzyme and the RNaseOUT™ RNase inhibitor in 20μL total reaction volume. Samples were incubated at 25 °C for 10

min, followed by 42 °C for 60-75 min to allow for cDNA synthesis. Reactions are terminated by a 5 min incubation at 85 °C. For cDNA synthesis using the Advantaged RT-for-PCR Kit, up to 1 µg of total RNA was diluted with DEPC-treated water to a total volume of 12.5µL, 1 µL of equimolar amounts of Oligo(dT) and random hexamer primers were added and reactions were incubated at 70 °C for 2 min to allow RNA to denature and primers to anneal, before placing samples on ice. Thereafter, a reagent master mix containing 4 µL of 5×reaction buffer, 1 µL of dNTP Mix containing 10mM of each nucleotide, 0.5 µL of Recombinant RNase Inhibitor and 1 µL of MMLV Reverse transcriptase enzyme was added, and cDNA synthesis was carried out for 60 min at 42 °C, before the reaction was terminated by incubation at 94 °C for 5 min. Reactions setup without the Reverse Transcriptase enzyme (-RT control), as well as reactions setup with DEPC-treated water instead of RNA (H_2O control) were used as negative controls. Depending on the amount of RNA used as a template for first-strand cDNA synthesis, samples were diluted 1:5- 1:100 using nuclease-free water (Ambion®, Fisher Scientific) prior to PCR analysis.

3.2.4 Polymerase chain reaction

For polymerase chain reaction (PCR) amplification of PD-1 or ABCB5, 4 µL of diluted cDNA were combined with 45 µL of the Platinum PCR SuperMix High Fidelity Kit (Invitrogen) and 1 µL of primer mix, containing 10 µM each of the following gene-specific primer pairs:

Gene name (species)	Primer sequence
PDCD1 (human)	5'-ATGCAGATCCCACAGGCGCC-3' (forward) 5'-TCAGAGGGGCCAAGAGCAGTG-3' (reverse)
Pdcd1 (murine)	5'-ATGTGGGTCCGGCAGGTACC-3' (forward) 5'-TCAAAGAGGCCAAGAACAATGTC-3' (reverse)
ABCB5 (human)	5'-GCGAGCAAAGGTCGGACTACAATCGTGG-3' (forward) 5'-CCCAGAACCACAAAAGGCCATTCAGGC-3' (reverse)
GAPDH (human & murine)	5'-ACCACAGTCCATGCCATCAC-3' (forward) 5'-TCCACCACCCTGTTGCTGTA-3' (reverse)

Gene specific primer sequences were either previously published or designed using the primer 3 software (Untergasser et al., 2012), and custom primers were synthesized by Integrated DNA Technologies (IDT, Coralville, Iowa, USA). Thermocycling was carried out at 94 °C for 2 min, followed by 40 cycles at 94 °C for 15 s, 60 °C for 20 s and 68 °C for 1 min. The 867-base *PDCD1* and the 377-base ABCB5 PCR products were resolved on a 1% agarose gel, specific PCR products were purified using the QIAquick® PCR purification kit (Qiagen) (see below) and validated by bidirectional Sanger sequencing (Genewiz, South Plainfield, NJ, USA) using the amplification primer pairs, respectively.

3.2.5 Agarose gel electrophoresis of PCR products

For visualization and purification, PCR products were separated by size using agarose gel electrophoresis. Briefly, a 1% agarose gel was prepared by suspending 1g of agarose (Sigma-Aldrich) in 100 mL 1×TAE buffer (Boston Bioproducts, Ashland, MA, USA), boiled to completely dissolve the agarose, and left to cool to 60 °C before adding ethidium bromide (EtBr, Bio-Rad) to a final concentration of 0.5µg/mL. Next, the agarose solution was poured into a gel tray containing a well comb and left to solidify at room temperature for 30 min before transferring it to an electrophoresis unit containing 1×TAE buffer with

0.2µg/mL EtBr. Upon removal of the comb, 5-10 µL of PCR product or molecular weight ladder (NEB, Ipswich, MA, USA) were mixed with 6×gel loading dye (NEB) before samples were loaded into the wells of the gel. Gels were run at 80-100 Volt until separation of products was achieved, and PCR bands were visualized under UV light using the AlphaImager® EC (Alpha Innotech Corporation, San Jose, CA, USA).

3.2.6 Real-time quantitative polymerase chain reaction

To quantitate PD-1, PD-L1, PD-L2, ABCB1, ABCB5, ABCC3, ABCG2, Mart-1, tyrosinase and Mitf gene expression levels, real-time quantitative RT-PCR using the SYBR® Green chemistry was performed as described previously (Schatton et al., 2008, Schatton et al., 2010). Briefly, 2 µL of diluted cDNA was combined with 6.5 µL of 2×Fast SYBR® Green Master Mix (Applied Biosystems, Foster City, CA, USA), 3.5 µL of nuclease-free water (Ambion®, Fisher Scientific) and 1 µL of primer mix containing 10 µM of reverse and forward primer each, and kinetic PCR was performed on a StepOne Plus Real-Time PCR System (Applied Biosystems). All samples were run in triplicate. Gene specific primer sequences were either previously published or designed using the primer 3 software (Untergasser et al., 2012), and custom primers were synthesized by IDT. Primer sequences were as follows:

Gene name (species)	Primer sequence
PDCD1 (human)	5'- GACAGCGGCACCTACCTCTGTG -3' (forward) 5'- GACCCAGACTAGCAGCACCAGG -3' (reverse)
PDCD1LG1 (human)	5'- TGCCGACTACAAGCGAATTACTG -3' (forward) 5'- CTGCTTGTCCAGATGACTTCGG -3' (reverse)
PDCD1LG2 (human)	5'- CTCGTTCCACATACCTCAAGTCC -3' (forward) 5'- CTGGAACCTTTAGGATGTGAGTG -3' (reverse)
Pdcd1 (murine)	5'- CGGTTTCAAGGCATGGTCATTGG -3' (forward) 5'- TCAGAGTGTCGTCCTTGCTTCC -3' (reverse)
Pdcd1lg1 (murine)	5'- TGCGGACTACAAGCGAATCACG -3' (forward) 5'- CTCAGCTTCTGGATAACCCTCG -3' (reverse)
Pdcd1lg2 (murine)	5'- CTGGGACTACAAGTACCTGACG -3' (forward 5'- CTCTAGCCTGGCAGGTAAGCTG -3' (reverse)
ABCB1 (human)	5'- GCTGTCAAGGAAGCCAATGCCT -3' (forward) 5'- TGCAATGGCGATCCTCTGCTTC -3' (reverse)
ABCB5 (human)	5'- GCTGAGGAATCCACCCAATCT -3' (forward) 5'- CACAAAAGGCCATTCAGGCT -3' (reverse)
ABCC3 (human)	5'- GAGGAGAAAGCAGCCATTGGCA -3' (forward) 5'- TCCAATGGCAGCCGCACTTTGA -3' (reverse)
ABCG2 (human)	5'- GTTCTCAGCAGCTCTTCGGCTT -3' (forward) 5'- TCCTCCAGACACACCACGGATA -3' (reverse)
Mart-1 (murine)	5'- GACGAAGTGGATACAGAACCTTG -3' (forward) 5'- CTCTTGAGAAGACAGTCGGCTG-3' (reverse)
Mitf (murine)	5'- GATCGACCTCTACAGCAACCAG-3' (forward) 5'- GCTCTTGCTTCAGACTCTGTGG -3' (reverse)
Tyrosinase (murine)	5'- CAGGCTCCCATCTTCAGCAGAT -3' (forward) 5'- ATCCCTGTGAGTGGACTGGCAA-3' (reverse)
18S rRNA (human)	5'- GATGGGCGGCGGAAAATAG -3' (forward) 5'- GCGTGGATTCTGCATAATGGT -3' (reverse)
β-Actin (murine)	5'- CATCGTACTCCTGCTTGCTG -3' (forward) 5'- AGCGCAAGTACTCTGTGTGG -3' (reverse)

Annealing temperatures for each primer pair were determined via melt curve analysis of PCR products amplified from positive control samples. Amplification of human 18S rRNA or murine β-Actin was used for normalization, and the relative amounts of *PDCD1/Pdcd1*, *PDCD1LG1/Pdcd1lg1*, *PDCD1LG2/Pdcd1lg2, ABCB1, ABCB5, ABCC3, ABCG2, Mart-1,*

tyrosinase and Mitf transcripts were analyzed by the $2^{(-\Delta\Delta Ct)}$ method as described previously (Schatton et al., 2008, Schatton et al., 2010). Statistical differences between mRNA expression levels of the markers listed above were determined using the unpaired Student's t-test. A two-sided *P* value of $P < 0.05$ was considered significant.

3.2.7 Generation of stable PD-1 and PD-L1 knockdown or PD-1 overexpressing melanoma cell line variants

To generate stable PD-1 and PD-L1 KD cell line variants, melanoma cells were infected with lentiviral particles containing gene-specific short hairpin RNAs (shRNAs). Briefly, HEK 293-EBNA packaging cells that stably express the Epstein Barr Virus Nuclear Antigen-1 (EBNA-1) gene to ensure episomal maintenance of origin of plasmid replication (ori*P*) containing plasmids, as well as a neomycin resistence gene, were provided by Dr. S. Barthel (Brigham and Women's Hospital, Boston, MA, USA). HEK 293-EBNA cells were maintained in DMEM medium supplemented with 10% (v/v) Hi-FBS, 1% (v/v) penicillin/streptomycin (Gibco) and 1mg/mL geneticin (G418 sulfate, Thermo Fisher) in tissue culture treated flasks (Falcon®, Fisher Scientific) at 37 °C and 5% CO_2 in a humidified incubator using aseptic techniques, as described above.

For transfection, cells were grown to 70% confluency in tissue culture treated 6-well plates (Fisher Scientific) in growth media without geneticin. Lipofectamine® 2000 reagent (Fisher Scientific) was mixed with serum-free DMEM or Opti-MEM media (Gibco) and incubated with 2 µg pLKO.1 plasmids containing shRNAs against human PD-1 (*PDCD1*) (NM_005018.2, RNAi Screening Facility, Broad Institute, Boston, MA, USA), murine PD-1 (*Pdcd1*) (NM_008798, Mission shRNA, Sigma), murine PD-L1 (*Cd274*, also known as *Pdcd1lg1*) (NM_021893, Mission shRNA, Sigma) or scrambled shRNA-control (Addgene,

Cambridge, MA, USA), as well as 2 µg of the viral packaging plasmids pN8e-GagPolΔ8.1 and pN8e-VSV-G (kindly provided by Dr. S. Barhel) according to manufacturers instructions to form plasmid DNA-lipid complexes. The target 21mers were (5'-3'): GCCTAGAGAAGTTTCAGGGAA (shRNA-1) and CATTGTCTTTCCTAGCGGAAT (shRNA-2) for human *PDCD1*, GACATGAGGATGGACATTGTT (shRNA-1) and GCTCGTGGTAACAGAGAGAA (shRNA-2) for murine *Pdcd1*, and GCGTTGAAGATACAAGCTCAA for murine *Pdcd1lg1* KD. Plasmid DNA-lipid complexes were added to HEK 293-EBNA cells for transient transfection. Supernatants containing viral particles were harvested 48-72 hours after transfection. Viral supernatants were filtered through 0.45µm syringe filters (Corning, Fisher Scientific) to remove HEK 293-EBNA contaminants, aliquoted and stored at 4°C for immediate use or -80°C for long-term storage.

To generate stable PD-1 OE cell line variants, melanoma cells were infected with retroviral particles containing the PDCD1 gene under the control of the human cytomegalovirus immediate early promoter (P_{CMV}). Briefly, human *PDCD1*- or murine *Pdcd1* expression vectors were generated by PCR amplification of the full *PDCD1/Pdcd1* (CDS) from TrueClone® cDNA vectors (Origene, Rockeville, MD, USA) and addition of Hind III and Bgl II restricton sites by combining 20 µg of TrueClone® vectors with 45 µL of the Platinum PCR SuperMix High Fidelity Kit (Invitrogen) and 1 µL of primer mix, containing 10 µM each of the following primer sets recognizing human *PDCD1* or murine *Pdcd1*, respectively:

Gene name (species)	**Primer sequence**
PDCD1 (human)	5'- CGACAGATCTGCCACCATGCAGATCCCACAGGCGCC -3' (forw.) 5'- TCCGAAGCTTTCAGAGGGGCCAAGAGCAGTG -3' (reverse)
Pdcd1 (murine)	5'- CGACAGATCTGCCACCATGTGGGTCCGGCAGGTACC -3' (forw.) 5'- TCCGAAGCTTTCAAAGAGGCCAAGAACAATGTC -3' (reverse)

Thermocycling was carried out at 94 °C for 2 min, followed by 40 cycles at 94 °C for 15 s, 60 °C for 20 s and 68 °C for 1 min. The 867-base *PDCD1* PCR products were resolved on a 1% agarose gel to validate gene-specific amplification. PCR products were purified using the QIAquick® gel extraction kit (Qiagen) following manufacturer's instructions. Full-length human *PDCD1* or murine *Pdcd1* PCR products, and the retroviral pLNCX2 vector (Clontech) were digested with Hind III and Bgl II restriction enzymes (NEB) for 2-3h at 37°C, and 5' termini of the digested pLNCX2 plasmids were dephosphorylated using thermosensitive alkaline phosphatase (TSAP) (Promega, Madison, WI, USA) for 15min at 37°C. Next, cut PCR products were resolved on a 1% agarose gel and purified using the QIAquick gel extraction kit (Qiagen). PD-1 PCR products were then ligated into the pLNCX2 vector using the Rapid DNA Ligation kit (Roche, Indianapolis, IN, USA) according to the manufacturer's protocol. Ligated plasmids were transformed into chemically competent DH5α E.Coli cells (Invitrogen) via heat shock, and bacteria were propagated on ampicillin containing Luria-Bertani (LB) Agar plates (Becton Dickinson, Franklin Lakes, NJ, USA) for 12-16h at 37°C. Bacterial colonies were picked to inoculate ampicillin containing LB liquid cultures, which were grown for 12-16h at 37°C before plasmid DNA was isolated using the QIAprep spin miniprep kit (Qiagen) following manufacturer's instructions. Fidelity of PD-1 expression vectors was validated by bidirectional Sanger sequencing (Genewiz, South Plainfield, NJ, USA) using the human *PDCD1* or murine *Pdcd1* cloning primers described above. The PD-1 pLNCX2 expression vectors were mixed with the retroviral packaging plasmids pN8e-GagPolΔS and pN8e-VSV-G, medium and Lipofectamine® 2000 reagent as above to form plasmid DNA-lipid complexes and added to HEK293 EBNA packaging cells for transient transfection. The empty pLNCX2 vector was used as a control. Viral supernatants were harvested and processed as above.

Human A375, C8161, G3361, or murine B16-F0 or B16-F10 melanoma cells were infected with filtered lentiviral and/or retroviral supernatant for 5-12 hours at 37°C and 5% CO_2 in the presence of the polybrene (hexadimethrine bromide, Sigma Aldrich) to increase transduction efficiency. 48 hours post infection, cells were selected in either 0.75-2µg/ml puromycin (Puromycin Dihydrochloride, Life Technologies) and/or 300-500µg/ml geneticin (G418 sulfate, Life Technologies). The stably transduced melanoma cells were further sorted by fluorescence-activated cell sorting (FACS) for > 95% purity of human *PDCD1*-, murine *Pdcd1*- or *Pdcd1lg1* KD, human *PDCD1*- or murine *Pdcd1*-overexpressing populations and subsequently utilized in functional experiments. Human *PDCD1*- or murine *Pdcd1* KD or overexpression were confirmed by quantitative RT-PCR and flow cytometry prior to all *in vivo* tumorigenicity studies described below. *Pdcd1*-OE versus vector control B16-F10 melanoma cells, generated as above, were also co-transduced with *Pdcd1lg1*- or scrambled shRNA-control lentiviral particles, as described above.

3.2.8 Site-directed mutagenesis of the PD-1 receptor signaling motifs

To abrogate PD-1 signaling into the melanoma cell, tyrosine residues within the cytoplasmic PD-1 signaling motifs ITIM and/or ITSM were mutated to phenylalanine using the GENEART Site-Directed Mutagenesis System (Invitrogen) according to the manufacturer's protocol. The following complenentary mutagenic primers with centrally located PD-1 ITIM and ITSM mutation sites were used:

Species	Mutation	Primer sequence
human	ITIM site (Y223F)	5'-GCCACTGGAAATCCAGCTCCCCAAAGTCCACAGAGAACAC-3' (forward) 5'- TCTGTGGACTTTGGGGAGCTGGATTTCCAGTGGCGAGAG-3' (reverse)
human	ITSM site (Y248F)	5'-GCTAGGAAAGACAATGGTGGCAAACTCCGTCTGCTCAGGG-3' (forward) 5'- CAGACGGAGTTTGCCACCATTGTCTTTCCTAGCGGAATGG-3' (reverse)
murine	ITIM site (Y225F)	5'-CGTCCCTGGAAGTCCAGCTCCTCAAAGGCCACACTAGGGAC-3' (forward) 5'-CCCTAGTGTGGCCTTTGAGGAGCTGGACTTCCAGGGACGAGAG-3' (reverse)
murine	ITSM site (Y248F)	5'-CCTTCAGTGAAGACAATGGTGGCAAATTCTGTGTGCACACAGG-3' (forward) 5'- GTGCACACAGAATTTGCCACCATTGTCTTCACTGAAGGGCTGG-3' (reverse)

Briefly, wildtype PDCD1 containing pLNCX2 plasmids (cloned as described above) were methylated and amplified using the primers containing the PD-1 ITIM and ITSM mutations listed above following the manufacturer's protocol. Amplification was verified by analyzing 5µL PCR products on a 1% agarose gel as above. Plasmids were recombined *in vitro* as per manufacturer's instructions, transformed into chemically competent DH5α E.Coli cells (Invitrogen) via heat shock, and bacteria were propagated on ampicillin containing LB Agar plates followed by ampicillin containing LB liquid cultures, as above. Plasmid DNA was isolated using the QIAprep spin miniprep kit (Qiagen) following manufacturer's instructions. Fidelity of vectors was validated by bidirectional Sanger sequencing using the human *PDCD1* or murine *Pdcd1* cloning primers, as described above. Mutant human *PDCD1* or murine *Pdcd1* variants were packaged into retroviral particles as above, and used to infect human A375 or C8161, or murine B16-F0 or B16-F10 melanoma cell lines, respectively. Transduced cell lines were selected in geneticin

containing growth media as above and FACS-sorted for > 95% purity of mutated human or murine PD-1 overexpressing populations. Wildtype or mutant *PDCD1* overexpression was confirmed by quantitative RT-PCR and flow cytometry for all cell lines prior to the *in vitro* and *in vivo* tumorigenicity studies described.

3.2.9 Western blot analysis

The western blot analyses shown throughout this thesis were performed by Dr. C. Posch and Dr. S. Barthel.

Wildtype or PD-1 variant murine B16, human C8161 and G3361 melanoma cell lines were grown to subconfluency in 6-well plates under serum-starved conditions (0.1% (v/v) Hi-FBS for 12h in the presence or absence of anti-PD-1 mAb (clones 29F.1A12 or J116) or isotype control mAb (clones RTK2758 or MOPC-21) (Biolegend or BioXCell, 50µg/ml, respectively), following subsequent incubation with or without 5µg/ml recombinant PD-L1 Ig (R&D Systems) or control Ig (R&D Systems or Bethyl Laboratories) under serum-free conditions for 15 min, or following incubation in the presence or absence of rapamycin (100nM), PP242 (50-100nM), wortmannin (50-100nM), LY294001 (500nM) (Selleck Chemicals, Houston, TX, USA), or vehicle control (DMSO) for 30 minutes under serum-free conditions, as described (Posch et al., 2013), and subsequent addition of recombinant PD-L1 Ig or control Ig, as above. Cells were placed on ice, washed twice with ice-cold PBS, and lysed by incubating with radio-immunoprecipitation buffer (RIPA) (Pierce®, Thermo Scientific) supplemented with protease and phosphatase inhibitors (Complete Protease Inhibitor Cocktail and PhosSTOP, Roche) for 10 min on ice, before serial passage through a 31G insulin syringe (Beckton Dickinson). Samples were centrifuged for 30 min at 4 °C and 14,000×g, cleared lysates transferred to new microcentrifuge tubes and protein

concentrations were determined using the Pierce™ BCA protein assay kit (Thermo Scientific) according to the manufacturer's protocol. Total protein in 1× Laemmli buffer (Boston Bioproducts, Ashland, MA, USA) supplemented with 10% β-mercaptoethanol were resolved by sodium dodecyl sulfate polyacrylamide gel electrophoresis (SDS/PAGE) (Bio-Rad), transferred for 1h to immunoblot PVDF membranes (Bio-Rad), and blocked for 1h in 5% (wt/v) dry milk/Tris-buffered saline (TBS, Boston Bioproducts))/0.1% (v/v) Tween-20 (Acros, Thermo Fisher), as described (Posch et al., 2013). For detection of human and murine PD-1, membranes were blocked in Odyssey Blocking Buffer (LI-COR Biosciences, Lincoln, NE, USA) overnight, incubated with mouse anti-human PD-1 (2µg/ml), goat anti-mouse PD-1 (1.5µg/ml), or mouse anti-β-actin Ab (1:10,000 dilution) in Odyssey Blocking Buffer/0.1% (v/v) Tween-20 for 1 hour at room temperature. Subsequently, blots were washed in TBS/0.1% (v/v) Tween-20, stained with infrared fluorescent dye (IRDye) -conjugated secondary Abs (LI-COR Biosciences) (1:10,000 dilution, respectively) in Odyssey Blocking Buffer/0.1% (v/v) Tween-20 for 45 min at room temperature, washed in TBS/0.1% (v/v) Tween-20, and then scanned on an Odyssey CLx imaging system (LI-COR Biosciences). To determine expression levels of phosphorylated versus total ERK1/2, AKT and S6 ribosomal protein, blots were probed overnight at 4 °C with Ab raised against the protein of interest (Cell Signaling Technologies, Danvers, MA, USA), incubated with horseradish peroxidase (HRP)- or IRDye-conjugated secondary Ab for 1h, and developed using enhanced chemoluminescence (Pierce) or analyzed using an Odyssey CLx imaging system, as described (Posch et al., 2013).

3.3 Flow cytometric analysis and cell sorting

3.3.1 Flow cytometric analysis of surface marker expression

PD-1, PD-L1, PD-L2 and ABCB5 cell surface expression by established human and murine melanoma and human MCC cell lines was analyzed by single-color flow cytometry, and PD-1 and ABCB5 or PD-1 and PD-L1/PD-L2 co-expression by established melanoma and MCC lines, as well as PD-1, CD31 and CD45 surface expression by patient-derived melanoma single cell suspensions were analyzed by multi-color flow cytometry, as described previously (Schatton et al., 2008, Schatton et al., 2010). Briefly, 1×10^5 - 1×10^6 cells were resuspended in 200 µL PBS supplemented with 2% Hi-FBS (FACS buffer) in 5 mL polystyrene round-bottom tubes (Fisher Scientific). Cells were incubated with PE- or PerCP-eFluor 710-conjugated anti-human or anti-murine PD-1 (clone MIH4 or 29F.1A12), PD-L1 (clone 29E.2A3 or 10F.9G2), PD-L2 (clone 24F.10C12 or TY25) (Biolegend and eBiosciences), unconjugated ABCB5 (clone 3C2-1D12, kindly provided by Dr. M. Frank) mAbs or respective isotype control mAbs (Biolegend) (1-20 µg/mL, titrated for each cell type) for 30 minutes at 4°C protected from light. Cells were washed twice with 2ml ice-cold FACS buffer to remove excess Abs and resuspended in 200 µL FACS buffer. For ABCB5 staining, cells were subsequently incubated with APC- or eFluor 660-conjugated anti-mouse IgG secondary F(ab')2 fragments or FITC – or PE-conjugated goat anti-mouse IgG Ab (Biolegend and eBiosciences) for 30 minutes at 4°C to detect unconjugated anti-ABCB5 or mIgG1 isotype control mAbs. Cells were washed as above and resuspended in 200 µL FACS buffer. To analyze coexpression of ABCB5 and PD-1, cells were first incubated with unconjugated anti-ABCB5 or isotype control mAb, followed by counterstaining with conjugated anti-mouse IgG secondary F(ab')2 or goat anti-mouse mAb as above. Subsequently, cells were incubated with PE- or PerCP-eFluor 710-conjugated anti-human or anti-murine PD-1 or respective isotype control mAbs for 30

minutes at 4°C. In between each incubation step, cells were washed twice with 2ml ice-cold PBS. For analysis of PD-1, CD31 and CD45 surface expression by patient-derived melanoma single cell suspensions, 5×10^5-1×10^6 cells were resuspended in 200 µL FACS buffer, and simultaneously incubated with PerCP-eFluor 710-conjugated anti-human PD-1, FITC-conjugated anti-human CD45 (clone HI30), APC-conjugated anti-human CD31 (clone WM59) and/or respective isotype control mAbs for 30 minutes at 4°C. Cells were washed twice with 2mL ice-cold PBS to remove excess Ab, and resuspended in 200 µL FACS buffer as above. For multicolor flow cytometry, spectral overlap was corrected for using compensation controls for each fluorophore-conjugated Ab. In addition, fluorescence minus one (FMO) and isotype control stainings were included in each experiment to allow for proper gating of cell populations. Fluorescence emission was acquired on a FacsCanto (Becton Dickinson), as described (Schatton et al., 2008, Schatton et al., 2010) and analyzed using the FlowJo software (Tree Star, Ashland, OR, USA). Statistical differences were determined using the Student's t-test. A two-sided *P* value of $P<0.05$ was considered significant.

3.3.2 Flow cytometric analysis of tumor-infiltrating and circulating lymphocytes

To assess antitumor immune responses in B16 melanoma-bearing C57BL/6 mice, single-cell suspensions were prepared from spleens and tumor-draining lymph nodes, and tumor-infiltrating lymphocytes were enriched for using density centrifugation as described above. Cells were suspended in FACS buffer, transferred to 96-well round- or V-bottom plates, and incubated for 30 min at 4°C with directly-conjugated Abs recognizing the following cell surface antigens: anti-mouse CD45.2 (clone 104), anti-mouse CD3 (clones 17A2 and

145-2C11), anti-mouse CD4 (clone RM4-5), anti-mouse CD8 (clone 53-6.7), anti-mouse CD25 (clone 3C7), anti-mouse CD44 (clone IM7), anti-mouse CD62L (clone Mel-14), anti-mouse GR-1 (clone RB6-8C5), anti-mouse Ly-6C (clone HK1.4), anti-mouse Ly-6G (clone IA8), anti-mouse CD11b (clone M1/70), anti-mouse CD11c (clone N418) and respective isotype controls (Biolegend and eBiosciences) following manufacturers recommendations. Cells were washed twice with ice-cold PBS to remove excess Abs, and resuspended in 200 µL FACS buffer for acquisition. For intracellular cytokine staining (ICS), cells were resuspended in RPMI-1640 medium supplemented with 10% (v/v) Hi-FBS, 1% (v/v) penicillin/streptomycin (Gibco) and stimulated *in vitro* in 96-well round-bottom plates for 2 h with 100ng/mL phorbol 12-myristate 13-acetate (PMA) and 500ng/mL Ionomycin (Sigma) at 37°C and 5% CO_2, and the release of proteins through the Golgi apparatus was blocked using Golgi Stop (BD Biosciences) as per manufacturers instructions. Cells were washed twice with ice-cold PBS prior to staining for extracellular antigens as above. Next, cells were fixed for 30 minutes at 4°C in 100 µL FACS buffer containing 1% paraformaldehyde (Fix buffer) to stabilize and retain target proteins. To permeabilize the membrane, cells were washed twice in FACS buffer containing 0.1% (wt/v) of the mild detergent saponin (Sigma Aldrich) (Perm buffer), and incubated with anti-mouse FoxP3 (clone FJK-16), anti-mouse TNF-α (clone MP6-XT22), and anti-mouse INF-γ (clone XMG1.2) (Biolegend) in Perm buffer for 30 minutes at 4°C following manufacturers instructions. Cells were washed twice with Perm buffer, and suspended in 200 µL FACS buffer for acquisition. Samples were acquired on a LSRII flow cytometer (Becton Dickinson) and data was analyzed using the FlowJo software (Tree Star).

To assess NK cell-, macrophage-, and neutrophil depletion efficiency in the circulation of NSG mice (see below), blood was collected from the lateral tail vein into a tube coated with 4mM ethylenediaminetetraacetic acid (EDTA) (Sigma Aldrich) in PBS to prevent coagulation. Red blood cells were lysed in 1mL ACK lysis buffer (Lonza) as

above, cells washed twice with PBS and resuspended 200 µL FACS buffer. Cells were stained with the following directly conjugated Abs: anti-mouse CD3 (clone 17A2), anti-mouse CD45.1 (A20), anti-mouse CD49b (clone DX5), anti-mouse CD11b (clone M1/70), anti-mouse F4/80 (clone BM8), and anti-mouse CD11c (clone N418) for 30 minutes at 4°C following manufacturers instructions. Cells were washed twice with PBS, and suspended in 200 µL FACS buffer for acquisition. Fluorescence emission was acquired on a FacsCanto (Becton Dickinson), as described (Schatton et al., 2008, Schatton et al., 2010) and analyzed using the FlowJo software (Tree Star). Statistical differences were determined using the Student's t-test. A two-sided *P* value of $P<0.05$ was considered significant.

3.3.3 Flow cytometric analysis of cell viability

To assess the effects of anti-PD-1 or anti-ABCB5 mAb blockade on cell viability *in vitro*, melanoma or MCC cells were cultured in the presence of 20 µg/mL anti-PD-1 mAb (clone 29F.1A12, Biolegend or J116, BioXCell), anti-ABCB5 mAb (clone 3C2-1D12, kindly provided by Dr. M. Frank) or respective isotype control mAbs in a tissue culture treated 6-well dish for 48-72 hours at 37°C and 5% CO_2. Cell death was quantified by annexin V/ 7-amino-actinomycin D (7-AAD) staining and subsequent flow cytometric analysis as described (Schatton et al., 2010). Briefly, cells were harvested as above, washed twice with ice-cold PBS and suspended in 1× Annexin V Binding Buffer (BD Biosciences) at a concentration of 1×10^6 cells/mL. 100 µL cell suspension was transferred to 5 mL polystyrene round-bottom tubes, and cells were stained with 1 µL annexin V-Alexa Fluor 647 (Biolegend) and 5 µL 7-AAD (BD Biosciences) for 10 minutes at room temperature.

Next, 400 µL 1× Annexin V Binding Buffer were added to each tube, and samples were analyzed by dual-color flow cytometry within 30 minutes.

Cell viability of $ABCB5^+$ versus $ABCB5^-$ MCC cell subsets cultured for 72 hours at 37°C and 5% CO_2 in the presence or absence of cytotoxic levels of carboplatin (250 µM) or etoposide (5 µm) was assessed by calcein AM and ABCB5 co-staining, followed by dual-color flow cytometric analysis, as described (Schatton et al., 2008, Schatton et al., 2010). Briefly, cells were collected, washed twice with ice-cold PBS before staining for ABCB5 as above. Cells were then suspended in MCC growth media and incubated for 5 minutes at 37°C and 5% CO_2 with 0.5 µg/mL of the nonfluorescent dye calcein AM (Life Technologies), that, upon hydrolysis by live cells, converts into a green-fluorescent calcein dye. Cells were subsequently washed with FACS buffer, and samples were analyzed by dual-color flow cytometry on a FacsCanto, as described.

3.3.4 Rhodamine 123 efflux assay

The rhodamine 123 efflux assay shown in Figure 39D was performed by Dr. B. Wilson.

The efflux capacity of the ABCB5 transporter for the green fluorescent dye, rhodamine 123 (Rh123, Sigma Aldrich), was assessed by flow cytometry following incubation of MCC cells with the anti-ABCB5 blocking mAb or isotype control mAb, as described previously (Frank et al., 2003, Lin et al., 2013). Briefly, MKL-1 cells were harvested as above, concentrated at 5×10^5 cells/mL in MCC growth media, loaded with Rh123 at 1µg/mL and incubated for 15 min at 37°C and 5% CO_2. Cells were washed twice with media and subsequently incubated with anti-ABCB5 blocking mAb (clone 3C2-1D12) or isotype control mAb (clone MOPC-31) (50 µg/mL, respectively) for 120 min at 37°C and 5% CO_2. Rh123 loaded cells incubated at 4°C were used as a control, as ATP-hydrolysis

and therefore ABCB5 transporter function is blocked at this temperature. Cellular efflux of the green fluorescent dye Rh123 was measured on a FacsCanto and analyzed using FlowJo, as described above.

3.3.5 FACS sorting of PD-1$^+$ cancer cells

The FACS sorting of melanoma cells was performed at the Cell Sorting Core Facility at the Center for Neurologic Disease at Brigham and Women's Hospital and Harvard Medical School.

PD-1$^+$ and PD-1$^-$ populations were isolated by FACS sorting from established human and murine native, PD-1 OE and PD-1 KD melanoma cell line variants. Briefly, cells were stained for PD-1 surface protein expression as described above using aseptic technique. PD-1$^+$ and PD-1$^-$ populations were identified using isotype control stained samples, and purified using BD's FACS Aria cell sorting instrument (BD Biosciences).

3.3.6 Magnetic bead cell sorting of PD-1$^+$ and ABCB5$^+$ cancer cells

PD-1$^+$- and ABCB5$^+$-purified cells were isolated by positive selection, and PD-1$^-$ and ABCB5$^-$ cell populations were generated by depleting PD-1$^+$ or ABCB5$^+$ cells from cell suspensions using PD-1 and ABCB5 mAb labeling followed by magnetic bead cell sorting, as described (Schatton et al., 2008, Schatton et al., 2010). Briefly, human and murine melanoma cells were harvested and counted, and cells were labeled using either anti-PD-1 (clone 29F.1A12 or J116) or anti-ABCB5 (clone 3C2-1D12) Abs (20 μg/mL) in FACS buffer for 30 min at 4 °C, washed twice with cold PBS to remove excess Ab, followed by incubation with 20 μL of secondary anti-mouse IgG mAb-coated MACS® MicroBeads

(Miltenyi Biotec, San Diego, CA, USA) and 80 μL MACS buffer (calcium- and magnesium-free PBS containing 1% (wt/v) bovine serum albumin (BSA) and 2mM EDTA (Sigma)) per 1×10^7 cells for 30 min at 4 °C protected from light. Subsequently, cells were washed twice with MACS buffer to remove excess magnetic beads, and sorted into marker positive and marker negative cell fractions by dual-passage cell separation using MS or LS MACS Columns and MidiMACS Separators (Miltenyi Biotec) as per manufacturers recommendations. Purified subpopulations were washed twice with cold PBS and counted. Viability of sorted melanoma cells was assessed by the trypan-blue dye-exlusion assay or AO/PI staining as described above. Purities of sorted melanoma cell subpopulations were determined by subsequent flow cytometric analysis of sorted cells for ABCB5 or PD-1 expression, respectively.

3.4 Histopathology, immunohistochemistry, and immunofluorescence studies

3.4.1 Human subjects

Stage IV melanoma patients with surgical resection or biopsy of melanoma lesions prior to and after systemic anti-PD1 treatment between February 2013 and May 2015 were included in the study. The data set contained 30 observations on metastatic melanoma patients undergoing anti-PD1 targeted therapy at the Department of Dermatology, University Hospital Zurich, Switzerland and 4 patients at the Massachusetts General Hospital Cancer Center, Boston, MA, USA. Paraffin-embedded tumor tissue was available from all 34 patients prior to anti-PD1 treatment start. From 11 of the patients, matched tumor tissue from progressive lesions during or immediately after anti-PD1 therapy was also available. Melanoma lesions were morphologically identified by experienced

dermatopathologists. Additionally, immunohistochemical analyses of melanoma markers (MART-1 and S-100) were used. Studies were conducted in accordance with the Declaration of Helsinki and approved by the IRBs of the University of Zurich (KEK-ZH-Nr. 2014-0320) and the Dana-Farber/Harvard Cancer Center (IRB# 11-181). All patients agreed to the use of their tumor tissues according to the Biobank project 2014-0320ct (EK No. 647), funded by the University of Zurich Research Priority Program (URPP) in translational cancer biology or DF/HCC IRB approved protocol 11-181. Paraffin-embedded tumor tissue from Merkel cell carcinoma biopsies and healthy human skin were obtained from patients and healthy volunteers upon approval by the IRBs of Partners Health Care Research Management and the Dana-Farber Cancer Institute, Boston, MA, USA and in accordance with an assurance filed with and approved by the U.S. Department of Health and Human Services. Informed consent was obtained from all subjects.

3.4.2 Immunohistochemical and immunoflourescence analysis of clinical melanoma and MCC sections and tumor xenografts

The immunohistochemical and immunofluorescence stainings presented in this thesis were performed and analyzed by Prof. Dr. G. Murphy, Prof. Dr. C. Lian, Dr. Q. Zhan, Dr. C. Lezcano, Dr. P. Elco, Dr. C. Schlapbach, Dr. E. Guenova, Dr. W. Hoetzenecker, Dr. A. Cozzi, Prof. Dr. R. Dummer, and the Pathology Core facility at Brigham and Women's Hospital, Harvard Medical School.

Immunohistochemical analysis of p-S6 expression in clinical tumor biopsies obtained from melanoma patients was done as described previously (Schatton et al., 2008, Schatton et al., 2010). Briefly, 3-5 μm thick tumor biopsy sections were deparaffinized in xylene and

subsequently rehydrated with 100%, 95%, and 75% ethanol, and deionized H_2O. Sections were then placed in target retrieval solution (Dako, Carpinteria, CA, USA), boiled in a Pascal pressure chamber (Dako) at 125 °C for 30 seconds, 90 °C for 10 seconds, and then cooled down to room temperature. Subsequently, sections were stained with a 1:200 dilution of rabbit anti-p-S6 Ab for 1 hour at room temperature, following incubation with a 1:100 dilution of biotin-conjugated mouse anti-rabbit IgG for 30 min at room temperature and subsequent incubation with streptavidin-alkaline phosphatase (Roche) for 30 minutes at room temperature. p-S6 immunoreactivity was detected using the FAST Red Chromogen System (Biolegend), per the manufacturer's instructions. Nuclear counterstaining (blue) was performed with Meyer's haemalum. p-S6 immunoreactivity by melanoma cells was graded by three independent investigators blinded to the study outcome on a scale of 0-4 (0: no p-S6 expression by melanoma cells; 1: p-S6 expression in 1-25%; 2: 26-50%; 3: 51-75%; 4: >75% of melanoma cells). For each slide, at least two areas with the highest numbers of S-100$^+$ and MART-1$^+$ melanoma cells, as determined in serial sections, were selected for analysis. IHC analysis of PD-1 expression by murine B16 melanomas and human A375, C8161, and G3361 melanoma xenografts was performed as described (Schatton et al., 2008, Schatton et al., 2010) in formalin-fixed, paraffin-embedded tumors harvested 3 weeks (murine B16 melanomas) or 4-5 weeks (human melanoma xenografts) post tumor cell inoculation. Binding of *in vivo* administered rat anti-mouse PD-1 or mouse anti-human PD-1 mAb to tumor target tissue was visualized by secondary anti-rat or anti-mouse IgG staining of experimental tumors harvested 3 hours post intraperitoneal (i.p.) mAb injection, as described (Schatton et al., 2008). For quantification of *in vivo* tumor-bound Ab, representative images (n=5-10) of B16-F10 melanoma grafts (n=2-3) from wildtype C57BL6, PD-1(-/-) KO C57BL6, and NSG mice were analyzed by FIJI/Image J (NIH). Positive staining with 3,3'-diaminobenzedine (DAB) was determined as a fraction of total image area. Relative staining per cell was

approximated by dividing the DAB-positive fraction by total nuclei counted as a function of image area to correct for any variability in image composition.

For IHC analysis of ABCB5 expression by MCC biopsies (n = 85) and human MCC cell line-derived xenografts (n = 55), formalin-fixed paraffin-embedded tissue samples were stained for ABCB5 (10 μg/ml, respectively). Selected samples were also stained for cytokeratin 20 (CK20), cleaved caspase 3 (CC3), or secondary anti-mouse Ig, to visualize binding of *in vivo*-administered anti-ABCB5 mAb to tumor xenograft target tissue, per manufacturer's recommendations. All samples were deparaffinized as above, and subsequent epitope retrieval was achieved by placing tissue sections in a sodium citrate solution (pH 6.0) (Dako), boiling in a Pascal pressure chamber (Dako) at 125°C for 30 seconds, 90°C for 10 seconds, and cooling to room temperature. The sections were blocked with serum at room temperature for 1 hour, incubated with primary Abs overnight at 4°C, washed with TBS-0.005% tween 20, followed by HRP-conjugated secondary Abs (1:200) at room temperature for 1 hour. Immunoreactivity was detected by using NovaRED peroxidase substrate (Vector Laboratories, Burlingame, CA, USA). ABCB5 immunoreactivity in MCC patient samples obtained before or after chemotherapy and in MCC tumor xenografts, in experimental groups as below, was quantified using ImageJ software analysis, as described (Frank et al., 2011).

MART-1/PD-1 and CD45/PD-1 immunofluorescence (IF) double labeling of clinical melanoma specimens and MART/PD-1 IF double labeling of murine B16 melanoma grafts was carried out as described previously (Schatton et al., 2008, Schatton et al., 2010). Cytospin slides of WaGa cells were fixed in cold acetone for 10 minutes and incubated with anti-ABCB5 (Novus 10 μg/ml) as described above. Sections were subsequently incubated with AlexaFluor 594 secondary Ab (1:2000) for 1 hour at room temperature. Sections were analyzed with a DXM 1200F Nikon microscope (Nikon Instruments, Melville, NY, USA), and images were captured using the NIS-Elements software (BR

2.30, Nikon).

3.5 *In vivo* melanoma and MCC xenotransplantation and targeting experiments

3.5.1 Animal maintenance

C57BL/6, Rag(-/-) knockout (KO) C57BL/6 (Rag) and nonobese diabetic/severe combined immunodeficiency (NOD/SCID) interleukin (IL)-2R γ-chain (-/-) null (NSG) mice were purchased from The Jackson Laboratory (Bar Harbor, ME, USA). PD-1(-/-) KO C57BL/6 and PD-L1(-/-) KO Rag mice were kindly provided by Dr. A. Sharpe (Francisco et al., 2009, Latchman et al., 2001) and maintained at the Harvard Institutes of Medicine animal facility. Age- and sex-matched mice that were at least 6 weeks of age were used for all experiments. All mice were used according to the Harvard Medical School Standing Committee on Animals and National Institutes of Animal Healthcare Guidelines, and all animal protocols were approved by the Harvard Medical School's Standing Committee on Animals.

3.5.2 Human melanoma and MCC to mouse xenotransplantation experiments

Stable PD-1 (*Pdcd1*)- or PD-L1 (*Pdcd1lg1*) KD, wildtype *Pdcd1* OE with or without concurrent *Pdcd1lg1* KD, ITIM-, ITSM-mutant, or ITIM/ITSM double mutant *Pdcd1*-OE murine B16-F0 or B16-F10 or their respective control cell line variants, or PD-1^{+} or PD-1^{-}-

sorted native B16-F0 or B16-F10 cells were injected s.c. (2×10^5 cells/inoculum) into the flanks of recipient wildtype C57BL/6, NSG, Rag, PD-1(-/-) C57BL/6, and/or PD-L1(-/-) KO Rag mice. Stable *PDCD1*-KD, wildtype *PDCD1*-OE, ITIM- or ITSM-mutant, or ITIM/ITSM double mutant *PDCD1*-OE or sorted PD-1^+ or PD-1^- human A375, C8161, and/or G3361 or their respective control cell line variants (1×10^6 cells/ inoculum), and native MKL-1 or WaGa MCC cell lines (1×10^7 cells/inoculum) were injected s.c. into the flanks of recipient NSG mice, as described (Schatton et al., 2008). Age- and sex-matched recipient mice were randomly assigned to experimental groups. Tumor formation and growth was assessed every 2-4 days as a time course until the experimental endpoint, and tumor volume was calculated as described (Schatton et al., 2008). Tumors were harvested in their entirety 3 weeks (murine B16 melanomas) or 4-5 weeks (human melanoma and MCC xenografts) after tumor cell inoculation for histologic and qPCR analysis, unless excessive tumor size or disease state required protocol-stipulated euthanasia earlier. Mice that required euthanasia before the experimental endpoint were excluded from tumor growth analysis. These exclusion criteria were pre-established. While the assessment of tumor growth was not blinded, all pathologists who performed histologic characterizations of tumor specimens were blinded to the group allocation. Sample sizes were chosen to ensure statistical power of detection based on projected outcomes. Differences in tumor volume were statistically assessed using the unpaired Student's *t*-test, the nonparametric Mann-Whitney test, or repeated measures two-way ANOVA followed by the Bonferroni correction with two-tailed *P* values <0.05 considered significant (Schatton et al., 2008).

3.5.3 Tumorigenicity experiments with anti-PD-1 and anti-ABCB5 blocking antibodies

For *in vivo* PD-1 and PD-L1 targeting experiments, murine B16–F10 melanoma cells or *Pdcd1*-OE versus control B16-F10 melanoma variants were grafted s.c. into wildtype versus PD-1(-/-) KO C57BL/6, wildtype versus PD-L1(-/-) KO Rag, and wildtype versus innate immune cell-depleted NSG mice, as described above. Human A375, C8161 or G3361 melanoma cells, *PDCD1*-OE versus control C8161 melanoma variants, or single cell suspensions of clinical melanoma metastases derived from n=3 distinct melanoma patients were grafted s.c. into the flanks of recipient NSG mice, as described above. Mice were randomly assigned to experimental treatment groups and sample sizes chosen to ensure statistical power of detection based on projected outcomes. Animals were injected i.p. (200μg per injection, respectively) with anti-mouse PD-1 (clone 29F.1A12), PD-L1 (clone 10F.9G2), or anti-human PD-1 mAb (clone J116) versus respective isotype control mAb every other day starting 1 day before melanoma cell inoculation for the duration of 3 weeks (murine melanomas) or 4-5 weeks (human melanoma xenografts). For *in vivo* ABCB5 targeting experiments, human MCC cells were grafted s.c. into the flanks of recipient NSG mice. Mice were randomized to experimental treatment groups with tumor volumes not statistically different between experimental arms. Animals were injected i.p. with anti-ABCB5 mAb (clone 3C2-1D12) or control mAb daily (500 μg per injection, respectively) for 9 consecutive days or starting 72 hours prior to initiating 6 consecutive daily administrations of carboplatin or etoposide at 30 mg/kg or 5 mg/kg body weight, respectively. Tumor formation and growth was assayed as described above, until the experimental endpoint of 3-5 weeks, or when excessive tumor burden or disease state required protocol-stipulated euthanasia earlier. Mice that required euthanasia before the experimental endpoint were excluded from tumor growth analysis. These exclusion criteria

were pre-established. While the investigators assessing tumor growth were not blinded, all pathologists and laboratory personel who performed histologic or qPCR characterizations of tumor specimens were blinded to the group allocation. Differences in tumor volume were statistically assessed using the unpaired Student's *t*-test test or repeated measures two-way ANOVA followed by the Bonferroni correction, with two-tailed *P* values <0.05 considered significant.

3.5.4 Innate immune cell depletion studies

NK cell depletion was achieved by i.p. injection of 50 µL undiluted anti-asialo GM1 Ab (Wako Pure Chemical Industries, Richmond, VA, USA) every 5 days, as described (Civenni et al., 2011) starting 3 days before melanoma cell engraftment, which resulted in >80% depletion of CD3-CD45.1$^+$CD49b(DX5)$^+$ NK cells in the circulation of NSG mice for the duration of the experiment, as determined by flow cytometry. Macrophages were depleted by i.p. injecting NSG mice with 200 µL of undiluted clodronate (dichloromethylene bisphosphonate) liposomes (Encapsula Nano Sciences, Brentwood, TN, USA) every 5 days, starting 3 days before melanoma cell engraftment (Fraser et al., 1995), resulting in >85% depletion of CD45.1$^+$CD11b$^+$F4/80$^+$ macrophages compared to untreated control mice. NSG mice were rendered neutropenic, as described (Jaeger et al., 2012) by i.p. injection of 100µg anti-Ly-6G mAb (clone RB6-8C5, BioXCell) on days -3, -1, 4, 9, 14, and 19 post tumor cell inoculation, resulting in >90% depletion of CD45.1$^+$CD11b$^+$CD11c$^-$ neutrophils in NSG mice. NK cell-, macrophage- and neutrophil depletion regimens, as above, were also used in combination to generate NSG mice lacking all three innate immune cell subtypes.

3.5.5 *In vivo* chemotherapy treatment

At day 34 post tumor cell inoculation, mice were randomized to carboplatin, etoposide or vehicle control treatment groups with tumor volumes not statistically different between experimental arms. Carboplatin (Novaplus pharmaceuticals, Limeport, PA, USA) or etoposide (APP pharmaceuticals Lake Zurich, IL, USA) were administered daily by i.p. injection for 6 consecutive days, at 75 mg/kg or 10 mg/kg body weight, respectively, and control animals were given vehicle at equal volumes as previously described (Fichtner et al., 2008). Tumor volumes were measured daily for the duration of the treatment, xenografts harvested 1 day following administration of the final treatment dose for subsequent qPCR and immunohistochemical analysis, unless excessive tumor size or disease state required protocol-stipulated euthanasia earlier. While the investigators assessing tumor growth were not blinded, all pathologists and laboratory personnel who performed histologic or qPCR characterizations of tumor specimens were blinded to the group allocation. Sample sizes were chosen using contingency table analyses to ensure statistical power of detection based on projected outcomes.

3.5.6 Assessment of PD-1 antibody titer by ELISA.

To determine the concentration of PD-1 Ab in the serum of wildtype C57BL/6, PD-1(-/-) KO C57BL/6, and NSG mice, animals were grafted with B16-F10 melanoma cells and treated with 200µg of anti-PD-1 Ab per 20g of body weight. Two weeks post melanoma cell inoculation and 12 hours post final administration of the PD-1 Ab, mouse blood was collected by cardiac puncture and serum prepared using serum separator tubes (BD Biosciences). Serum obtained from C57BL/6, PD-1(-/-) KO C57BL/6, and NSG mice that had not been treated with anti-PD-1 Ab was used as a negative control. Subsequently, the

serum concentration of rat anti-mouse PD-1 Ab was measured using a rat IgG2a-specific enzyme-linked immunosorbent assay (ELISA) kit (Bethyl Laboratories), per the manufacturers instructions.

3.6 Statistical analysis.

Statistical differences between gene and protein expression levels, *in vitro* tumor spheroid and *in vivo* melanoma and MCC growth were compared statistically using the unpaired Student's *t* test or the nonparametric Mann-Whitney test (comparison of two experimental groups) or repeated measures two-way ANOVA followed by the Bonferroni correction (comparison of three or more experimental groups). Data was tested for normal distribution using the D'Agostino and Pearson omnibus normality test. Analyses were performed using the PRISM software (version 5 for Macintosh, GraphPad Inc.)

Kaplan-Meier estimates and the log-rank test were used to analyze statistical differences in progression-free and overall survival between melanoma patients treated systemic anti-PD-1 Ab-based therapy whose pre-treatment tumor biopsies showed low (<25%) versus high (>25%) melanoma cell expression of p-S6. The corresponding hazard ratio was estimated using the Cox proportional hazards model. Progression-free survival was defined as the time from the first administration of anti-PD1-based therapy to the first documented radiographic evidence of progressive disease. Overall survival was defined as the time from the first administration of anti-PD1-based therapy to the date of death, regardless of cause. Statistical analyses were performed using the R programming language (version 3.02) and Origin Pro 9.1G Software (OriginLab). Differences in p-S6 expression in patient-matched tumor biospecimens obtained before and after PD-1 therapy were statistically compared using the paired Student's *t* test. Data was tested for normal

distribution using the D'Agostino and Pearson omnibus normality test. A two-sided value of $P<0.05$ was considered statistically significant.

4 Results

4.1 The immune checkpoint receptor PD-1 is expressed by tumorigenic melanoma subpopulations.

Parts of this chapter have been previously published in *Kleffel S. et al. Melanoma Cell-Intrinsic PD-1 Receptor Functions Promote Tumor Growth. Cell 2015;162(6):1242-56.* Published data is highlighted in the individual figure legends.

4.1.1 Introduction

Immune checkpoints are critical regulatory pathways that modulate the duration, amplitude and quality of immune responses and maintain self-tolerance (Pardoll, 2012). Cancer cells commonly exploit immune checkpoints to escape immune-mediated rejection, for example by promoting functional exhaustion of tumor-reactive cytotoxic T lymphocytes (CTLs). PD-1 is a prominent immune checkpoint receptor that, upon engagement by its ligands, PD-L1 or PD-L2, dampens T effector functions by inhibiting signaling downstream of the TCR (Topalian et al., 2012a). Thus, expression of PD-1 ligands, particularly PD-L1, in the TME protects cancers from tumor-specific immunity (Dong et al., 2002a, Topalian et al., 2012a). Antibody-based therapeutics targeting the PD-1:PD-1 ligand axis have demonstrated unprecedented response rates and encouraging safety profiles in patients with advanced-stage cancers of various etiology, including melanoma (Ansell et al., 2015, Borghaei et al., 2015, Brahmer et al., 2015, Garon et al., 2015, Hamid et al., 2013, Kaufman et al., 2016, Larkin et al., 2015, Motzer et al., 2015, Nghiem, 2015, Pai et al., 2016, Postow et al., 2015a, Ribas et al., 2015, Robert et al., 2015a, Robert et al., 2015b, Rosenberg et al., 2016, Topalian et al., 2012b, Topalian et al., 2014, Weber et al., 2015, Wolchok et al., 2013). This has led to the FDA approval of two anti-PD-1 Abs, nivolumab

(Opdivo®) and pembrolizumab (Keytruda®), for the treatment of patients with advanced melanoma, RCC, NSCLC, head and neck squamous cell carcinoma and Hodgkin's Lymphoma, and one Ab inhibiting PD-L1, atezolizumab (Tecentriq®), for the treatment of urothelial carcinoma. Clinical responses to PD-1 pathway blockade have been associated with: (i) PD-L1 expression by cancer cells and TILs (Herbst et al., 2014, Topalian et al., 2012b, Tumeh et al., 2014), (ii) presence of Th1-associated inflammatory mediators (Herbst et al., 2014, Tumeh et al., 2014), (iii) increased density and proliferation of intratumoral $CD8^+$ T cells with clonally expanded TCR repertoires (Tumeh et al., 2014), and (iv) elevated frequencies of tumor-associated neoantigens within the TME (Gubin et al., 2014, Johnson et al., 2016b, Rizvi et al., 2015, Yadav et al., 2014). This suggests that therapeutic efficacy of PD-1 pathway blockade requires re-activation and expansion of tumor-specific T cell immunity.

PD-1 pathway blockade has also yielded meaningful clinical activity in patients with lesser immunogenic cancers that do not typically respond to immunotherapy (Borghaei et al., 2015, Herbst et al., 2014, Topalian et al., 2012b), in addition to benefiting patients afflicted with immunogenic cancers, such as melanoma (Hamid et al., 2013, Herbst et al., 2014, Topalian et al., 2012b, Wolchok et al., 2013). The proposed mechanism of action for both PD-1 and CTLA-4 pathway blockade is re-activation of tumor-specific immune responses. Accordingly, the presence of immunogenic neoantigens and an immune-active TME are associated with favorable outcomes in cancer patients treated with either PD-1- (Gubin et al., 2014, Johnson et al., 2016b, Rizvi et al., 2015, Yadav et al., 2014) or CTLA-4-directed checkpoint blockade (Snyder et al., 2014a). Yet, evidence suggests that PD-1 inhibitors produce greater anticancer activity and fewer immune-related adverse events compared to the anti-CTLA-4 Ab ipilimumab (Menzies et al., 2016, Postow et al., 2015a, Robert et al., 2015b, Weber et al., 2013). Moreover, patients with advanced melanoma refractory to therapies targeting the immune checkpoint CTLA-4 showed marked clinical

responses to anti-PD-1 therapy (Hamid et al., 2013, Menzies et al., 2016, Ribas et al., 2015, Weber et al., 2015). The superior clinical efficacy of anti-PD-1 compared to anti-CTLA-4 blockade raises the possibility that anti-PD-1 therapy might also inhibit tumor cell-intrinsic or other pro-tumorigenic mechanisms, in addition to re-activating T cell-specific antitumor immunity.

PD-1 was previously shown to be expressed by subpopulations of $ABCB5^+$ dermal cells (Schatton et al., 2015) and $ABCB5^+$ melanoma initiating cells (Schatton et al., 2010), in addition to immune cells. The latter study also revealed that isolated $PD\text{-}1^+$ melanoma cells are significantly more tumorigenic compared to their $PD\text{-}1^-$ counterparts in an experimental tumor xenograft model that lacks adaptive immunity (Schatton et al., 2010). It was therefore hypothesized that the tumor growth-suppressive effects of anti-PD-1 therapy may result, at least in part, from direct inhibition of PD-1 on melanoma cells. PD-1 expression by established human and murine melanoma cell lines, syngeneic and xenogeneic tumor grafts, and clinical melanomas was thoroughly characterized. To date, the mechanisms underlying the clinical effectiveness of PD-1 blockade are not entirely understood. Studies geared towards further elucidating the molecular mechanisms of PD-1-driven tumorigenesis, and by extension, PD-1-targeted therapies, including potential immune-independent effects, are therefore of critical importance to further improve clinical efficacy.

4.1.2 PD-1 is expressed by melanoma cells

4.1.2.1 PD-1 is expressed by clinical melanomas

PD-1 expression was examined in a series of melanoma patient samples, to further expand upon the potential clinical significance of the previous finding that melanoma cells can express PD-1 (Schatton et al., 2010). Flow cytometric analysis of single cell suspensions

derived from clinical tumor specimens (*n*=8 patients) revealed PD-1 surface protein expression by melanoma subpopulations negative for the pan-lymphocyte marker, CD45, and the endothelial marker, CD31, in all melanoma specimens examined. Frequencies of PD-1^+ tumor cells ranged from 3.5% to 16.5% among $CD45^-$ live cells (cell frequency 8.7% ± 1.5%, mean ± SEM, Figure 2A). The gating strategy used for the detection of melanoma-expressed PD-1 is outlined in Figure 2B. Immunofluorescence double labeling of clinical melanoma biopsies (*n*=50) for PD-1 and the melanoma antigen recognized by T cells (MART)-1 confirmed PD-1 protein expression by subpopulations of MART-1^+ melanoma cells that were cytologically distinct from $CD45^+$ lymphocytes (Figure 2C). Overall *n*=22/36 melanoma patients demonstrated melanoma-PD-1 positivity in at least one of their tumor lesions (Table 1).

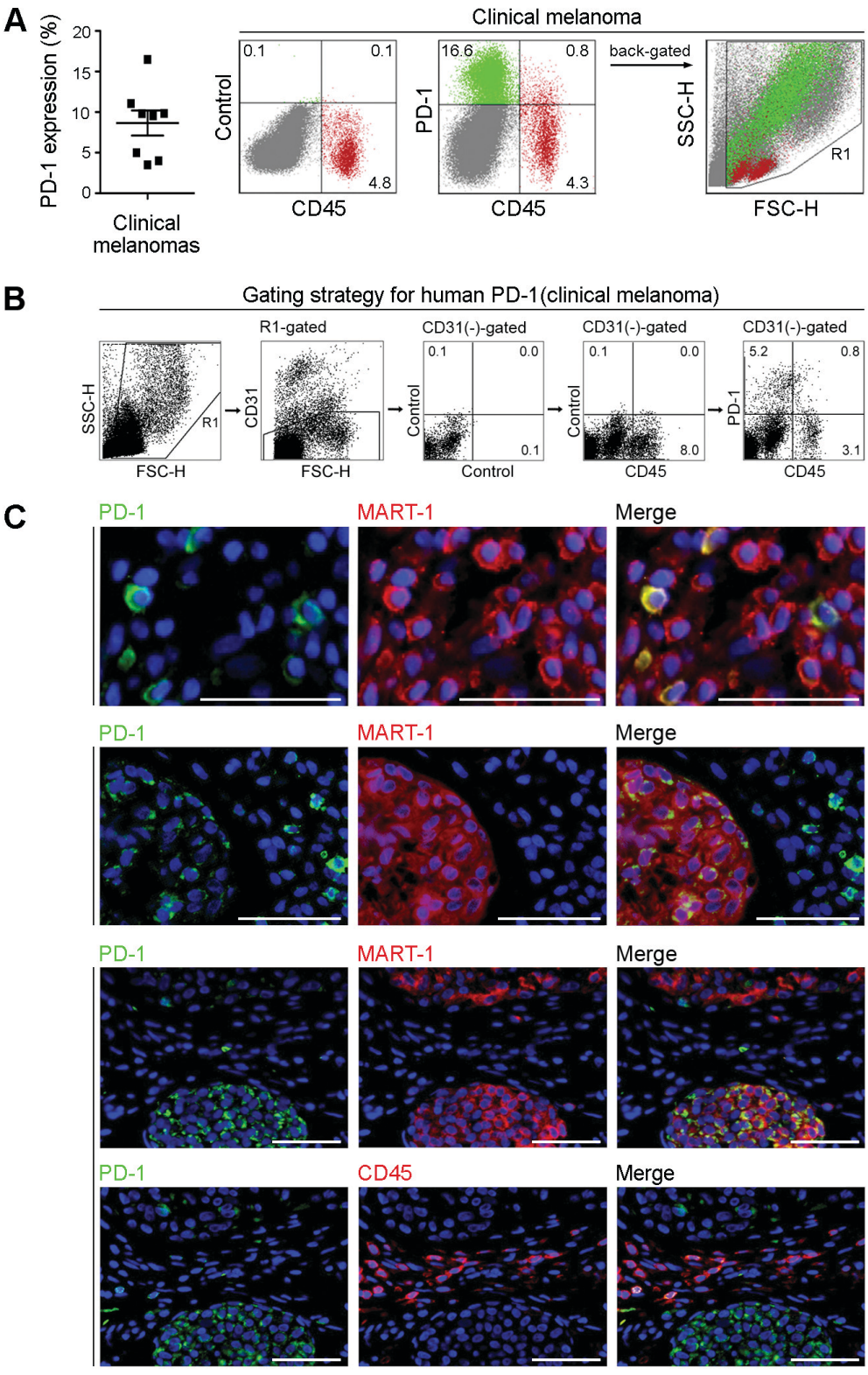

Figure 2. PD-1 expression by clinical melanomas. (A) Percentages (mean ± SEM) (left) and representative flow cytometry plots (right) of PD-1 surface protein expression by clinical tumor biopsy-derived melanoma cells (green) from n=8 distinct melanoma patients. These cells are negative for the CD45 lymphocyte common antigen (red) and the CD31 endothelial marker. (B) Gating strategy for the flow cytometric analysis of PD-1

surface protein expression by $CD31^-/CD45^-$ melanoma cells derived from a clinical tumor biospecimen, as shown in (A). (C) Representative immunofluorescence double stainings of three clinical melanoma biopsies for co-expression of PD-1 (green) and MART-1 (red) or of PD-1 (green) and CD45 (red) on a serial tissue section. Nuclei were counterstained with 4',6-Diamidino-2-Phenylindole (DAPI) (blue). Size bars, 100µm. Representatives of n=22/36 melanoma patients demonstrating melanoma-PD-1 positivity. A patient was considered melanoma-PD-1 positive if any tumor biopsy (total of n=50) showed expression of PD-1 by $MART\text{-}1^+$ and/or $CD45^-$ cells. Please see also Table 1. The data presented in this figure, with the exception of the top panels of Fig. 2C, has been previously published (Kleffel et al., 2015).

4.1.2.2 PD-1 is expressed by established human melanoma cell lines

To mechanistically dissect the role of melanoma-expressed PD-1 in experimental tumor growth, PD-1 expression by established human melanoma cell lines was characterized next. RT-PCR amplification and sequencing of the full coding sequence (CDS) of the human PD-1 (*PDCD1*) gene revealed *PDCD1* mRNA expression (Figure 3A), and immunoblot analysis demonstrated PD-1 protein expression by human A375, C8161 and G3361 melanoma cells (Figure 3B). Flow cytometric analyses showed PD-1 surface protein expression in 8/8 melanoma lines tested, with $PD\text{-}1^+$ tumor cell frequencies ranging from 11.3% ± 1.2% to 29.5% ± 3.7% (mean ± SEM, Figure 3C). Notably, PD-1 mRNA and protein were preferentially expressed by melanoma cell subsets positive for the tumor-initiating cell determinant (Schatton et al., 2008) ABCB5 in 8/8 cell lines studied (Figure 3D). This finding was consistent with the previous demonstration of PD-1 expression by $ABCB5^+$ melanoma-initiating cells (Schatton et al., 2010). Human A375, C8161 and G3361 melanoma lines also demonstrated positivity for both PD-1 ligands, with PD-L1 frequencies ranging from 2.4% ± 0.1% to 99.2% ± 0.1% (Figure 3E), and PD-L2 frequencies ranging from 0.6% ± 0.1% to 88.9% ± 2.6% of cells (mean ± SEM) (Figure

3F). PD-1 was also found to be co-expressed with both ligands, PD-L1 and PD-L2 (data not shown).

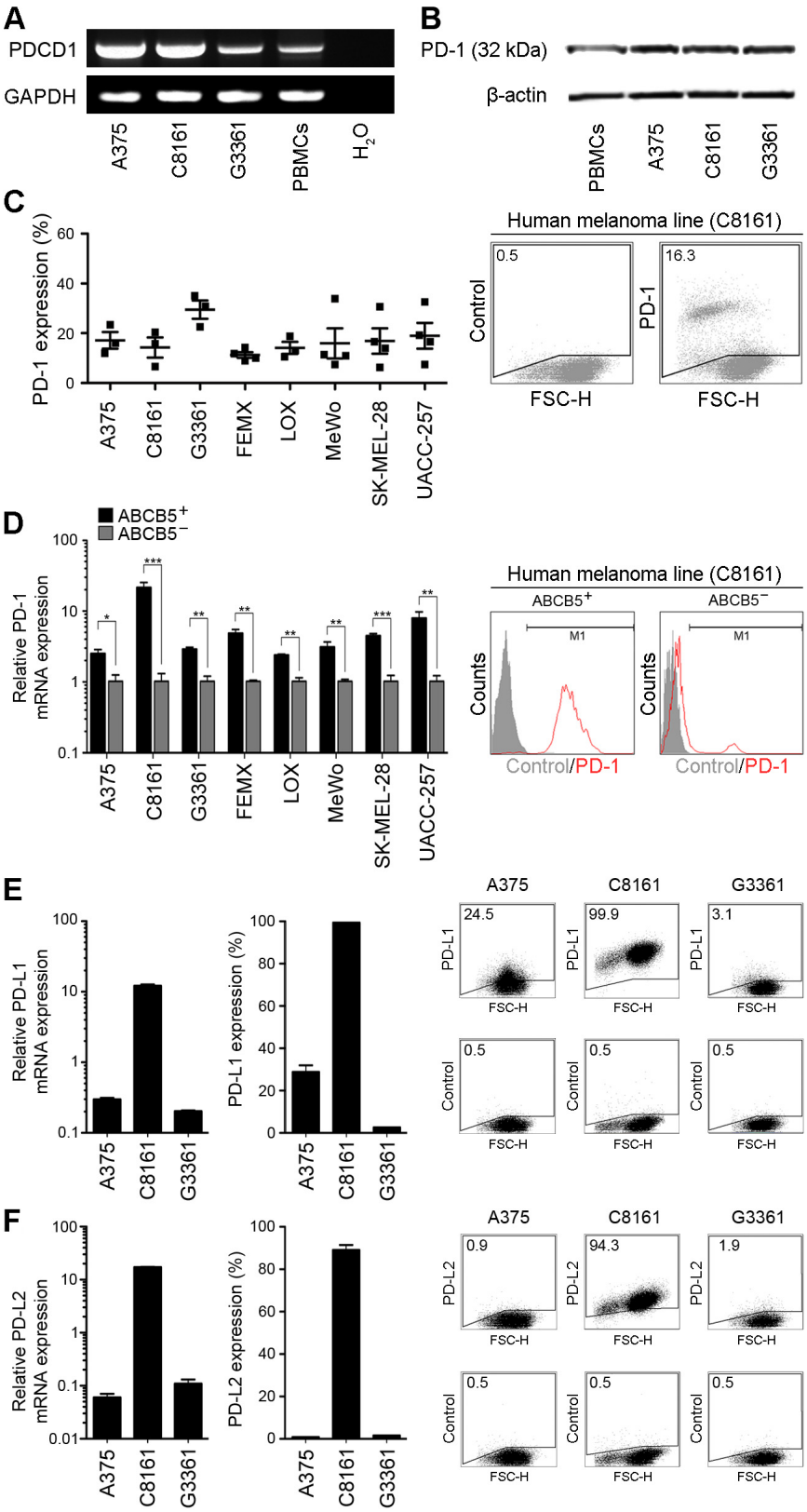

Figure 3. PD-1 expression by established human melanoma cells. (A) RT-PCR expression analysis of full-length PD-1 (*PDCD1*) mRNA and (B) immunoblot of PD-1

protein expression by established human melanoma lines and PBMCs. (C) Percentages (mean ± SEM, left) and representative flow cytometry plots (right) of PD-1 surface protein expression by human melanoma lines (*n*=3-4 independent experiments, respectively). (D) Relative PD-1 mRNA expression by sorted ABCB5^{+} versus ABCB5^{-} melanoma cells isolated from established human melanoma lines as determined by quantitative RT-PCR. Illustrated are PD-1 mRNA expression levels relative to those of ABCB5^{-} subsets for *n*=3 replicate experiments, respectively (left). Representative flow cytometry plots of PD-1 protein expression by ABCB5^{+} versus ABCB5^{-} human C8161 melanoma cells are shown on the right. (E) Relative PD-L1 and (F) PD-L2 mRNA expression by established human melanoma cells compared to PBMCs, as determined by quantitative RT-PCR (left). Percentages of PD-L1 and PD-L2 surface protein expression (mean ± SEM) by melanoma cells as determined by single-color flow cytometry (center) and representative flow cytometry plots (right). The data presented in this figure has been previously published (Kleffel et al., 2015).

4.1.2.3 PD-1 is expressed by established murine melanoma cell lines

In humans, melanoma development is tightly regulated by interactions between the immune system and malignantly transformed cells. The syngeneic murine C57BL/6-derived B16 melanoma model mimics the complex crosstalk between cancer and immune cells in the TME. PD-1 expression by established murine B16-F0 and B16-F10 melanoma cells was characterized to determine whether B16 melanoma is a translationally relevant model to study the effects of melanoma-expressed PD-1 on antitumor immunity and melanomagenesis. Similar to human melanomas, murine B16 cultures expressed PD-1 (*Pdcd1*) mRNA, as determined by amplification and sequencing of the full *Pdcd1* CDS (Figure 4A), and PD-1 protein as determined by immunoblotting (Figure 4B). Flow cytometric analysis revealed PD-1 surface protein expression by B16-F0 and B16-F10 melanoma lines, with PD-1^{+} tumor cell frequencies of 9.4% ± 2.5% and 6.6% ± 2.4%, respectively (mean ± SEM, Figure 4C). B16 melanoma grafts grown in NSG mice that

lack adaptive immunity also demonstrated PD-1 expression by MART-1^+ melanoma cells (Figure 4D). Both B16-F0 and B16-F10 cultures contained cell subsets that express ABCB5 (Figure 4E), consistent with previous demonstrations of ABCB5 expression in human and murine melanoma (Schatton et al., 2008, Zhang et al., 2016b). PD-1 mRNA and protein was preferentially expressed by murine $ABCB5^+$ melanoma cell subsets (Figure 4F), paralleling findings in human melanoma (Schatton et al., 2010). Murine B16-F0 and B16-F10 melanoma cells expressed PD-L1 with frequencies of 43.4% ± 9.4%, and 37.5% ± 2.3%, respectively (Figure 4G), but not PD-L2 surface protein (Figure 4H). PD-1 was also found to be co-expressed with its ligand PD-L1 (data not shown).

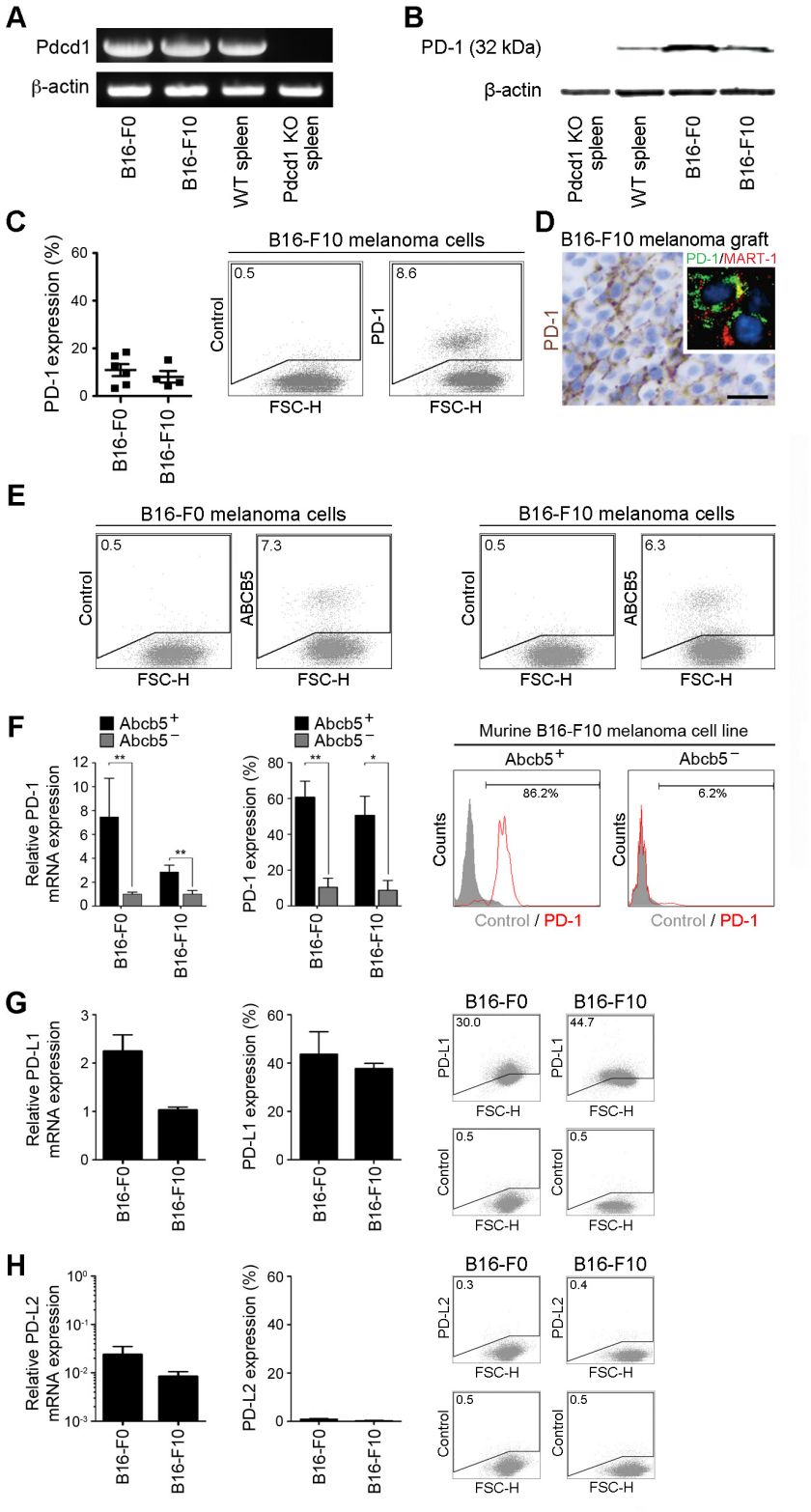

Figure 4. PD-1 expression by established murine melanoma cells. (A) RT-PCR expression analysis of full-length PD-1 (*Pdcd1*) mRNA and (B) immunoblot of PD-1 protein expression by murine B16-F0 and B16-F10 melanoma cells, wildtype (WT) and *Pdcd1* KO C57BL/6-derived splenocytes. (C) Percentages (mean ± SEM, left) and representative flow cytometry plots (right) of PD-1 surface protein expression by B16 cells

(*n*=4-6 independent experiments, respectively). (D) Representative PD-1 IHC and immunofluorescence double staining for co-expression of PD-1 (green) with MART-1 (red) (inset photomicrograph) of a B16-F10 melanoma graft grown in NSG mice (size bar, 50μm). (E) Representative flow cytometry plots of ABCB5 surface protein expression by B16 cells. (F) Relative PD-1 mRNA expression by sorted $ABCB5^+$ versus $ABCB5^-$ melanoma cells isolated from established murine melanoma lines as determined by quantitative RT-PCR. Illustrated are PD-1 mRNA expression levels relative to those of $ABCB5^-$ subsets for *n*=3 replicate experiments, respectively (left). PD-1 protein expression by $ABCB5^+$ versus $ABCB5^-$ murine B16 (*n*=3-4 replicate experiments per cell line, center). Representative flow cytometry plots are shown on the right. (G) Relative PD-L1 and (H) PD-L2 mRNA expression by established murine B16-F0 and B16-F10 melanoma cells compared to C57BL/6 splenocytes, as determined by quantitative RT-PCR (left), and percentages of PD-L1 and PD-L2 surface protein expression (mean ± SEM) by B16-F0 and B16-F10 cells (center). Representative flow cytometry plots are shown on the right. The data presented in this figure, with the exception of Fig. 4E, has been previously published (Kleffel et al., 2015).

To assess the tumorigenic capacity of native $ABCB5^+$ compared to $ABCB5^-$ B16-F0 and B16-F10 melanoma subpopulations, sorted cells were grafted to syngeneic C57BL/6 mice. Murine $ABCB5^+$ subpopulations demonstrated significantly increased *in vivo* tumor growth compared to $ABCB5^-$ tumor cells (Figure 5A), consistent with previous demonstrations in human melanoma (Schatton et al., 2008). In addition, $ABCB5^+$-sorted B16-F0 and B16-F10 melanoma cells expressed significantly lower levels of the MAAs microphthalmia-associated transcription factor (Mitf) and tyrosinase compared to $ABCB5^-$ melanoma populations (Figure 5B). Mart-1 expression was significantly decreased in $ABCB5^+$- versus $ABCB5^-$-sorted B16-F0, but not B16-F10 melanoma cells, suggesting a greater variability in expression levels of this marker compared to Mitf and Tyrosinase (Figure 5B). Similarly, human $ABCB5^+$ melanoma cells demonstrate decreased MAA expression compared to their $ABCB5^-$ counterparts (Schatton et al., 2010).

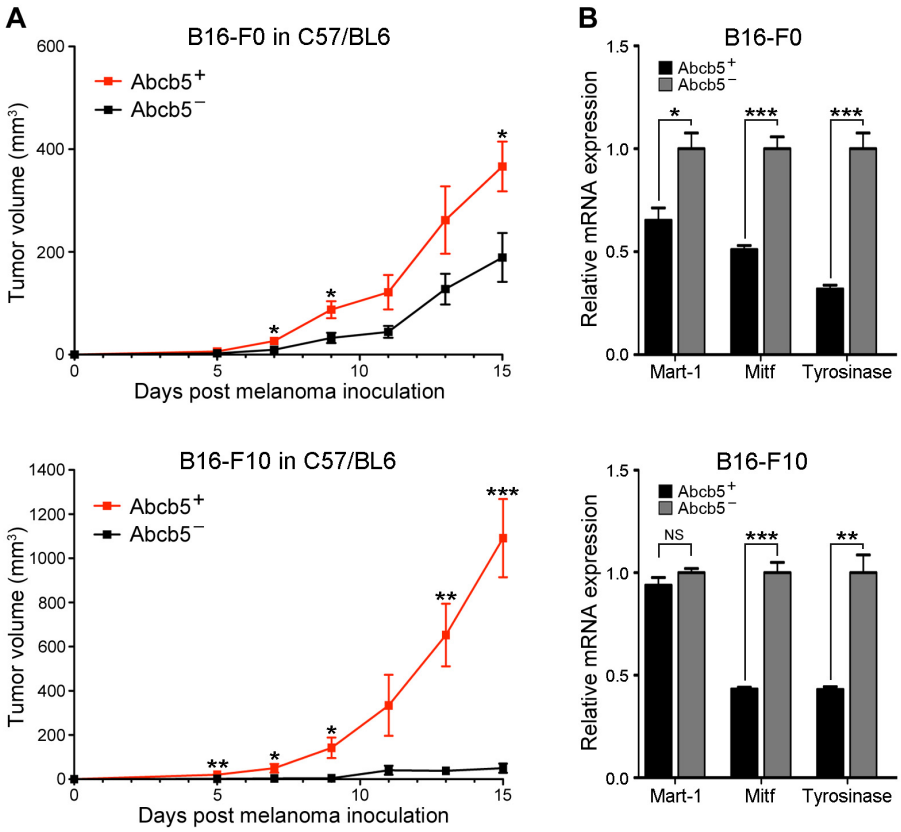

Figure 5. ABCB5 promotes tumorigenicity in a syngeneic murine melanoma model. (A) Tumor growth kinetics (mean ± SD) of sorted ABCB5$^+$ versus ABCB5$^-$ B16-F0 and B16-F10 melanoma cells grafted to C57BL/6 mice (n=10 each). (B) Relative mRNA expression of Mart-1, Mitf and Tyrosinase by sorted ABCB5$^+$ versus ABCB5$^-$ melanoma cells isolated from established murine melanoma lines as determined by quantitative RT-PCR. Illustrated are mRNA expression levels relative to those of ABCB5$^-$ subsets for n=3 replicate experiments, respectively. (NS: not significant, *P<0.05, **P<0.01, ***P<0.001). This figure shows previously unpublished data.

4.1.3 Discussion

This chapter provides a comprehensive characterization of PD-1 transcript and protein expression by cancer cells in clinical melanoma biopsies and established human and murine melanoma lines. Previously, PD-1 expression had been mainly reported in immune-competent cells of the hematopoietic lineage (Topalian et al., 2012a). Using

various independent methods, including RT-PCR, immunoblotting, and flow cytometric analysis, the herein presented data revealed that all melanoma cell lines and surgical specimens examined harbored PD-1-expressing cancer cells. Furthermore, immunofluorescence double labeling similarly showed PD-1 expression by melanoma subpopulations in clinical biopsy specimens obtained from >60% of melanoma patients. However, PD-1 was not uniformly present on all melanoma cells among heterogeneous tumor samples. Rather, it was restricted to small melanoma subpopulations. Similarly, ABCB5 expression is limited to subsets of melanoma cells that are nonetheless critically important for tumor initiation and growth (Schatton et al., 2008, Zhang et al., 2016b). Interestingly, both PD-1 and ABCB5 proteins were preferentially co-expressed by human and murine melanoma cells, consistent with previous reports (Schatton et al., 2010). Comparably, melanoma cell expression of the PD-1 ligand, PD-L1, is often confined to small subsets of cancer cells within clinical tumor specimens (Herbst et al., 2014, Kakavand et al., 2015, Topalian et al., 2012b), and PD-1 and PD-L1 were also co-expressed by established human and murine melanoma cell lines in this study.

$ABCB5^+$-sorted native B16 melanoma cells demonstrated significantly increased tumor growth *in vivo,* compared to $ABCB5^-$ cell subsets, consistent with previous reports of preferential tumorigenicity of $ABCB5^+$ human and murine melanoma cells (Schatton et al., 2008, Zhang et al., 2016b). In addition, murine $ABCB5^+$ B16 melanoma subpopulations also expressed markedly reduced levels of MAAs compared to $ABCB5^-$ cell subsets, paralleling previous findings in human $ABCB5^+$ melanoma cells (Schatton et al., 2010). Due to the similarity to human disease, the syngeneic B16 mouse model was deemed translationally relevant to study the immunoregulatory functions of cancer cell-expressed PD-1 in melanoma growth. Tumorigenic murine B16 melanoma cells may be capable of regulating antitumor immunity because they preferentially co-express the checkpoint inhibitor PD-1 and ABCB5, and downmodulate the expression of MAAs. In

support, ABCB5^{+} dermal cells have been shown to inhibit T cell proliferation and induce Tregs, at least partly, via dermal cell-expressed PD-1 (Schatton et al., 2015). Moreover, ABCB5^{+}PD-1^{+} melanoma cell subsets impair T cell proliferation, and induce Tregs and secretion of the immunosuppressive cytokine IL-10 (Schatton et al., 2010).

In summary, clinical melanoma specimens and established human and murine melanoma cell lines contain PD-1^{+} cancer cell subsets that preferentially co-express ABCB5, a marker of immunoregulatory dermal cells and tumor-initiating cells in human melanoma (Schatton et al., 2008, Schatton et al., 2010, Schatton et al., 2015). Figure 6 highlights the key findings presented in this chapter.

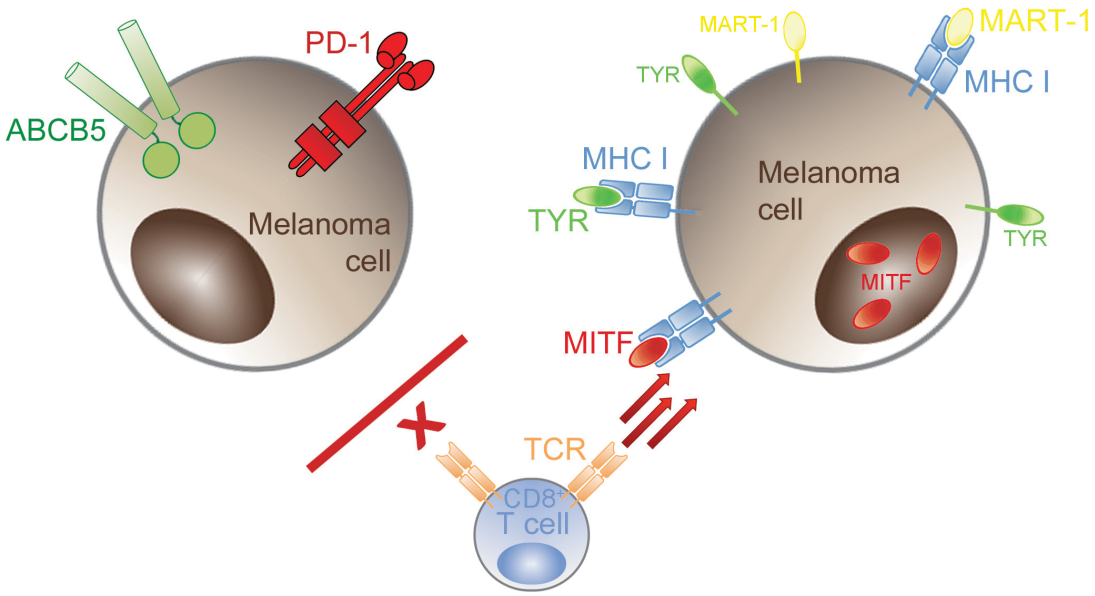

Figure 6. PD-1 expression by melanoma cells. Melanoma cells in clinical tumor biopsies and established human and murine melanoma cell lines frequently contain PD-1 expressing subpopulations. PD-1 is preferentially expressed by tumorigenic ABCB5^{+} melanoma cell subsets. ABCB5^{+} melanoma cells express decreased levels of MAAs like Mart-1, Mitf and tyrosinase compared to ABCB5^{-} cell subsets. Both, expression of the inhibitory immune checkpoint receptor PD-1 and decreased expression of MAAs may serve as a potential mechanism to evade recognition by tumor-specific immune cells like CD8^{+} CTLs.

4.2 Melanoma-expressed PD-1 modulates antitumor immune responses.

Parts of this chapter have been previously published in *Kleffel S. et al. Melanoma Cell-Intrinsic PD-1 Receptor Functions Promote Tumor Growth. Cell 2015;162(6):1242-56.* Published data is highlighted in the individual figure legends.

4.2.1 Introduction

The PD-1 receptor and its two known ligands, PD-L1 and PD-L2, are expressed by a wide variety of immune cells known to infiltrate tumors, including T cells and MDSCs (Francisco et al., 2010). Both, frequency and level of PD-1 expression by effector and regulatory T cells are markedly increased in the TME compared to physiologic tissues (Ahmadzadeh et al., 2009, Baitsch et al., 2011a, Krempski et al., 2011, Nishikawa and Sakaguchi, 2010). In addition, the inflammatory milieu of the TME promotes the expression of PD-1 ligands by tumor, immune, and stromal cells. Indeed, the major PD-1 ligand, PD-L1, is expressed by subpopulations of melanoma cells that are in close proximity to PD-1^+ T cells in ~ 40% of clinical melanoma biopsies (Kakavand et al., 2015, Taube et al., 2012). Binding of TME-expressed PD-1 ligand to the PD-1 receptor on tumor-infiltrating T cells can trigger functional exhaustion, anergy, or apoptosis of tumor-specific CTLs, thereby protecting cancers from immune-mediated rejection (Wherry, 2011). In addition, cancer cells exploit the PD-1 pathway to regulate the expansion and immunosuppressive capacity of tolerogenic cell subsets, like Tregs and MDSCs, both of which are capable of shaping tumor-specific T cell immunity (Highfill et al., 2014, Nishikawa and Sakaguchi, 2014). For example, PD-1 receptor signaling promotes Treg development and enhances their suppressive function (Amarnath et al., 2011, Francisco et al., 2009). PD-L1 also plays a critical role in Treg induction and maintenance (Habicht et al., 2007, Krupnick et al., 2005). The role of MDSC-expressed PD-1 remains controversial

(Green et al., 2013), however PD-L1 is highly expressed by MDSCs and mediates suppression of T cell-dependent immunity (Highfill et al., 2014, Lei et al., 2015, Noman et al., 2014).

PD-1 has been previously shown to define immunoregulatory cell subpopulations in normal skin and melanoma (Schatton et al., 2010, Schatton et al., 2015). Subsets of dermal cells suppress T cell function and induce Tregs, at least in part, via dermal cell-expressed PD-1 signaling (Schatton et al., 2015). Moreover, virulent melanoma cells that express PD-1 also impair T cell function and promote Treg maintenance (Schatton et al., 2010). Consistently, recent evidence suggests that both PD-L1 and PD-L2 can serve as receptors and transmit bi-directional signals upon engagement to PD-1 that can be immunoinhibitory or -stimulatory, depending on the cellular context, adding to the complexity of the PD-1:PD-1 ligand axis in immunomodulation (Azuma et al., 2008, Francisco et al., 2010). It was therefore hypothesized that melanoma-PD-1:lymphocyte-PD-1 ligand interactions confer immunoevasive and protumorigenic properties to melanoma cells. Determining TME-specific and systemic effects of melanoma-expressed PD-1 on the composition of effector and regulatory T cells and MDSC, and understanding how the crosstalk between immune cells and cancer cells within the TME regulates tumor progression and metastasis is crucial for improving immunotherapy, and was therefore assessed in the syngeneic B16 melanoma model.

4.2.2 Melanoma-expressed PD-1 promotes tumor growth in immunocompetent mice

To dissect the potential role of melanoma-expressed PD-1 in tumor immune evasion and cancer growth, stable *Pdcd1* KD and *Pdcd1*-OE B16 melanoma lines were generated.

Transduction of B16-F0 and B16-F10 cells with two distinct shRNAs targeting *Pdcd1* inhibited murine PD-1 mRNA expression by ≥59% and significantly blocked PD-1 protein expression compared to controls (Figure 7A), but did not significantly alter expression of PD-L1 or PD-L2 (data not shown). Conversely, transduction of B16 cells with *Pdcd1*-encoding constructs resulted in marked upregulation of PD-1, both at the mRNA and protein level (Figure 7B). Melanoma-specific *Pdcd1*-KD resulted in significantly decreased and *Pdcd1*-OE in markedly increased B16-F0 and B16-F10 melanoma growth in immunocompetent C57BL/6 mice compared to that of vector controls (Figure 7C). *Pdcd1*-KD melanoma grafts demonstrated diminished (Figure 7D) and *Pdcd1*-OE melanomas significantly enhanced *Pdcd1* mRNA and PD-1 protein expression compared to control tumors at the experimental endpoint (Figure 7E).

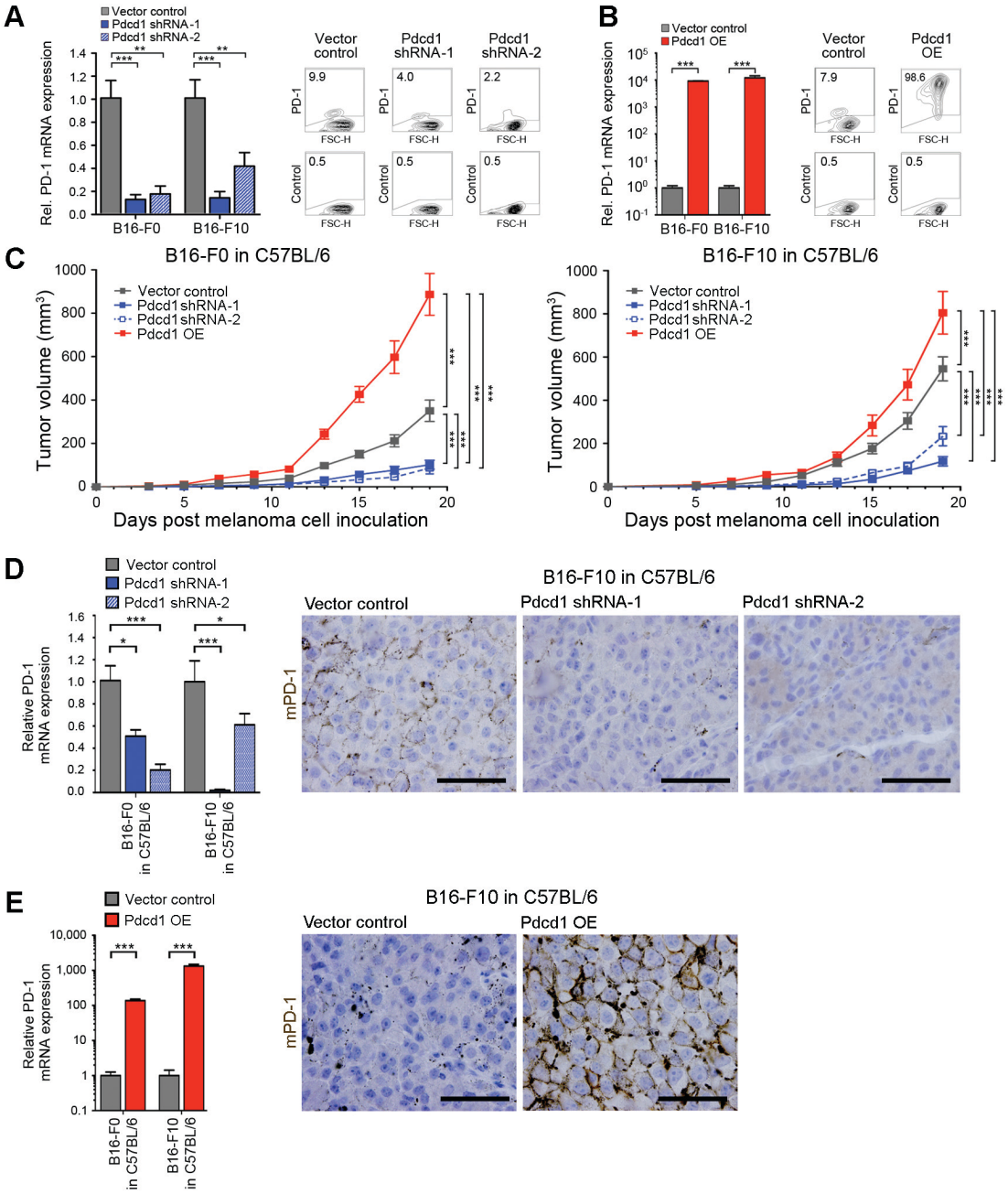

Figure 7. Melanoma-expressed PD-1 promotes tumorigenicity in immunocompetent mice. (A) Relative PD-1 mRNA expression (mean ± SEM) by *Pdcd1*-shRNA-1 and *Pdcd1*-shRNA-2 versus vector control and by (B) *Pdcd1*-OE versus vector control B16-F0 or B16-F10 melanoma cells, as determined by quantitative RT-PCR. Illustrated are PD-1 mRNA expression levels relative to those of vector control-transduced cells (left). Representative flow cytometry plots show PD-1 protein expression in B16-F10 melanoma variants (right). (C) Tumor growth kinetics (mean ± SD) of *Pdcd1*-shRNA-1/-2 versus *Pdcd1*-OE versus vector control B16-F0 or B16-F10 melanomas in C57BL/6 mice (n=10-30 each). (D) PD-1 mRNA expression (mean ± SEM) as determined by quantitative RT-PCR (left) and representative IHC images of PD-1 protein expression (B16-F10, right) of

murine B16 melanomas harvested 19 days post inoculation of *Pdcd1*-shRNA-1/-2- versus vector control- or of (E) *Pdcd1*-OE- versus vector control-transduced B16-F0 or B16-F10 melanoma cells to C57BL/6 mice, respectively. Similar IHC results were obtained for B16-F0 melanoma variant grafts (not shown). Size bars, 50µm. (* P<0.05, ** P<0.01, *** P<0.001). The data presented in this figure has been previously published (Kleffel et al., 2015).

To determine the tumorigenic capacity of PD-1 expressed by native melanoma cells, B16-F0 and B16-F10 cultures were sorted into PD-1$^+$ versus PD-1$^-$ melanoma cell subsets using fluorescence activated cell sorting (Figure 8A). PD-1$^+$ B16 melanoma subpopulations demonstrated significantly increased tumor growth in syngeneic C57BL/6 mice compared to PD-1$^-$ cells (Figure 8B). Together, these findings identify melanoma-expressed PD-1 as a protumorigenic mechanism.

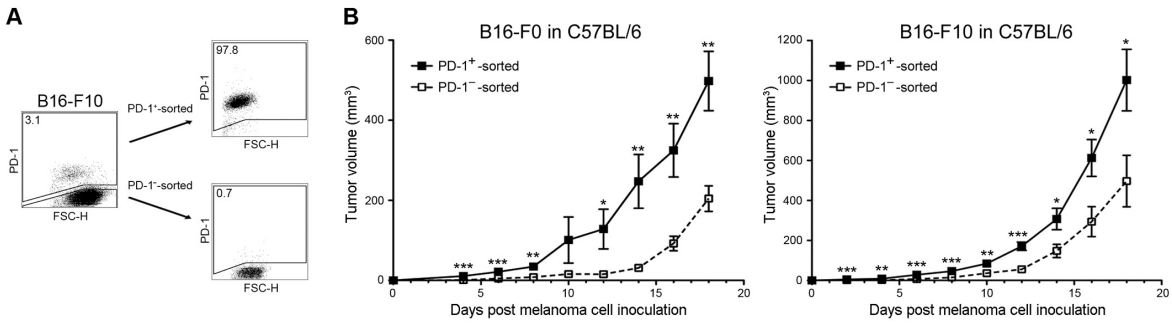

Figure 8. Native PD-1$^+$ melanoma cells promote tumorigenicity in immunocompetent mice. (A) Representative flow cytometry plots of PD-1 surface protein expression by B16 cells pre- (left) and post-sort for PD-1$^+$ versus PD-1$^-$ cell populations (right). (B) Tumor growth kinetics (mean ± SD) of sorted PD-1$^+$ versus PD-1$^-$ B16-F0 and B16-F10 melanoma cells grafted to C57BL/6 mice (n=10 each). (* P<0.05, ** P<0.01, *** P<0.001). The data presented in this figure has been previously published (Kleffel et al., 2015).

4.2.3 Melanoma-expressed PD-1 inhibits T effector cell functions in the tumor microenvironment

PD-1 expressed by immune cells plays a well-defined role in inhibiting antitumor immunity (Topalian et al., 2012a). To determine whether the observed tumor growth-accelerating effects of melanoma-expressed PD-1 are associated with the suppression of T cell immunity in the TME, the frequencies and phenotypes of T cells in tumor-bearing mice were assessed next.

Flow cytometric characterization of TILs isolated from *Pdcd1*-KD versus control B16-F10 melanomas revealed significantly increased frequencies of $CD4^+$ T cells producing the effector cytokines IFN-γ, TNF-α, and both IFN-γ and TNF-α (Figure 9A, top). *Pdcd1*-KD tumors also contained increased frequencies of TNF-α-producing $CD8^+$ TILs compared to controls (Figure 9A, bottom). Consistently, significantly decreased frequencies of activated $CD44^+CD62L^-$ $CD4^+$ and $CD8^+$ T effector cells were found in *Pdcd1*-OE versus control B16 melanomas (Figure 9B). Furthermore, overexpression of PD-1 markedly inhibited production of IFN-γ, TNF-α, and both IFN-γ and TNF-α by $CD4^+$ and by $CD8^+$ TILs compared to controls (Figure 9B).

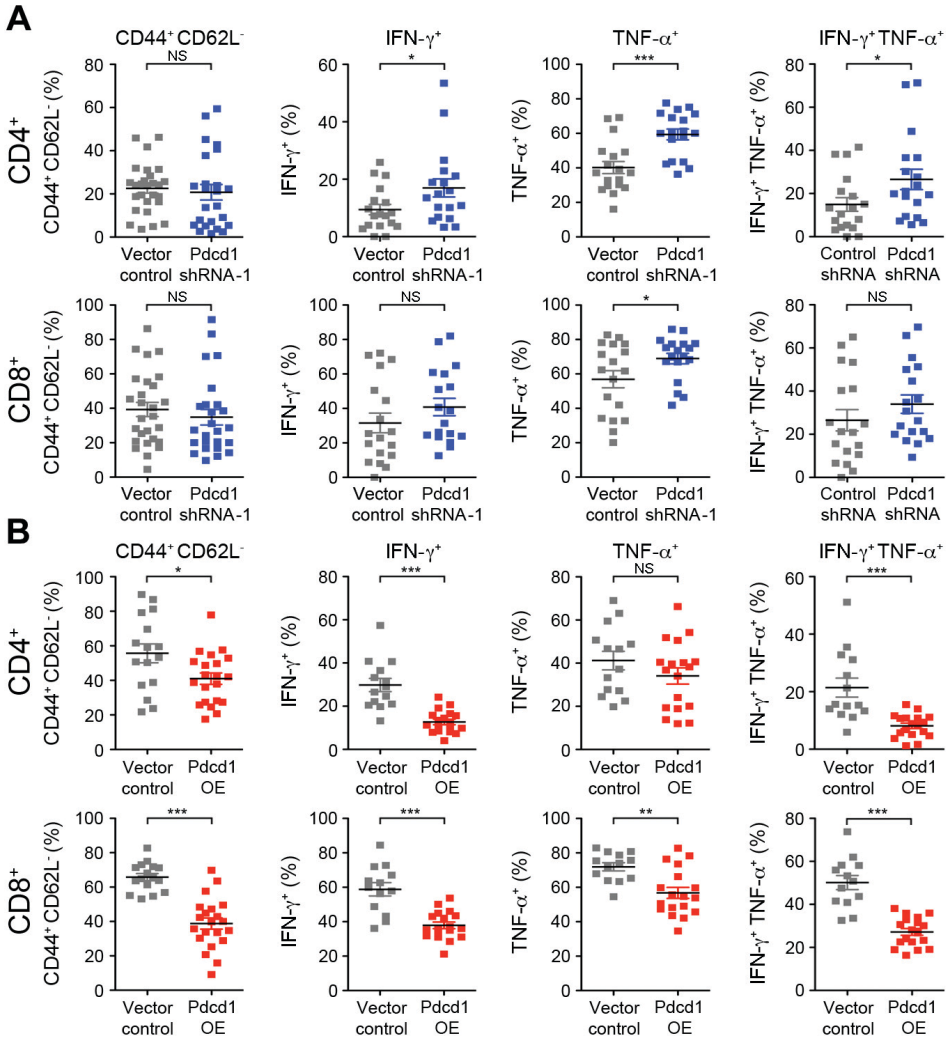

Figure 9. Melanoma-expressed PD-1 regulates T cell immunity in the tumor microenvironment. (A) Flow cytometric characterization of T cells infiltrating Pdcd1-shRNA-1 versus vector control, or (B) Pdcd1-OE versus vector control B16-F10 melanoma grafts in C57BL/6 mice 14-18 days post tumor cell inoculation, respectively. Frequencies (mean ± SEM) of $CD44^+CD62L^-$, IFN-γ^+, TNF-α^+, and IFN-γ^+TNF-α^+ cells among $CD4^+$ (top) or $CD8^+$ TILs (bottom) are illustrated. (NS: not significant, *P<0.05, **P<0.01, ***P<0.001). This figure shows previously unpublished data.

Importantly, frequencies of $CD44^+CD62L^-$ T effector cells, and IFN-γ-, TNF-α-producing, or IFN-γ-TNF-α double-producing $CD4^+$ or $CD8^+$ T cells were not significantly different in tumor-draining lymph nodes (dLNs) or spleens of *Pdcd1*-KD versus control (Figure 10A) or *Pdcd1*-OE versus control B16 melanoma-bearing mice (Figure 10B).

Together, these findings suggest that melanoma-expressed PD-1 mediates a local, TME-specific, but not systemic inhibition of T effector cell functions.

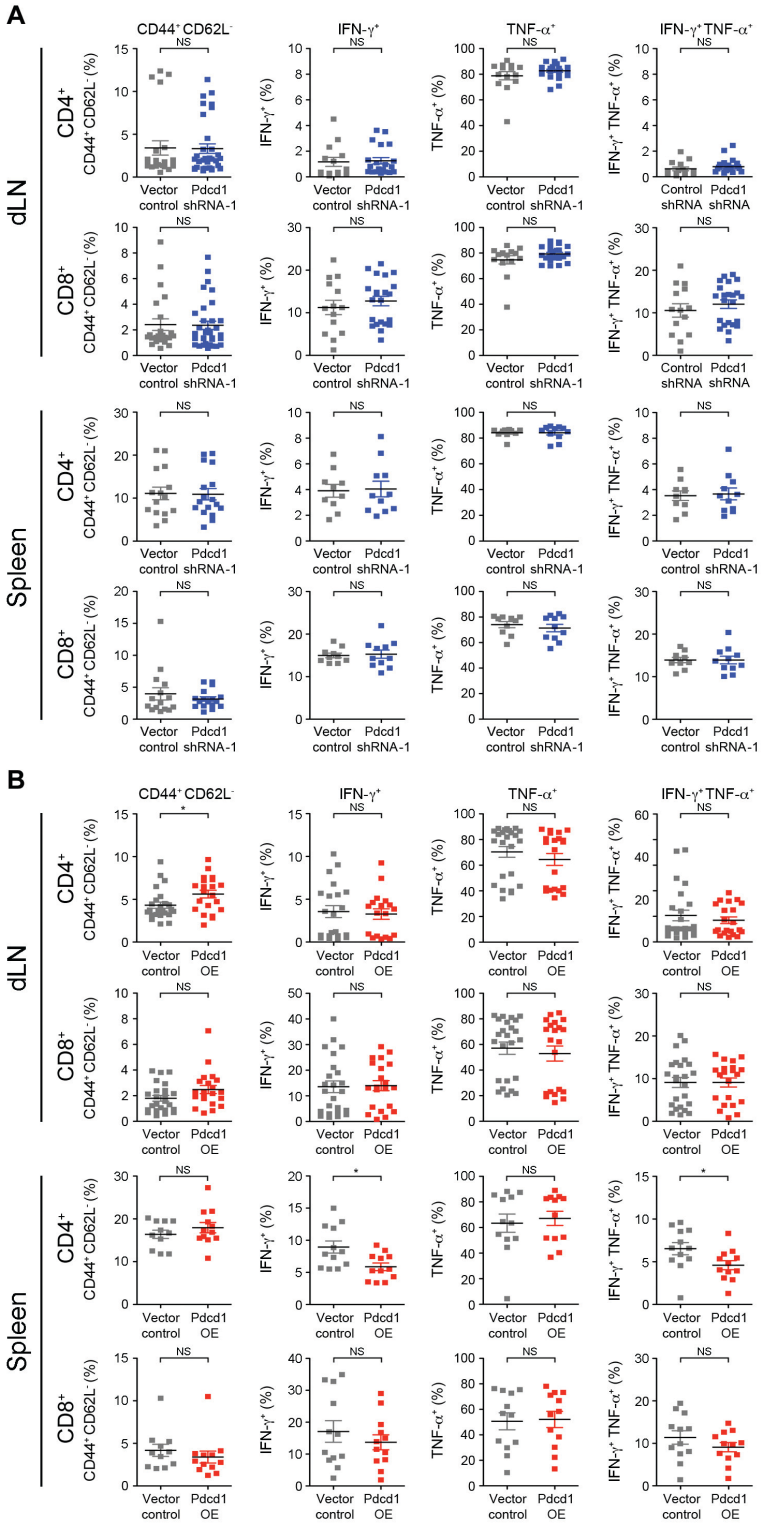

Figure 10. Melanoma-expressed PD-1 does not modulate systemic T effector cell functions. (A) Frequencies (mean ± SEM) of $CD44^{+}CD62L^{-}$, IFN-γ^{+}, TNF-α^{+}, and IFN- γ^{+}

TNF-α^+ cells among $CD4^+$ or $CD8^+$ T cells isolated from tumor dLNs (top) or spleens (bottom) of Pdcd1-shRNA-1 versus vector control or (B) Pdcd1-OE- versus vector control B16-F10 melanoma-bearing C57BL/6 mice 14-18 days post tumor cell inoculation, respectively. (NS: not significant, * P<0.05). This figure shows previously unpublished data.

To determine whether this inhibition of TIL effector functions by melanoma-expressed PD-1 results from the induction and/or local expansion of tolerogenic immune cells, the frequency of Tregs in tumor-bearing mice was assessed. The analysis of $CD4^+Foxp3^+$ Treg frequencies among lymphocytes isolated from the TME, dLNs and spleens of *Pdcd1*-KD versus control (Figure 11A), or *Pdcd1*-OE versus control melanoma-bearing mice did not reveal any significant differences (Figure 11B). This suggests that melanoma-expressed PD-1 regulates activation and function of T effector cell populations, rather than affecting Treg frequencies in this experimental model.

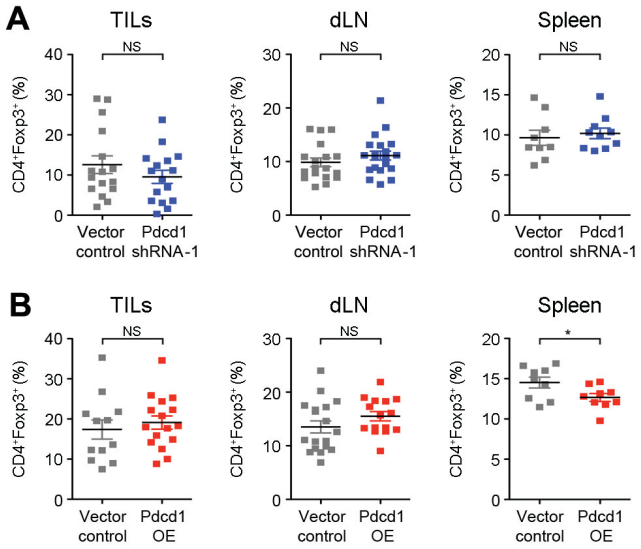

Figure 11. PD-1 expression by melanoma grafts does not alter frequencies of regulatory T cells in tumor bearing mice. (A) $FoxP3^+$ Treg frequencies (mean ± SEM) among $CD4^+$ T cells isolated from tumor tissue (left), tumor dLNs (center) or spleens (right) of Pdcd1-shRNA-1 versus vector control or (B) Pdcd1-OE versus vector control-transduced B16-F10 melanoma-bearing C57BL/6 mice 14-18 days post tumor cell

inoculation, respectively, as determined by flow cytometry. (NS: not significant, * $P<0.05$). This figure shows previously unpublished data.

4.2.4 Melanoma-PD-1 induces tolerogenic myeloid derived suppressor cells

MDSC-expressed PD-L1 has been shown to further up-regulate PD-1 expression by T cells, thereby decreasing the frequencies of IFN-γ producing $CD4^+$ and $CD8^+$ T cells, while expanding Tregs (Noman et al., 2014, Pinton et al., 2015). To determine whether MDSCs contribute to the observed effects of enhanced tumor growth and reduced T cell activation, the frequency and phenotype of MDSCs in tumor-bearing mice was analyzed. Flow cytometric analysis revealed a trend toward increased frequencies of monocytic $CD11b^+Ly6C^+$ MDSCs in the TME of wildtype C57BL/6 recipient mice grafted with *Pdcd*-1 OE versus control B16-F10 melanoma cells (Figure 12A). No differences in frequencies of granulocytic $CD11b^+Ly6G^+$ MDSCs were observed in the TME of *Pdcd-1*-OE compared to control B16-F10 melanoma bearing mice (data not shown).

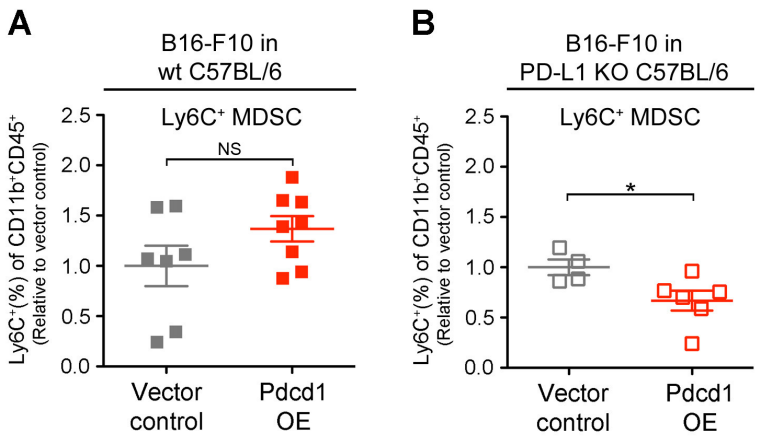

Figure 12. Melanoma-expressed PD-1 modulates frequencies of intratumoral myeloid-derived suppressor cells. (A) Frequencies (mean ± SEM) of Ly-6C$^+$

$CD11b^+CD45^+$ monocytic MDSCs isolated from Pdcd1-OE- versus vector control B16-F10 melanomas 14-18 days post tumor cell inoculation of wt or (B) PD-L1 KO C57BL/6 mice, respectively. (NS: not significant, * $P<0.05$). This figure shows previously unpublished data.

In previous studies, PD-L1 expression by MDSCs was upregulated in the hypoxic environment of solid tumors like melanoma, and PD-L1 signaling promoted MDSC suppressive function (Noman et al., 2014). To test whether melanoma-PD-1:MDSC-PD-L1 interactions are required for the maintenance of immunosuppressive monocytic MDSCs within the TME, *Pdcd1*-OE versus control B16-F10 melanoma cells were grafted to wildtype C57BL/6 versus PD-L1 (-/-) KO recipient mice(Latchman et al., 2004). Significantly lower frequencies of $CD11b^+Ly6C^+$ MDSC were observed in the TME of PD-L1 (-/-) KO mice grafted with *Pdcd1*-OE versus vector control B16 melanoma cells (Figure 12B), suggesting that ligation of melanoma-PD-1 to MDSC:PD-L1 may drive the recruitment of MDSCs to the TME and/or their local expansion.

4.2.5 Discussion

Expression of the major PD-1 ligand, PD-L1, by melanoma cells and its roles in promoting tumor immune evasion and melanoma progression are well established (Dong et al., 2002a, Taube et al., 2012). However, the potential role of melanoma-expressed PD-1 in tumor growth had not been addressed previously. To test whether melanoma-expressed PD-1 drives tumor growth, stable *Pdcd1*-KD and *Pdcd1*- OE B16 melanoma lines were generated. Interestingly, PD-1 KD inhibited and enforced PD-1 expression promoted tumor growth in syngeneic, immunocompetent C57BL/6 mice. Consistently, $PD\text{-}1^+$-sorted native B16 melanoma cell subsets also demonstrated accelerated tumorigenicity *in vivo*

compared to PD-1$^-$-sorted cell isolates. These findings are consistent with the tumor growth-inhibitory effects of PD-1 blockade observed in the clinic.

To dissect whether melanoma-expressed PD-1 promotes tumor growth by negatively regulating anti-tumor immunity, the effects of melanoma-PD-1:T cell PD-1 ligand interactions on T effector cell function were studied. PD-1 expressed by melanoma cells markedly inhibited production of the effector cytokines, IFN-γ and TNF-α, by tumor infiltrating CD4$^+$ and CD8$^+$ T cells, consistent with the inhibitory role of T cell-expressed PD-1 in limiting T effector functions (Francisco et al., 2010). Importantly, the observed inhibition of T effector cell cytokine production was TME-specific rather than systemic, since no differences in IFN-γ and TNF-α production by T cells were observed in draining lymph nodes and spleens of tumor-bearing mice. This melanoma-PD-1-mediated inhibition of T cell immunity is consistent with the herein described tumor growth-promoting effects of cancer cell-expressed PD-1.

Tolerogenic Tregs and MDSCs frequently infiltrate melanomas and maintain an immunosuppressive TME by inhibiting TAg-specific T cell responses (Nishikawa and Sakaguchi, 2014, Noman et al., 2014). Since PD-L1 plays an important role in Treg maintenance and suppressive capacity (Habicht et al., 2007, Krupnick et al., 2005), changes in Treg frequency in response to melanoma expressed-PD-1 were assessed. Melanoma-specific PD-1 KD or OE, however, did not affect Treg frequencies in the TME, dLNs or spleens in the B16 melanoma model. Whether melanoma-expressed PD-1 modulates the suppressive capacity of Tregs, thereby inhibiting T effector cell functions, requires further elucidation.

Melanoma-expressed PD-1 increased the frequency of monocytic CD11b$^+$Ly6C$^+$, but not granulocytic CD11b$^+$Ly6G$^+$ MDSCs within tumors. Monocytic MDSCs are capable of inhibiting both antigen-specific and non-specific T cell responses, and have stronger suppressive capacity on a per cell basis, compared to granulocytic MDSCs (Gabrilovich et

al., 2012). PD-L1 activation is important for MDSC maintenance and suppressive functions, at least in part, via MDSC-PD-L1-dependent up-regulation of PD-1 expression by activated T effector and Treg cells (Highfill et al., 2014, Lei et al., 2015, Pinton et al., 2015). Consistently, the observed increase in monocytic MDSCs by melanoma-expressed PD-1 was abrogated in PD-L1-deficient tumor-bearing recipient mice. Understanding whether interactions of melanoma-expressed PD-1 with MDSC-expressed PD-L1 directly modulate the immunosuppressive capacity of MDSCs, or whether melanoma-PD-1 mediated activation of MDSCs indirectly modulates antitumor immunity by inhibiting T effector cell functions requires further investigation. In addition, melanoma-PD-1 engagement by MDSC-expressed PD-L2 might also affect MDSC function, thereby adding to the complexity.

Melanoma-expressed PD-1 may also control the differentiation and functional activity of additional PD-1 ligand-expressing immune cell types to further promote the immunosuppressive network at the tumor site. To elucidate the effects of melanoma-expressed PD-1 on other immune compartments, and to help dissect the molecular and cellular factors underlying melanoma-PD-1-dependent modulation of antitumor immunity and cancer growth, additional dedicated studies are required. Due to the relatively low immunogenicity of B16 tumors (Celik et al., 1983) it is inherently difficult to study melanoma-specific immune responses using the B16 model. Switching to a transgenic model, for example B16-OVA cells grafted to OT-1 mice, in which all T cells are committed to one specific antigen and thus elicit reproducible immune responses might provide a framework to further dissect the effects of melanoma-expressed PD-1 on regulating antitumor immunity. To this end, the Ph.D. candidate engineered *Pdcd1*-OE and *Pdcd1*-KD B16-OVA melanoma variants. Transplantation of these PD-1 variant B16-OVA cells to commercially available OT-1 mice would provide an antigen-specific T cell

response, which may help to further characterize the effects of melanoma-expressed PD-1 on tumor-specific immunity.

In summary, the herein presented data identify melanoma-expressed PD-1 as a novel, previously unrecognized immunoregulatory and tumor growth-accelerating mechanism. To date, PD-1 receptor functions have mainly been studied in T cells. Elucidating the role of melanoma-PD-1:immune cell-PD-1 ligand signaling interactions in tumor immune evasion and melanoma growth may critically enhance current understanding of melanoma progression. In addition, elucidating the complex PD-1 pathway interactions between cancers and immune cells in the TME might help identify additional factors and pathways that could be targeted in combination with anti-PD-1 treatment to improve clinical benefit. The key findings discussed in this chapter are summarized in Figure 13.

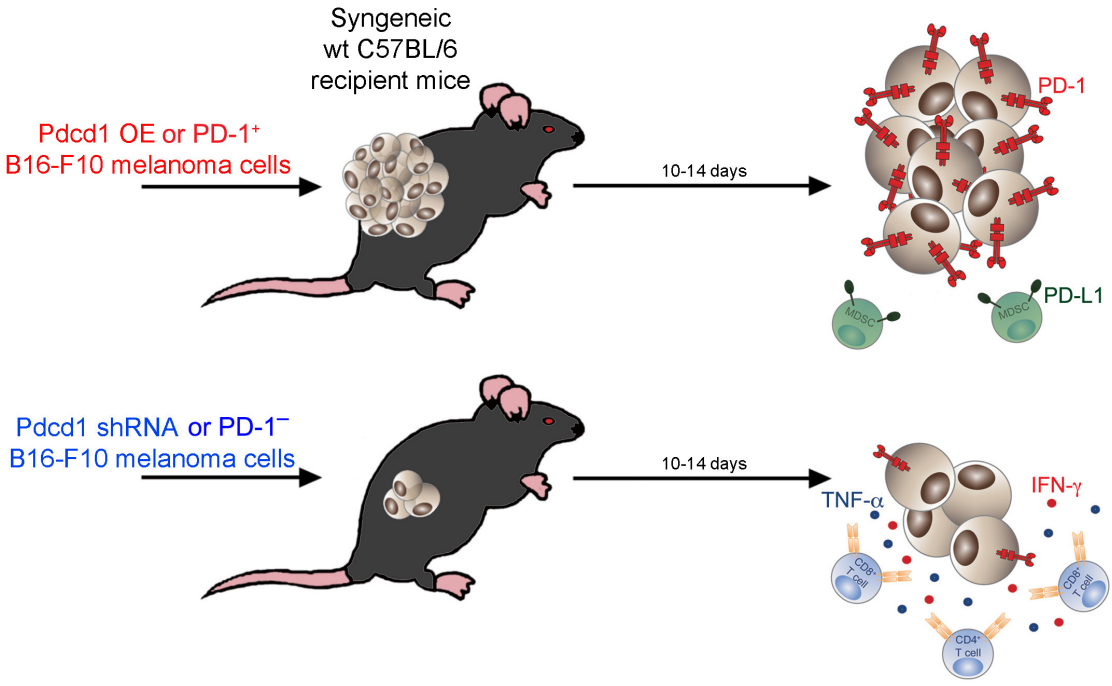

Figure 13. Melanoma-expressed PD-1 promotes tumorigenicity and modulates antitumor immunity. Enforced expression of PD-1 by melanoma cells and PD-1^{+} sorted native melanoma cells results in significantly increased B16-F0 and F10 melanoma growth in immunocompetent syngeneic C57BL/6 recipient mice, while both PD-1 KD and PD-1^{-} sorted melanoma cells yield significantly decreased tumor burden compared to respective

controls. This observed protumorigenic effect of melanoma-expressed PD-1 may, in part, be due to the fact that PD-1^+ tumor cells inhibit local, but not systemic antitumor immune responses in the B16 melanoma model. Particularly, PD-1 OE melanomas harbor decreased frequencies of $CD44^+CD62L^-$ effector T cells and IFN-γ^+, TNF-α^+, and IFN- γ^+ TNF-α^+ $CD4^+$ and $CD8^+$ T cells compared to control tumors. PD-1 KD, on the other hand, resulted in increased frequencies of activated T cells producing the effector cytokines IFN-γ^+ and TNF-α^+ compared to TILs isolated from control melanoma grafts.

4.3 Melanoma cell-intrinsic PD-1 receptor functions promote tumor growth

Parts of this chapter have been previously published in *Kleffel S. et al. Melanoma Cell-Intrinsic PD-1 Receptor Functions Promote Tumor Growth. Cell 2015;162(6):1242-56.* Published data is highlighted in the individual figure legends.

4.3.1 Introduction

Melanoma-expressed PD-1 promoted tumor growth in immunocompetent C57BL/6 mice and helped maintain an immunosuppressive TME by regulating intra-tumoral T effector cell functions and MDSC frequencies. Interestingly, a study by Drs. Markus Frank and Tobias Schatton previously demonstrated increased tumorigenicity of patient-derived PD-1^+ compared to PD-1^- melanoma cell subsets in mice lacking adaptive immunity (Schatton et al., 2010). It was therefore hypothesized that melanoma-expressed PD-1 promotes tumor growth via additional, melanoma cell-intrinsic PD-1 functions. Thus, the superior anticancer activity of antibody-based therapeutics targeting the PD-1 pathway versus the alternate immune checkpoint CTLA-4 could, at least in part, result from the direct inhibition of melanoma-PD-1-dependent protumorigenic mechanisms.

PD-1 immunobiology has been mainly studied in immune cells (Topalian et al., 2012a). In T cells, the PD-1 receptor controls MAPK/ERK, PI3K/AKT and mTOR signaling downstream of the TCR complex (Patsoukis et al., 2012, Riley, 2009, Sheppard et al., 2004). These pathways are also critically important for melanomagenesis (Flaherty et al., 2012). Therefore, melanoma-expressed PD-1 was hypothesized to promote tumor growth by activating cancer cell-intrinsic oncogenic signaling cascades, such as MAPK/ERK, PI3K/AKT and/or mTOR. Consistently, activation of the PD-1:PD-L1 axis in cancer cells has previously been shown to activate tumor cell-intrinsic mTOR signaling and promote metastasis (Black et al., 2016, Chang et al., 2015).

Although PD-1 pathway blockade has yielded unprecedented response rates and durable cancer regression, the majority of melanoma patients do not respond to treatment. Elucidating the role of cancer cell-expressed PD-1 in melanomagenesis may identify reliable biomarkers to predict which patient will benefit from PD-1 blockade and guide treatment selection. In addition, understanding the molecular function of PD-1 signaling in melanoma cells could further guide the combination of therapies that might have synergistic effects in cancer patients. To assess the potential translational relevance of melanoma cell-intrinsic PD-1 receptor signaling, the effects of Ab-mediated PD-1 blockade on oncogenic signaling were also assessed in clinical tumor specimen from patients undergoing PD-1 therapy.

4.3.2 Melanoma-expressed PD-1 promotes murine tumor growth independently of adaptive immunity

Melanoma-expressed PD-1 promotes tumor growth in immunocompetent C57BL/6 mice. To determine whether the observed protumorigenic effects depend on melanoma-PD-

1:lymphocyte-PD-1 ligand interactions, the abilities of *Pdcd1*-KD and *Pdcd1*-OE versus control B16 melanomas to initiate tumor growth in immunocompromised, T and B cell-deficient NSG mice were compared. Interestingly, *Pdcd1* knockdown inhibited and *Pdcd1* overexpression increased tumorigenicity of B16-F0 and B16-F10 melanomas in NSG mice compared to controls (Figure 14A), suggesting lymphocyte-independent roles of melanoma-PD-1 in tumorigenesis. Significant *Pdcd1* KD (Figure 14B) and overexpression (Figure 14C) compared to control B16 melanoma grafts was confirmed after *in vivo* growth at the experimental endpoint.

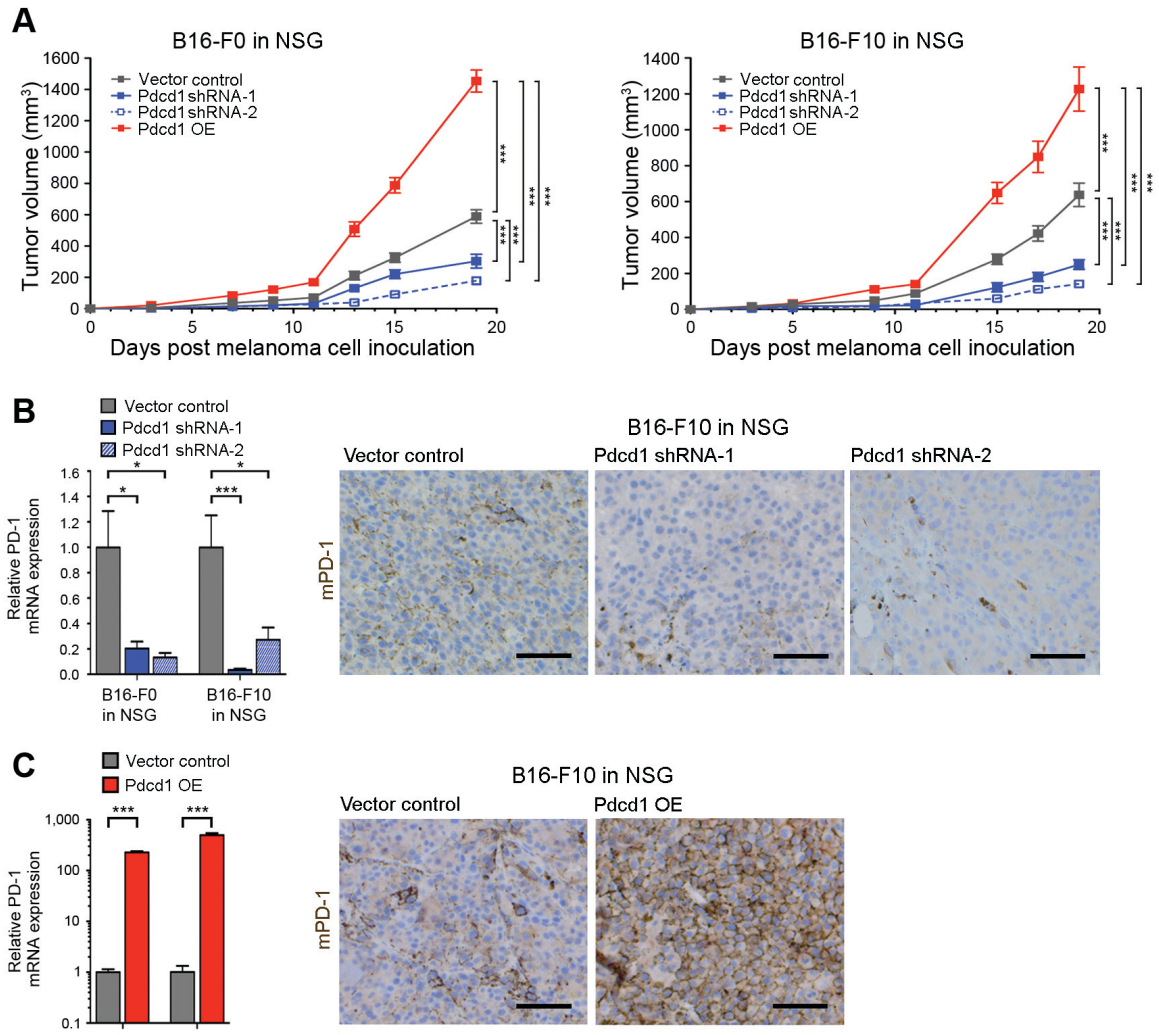

Figure 14. Melanoma-expressed PD-1 promotes tumorigenicity independent of adaptive immunity. (A) Tumor growth kinetics (mean ± SD) of *Pdcd1*-shRNA-1/-2

versus *Pdcd1*-OE versus vector control B16-F0 or B16-F10 melanomas in NSG mice (*n*=10-20 each). (B) PD-1 mRNA expression (mean ± SEM) determined by quantitative RT-PCR (left) and representative IHC images of PD-1 protein expression (B16-F10, right) of murine B16 melanomas harvested 19 days post inoculation of *Pdcd1*-shRNA-1/-2- versus vector control- or of (C) *Pdcd1*-OE- versus vector control-transduced B16-F0 or B16-F10 melanoma cells to NSG mice, respectively. Similar IHC results were obtained for B16-F0 melanoma variant grafts (not shown). Size bars, 50µm. (* P<0.05, *** P<0.001). The data presented in this figure has been previously published (Kleffel et al., 2015).

Consistent with the observed increased tumorigenicity of *Pdccd1*-OE melanoma variants, PD-1^{+} melanoma subpopulations purified from native B16-F0 and B16-F10 lines (Figure 8A) demonstrated accelerated tumor growth in NSG mice compared to PD-1^{-} cell isolates (Figure 15).

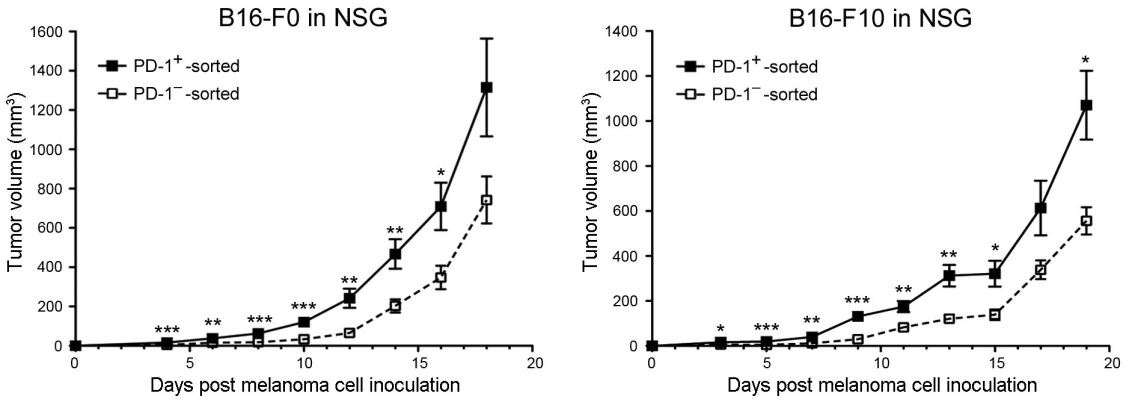

Figure 15. Native PD-1^{+} melanoma cells promote tumorigenicity in immunocompromised mice. Tumor growth kinetics (mean ± SD) of sorted, PD-1^{+} versus PD-1^{-} B16-F0 or B16-F10 melanoma cells grafted to NSG mice (*n*=8-10 each). (* P<0.05, ** P<0.01, *** P<0.001). The data presented in this figure has been previously published (Kleffel et al., 2015).

To examine whether melanoma-specific *Pdcd1* silencing or overexpression affects melanoma cell growth *in vitro* in the complete absence of immune cells, melanoma

variants were cultured in an established system designed for the study of tumorigenic minority populations (Aceto et al., 2012, Civenni et al., 2011). Consistent with *in vivo* findings, *Pdcd1*-KD impaired and *Pdcd1*-OE promoted *in vitro* three-dimensional B16-F0 and B16-F10 culture growth compared to respective controls (Figure 16A). PD-1 receptor signaling in T cells modulates several downstream pathways (Riley, 2009) that also serve critical roles in melanomagenesis (Flaherty et al., 2012), such as MAPK/ERK and PI3K/AKT/mTOR signaling. Thus, melanoma-PD-1-specific changes in phospho (p)-ERK1/2, p-AKT, and p-S6 ribosomal protein levels were examined next. *Pdcd1*-KD reduced and *Pdcd1*-OE increased the phosphorylation of the mTOR effector molecule, S6, compared to control B16 melanoma cells (Figure 16B), indicating PD-1-mediated melanoma cell-intrinsic induction of protumorigenic mTOR pathway activity. Together, these *in vitro* findings suggest that lymphocyte-independent, cancer cell-intrinsic functions of melanoma-expressed PD-1 promote tumor growth.

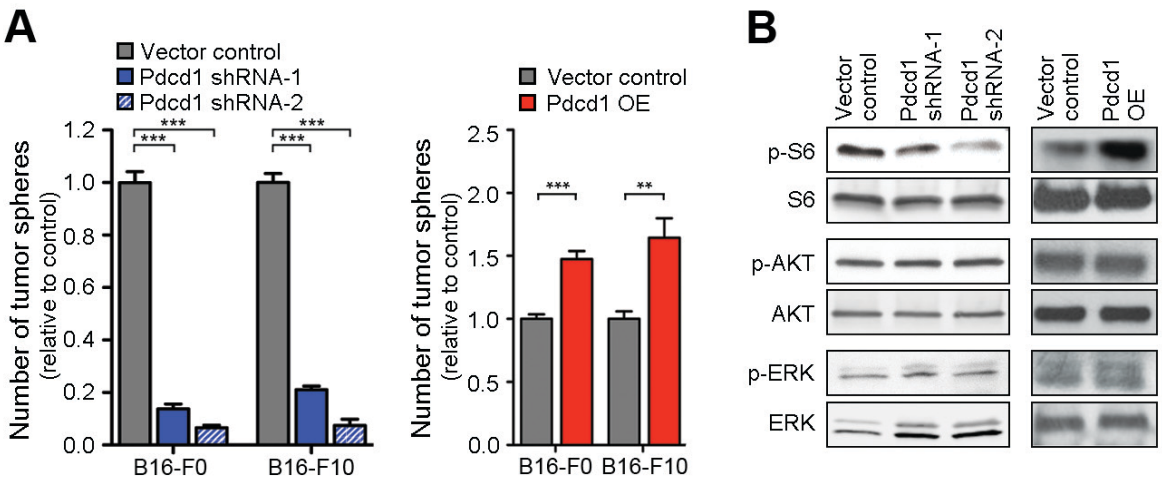

Figure 16. Melanoma-expressed PD-1 promotes spheroid growth and activates the mTOR effector molecule, S6, independent of immunity. (A) Mean number of tumor spheres ± SEM and (B) immunoblot analysis of phosphorylated (p) and total S6, AKT, and ERK in *Pdcd1*-shRNA-1/-2 versus control (left) and *Pdcd1*-OE versus vector control (right) B16 melanoma variants. Results are representative of *n*=2-3 independent

experiments (**P<0.01, ***P<0.001). The data presented in this figure has been previously published (Kleffel et al., 2015).

4.3.3 Melanoma-PD-1:PD-L1 interactions promote murine melanoma growth

To determine whether activation of melanoma-PD-1 by its ligands, PD-L1 and PD-L2, is required for PD-1 driven tumorigenesis, *Pdcd1*-OE versus control B16-F10 cells were grafted to wildtype C57BL/6 versus PD-L1 (-/-) KO, PD-L2 (-/-) KO and PD-L1 (-/-) / PD-L2 (-/-) double (D) KO C57BL/6 recipient mice (Keir et al., 2006, Latchman et al., 2004). Enforced expression of PD-1 resulted in significantly increased B16-F10 melanoma growth compared to that of vector control B16 melanomas in PD-L2 (-/-) KO C57BL/6 recipient mice (Figure 17A), consistent with previous findings in wt C57BL/6 mice (Figure 7C). However, no significant differences in tumorigenicity between *Pdcd1*-OE versus vector control B16 cells were observed in PD-L1 (-/-) KO and PD-L1 (-/-) / PD-L2 (-/-) DKO C57BL/6 recipient mice (Figure 17A). This finding suggests that ligation of melanoma-PD-1 to host-PD-L1, but not host-PD-L2, is required for PD-1-driven tumorigenesis. To test whether melanoma-PD-1:host-PD-L1 interactions also promote tumor growth in the absence of adaptive immunity, *Pdcd1*-OE versus control B16-F10 cells were grafted to wildtype Rag(-/-) versus PD-L1(-/-) KO Rag(-/-) mice (Francisco et al., 2009). The growth of *Pdcd1*-OE melanomas was attenuated in PD-L1(-/-) KO Rag(-/-) compared to PD-L1(+/+) Rag(-/-) recipients (Figure 17B), consistent with findings in immunocompetent PD-L1 (-/-) KO C57BL/6 mice (Figure 17A). To examine if PD-L1 expressed by melanoma cells (Figure 4G) also contributes to melanoma-PD-1-dependent tumorigenesis, PD-L1(-/-) KO Rag(-/-) versus wildtype Rag(-/-) mice grafted with *Pdcd1*-OE melanomas were treated with a PD-L1 blocking Ab. Antibody-mediated PD-L1

blockade inhibited *Pdcd1*-OE B16-F10 melanoma growth compared to isotype control treatment in PD-L1(-/-) KO mice (Figure 17C). Additionally, PD-L1 Ab treatment resulted in significantly reduced tumor growth of *Pdcd1*-OE melanomas in PD-L1(-/-) KO Rag(-/-) compared to wildtype Rag(-/-) mice (Figure 17C). These findings suggest growth-accelerating functions not only of host-PD-L1:melanoma-PD-1, but also of melanoma-PD-L1:melanoma-PD-1 interactions.

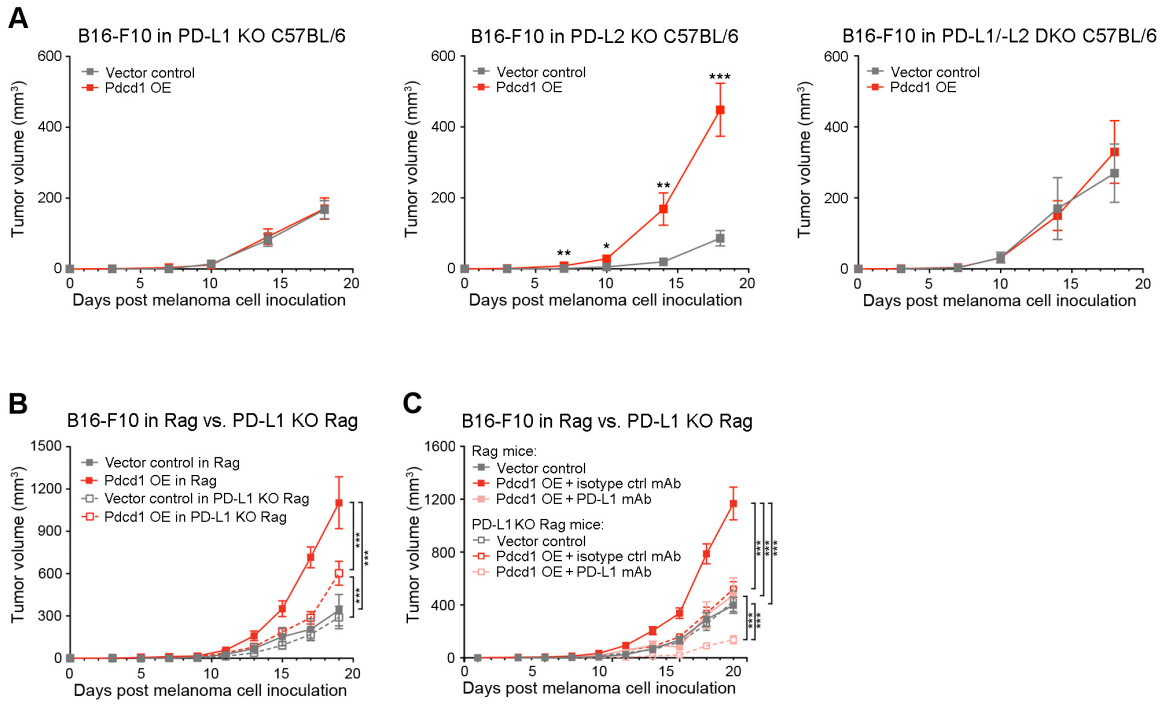

Figure 17. Melanoma-PD-1 engagement by its ligand, PD-L1, promotes murine melanoma growth. (A) Growth kinetics (mean ± SD) of *Pdcd1*-OE versus vector control B16-F10 melanomas in PD-L1(-/-) KO, PD-L2 (-/-) KO and PD-L1(-/-)/PD-L2 (-/-) DKO C57BL/6 recipient mice (n=8-12 each), (B) in wildtype Rag(-/-) KO (n=6 each) versus PD-L1(-/-) KO Rag(-/-) KO mice (n=10 versus 8), and (C) in wildtype Rag(-/-) KO recipients (n=14 versus 14 versus 8) versus PD-L1(-/-) KO Rag(-/-) KO (n=14 versus 20 versus 10) treated with anti-PD-L1- versus isotype control mAb. (* P<0.05, ** P<0.01, *** P<0.001). Figure 2A contains unpublished data, however, the data shown in Figures 2B and C has been previously published (Kleffel et al., 2015).

To further demonstrate protumorigenic melanoma-PD-L1 effects in the absence of adaptive immunity, stable PD-L1 gene (*Cd274*, also known as *Pdcd1lg1*)-KD B16-F10 melanoma cells were generated (Figure 18A) and tested for their ability to maintain culture growth and form tumors. Compared to vector control, *Pdcd1lg1* silencing impaired three-dimensional B16 melanoma growth *in vitro* (Figure 18B) and *in vivo* tumorigenesis in both immunocompetent C57BL/6 and immunocompromised NSG mice (Figure 18C). Moreover, concurrent *Pdcd1lg1*-KD reversed the significant increase in tumorigenicity of *Pdcd1*-OE versus vector control B16-F10 melanoma cells in C57BL/6 and NSG mice (Figure 18D).

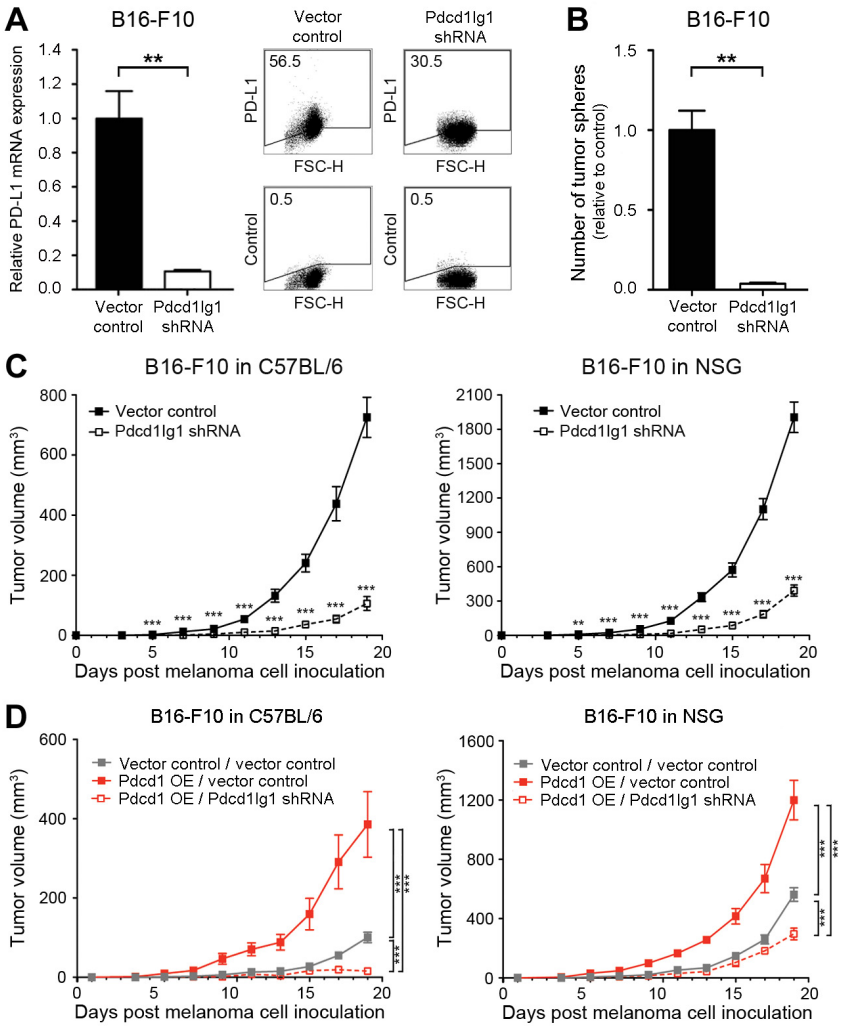

Figure 18. The melanoma-PD-1:melanoma-PD-L1 axis promotes tumorigenesis. (A) PD-L1 (*Cd274*, also known as *Pdcd1lg1*) mRNA expression (mean ± SEM), as determined

by quantitative RT-PCR (left) and PD-L1 protein expression, as determined by single-color flow cytometric analysis (right), and (B) mean number of tumor spheres ± SEM in three-dimensional *in vitro* cultures of *Pdcd1lg1*-shRNA- compared to control-shRNA-transduced B16-F10 melanomas. (C) Tumor growth kinetics (mean ± SD) in C57BL/6 (left) and NSG mice (right) of *Pdcd1lg1*-shRNA- versus control-shRNA-transduced B16-F10 melanomas (n=10 each). (D) Tumor growth kinetics (mean ± SD) in C57BL/6 (left) and NSG mice (right) of *Pdcd1*-OE B16-F10 cells co-transduced with PD-L1-shRNA versus vector control compared to vector controls (n=10 each). (** P<0.01, *** P<0.001). The data presented in this figure has been previously published (Kleffel et al., 2015).

To further demonstrate that PD-L1 interactions with melanoma-PD-1 promote melanoma growth, native B16-F0 and B16-F10 cultures were treated with a recombinant PD-L1 Fc-fusion protein (PD-L1 Ig), known to elicit changes in PD-1 receptor signaling in T cells (Francisco et al., 2009). Compared to control Ig treatment, addition of PD-L1 Ig to B16 cultures significantly augmented three-dimensional growth and phosphorylation of S6 ribosomal protein (Figure 19A). Because both PI3K/AKT and mTOR signaling cascades feed into downstream S6 phosphorylation, it was examined whether pharmacologic inhibition of either pathway could reverse the observed increase in p-S6 expression. mTOR pathway blockade (via rapamycin or PP242), but not PI3K inhibition (via wortmannin or LY294002), suppressed the PD-L1 Ig-dependent phosphorylation of S6 in murine B16-F10 melanoma cells (Figure 19B). Together, these findings demonstrate that interactions between melanoma-expressed PD-1 with its ligand, PD-L1, promote tumor growth and activate mTOR signaling.

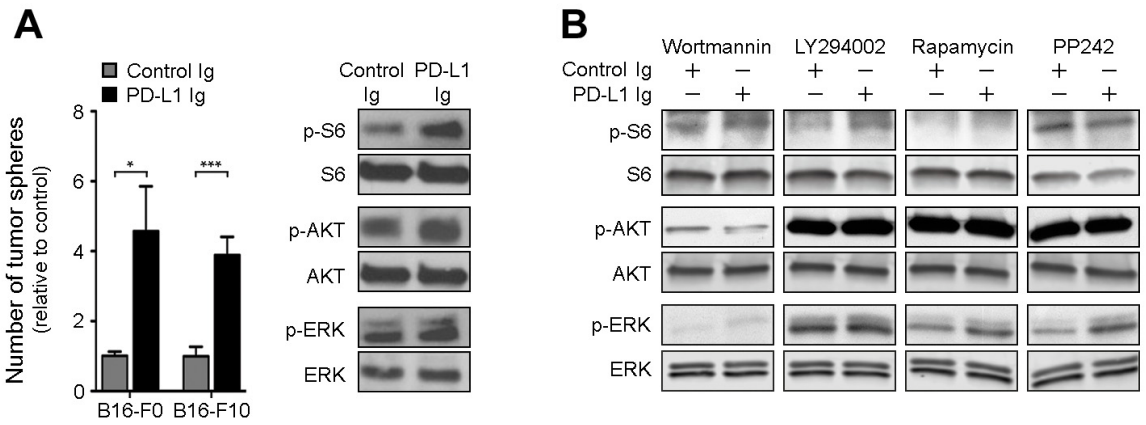

Figure 19. Exogenous PD-L1 activates the protumorigenic mTOR pathway in melanoma cells. (A) Mean number of tumor spheres ± SEM (left), and immunoblot analysis of p- and total S6, AKT, and ERK in PD-L1 Ig versus control Ig-treated B16 cultures (right). (B) Immunoblot analysis of p- and total S6, AKT, and ERK in PD-L1 Ig versus control Ig-treated B16-F10 melanoma cells cultured in the presence of the pharmacologic PI3K inhibitors, wortmannin or LY294002, or the mTOR pathway inhibitors, rapamycin or PP242. (* $P<0.05$, *** $P<0.001$). The data presented in this figure has been previously published (Kleffel et al., 2015).

4.3.4 Tumor cell-intrinsic PD-1 signaling is required for efficient murine melanoma growth.

To determine whether melanoma cell-intrinsic PD-1 signaling is required for efficient tumor growth, *Pdcd1*-OE B16 variants containing tyrosine to phenylalanine single point mutations in the two PD-1 signaling motifs, ITIM (disrupted by Y225F mutation) and ITSM (disrupted by Y248F mutation), within the cytoplasmic tail of melanoma-PD-1 were generated (Figure 20A). A construct containing point mutations of both tyrosines (Y225F/Y248F) was also created. In immune cells, ITIM and ITSM play pivotal roles in PD-1 signaling (Riley, 2009). Transduction of wildtype versus mutant *Pdcd1*-constructs into B16-F0 or B16-F10 melanoma cells resulted in similarly high expression levels of PD-1, both at the mRNA and at the protein level (Figure 20B), permitting a direct comparison

between wildtype *Pdcd1*-OE and each of the mutant variants. Strikingly, mutation of either one (Y225F or Y248F) or both (Y225F/Y248F) melanoma-PD-1 signaling motifs significantly abrogated the increased tumor growth observed in both C57BL/6 and NSG mice grafted with wildtype *Pdcd1*-OE versus vector-control B16 melanoma variants (Figure 20C). Moreover, mutation of melanoma-PD-1 ITIM and/or ITSM motifs suppressed three-dimensional tumor growth *in vitro* (Figure 20D), and phosphorylation of S6 ribosomal protein (Figure 20E) compared to enforced expression of wildtype *Pdcd1*. Together, these findings suggest that cancer cell-intrinsic PD-1 signaling via its ITIM and ITSM motifs is required for tumor growth and mTOR activation of PD-1^{+} melanoma cells.

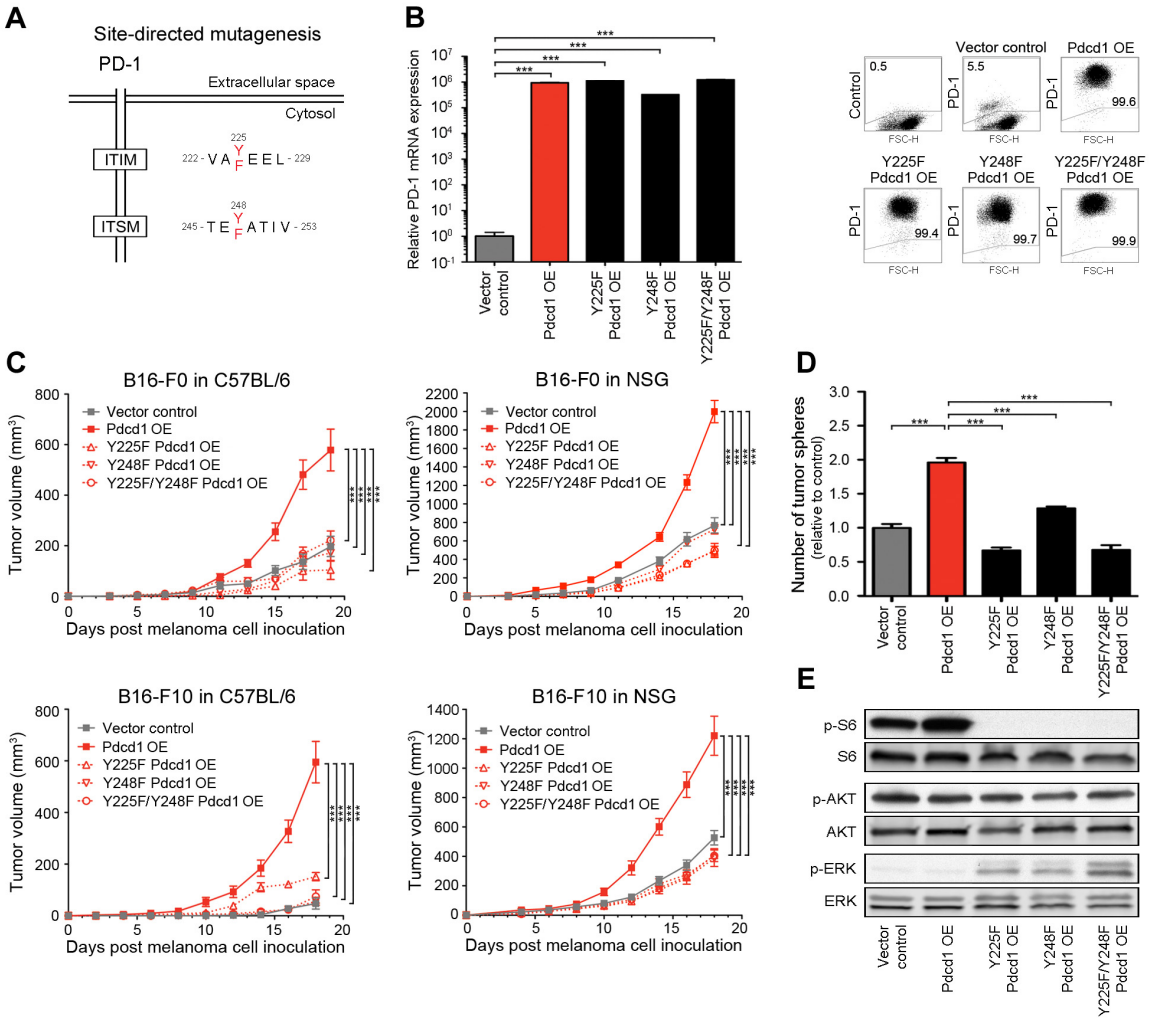

Figure 20. Tumor cell-intrinsic PD-1 signaling promotes murine melanoma growth. (A) Schematic diagram illustrating the introduction of tyrosine to phenylalanine mutations

to murine PD-1 signaling motifs via site-directed mutagenesis. (B) Relative *Pdcd1* mRNA expression (left, mean ± SEM) and representative flow cytometry plots of PD-1 surface protein expression (right) by wildtype *Pdcd1*-OE versus Y225F-*Pdcd1*-OE, Y248F-*Pdcd1*-OE, Y225F/Y248F-*Pdcd1*-OE, and vector control B16-F10 variants. (C) Tumor growth kinetics in C57BL/6 (left, *n*=10-14 each) and NSG mice (right, *n*=8-10 each), (D) mean number of tumor spheres ± SEM, and (E) immunoblot analysis of p- and total S6, AKT, and ERK in B16-F10 melanoma variants as in (B). (***$P<0.001$). The data presented in this figure has been previously published (Kleffel et al., 2015).

4.3.5 Melanoma cell-intrinsic PD-1 enhances human tumor xenograft growth

The effects of melanoma-specific PD-1 knockdown versus PD-1 overexpression on human melanoma xenograft growth was analyzed next. Transduction of established human A375, C8161, or G3361 melanoma cells with two distinct *PDCD1*-shRNAs significantly inhibited PD-1 mRNA expression and blocked PD-1 protein expression between 53-75% (Figure 21A). Infection with *PDCD1*-OE constructs resulted in marked upregulation of PD-1, both at the mRNA and protein level (>90% positivity), respectively (Figure 21B).

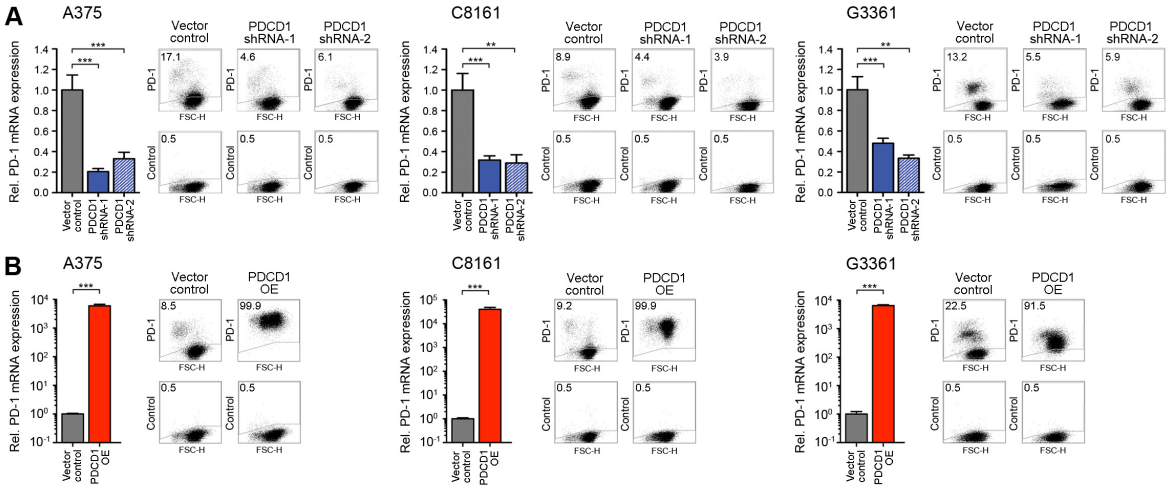

Figure 21. Characterization of PD-1 knockdown and PD-1 overexpressing human melanoma cell lines. (A) Stable *PDCD1* KD human A375, C8161 and G3361 melanoma cell line variants were generated by shRNA-mediated gene silencing (*PDCD1*-shRNA-1 and *PDCD1*-shRNA-2), and (B), stable *PDCD1*-OE human melanoma cell lines by transduction with vectors containing the full-length human *PDCD1* CDS. PD-1 KD or overexpression compared to respective vector control-transduced cells was confirmed at the mRNA level (mean ± SEM) by quantitative RT-PCR (left) and at the protein level by single-color flow cytometry (right), respectively. (** P<0.01, *** P<0.001). The data presented in this figure has been previously published (Kleffel et al., 2015).

PDCD1-KD significantly inhibited, and *PDCD1*-OE markedly increased human melanoma xenograft growth in NSG mice compared to vector control-transduced A375, C8161, or G3361 tumors (Figure 22A). *PDCD1* silencing (Figure 22B) and overexpression (Figure 22C) was preserved in all melanoma xenografts at the experimental endpoint, respectively.

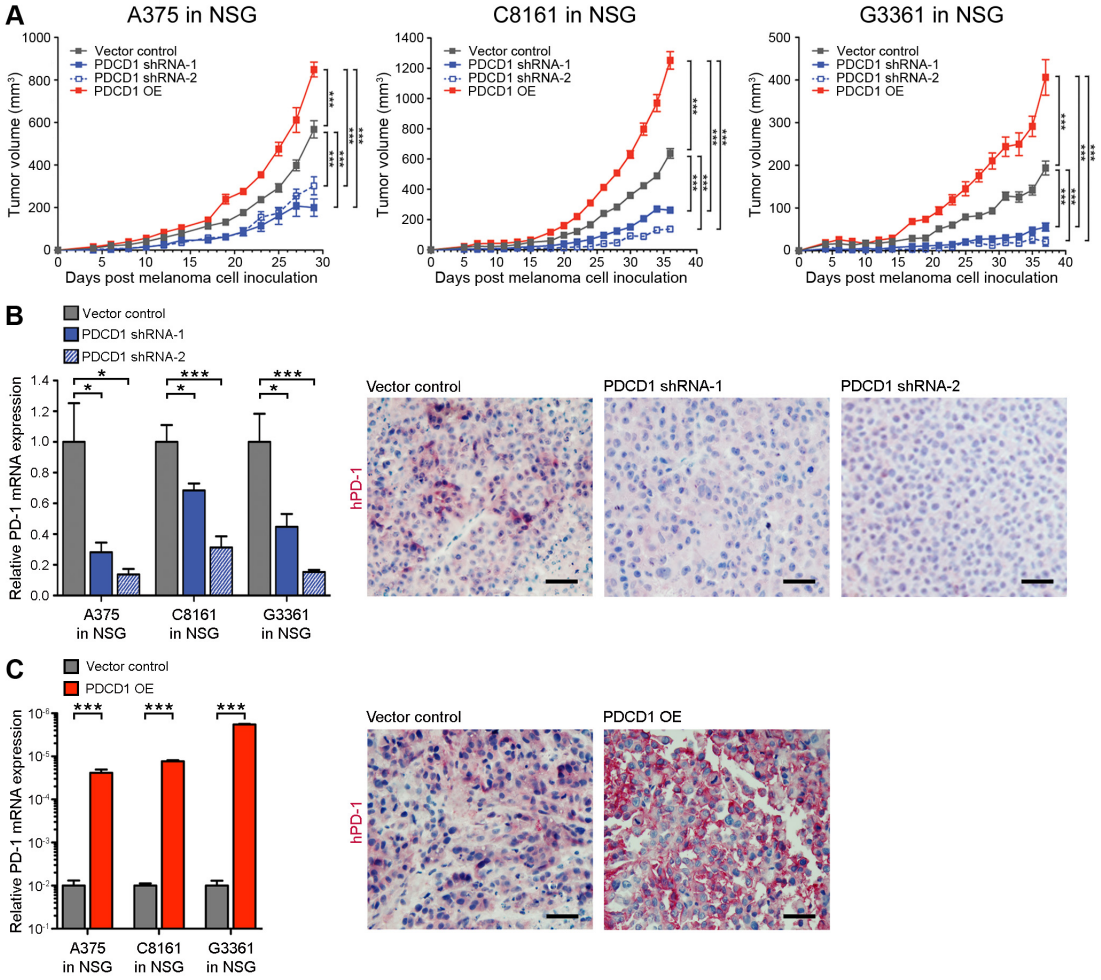

Figure 22. PD-1 expression by human melanoma cells promotes experimental tumor growth. (A) Tumor growth kinetics (mean ± SD) of *PDCD1*-shRNA-1, *PDCD1*-shRNA-2, and *PDCD1*-OE versus vector control human A375 (left), C8161 (center), and G3361 melanoma cells (right) grafted to NSG mice (n=8-20 each). (B) Relative PD-1 mRNA expression (mean ± SEM) determined by quantitative RT-PCR (left) and representative IHC images of PD-1 protein expression (right) of human melanoma xenografts (n=4-8, respectively) harvested 29-37 days post inoculation of *PDCD1*-shRNA-1/-2- versus vector control- or (C), *PDCD1*-OE- versus vector control-transduced A375, C8161, and G3361 melanoma cells to NSG mice. Size bars, 50µm. Representative IHC images depict A375 melanoma xenografts. (* P<0.05, ** P<0.01, *** P<0.001). The data presented in this figure has been previously published (Kleffel et al., 2015).

Moreover, PD-1$^+$ cancer cell subsets purified from native C8161 cultures using FACS sorting (Figure 23A) showed significantly increased tumorigenicity in NSG mice compared to PD-1$^-$ sorted C8161 cell subsets (Figure 23B).

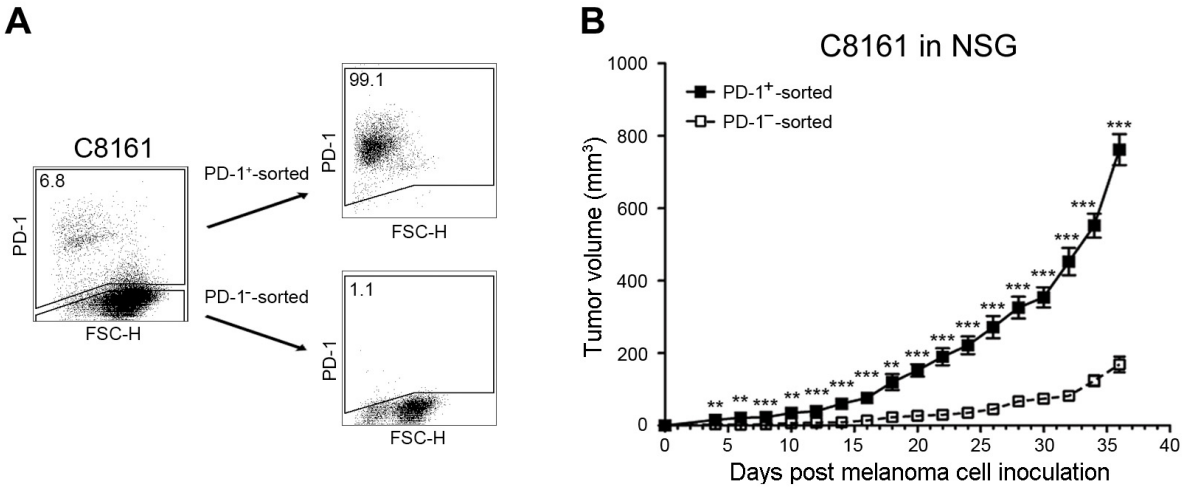

Figure 23. Native PD-1$^+$ human melanoma cells promote tumorigenicity. (A) Representative flow cytometry plots of PD-1 surface protein expression by C8161 cells pre- (left) and post-sort (right) for PD-1$^+$ versus PD-1$^-$ cell populations. (B) Tumor growth kinetics (mean ± SD) of sorted, PD-1$^+$ versus PD-1$^-$ C8161 melanoma cells grafted to NSG mice (n=5 each). (** P<0.01, *** P<0.001). The data presented in this figure has been previously published (Kleffel et al., 2015).

Consistent with *in vivo* findings, *PDCD1*-KD impaired and *PDCD1*-OE promoted three-dimensional A375, C8161, and G3361 culture growth compared to controls (Figure 24A). Furthermore, relative to control Ig treatment, addition of human PD-L1 Ig augmented tumor sphere formation of A375 and G3361, but not C8161 melanoma cultures (Figure 24B). Native C8161 express greater than 3-fold higher endogenous PD-L1 levels than A375 and G3361 cells (Figure 3E). Human *PDCD1*-KD lines showed a reduction, and *PDCD1*-OE and PD-L1 Ig-treated human G3361 melanoma cells an increase in p-S6 levels compared to respective controls (Figure 24C), paralleling findings in murine B16 cells. Additionally, pharmacologic inhibition of mTOR, but not PI3K signaling, blocked

the increase in p-S6 expression in PD-L1 Ig compared to control Ig-treated human G3361 melanoma cells (Figure 24D). This indicates that S6 phosphorylation downstream of the melanoma-PD-1 receptor depends on mTOR pathway activation, consistent with findings in murine B16 melanoma cells (Figure 19B).

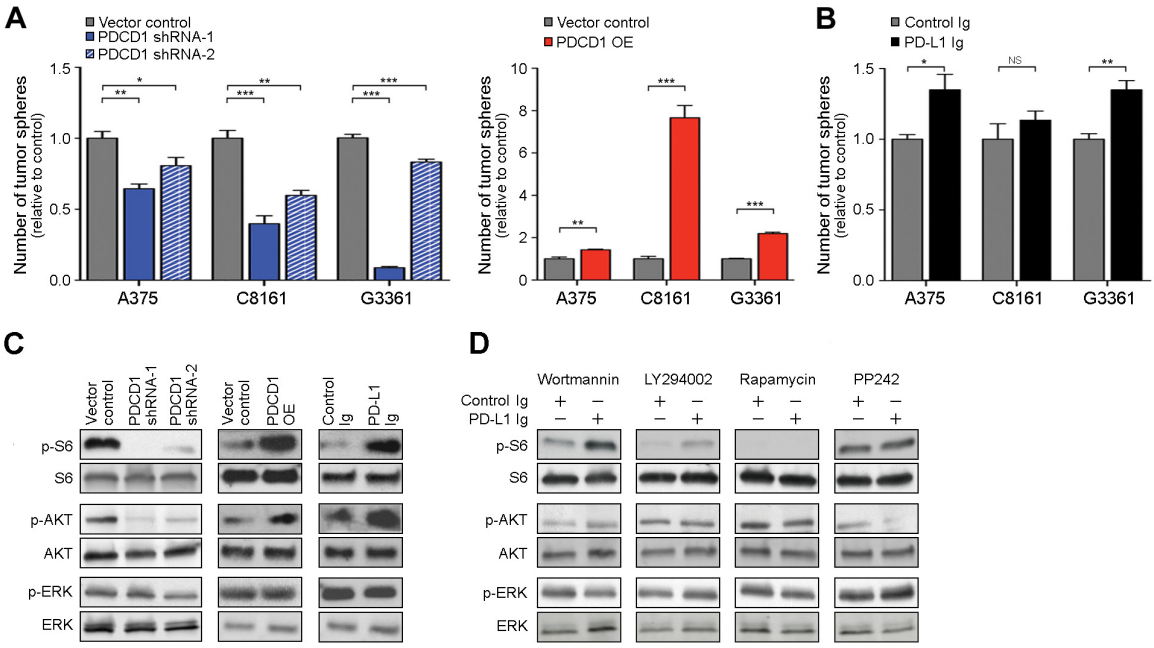

Figure 24. The melanoma-PD-1:PD-L1 axis activates the mTOR mediator, S6. (A) Mean number of tumor spheres ± SEM of *PDCD1*-shRNA-1/-2 versus vector control (left), *PDCD1*-OE versus vector control (right), and (B) PD-L1 Ig- versus control Ig-treated human A375, C8161, and G3361 melanoma cultures. (C) Immunoblot analysis of p- and total ribosomal protein S6, AKT, and ERK in *PDCD1*-shRNA-1/-2 versus vector control, *PDCD1*-OE versus vector control, and PD-L1 Ig- versus control Ig-treated human G3361 melanoma cultures. (D) Immunoblot analysis of p- and total S6, AKT, and ERK in PD-L1 Ig versus control Ig-treated G3361 melanoma cells cultured in the presence of the pharmacologic PI3K inhibitors, wortmannin or LY294002, or the mTOR pathway inhibitors, rapamycin or PP242. (* $P<0.05$, ** $P<0.01$, *** $P<0.001$). The data presented in this figure has been previously published (Kleffel et al., 2015).

To assess whether melanoma cell-intrinsic PD-1 signaling is also required for efficient growth of human melanoma cells, A375 and C8161 melanoma cells were transduced with wildtype versus ITIM (disrupted by Y223F mutation) and/or ITSM (disrupted by Y248F mutation) mutant PDCD1-OE constructs (Figure 25A). These engineered A375 and C8161 variants expressed similarly high levels of PD-1 mRNA (Figure 25B) and PD-1 protein (Figure 25C), allowing a direct comparison between wildtype and each of the mutant *PDCD1*-OE variants. Mutation of either one (Y223F or Y248F) or both (Y223F/Y248F) signaling motifs within the melanoma-PD-1 cytoplasmic tail abrogated the increased tumor growth observed in NSG mice grafted with wildtype *PDCD1*-OE versus vector-control A375 or C8161 variants (Figure 25D). Additionally, Y223F-, Y248F-, and Y223F/Y248F-mutant *PDCD1*-OE C8161 melanoma cells demonstrated significantly impaired three-dimensional culture growth (Figure 25E) and reduced p-S6 levels compared to wildtype *PDCD1*-OE C8161 cells (Figure 25F). Together, these findings identify PD-1 expressed by human melanoma cells as a lymphocyte-independent tumor growth-accelerating mechanism.

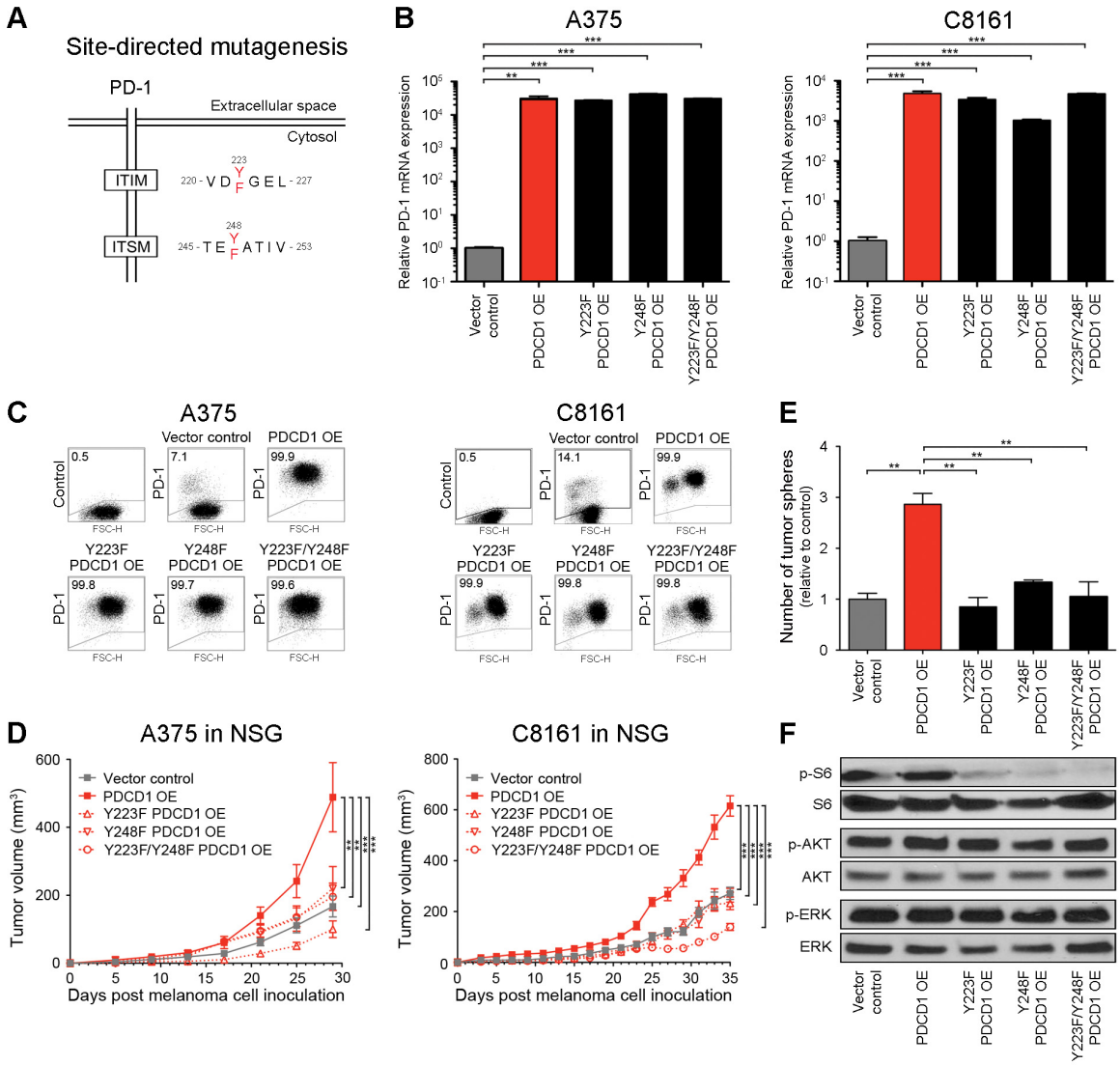

Figure 25. Tumor cell-intrinsic PD-1 signaling promotes human melanoma growth. (A) Schematic diagram illustrating the introduction of tyrosine to phenylalanine mutations to human PD-1 ITIM and ITSM signaling motifs via site-directed mutagenesis. (B) Relative *Pdcd1* mRNA expression (mean ± SEM), (C) representative flow cytometry plots of PD-1 surface protein expression, and (D) tumor growth kinetics (mean ± SD) of wildtype *PDCD1*-OE versus Y223F-*PDCD1*-OE, Y248F-*PDCD1*-OE, Y223F/Y248F-*PDCD1*-OE, and vector control human A375 (left, *n*=10-24) and C8161 melanomas (right, *n*=10-12) in NSG mice, respectively. (E) Mean number of tumor spheres ± SEM and (F) immunoblot analysis of p- and total S6, AKT, and ERK in C8161 melanoma variants as in (D). (**P<0.01, ***P<0.001). The data presented in this figure, with the exception of Figure 25B, has been previously published (Kleffel et al., 2015).

4.3.6 Antibody-mediated blockade of PD-1 on melanoma cells inhibits murine melanoma growth.

Based upon the herein demonstrated melanoma cell-intrinsic, protumorigenic PD-1 receptor functions, Ab-mediated blockade of melanoma-PD-1 was hypothesized to significantly inhibit tumor growth, even in immunocompromised NSG hosts. Administration of PD-1 blocking Ab to immunocompetent C57BL/6 recipient mice starting one day before inoculation with B16-F10 cells resulted in modest inhibition of melanoma growth between days 5 and 11 post inoculation ($P<0.01$), but showed no significant differences in tumorigenicity compared to isotype control Ab-treatment at later time points (Figure 26A), consistent with previous studies (Peng et al., 2012, Woo et al., 2012). However, antibody-mediated PD-1 blockade significantly ($P<0.05$) inhibited B16-F10 melanoma growth in PD-1(-/-) KO C57BL/6 mice compared to controls, for the entire duration of the experiment (Figure 26B). Immunohistochemical examination of melanoma grafts harvested at the experimental endpoint revealed >5-fold increased binding ($P<0.05$) of *in vivo*-administered anti-PD-1 Ab to B16 melanoma target tissue in PD-1(-/-) KO (Figure 26B) compared to wildtype C57BL/6 hosts (Figure 26A). This observation is consistent with a more pronounced PD-1 Ab effect on melanoma cell growth in PD-1(-/-) KO versus PD-1(+/+) wildtype mice.

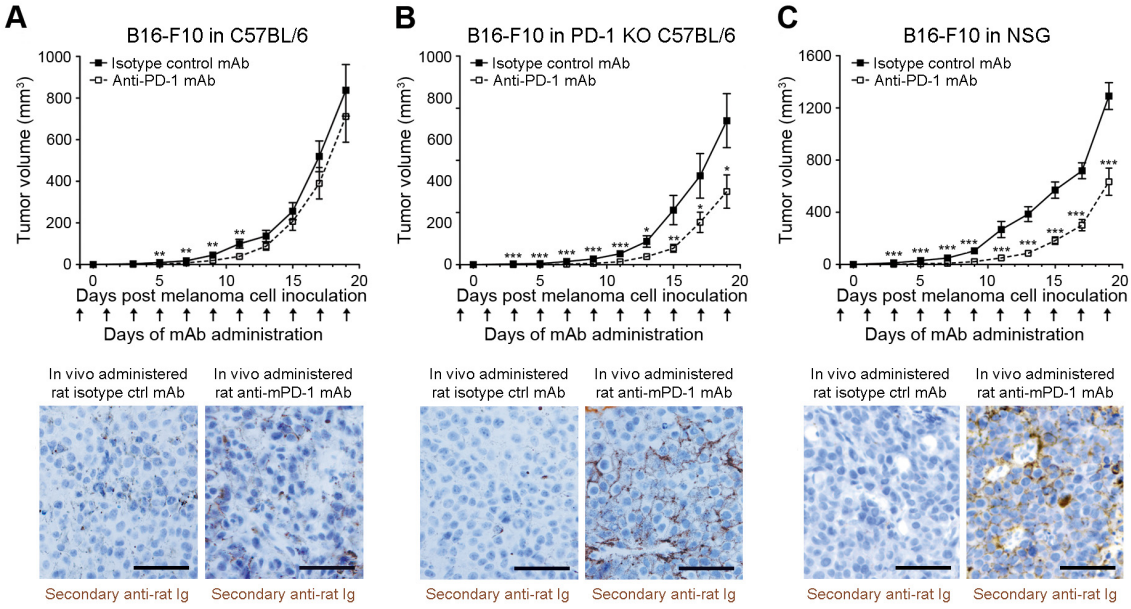

Figure 26. Anti-PD-1 blocking Ab inhibits murine melanoma growth in immunocompetent, immunocompromised and PD-1-deficient tumor graft recipient mice. (A) Tumor growth kinetics (mean ± SD) of B16-F10 melanomas in wildtype C57BL/6 (*n*=32 versus 34), (B) PD-1(-/-) KO C57BL/6 (*n*=20 versus 16), and (C) NSG (*n*=20 versus 18) treated with anti-PD-1- versus isotype control Ab. Arrows indicate days of Ab administration. Representative IHC images illustrate binding of *in vivo*-administered rat anti-mouse PD-1 blocking, but not isotype control mAb, to the respective B16-F10 melanoma grafts (size bars, 50µm). (* $P<0.05$, ** $P<0.01$, *** $P<0.001$). The data presented in this figure has been previously published (Kleffel et al., 2015).

A >20% increase in PD-1 Ab titer in the serum of PD-1(-/-) KO compared to PD-1(+/+) C57BL/6 hosts was determined by rat-IgG2a-specific ELISA (Figure 27A). This further indicated that increased PD-1 Ab availability might, at least in part, contribute to the growth-inhibitory effect of PD-1 blockade observed in PD-1(-/-) KO hosts. Anti-PD-1 Ab administration to NSG mice also significantly ($P<0.001$) diminished B16-F10 melanoma growth compared to isotype control Ab treatment (Figure 26C). B16 melanomas grafted to NSG mice tended to show increased anti-PD-1 Ab binding compared to B16 melanoma grafts grown in C57BL/6 mice (Figure 26C). Interestingly, Ab titers were not increased in NSG versus C57BL/6 mouse serum (Figure 27A), suggesting strain-specific differences in

PD-1 Ab kinetics.

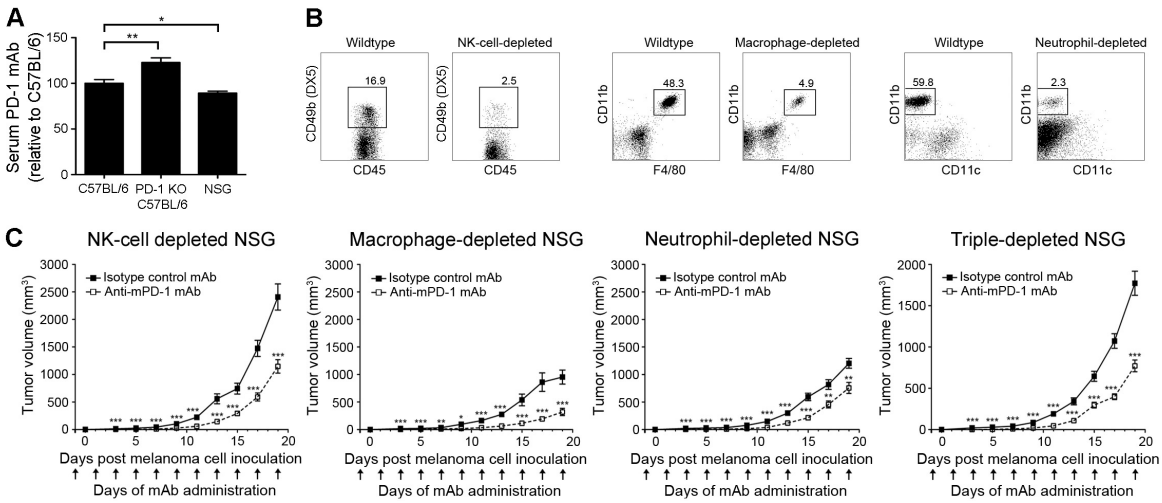

Figure 27. Serum level of anti-PD-1 Ab in wildtype C57BL/6, PD-1(-/-) KO C57BL/6, and NSG mice, and effects of anti-PD-1 blocking Ab on murine melanoma growth in innate immune cell-depleted NSG mice. (A) Relative PD-1 Ab titer (mean ± SEM) in serum obtained from PD-1(-/-) KO C57BL/6 and NSG mice compared to that in wildtype C57BL/6 mice (*n*=3 mice each) 12 hours post i.p. administration of rat anti-mouse PD-1 blocking Ab, as determined by rat-IgG2a-specific ELISA. (B) Representative flow cytometry plots demonstrating successful reduction of NK cell, macrophage, and neutrophil frequencies in NSG mice depleted of the respective immune cell subtypes compared to non-depleted (wildtype) NSG mice. (C) Tumor growth kinetics (mean ± SD) of B16-F10 melanomas in natural killer (NK) cell- (*n*=10 each), macrophage- (*n*=10 versus 8), neutrophil- (*n*=10 each), and NK cell/macrophage/neutrophil triple-depleted NSG mice (*n*=10 each) treated with anti-PD-1 versus isotype control mAb. Arrows indicate days of Ab administration. (* $P<0.05$, ** $P<0.01$, *** $P<0.001$). The data presented in this figure has been previously published (Kleffel et al., 2015).

To control for the possibility that the observed growth-inhibitory effects might result from antibody-mediated blockade of PD-1-expressing innate immune cell subtypes present in NSG mice, anti-PD-1 Ab was administered to NK cell-, macrophage-, and neutrophil-depleted NSG recipients of B16-F10 melanoma cells (Figure 27B). NSG mice depleted of

all three innate immune effector subsets were also generated. Anti-PD-1 Ab treatment inhibited B16 melanoma growth compared to isotype control Ab in all innate immune cell-depleted NSG hosts (Figure 27C).

To further confirm melanoma-specific PD-1 inhibition of the PD-1 blocking Ab, the anti-PD-1 Ab was administered to C57BL/6 and NSG mice grafted with *Pdcd1*-OE versus vector control B16-F10 melanoma cells. Anti-PD-1 Ab treatment reversed the increase in tumor growth of isotype control-treated *Pdcd1*-OE compared to vector-control B16 melanomas in both C57BL/6 (Figure 28A) and NSG mice, concomitant with binding of *in vivo*-administered anti-PD-1 Ab to B16 melanomas (Figure 28B). This experiment confirmed recognition of melanoma-PD-1 by the PD-1 blocking Ab.

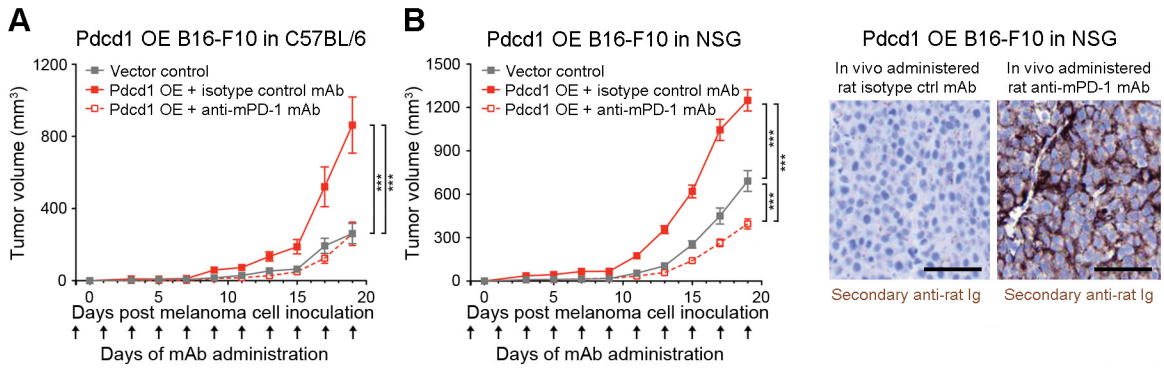

Figure 28. Anti-PD-1 blocking Ab reverses the increased tumorigenicity of PD-1 OE melanoma cells. (A) Tumor growth kinetics (mean ± SD) of *Pdcd1*-OE versus vector control B16-F10 melanomas in C57BL/6 (*n*=10 each) or (B) NSG mice (*n*=10 each) treated with anti-PD-1- versus isotype control Ab. Arrows indicate days of Ab administration. A representative IHC image illustrates binding of *in vivo*-administered rat anti-mouse PD-1 blocking Ab, but not isotype control Ab, to the respective B16-F10 melanoma grafts (size bars, 50µm). (*** $P<0.001$). The data presented in this figure has been previously published (Kleffel et al., 2015).

Antibody-mediated PD-1 blockade also reduced three-dimensional B16-F0 and B16-F10 melanoma growth *in vitro* (Figure 29A), but did not induce significant cell death

compared to isotype control Ab-treatment (Figure 29B), as determined by Annexin V/7-AAD positivity. Moreover, treatment of B16 melanoma cultures with anti-PD-1, but not isotype control Ab, inhibited PD-L1 Ig-induced phosphorylation of S6 ribosomal protein (Figure 29C). Together, these findings show that antibody-mediated PD-1 blockade directly on melanoma cells inhibits tumor cell-intrinsic, protumorigenic PD-1 functions, including in the absence of adaptive immunity.

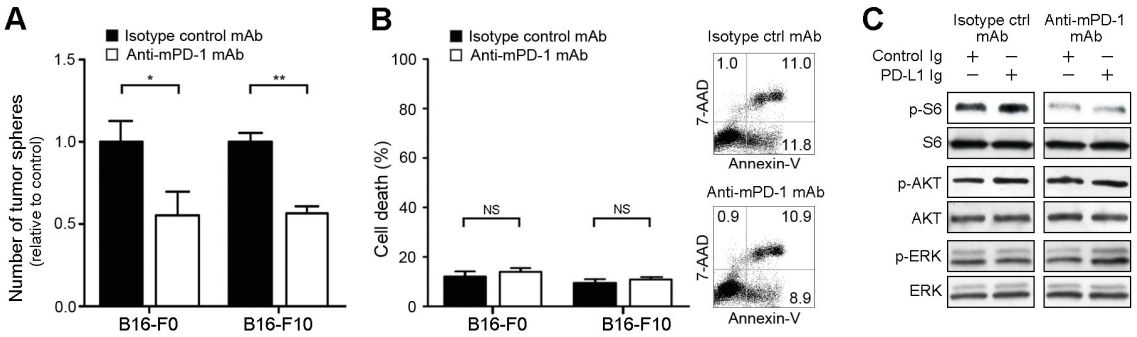

Figure 29. Antibody-mediated PD-1 blockade inhibits the protumorigenic effects of murine melanoma-expressed PD-1 without inducing cell death. (A) Mean number of tumor spheres ± SEM, (B) flow cytometric assessment of cell death (percent $AnnexinV^+/7AAD^+$ cells, mean ± SEM) (left) and representative flow cytometry plots (right) of anti-PD-1- versus isotype control mAb-treated murine B16-F0 and B16-F10 melanoma cultures. (C) Immunoblot analysis (representative of n=2 independent experiments) of p- and total ribosomal protein S6, AKT, and ERK in B16 cultures concurrently treated with PD-L1 Ig versus control Ig and/or anti-PD-1- versus isotype control mAb (NS: not significant, *P<0.05, **P<0.01). The data presented in this figure has been previously published (Kleffel et al., 2015).

4.3.7 Antibody-mediated PD-1 blockade inhibits human melanoma xenograft growth in immunodeficient mice.

To assess the translational relevance of targeting melanoma cell-intrinsic PD-1 to impede tumor growth, the effects of antibody-mediated PD-1 blockade on human melanoma growth in NSG mice were examined next. First, anti-PD-1 Ab was administered to NSG mice grafted with patient-derived melanoma cells. *In vivo* anti-PD-1 Ab administration to NSG mice significantly inhibited mean tumor volumes of clinical melanoma xenografts derived from three distinct melanoma patients (Figure 30A), consistent with findings in murine B16 models (Figure 26C). Anti-PD-1 Ab treatment also significantly inhibited the growth of human A375, C8161, and G3361 melanoma xenografts in NSG mice compared to that of the respective isotype control Ab-treated melanomas (Figure 30B). Immunohistochemical analysis revealed binding of *in vivo*-administered anti-human PD-1 Ab to melanoma xenografts (Figure 30C). Administration of anti-PD-1 Ab to NSG mice also abrogated the increased melanoma xenograft growth of isotype control-treated human *PDCD1*-OE compared to vector-control C8161 xenografts (Figure 30D). Marked melanoma binding of *in vivo*-administered anti-PD-1 Ab to *PDCD1*-OE C8161 melanomas (Figure 30D) confirmed melanoma-PD-1 reactivity of the human anti-PD-1 blocking Ab.

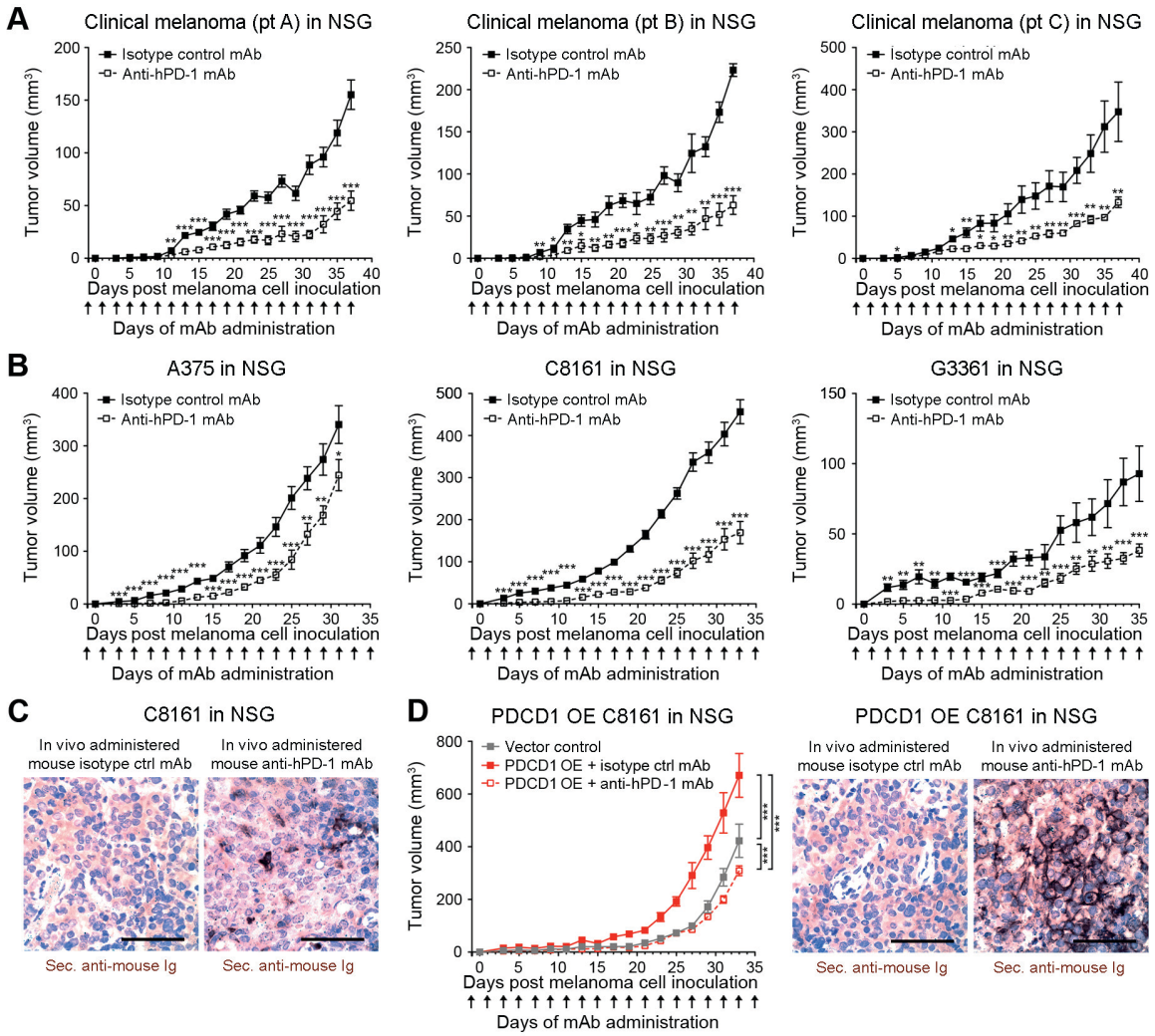

Figure 30. Anti-PD-1 blocking Ab inhibits human melanoma xenograft growth in immunocompromised mice. (A) Kinetics (mean ± SD) of clinical melanoma xenograft growth in NSG mice treated with anti-human PD-1 or isotype control Ab (patient A, *n*=7 each; patient B, *n*=5 versus 4; patient C: *n*=10 each). (B) Tumor growth kinetics (mean ± SD) and (C) representative secondary Ab staining of mouse anti-human PD-1 versus isotype control Ab-treated human A375 (*n*=14 each), C8161 (*n*=14 each), or G3361 melanoma xenografts (*n*=16 versus 12) or of (D) human *PDCD1*-OE versus vector control-transduced C8161 xenografts in NSG mice (*n*=10 each). IHC images illustrate binding of *in vivo*-administered mouse anti-human PD-1 blocking but not isotype control Ab to the respective human melanoma xenograft. Arrows indicate days of Ab administration. (size bars, 50µm). (* $P<0.05$, ** $P<0.01$, *** $P<0.001$). The data presented in this figure has been previously published (Kleffel et al., 2015).

Compared to isotype control Ab-treatment, PD-1 blockade also decreased three-dimensional melanoma growth *in vitro* (Figure 31A), but did not significantly induce apoptosis in human A375, C8161, or G3361 melanoma cultures (Figure 31B). Finally, treatment of G3361 melanoma cells with anti-PD-1, but not isotype control Ab, inhibited the PD-L1 Ig-dependent phosphorylation of S6 ribosomal protein (Figure 31C). Together, these findings in NSG mice indicate that anti-PD-1-mediated melanoma growth inhibition results from direct interference with melanoma-expressed PD-1 and is not necessarily dependent on adaptive immunity.

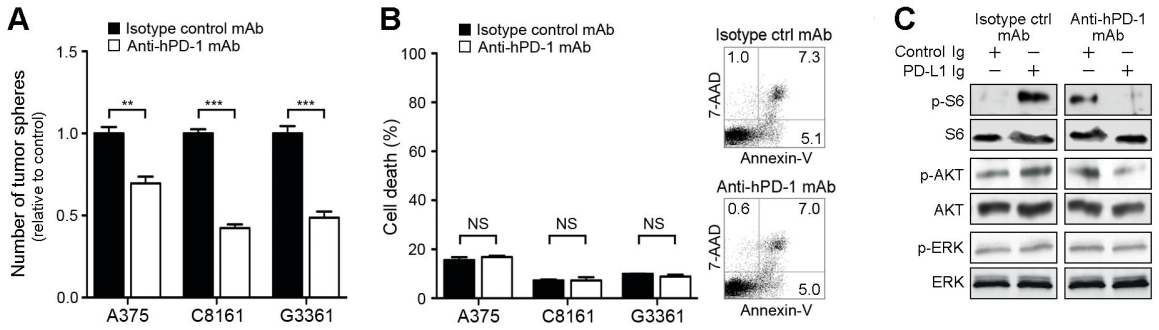

Figure 31. Antibody-mediated PD-1 blockade inhibits protumorigenic effects of PD-1-expressing human melanoma cells without inducing cell death. (A) Mean number of tumor spheres ± SEM, (B) flow cytometric assessment of cell death (percent $AnnexinV^+/7AAD^+$ cells, mean ± SEM) (left) and representative flow cytometry plots (right) of anti-PD-1- versus isotype control mAb-treated human A375, C8161, and G3361 melanoma cultures. (C) Immunoblot analysis (representative of n=3 independent experiments) of p- and total ribosomal protein S6, AKT, and ERK in G3361 cultures concurrently treated with PD-L1 Ig versus control Ig and/or anti-PD-1- versus isotype control mAb. (NS: not significant, $^{**}P<0.01$, $^{***}P<0.001$). The data presented in this figure has been previously published (Kleffel et al., 2015).

4.3.8 Melanoma cell expression of the PD-1 receptor target, p-S6, correlates with response to PD-1 therapy in cancer patients

To further assess the translational relevance of melanoma cell-intrinsic PD-1 receptor signaling, p-S6 staining was performed and melanoma-p-S6 positivity was quantitatively assessed in pre-treatment versus post-treatment tumor biopsies obtained from *n*=11 melanoma patients undergoing anti-PD-1 therapy. Interestingly, melanoma biospecimens sampled post PD-1 therapy demonstrated significantly (*P*=0.005) decreased p-S6 expression compared to patient-matched pre-treatment biopsies (Figure 32A), consistent with findings in PD-1 Ab-treated melanoma cell lines (Figures 29C and 31C). Additionally, in a cohort of *n*=34 melanoma patients where pre-treatment tumor tissue was available for analysis, patients with high p-S6 expression (>25% of melanoma cells, Figure 32B) prior to treatment showed a >3-fold increase in progression-free survival (mean progression-free survival: 17.0 versus 4.5 months, *P*=0.001, Figure 32C) and significantly (*P*<0.05) enhanced overall survival (mean overall survival: 25.1 versus 13.0 months, Figure 32D) compared to melanoma patients with low p-S6 levels (<25% of melanoma cells, Figure 32B) in pre-treatment tumor biospecimens (Table 2). These findings suggest a relationship between p-S6 and response to PD-1 pathway blockade, thereby indicating the potential translational relevance of melanoma cell-intrinsic PD-1 receptor functions.

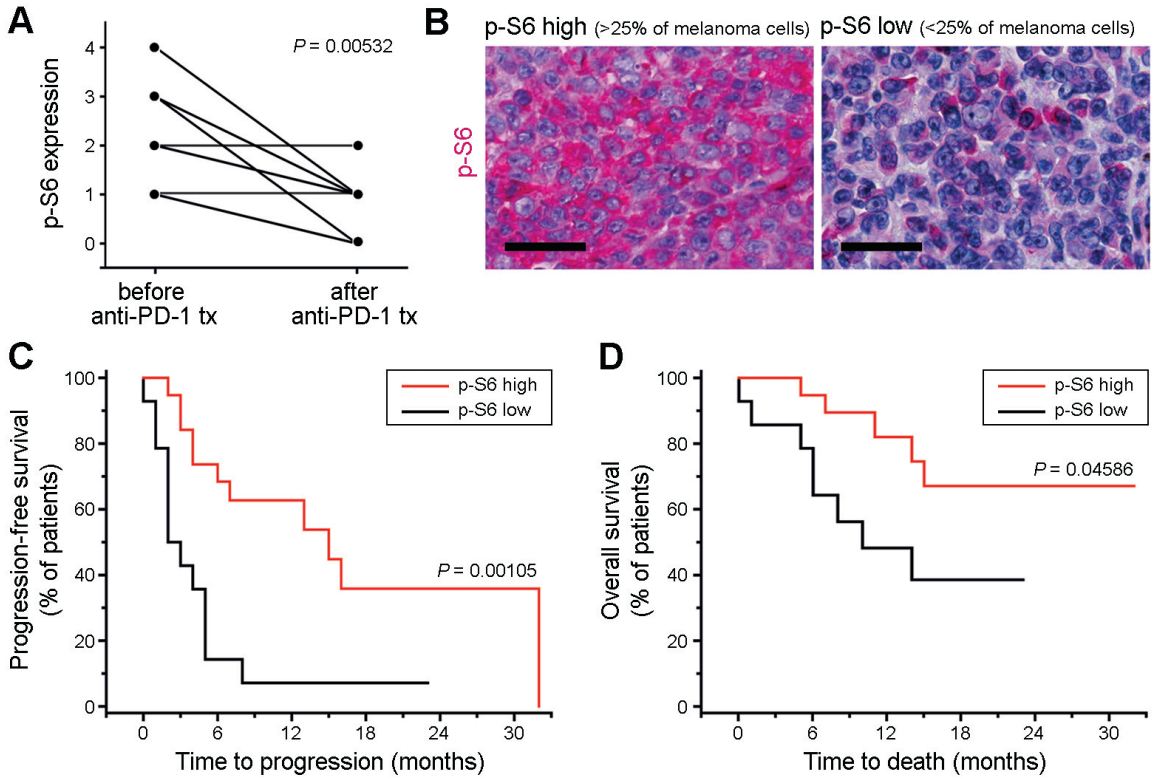

Figure 32. Analysis of p-S6 expression in tumor biospecimens obtained from patients with advanced-stage melanoma undergoing anti-PD-1 Ab therapy. (A) Expression of p-S6 ribosomal protein by melanoma cells in tumor biospecimens obtained from *n*=11 patients with stage IV melanoma before treatment start, compared to that in patient-matched progressive lesions sampled after initiation of anti-PD-1 Ab therapy. p-S6 expression by melanoma cells was determined by IHC analysis and graded by three independent investigators blinded to the study outcome on a scale of 0-4 (0: no p-S6 expression by melanoma cells; 1: p-S6 expression in 1-25%; 2: 26-50%; 3: 51-75%; 4: >75% of melanoma cells). (B) Representative p-S6 IHC of tumor biospecimens obtained from melanoma patients before initiation with systemic anti-PD-1 Ab therapy showing low (<25%) versus high (>25%) melanoma cell expression of p-S6. Size bars, 50µm. (C) Kaplan-Meier estimates of progression-free survival and (D) of overall survival probability in stage IV melanoma patients (*n*=34) demonstrating low (<25%, *n*=14 patients) versus high melanoma cell-expression of p-S6 (>25%, *n*=20 patients) in tumor biospecimens obtained before initiation of systemic anti-PD-1 Ab treatment. See also Table 2. The data presented in this figure has been previously published (Kleffel et al., 2015).

4.3.9 Discussion

Melanoma-expressed PD-1 was identified as a novel, immune independent protumorigenic mechanism in multiple independent experimental *in vitro* and *in vivo* systems. Enforced PD-1 expression by melanoma cells promoted, while melanoma-intrinsic PD-1 knockdown, mutagenesis of PD-1 signaling motifs, and antibody-mediated PD-1 blockade inhibited tumor growth in melanoma cultures completely devoid of immune cells, and in severely immunocompromised T cell-, B cell-, and innate immune cell-deficient hosts. Moreover, efficient PD-1-driven tumorigenesis required melanoma-PD-1 interactions with host- or melanoma-expressed PD-L1, because both PD-L1-deficient and PD-L1 Ab-treated mice grafted with *Pdcd1*-OE melanomas demonstrated decreased tumor growth compared to respective controls. Additionally, PD-L1 silencing reversed melanoma-PD-1-driven tumorigenesis, while recombinant PD-L1 Ig treatment promoted melanoma spheroid growth. Thus, beyond promoting cancer progression by limiting tumor-specific immune responses of PD-1 expressing lymphocytes, the herein presented data suggests that melanoma-expressed PD-L1 might also promote tumor growth directly via paracrine or autocrine activation of the melanoma-PD-1 receptor.

In T cells, PD-1 engagement by its ligands, PD-L1 or PD-L2, controls signaling networks downstream of the TCR complex, including mTOR and PI3K/AKT (Patsoukis et al., 2012, Riley, 2009, Sheppard et al., 2004). These oncogenic pathways also play important roles in melanoma survival and proliferation (Flaherty et al., 2012). Consistent with the herein described protumorigenic effects of melanoma-PD-1, *PDCD1*-KD, antibody-mediated PD-1 blockade, and mutagenesis of melanoma-PD-1 signaling motifs were found to decrease, while *PDCD1*-OE and PD-L1 Ig-treatment increased phosphorylation of the mTOR effector molecule (Corcoran et al., 2013), ribosomal protein S6. Melanoma-PD-1-dependent S6 phosphorylation was reversed via pharmacologic inhibition of mTOR but not PI3K, suggesting that the PD-1 receptor on melanoma cells

activates downstream mTOR signaling through a PI3K/AKT-independent pathway. However, whereas PD-1 activation augments p-S6 levels in melanoma cells and enhances tumor growth, it dampens mTOR signaling in T cells leading to diminished proliferation (Riley, 2009). Because S6 phosphorylation represents a point of convergence that integrates multiple upstream signaling networks (Corcoran et al., 2013, Flaherty et al., 2012), it is possible that melanoma-PD-1 might also modulate several alternative signaling networks, in addition to the mTOR pathway.

PD-1 ligation in T lymphocytes recruits phosphatases SHP-1 and SHP-2 to its ITIM and ITSM cytosolic loci. This induces dephosphorylation of proximal TCR signaling intermediaries and subsequent suppression of several pathways downstream of the TCR, including mTOR (Riley, 2009, Yokosuka et al., 2012). SHP-2 is also expressed by melanoma cells (Ostman et al., 2006, Win-Piazza et al., 2012) and tumor-initiating cell subsets in other cancers (Aceto et al., 2012, Liu et al., 2011), consistent with the preferential expression of PD-1 by melanoma-initiating cells demonstrated in chapter 4.1 and previously reported (Schatton et al., 2010). In cancer cells, SHP-2-dependent signaling promotes activation of protumorigenic pathways, including mTOR (Liu et al., 2011, Ostman et al., 2006). The divergent effects of PD-1 ligation on mTOR signaling in melanoma cells compared to T cells are thus entirely consistent with the opposing, protumorigenic versus growth-inhibitory roles of SHP-2 in the respective cell types.

PD-1 pathway interference inhibited tumor growth, including in the absence of immunity. These results suggest that antibody-mediated blockade of PD-1 directly on melanoma cells might represent an important additional, tumor cell-intrinsic mechanism that could contribute to the clinical effectiveness of PD-1 cancer therapy. Notably, clinical trials of therapeutic PD-1 pathway inhibitors report superior clinical activity and fewer immune-related adverse events compared to Abs targeting the alternate immune checkpoint, CTLA-4, in patients with advanced melanoma (Larkin et al., 2015, Robert et

al., 2015b). Moreover, PD-1 pathway interference has clinical benefits, even in patients that are refractory to CTLA-4 blockade (Ribas et al., 2015, Weber et al., 2013), patients with lesser immunogenic cancers that typically do not respond to immunotherapeutic regimens (Borghaei et al., 2015, Herbst et al., 2014, Topalian et al., 2012b), patients with pre-existing autoimmune disorders, and those suffering from major irAE during treatment with ipilimumab (Menzies et al., 2016).

To date, the majority of melanoma patients do not respond to PD-1 immunotherapy. Current research aims to identify biomarkers that can predict which patients will benefit from PD-1 pathway interference, in order to effectively guide treatment selection and improve patient outcome. Consistent with the protumorigenic effects of the melanoma-PD-1:PD-L1 axis, clinical trial data initially suggested a correlation between cancer cell- and TIL-PD-L1 expression and objective responses to PD-1 checkpoint blockade (Herbst et al., 2014, Topalian et al., 2012b, Tumeh et al., 2014). PD-L1 expression is heterogenous among cancer and immune cells, and is highly dynamic depending on cues from the TME. Because patients with PD-L1 negative tumors have been shown to respond to anti-PD-1 therapy, the use of PD-L1 IHC as a biomarker for treatment selection is not advised (Kakavand et al., 2015, Larkin et al., 2015, Postow et al., 2015b). To assess the potential translational relevance of the herein identified PD-1 receptor signaling mediator, p-S6, clinical melanoma biopsies from patients undergoing PD-1 targeted therapy were examined for p-S6 status. In this pilot study, data obtained from a small cohort of patients with stage IV disease suggests that tumoral expression of p-S6 correlates with clinical responses to anti-PD-1 Abs. However, the possible utility of p-S6 as a potential biomarker of PD-1 inhibitor sensitivity will require independent validation in larger prospective cohorts studies.

In summary, the results presented in this chapter identify PD-1 expressed by melanoma cells as a growth-promoting receptor and molecular mediator of melanoma cell-

intrinsic mTOR signaling. However, while T cell-PD-1 facilitates cancer progression by dampening antitumor immune responses, melanoma-PD-1 fuels tumor growth by inducing oncogenic signaling, even in the absence of adaptive immunity. Recognition of melanoma-PD-1-driven tumorigenesis critically enhances current understanding of the mechanisms underlying melanoma progression. In addition, identifying tumor growth-inhibitory effects of antibody-mediated PD-1 blockade at the level of the melanoma cell might help refine PD-1-targeted therapies to further improve outcome in patients with advanced stage cancers. The key findings presented in this chapter are summarized in Figure 33.

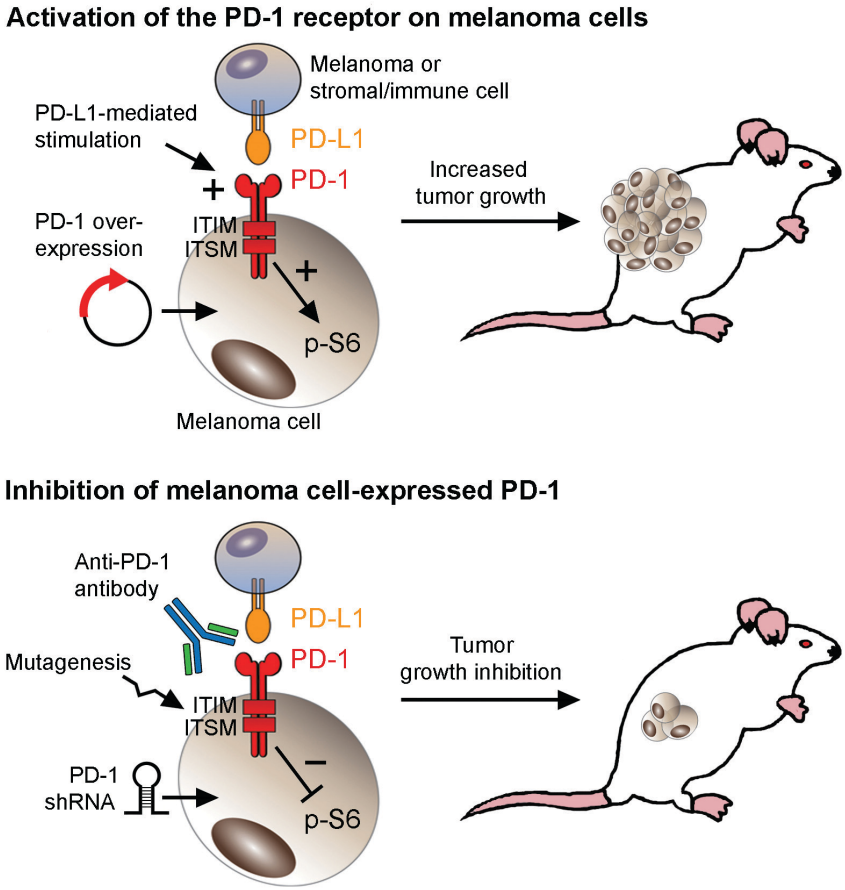

Figure 33. Melanoma cell-intrinsic PD-1 receptor functions promote tumor growth even in the absence of adaptive immunity. Melanoma-specific PD-1 overexpression promotes tumor growth, while inhibition of melanoma-PD-1 using PDCD1 specific shRNAs or PD-1 blocking Abs reduces tumor growth, independent of adaptive immunity. Engagement of melanoma-expressed PD-1 by its dominant ligand, PD-L1, and tumor-cell intrinsic PD-1 signaling via its ITIM and ITSM motifs is required for efficient tumor growth and S6, at least in part, via activation of the protumorigenic mTOR pathway.

4.4 ABCB5 marks therapy-refractory cell populations in Merkel cell carcinoma

Parts of this chapter have been previously published in *Kleffel S. et al. ABCB5-targeted chemoresistance reversal inhibits Merkel cell carcinoma growth. J Invest Dermatol. 2016;136(4):838-46.* Published data is highlighted in the individual figure legends.

4.4.1 Introduction

MCC is a rare, but highly aggressive neuroendocrine skin cancer with a mortality rate that is three-times higher than in melanoma (Lemos et al., 2010, Poulsen, 2004). Although MCC is an orphan malignancy with only an estimated 1500 cases per year in the United States, the MCC incidence rate has tripled over the past 20 years and continues to rise by 8% annually, due to improved detection and increased prevalence of patients with relevant risk factors (Bhatia et al., 2011, Hodgson, 2005). While surgical resection followed by adjuvant radiation therapy may initially clear patients of local disease, relapses are frequent and often fatal (Bhatia et al., 2011, Eng et al., 2007). Patients with metastatic disease are typically treated with systemic chemotherapy. Combination therapy with carboplatin and etoposide, the first-line chemotherapeutic agents used for treating advanced-stage MCC, initially yield response rates of up to 60%. However, clinical benefit is usually of limited duration, as tumors become chemoresistant (Bhatia et al., 2011, Fitzgerald et al., 2015, Tai et al., 2000). There are currently no well-established second-line treatment options for patients that progress, and ten-year survival has not changed over decades (Bhatia et al., 2011, Thakuria et al., 2014). Mechanisms of MCC chemotherapy resistance are largely understudied because of the limited availability of human MCC cell lines and patient samples from this rare form of cancer (Becker, 2010). This highlights the need for studies

aimed at elucidating the molecular mechanisms underlying MCC therapeutic resistance to identify novel treatment modalities and improve patient survival.

The laboratory of Dr. Markus Frank has previously cloned and characterized the ABCB5 transporter (Frank et al., 2005, Frank et al., 2003, Frank et al., 2011, Ksander et al., 2014, Lin et al., 2013, Schatton et al., 2008, Schatton et al., 2010, Schatton et al., 2015, Wilson et al., 2014, Wilson et al., 2011), which has been shown to serve as a clinically relevant multidrug resistance (MDR) mediator in human melanoma (Chartrain et al., 2012, Frank et al., 2005, Wilson et al., 2014), colorectal cancer (Wilson et al., 2011), hepatocellular carcinoma (Cheung et al., 2011b) and osteosarcoma (Wang and Teng, 2016). ABCB5 functions as an ATP-dependent drug efflux transporter that effuses multiple, structurally and functionally unrelated chemotherapeutic drugs, to decrease intracellular accumulation. Blockade of ABCB5-mediated efflux augments intracellular drug concentrations, thereby sensitizing cancer cells to chemotherapy-induced apoptosis (Frank et al., 2005, Wilson et al., 2011). In addition, ABCB5 expression correlates with tumor virulence and clinical cancer progression (Cheung et al., 2011b, Gambichler et al., 2016, Gazzaniga et al., 2010, Schatton et al., 2008, Sharma et al., 2010, Wilson et al., 2011). Given its role in MDR in cancers of various etiologies, including melanoma, ABCB5 was hypothesized to also contribute to chemotherapy resistance in MCC.

The herein reported results establish ABCB5 expression in MCC, and show that ABCB5 marks therapy-refractory tumor subpopulations in MCC patients after standard-of-care carboplatin- and etoposide-based combinatorial therapy. Similarly, $ABCB5^{+}$ tumor cells preferentially survived carboplatin- and etoposide-induced cytotoxicity in MCC xenotransplantation models. Moreover, antibody-mediated ABCB5 blockade sensitized MCC cells to carboplatin- and etoposide-mediated cell killing and significantly increased inhibition of MCC xenograft growth.

4.4.2 ABCB5 is expressed by MCC cells and expression levels are elevated post-chemotherapy

In healthy human skin, ABCB5 is expressed only on rare subsets of cells (Frank et al., 2003, Schatton et al., 2015). Similarly, in human melanoma, ABCB5 expression is confined to relatively rare tumorigenic minority populations (Schatton et al., 2008). In contrast, clinical human MCC specimens obtained at various stages of disease progression (n = 85) demonstrated marked ABCB5 membrane expression by CK20-positive MCC cells (Figure 34A). Although cell-cell membrane apposition made it difficult to enumerate the exact number of positive cells and specimens displayed heterogeneity for ABCB5 expression, ABCB5 immunoreactivity was typically observed in the majority of tumor cells. Table 3 summarizes the clinical parameters for all MCC biopsies analyzed. Aggregate quantitative RT-PCR-based analysis of all tissue specimens showed significantly higher (P<0.001) ABCB5 mRNA expression in MCC patient biopsies (n = 85) compared with normal human skin (n = 10) (Figure 34B). Previous studies described correlation between ABCB5 frequency and disease progression in melanoma (Schatton et al., 2008, Setia et al., 2012) and other cancers (Cheung et al., 2011b). Accordingly, ABCB5 expression levels in MCC biopsies obtained before and after first-line chemotherapy from three patients afflicted by this extraordinarily rare disease were examined next. Analysis of patient-matched pre- and post-chemotherapy MCC specimens revealed significantly increased ABCB5 mRNA expression in post-chemotherapy local recurrences compared with pre-chemotherapy biopsy specimens, both at the mRNA (Figure 34C) and immunoreactive protein levels (cell frequency 59.2 ± 4.1% post-chemotherapy versus 14.0 ± 1.0% pre-chemotherapy, mean ± SEM, respectively, P<0.001) (Figure 34D). These findings in patient specimens support the possibility that ABCB5$^+$

MCC cells are preferentially resistant to treatment with the first-line chemotherapeutic agents, carboplatin and etoposide.

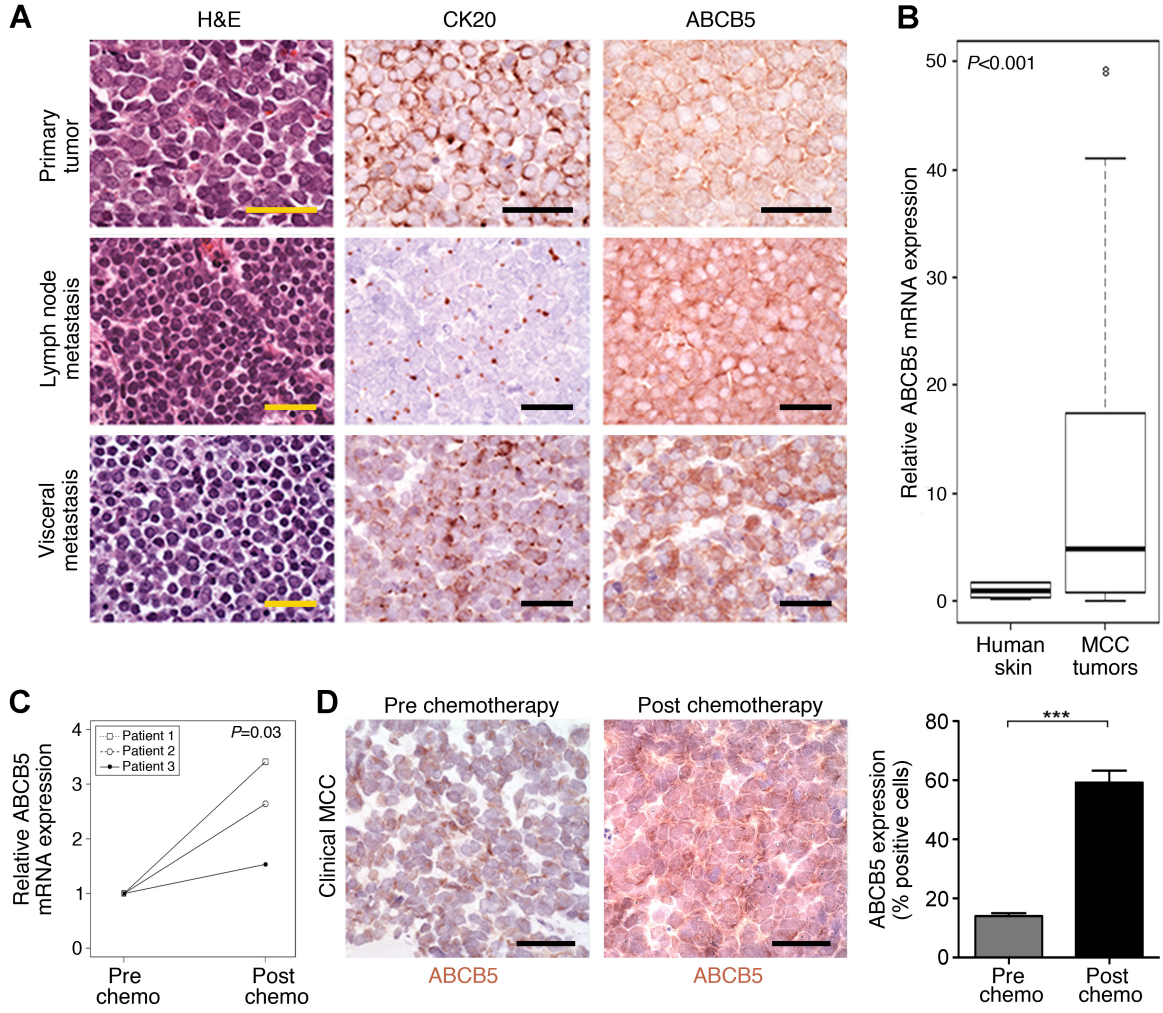

Figure 34. Clinical MCC specimens express higher ABCB5 levels post first-line chemotherapy. (A) Representative hematoxylin and eosin (H&E), CK20 and ABCB5 IHC of a primary MCC tumor, a lymph node and visceral metastasis. (B) Relative ABCB5 mRNA expression in normal human skin (*n*=10) versus clinical MCC specimens (*n*=85), as determined by quantitative RT-PCR. (C) Relative ABCB5 mRNA expression and (D) immunohistochemically-determined ABCB5 protein expression (mean ± SEM) by patient-matched pre- and post-chemotherapy MCC biospecimens (*n*=3, respectively). Size bars, 50 µm. (NS: not significant, *** P<0.001). The data presented in this figure has been previously published (Kleffel et al., 2016).

4.4.3 ABCB5^{+} MCC cells preferentially survive chemotherapy-induced cytotoxicity

Because it was previously demonstrated that ABCB5 expression confers chemotherapeutic resistance in several human cancers (Chartrain et al., 2012, Cheung et al., 2011b, Frank et al., 2005, Wilson et al., 2014, Wilson et al., 2011), the potential functional contribution of ABCB5 to carboplatin and/or etoposide resistance in MCC was examined next. ABCB5 mRNA expression in the established human MCC cell lines MKL-1, MKL-2, MS-1, and WaGa (Guastafierro et al., 2013, Houben et al., 2010, Rodig et al., 2012a, Rosen et al., 1987) was determined by RT-PCR amplification and sequencing (Figure 35A). Established MCC cell lines also showed ABCB5 surface protein expression, as determined by immunofluorescence staining (Figure 35B). Flow cytometric analysis revealed ABCB5 protein expression, with cell frequencies averaging 10.0 ± 1.8% for MKL-1, 9.1 ± 2.4% for MKL-2, 8.3 ± 1.5% for MS-1 and 16.9 ± 5.4% for WaGa cells (mean ± SEM) (Figure 35C).

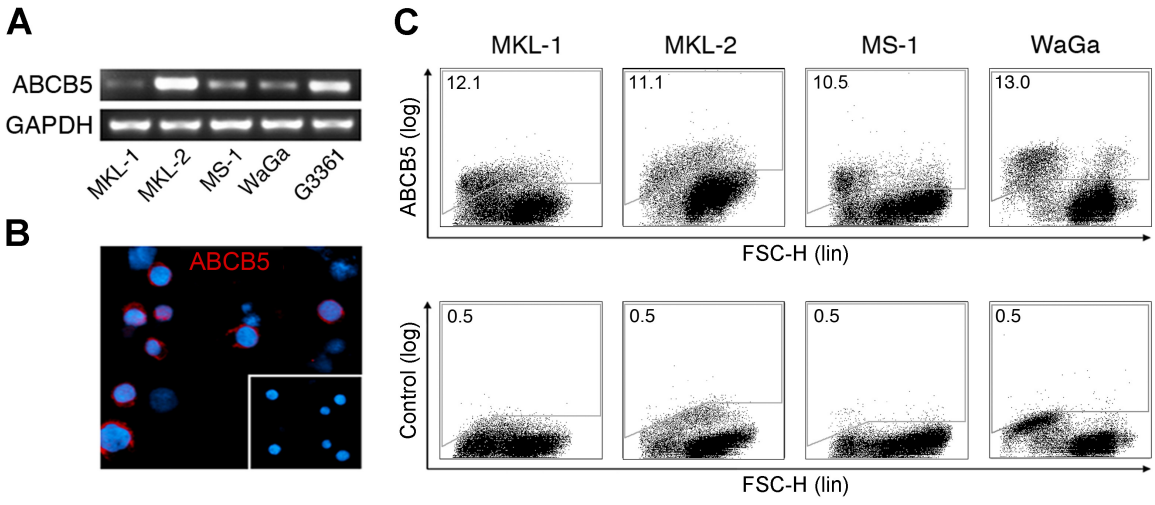

Figure 35. ABCB5 expression by established human MCC cells. (A) ABCB5 mRNA expression by MKL-1, MKL-2, MS-1, and WaGa MCC cell lines, as determined by RT-PCR (positive control: G3361 melanoma cells). (B) Representative ABCB5

immunofluorescence staining (red) of a cytospin preparation of WaGa cells (inset: isotype control Ab staining). Nuclei are counterstained with DAPI (blue). (C) Representative flow cytometry plots of ABCB5 protein expression by MKL-1, MKL-2, MS-1, and WaGa cells (*n*=6 independent experiments). The data presented in this figure has been previously published (Kleffel et al., 2016).

To explore the potential role of ABCB5 in MCC refractoriness to first-line chemotherapy, ABCB5 expression was assessed in control (wildtype) versus MCC-lines rendered drug-resistant via continuous exposure to carboplatin or etoposide over a 2-month period. First, preferential survival of carboplatin- and etoposide-resistant compared with wildtype MCC cells was confirmed for the respective drugs (Figure 36).

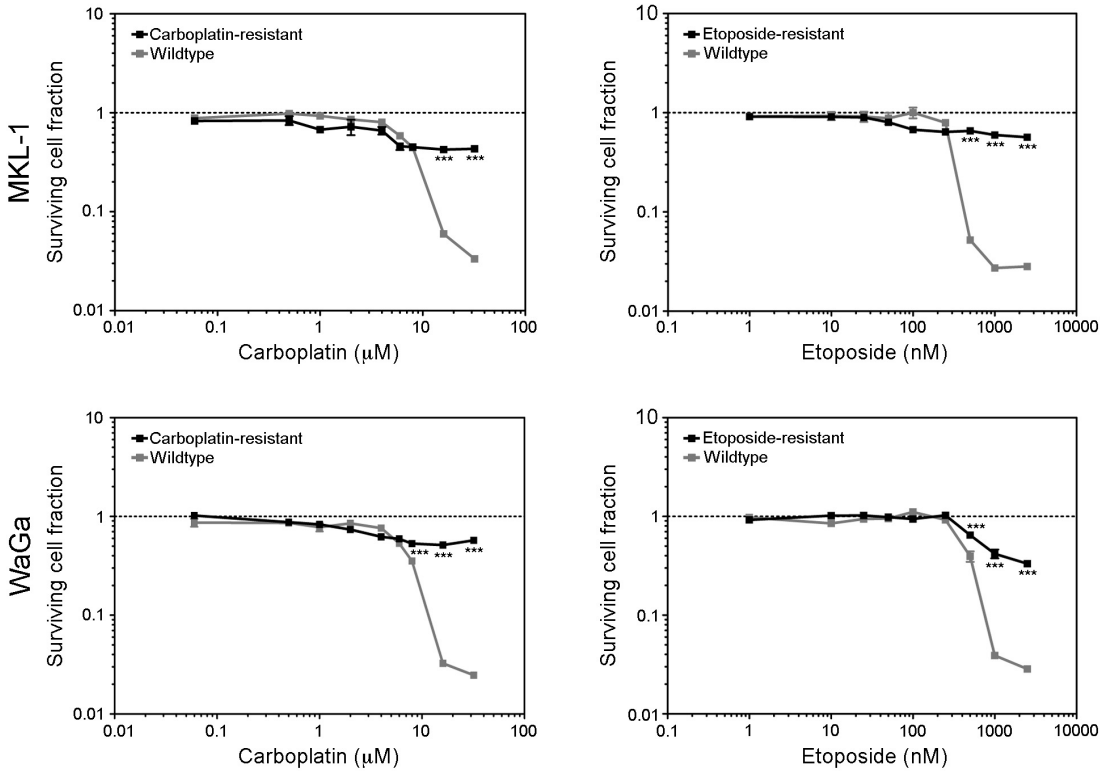

Figure 36. **Characterization of carboplatin- and etoposide-resistant MCC cell lines.** Carboplatin- and etoposide-dependent cell killing of wildtype versus carboplatin- or etoposide-resistant MKL-1 (top) and WaGa cells (bottom), as determined by the MTT assay. Surviving cell fractions are plotted as a function of carboplatin or etoposide concentration (n = 6 replicates each, representative of n = 3 independent experiments,

respectively). (*** P<0.001). The data presented in this figure has been previously published (Kleffel et al., 2016).

Subsequent quantitative RT-PCR analyses revealed markedly increased ABCB5 mRNA expression levels in both carboplatin- and etoposide-resistant MKL-1, MKL-2, MS-1 and WaGa cell lines compared to controls (Figure 37A). At the protein level, exposure to cytotoxic levels of carboplatin or etoposide resulted in significantly increased ABCB5 expression among viable MKL-1, MKL-2, MS-1, and WaGa cells compared with vehicle-treated controls, respectively (Figure 37B and C). Although the percentage of $ABCB5^+$ cells was markedly enhanced in chemorefractory MCC cell lines, a significant proportion of carboplatin- and etoposide-resistant cells did not display ABCB5 expression. The viability of $ABCB5^+$ versus $ABCB5^-$ MKL-1 and WaGa cells grown in the presence of cytotoxic carboplatin or etoposide levels was compared next, to directly demonstrate that $ABCB5^+$ tumor cell subsets preferentially survive carboplatin- and etoposide-induced cytotoxicity. Indeed, $ABCB5^+$ cells cultured under these conditions demonstrated increased viability compared to $ABCB5^-$ MCC populations (Figure 37D). This suggests that $ABCB5^+$ MCC subsets preferentially survive drug-induced cell killing.

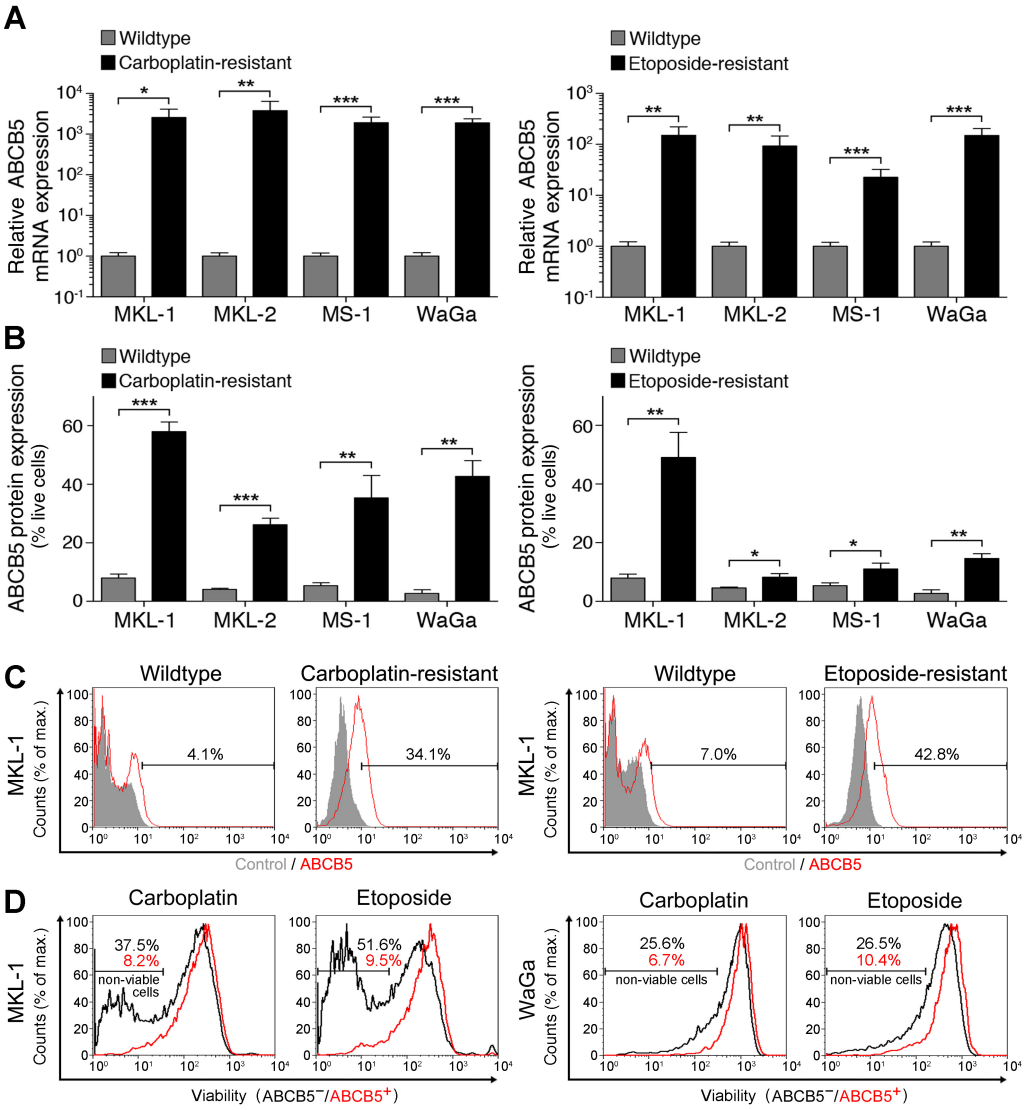

Figure 37. ABCB5 expression in response to *in vitro* carboplatin and etoposide treatment. (A) Relative ABCB5 mRNA expression (mean ± SEM) by MCC cells resistant to 50-150 µM carboplatin or 1-3 µM etoposide compared with that in wildtype MCC cells, as determined by quantitative RT-PCR (*n*=6-9 each, representative of 2-3 independent experiments). (B) Flow cytometrically determined ABCB5 protein expression (% live cells, mean ± SEM) in wildtype versus carboplatin- or etoposide-resistant MCC cells (*n*=3-8 independent experiments, respectively). (C) Representative histogram plots of ABCB5 protein expression (MKL-1) in experimental groups as in (B) and of (D) cell viability (calcein AM positivity) of wildtype ABCB5$^+$ versus ABCB5$^-$ MCC cells cultured in the presence of cytotoxic carboplatin (250 µM) or etoposide (5 µM) concentrations. (* P<0.05, ** P<0.01, *** P<0.001). The data presented in this figure has been previously published (Kleffel et al., 2016).

However, the possibility of induction of ABCB5 expression, as opposed to preferential survival of ABCB5^{+} MCC cells cannot be excluded entirely based on this data. Because other ABC transporters, including ABCB1, ABCC3, and ABCG2, are known mediators of carboplatin and etoposide resistance in other cancers (Dean et al., 2001), it was examined whether drug-resistant MCC lines also expressed high levels of these ABC transporters, in addition to ABCB5. All drug-resistant MCC cell lines examined, with the exception of etoposide-resistant MKL-1 cells, showed a significant increase in ABCB1 and ABCC3, but not ABCG2 transcript expression compared to the respective wildtype cell lines (Figure 38). This raises the possibility that several ABC transporters, in addition to ABCB5, might contribute to chemoresistance in drug-induced MCC cell lines. Together, these results suggest a direct relationship between therapeutic resistance to carboplatin and etoposide and ABCB5 expression in the MCC lines. However, additional ABC transporters, including ABCB1 and ABCC3, may potentially contribute to MCC chemoresistance.

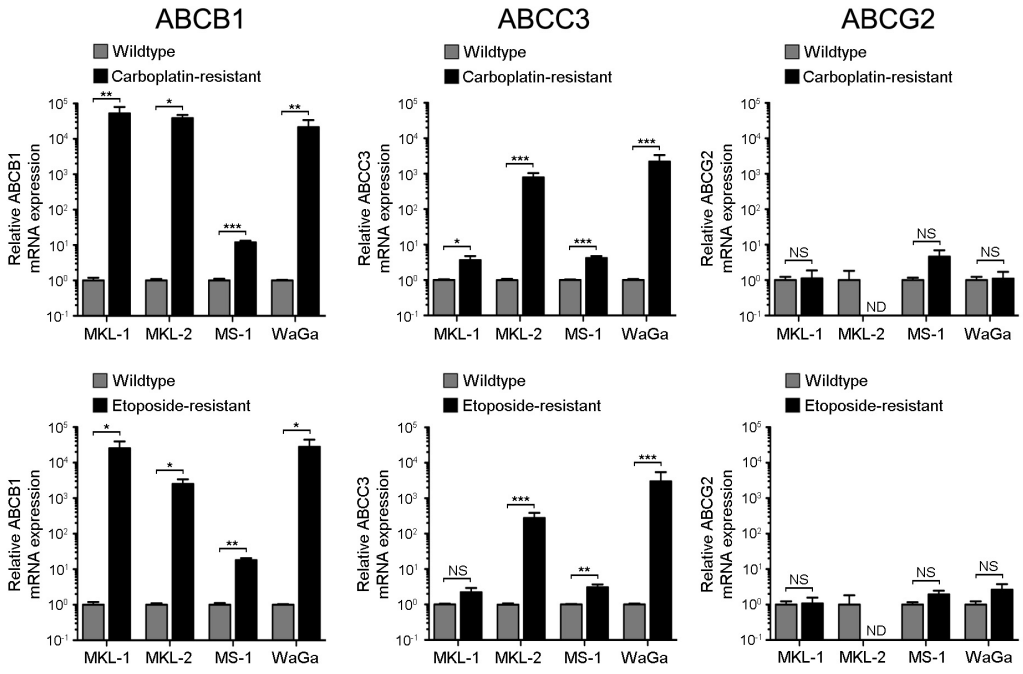

Figure 38. Expression of ABC transporters by carboplatin- and etoposide-resistant MCC cell lines. Relative ABCB1, ABCC3, and ABCG2 mRNA expression (mean ± SEM) by MCC cells resistant to carboplatin (top) or etoposide (bottom) compared to

wildtype MCC cells, as determined by quantitative RT-PCR (n = 3-12, respectively). (ND: not detected, NS: not significant, * P<0.05, ** P<0.01, *** P<0.001). The data presented in this figure has been previously published (Kleffel et al., 2016).

4.4.4 Antibody-mediated ABCB5 blockade reverses MCC resistance to chemotherapy

To explore the potential role of ABCB5 as a mediator of carboplatin- and etoposide resistance in MCC, the cell viability in MCC cultures exposed to increasing concentrations of carboplatin or etoposide in the presence of an anti-ABCB5 blocking mAb (Frank et al., 2005, Frank et al., 2003, Ksander et al., 2014, Schatton et al., 2008, Wilson et al., 2014) versus isotype control mAb was evaluated. ABCB5 blockade reversed carboplatin and etoposide resistance of both MKL-1 and WaGa cells (Figure 39A), resulting in significantly enhanced cell killing at all carboplatin concentrations greater than 1 μM versus controls and at etoposide concentrations as low as 10 nM in MKL-1 cells. Concomitantly, LD_{50} values were reduced in both MKL-1 cells (Carboplatin: LD_{50} 2.3 μM versus 5.9 μM and Etoposide: LD_{50} 25.0 nM versus 62.4 nM, respectively) and WaGa cells (Carboplatin: LD_{50} 3.1 μM versus 7.6 μM and Etoposide: LD_{50} 98.4 nM versus 130.4 nM, respectively) treated with anti-ABCB5 versus isotype control mAb (Figure 39A). Drug-induced selection for $ABCB5^{+}$ MCC cells (Figure 37) might hereby explain why the ABCB5 blocking mAb mediates carboplatin- and etoposide-induced cytotoxicity in proportions of MCC cells that exceeded those frequencies observed in native cell lines (Figure 35C), especially at higher drug concentrations. Treatment with the anti-ABCB5 mAb alone had no significant effect on *in vitro* cell survival (Figure 39B). However, in line with its blocking specificity, anti-ABCB5 mAb induced compensatory increases in ABCB5 mRNA expression compared to isotype control mAb treatment (Figure 39C). To

more rigorously demonstrate that the anti-ABCB5 mAb used in this study blocks ABCB5 function in MCC, the ability to block cellular efflux of the green fluorescent dye and known ABCB5 substrate (Frank et al., 2003, Lin et al., 2013), rhodamine 123 (Rh123) in MCC cells was examined next. Compared with isotype control mAb-treated MCC cells, of which a subpopulation of 19.0%±2.8% (mean ± SEM, n = 3) effluxed Rh123 over a 120 minute incubation period at 37°C, mAb-mediated ABCB5 blockade significantly (P<0.05) inhibited Rh123 efflux by >60% (Figure 39D). The effect of ABCB5 blockade on Rh123 efflux was assessed compared with incubation of MCC cells for 120 minutes at 4°C (Figure 39D), which blocks ATP hydrolysis and hence ABC transport function (Frank et al., 2003, Lin et al., 2013). Together, these results established that ABCB5 is expressed as a functional xenobiotic efflux transporter in MCC, and that ABCB5 blockade reverses carboplatin and etoposide resistance in this malignancy.

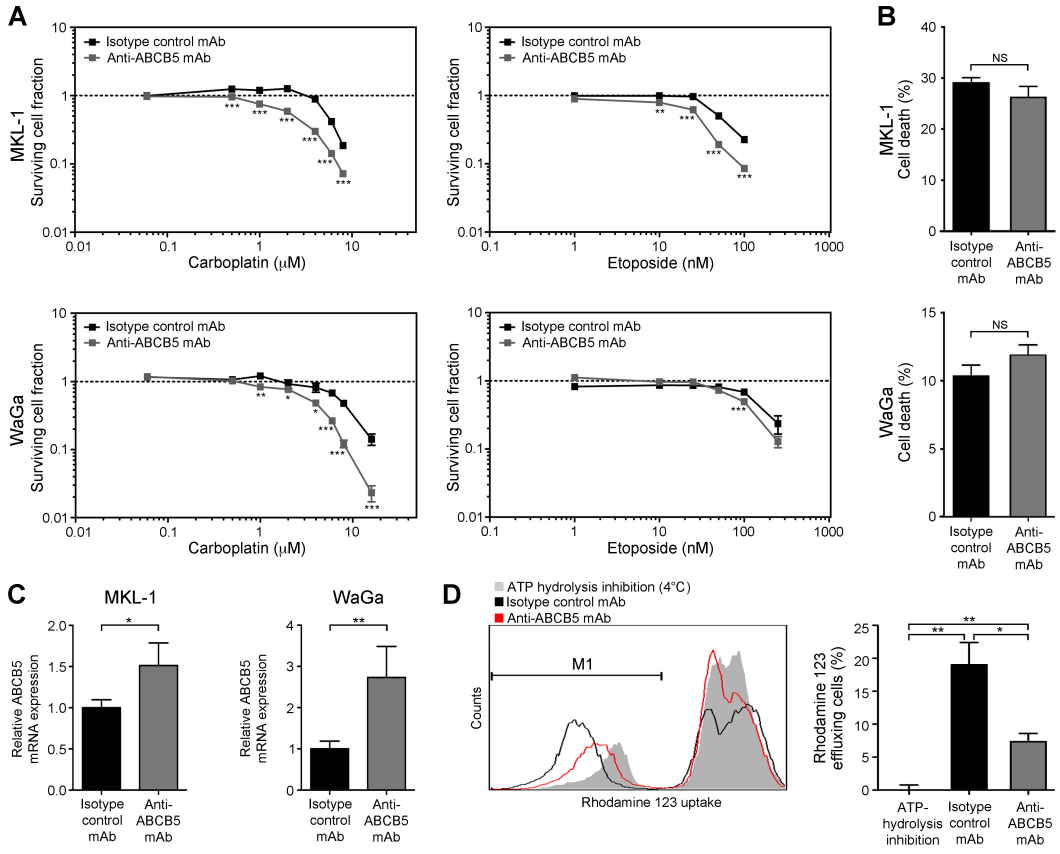

Figure 39. Chemoresistance reversal of MCC cells by ABCB5 inhibition. (A) Effects of anti-ABCB5 versus isotype control Ab on carboplatin- or etoposide-induced MKL-1

and WaGa cell killing, as determined by the MTT assay. Surviving cell fractions are plotted against drug concentration (n=6 each, representative of n=3 independent experiments). (B) Flow cytometric assessment of cell death (percent Annexin-V^+/$7AAD^+$ cells, mean ± SEM, n=3) and (C) relative ABCB5 mRNA expression (mean ± SEM) in isotype control- versus anti-ABCB5 Ab-treated MCC cultures (n=3-9, respectively). (D) Representative histogram plot and percent Rh123-effluxing wildtype MKL-1 cells (mean ± SEM) under conditions of isotype control or ABCB5-blocking Ab treatment (37°C), or with incubation at 4°C to block ATP-dependent efflux (n=3 independent experiments). (NS: not significant, * P<0.05, ** P<0.01, *** P<0.001). The data presented in this figure has been previously published (Kleffel et al., 2016).

4.4.5 MCC tumor xenografts express increased ABCB5 levels post chemotherapy

The relationship between ABCB5 and first-line chemotherapy resistance in MCC was investigated utilizing an established *in vivo* model system (Lezcano et al., 2014). MKL-1 and WaGa tumors grew at similar rates (Figure 40A) and exhibited CK20 and ABCB5 expression profiles similar to those found in patient MCC samples (Figure 40B).

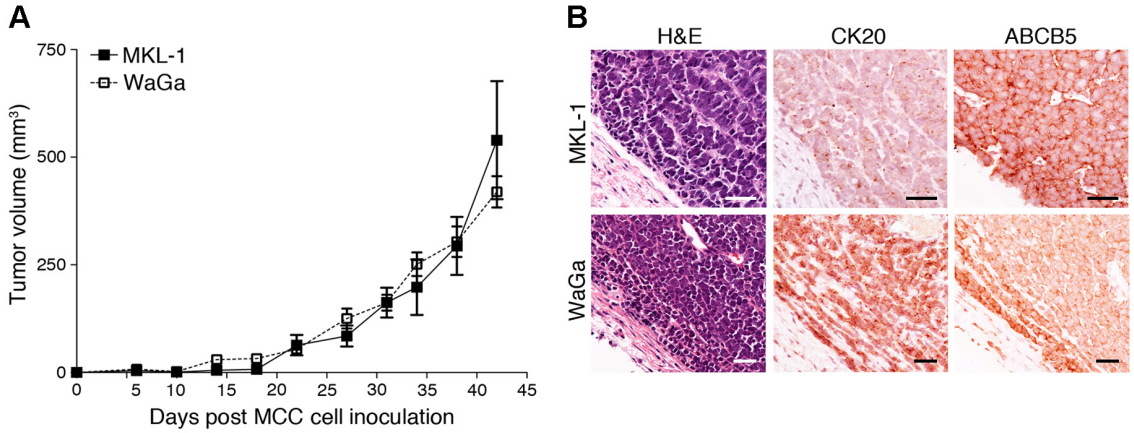

Figure 40. ABCB5 expression in MCC tumor xenografts. (A) MCC tumor volumes (mm^3, mean ± SD) plotted against days post xenotransplantation of MKL-1 and WaGa

cells to NSG mice (n = 4-6, respectively) and (B) representative H&E staining, CK20, and ABCB5 IHC of the respective MCC tumor xenografts at the experimental endpoint. Size bars, 50 μm. The data presented in this figure has been previously published (Kleffel et al., 2016).

Next, the response of $ABCB5^+$ cancer cell populations to treatment with carboplatin or etoposide was examined in NSG mice bearing MKL-1 or WaGa xenografts. Administration of carboplatin or etoposide to NSG mice for six consecutive days using previously established doses (Fichtner et al., 2008) resulted in significant volume reduction of pre-established MKL-1 and WaGa xenograft tumors, whereas vehicle-treated controls showed continued tumor growth (Figure 41A). Quantitative RT-PCR analysis revealed greater than 8-fold elevation of ABCB5 mRNA expression by tumor xenograft tissue harvested from carboplatin- and etoposide-treated versus vehicle control-treated MKL-1 ($P<0.001$) or WaGa xenograft-bearing mice ($P<0.05$), respectively (Figure 41B). Compared to tumor xenografts of vehicle control-treated mice, residual MKL-1 and WaGa specimens resected from NSG mice treated with carboplatin or etoposide also showed 2.0-4.3-fold enhanced ($P<0.001$, respectively) ABCB5 protein expression by viable MCC cells (Figure 41C), consistent with the *in vitro* results (Figure 37).

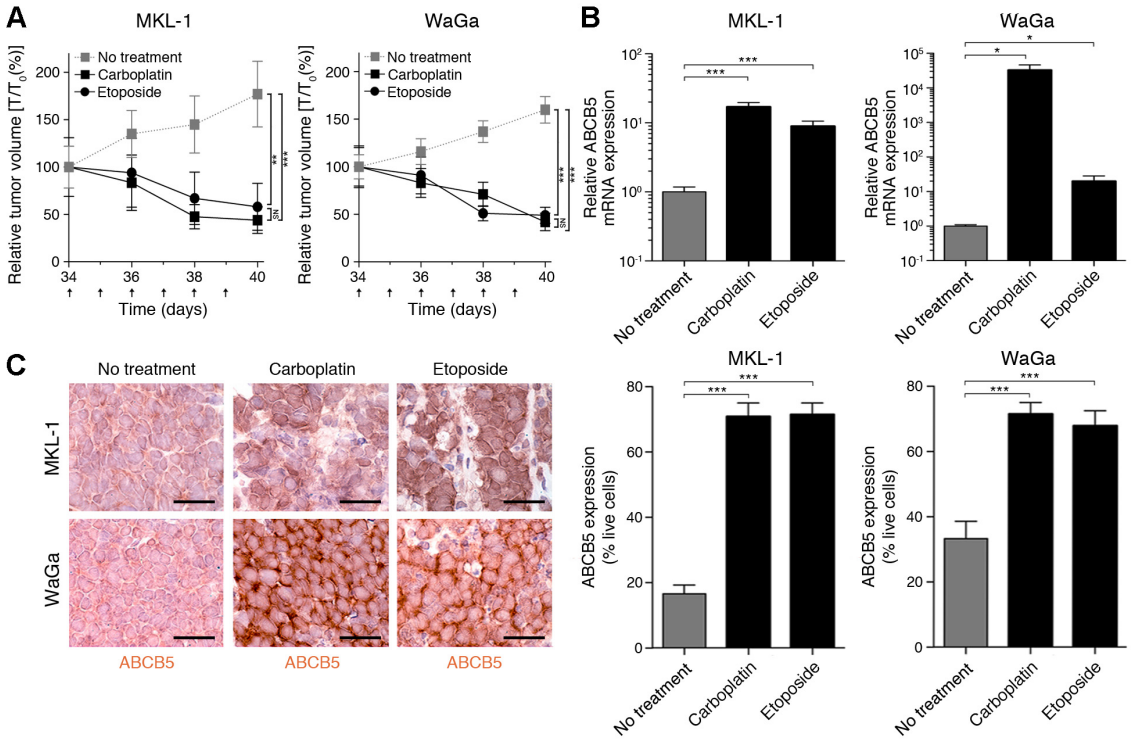

Figure 41. Response of ABCB5 expression to carboplatin and etoposide treatment in MCC tumor xenografts. (A) Tumor growth kinetics (mean ± SD) of vehicle control-, carboplatin- (75 mg/kg/d) or etoposide-treated (10 mg/kg/d) MKL-1 and WaGa xenografts in NSG mice (*n*=6-8, respectively). Arrows indicate days of carboplatin or etoposide administration. (B) Relative ABCB5 mRNA expression (mean ± SEM) determined by quantitative RT-PCR and (C) immunohistochemically determined ABCB5 protein expression (mean ± SEM) by MCC xenografts (*n*=6-8, respectively) harvested 40 days post inoculation to NSG mice, in experimental groups as in (A). Representative images of ABCB5 IHC are shown on the left. Size bars, 50 µm. (NS: not significant, * P<0.05, ** P<0.01, *** P<0.001). The data presented in this figure has been previously published (Kleffel et al., 2016).

In line with the herein presented *in vitro* findings, ABCB1 and ABCC3 transcript levels were also elevated in both MKL-1 and WaGa tumors resected from NSG mice treated with carboplatin or etoposide compared to those treated with vehicle control (Figure 42).

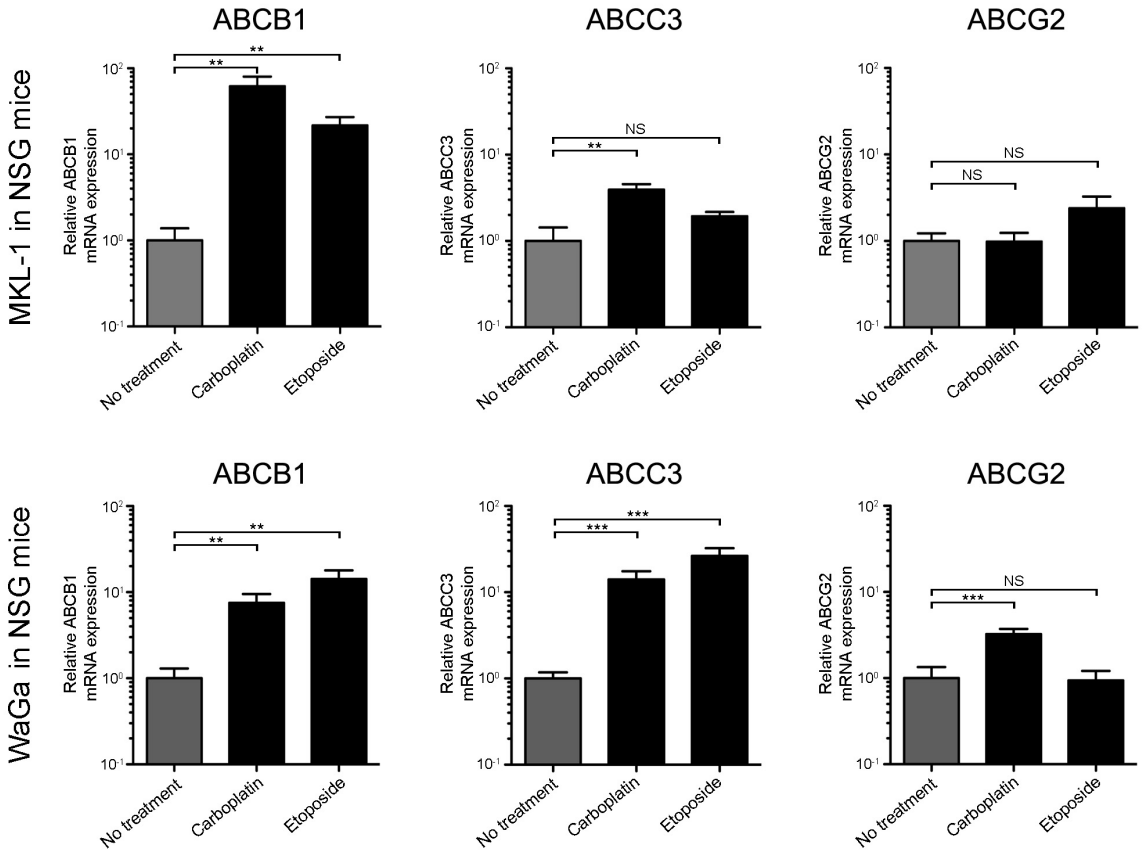

Figure 42. ABC transporter expression by MCC xenografts in response to carboplatin and etoposide treatment. Relative ABCB1, ABCC3, and ABCG2 mRNA expression (mean ± SEM) by MKL-1 (top) and WaGa (bottom) tumor xenografts harvested 40 days post inoculation to NSG mice treated with vehicle control (n = 4-7), carboplatin (n = 5), or etoposide (n = 5), respectively, as determined by quantitative RT-PCR. (NS: not significant, ** P<0.01, *** P<0.001). The data presented in this figure has been previously published (Kleffel et al., 2016).

4.4.6 Antibody-mediated blockade of ABCB5 sensitizes MCC cells to chemotherapy-induced killing and inhibits tumor growth

To determine if ABCB5 blockade in the context of carboplatin- or etoposide-based monotherapy has an additive inhibitory effect on MCC growth *in vivo*, submaximal doses of carboplatin (30 mg/kg) or etoposide (5 mg/kg) were administered in combination with

anti-ABCB5 mAb (Frank et al., 2005, Frank et al., 2003, Ksander et al., 2014, Lin et al., 2013, Schatton et al., 2008, Schatton et al., 2015, Wilson et al., 2014) or isotype control mAb to MKL-1 or WaGa tumor xenograft-bearing NSG mice. Compared with the respective vehicle control groups, low-dose carboplatin or etoposide treatment resulted in significantly (P<0.01) attenuated growth of both MKL-1 and WaGa tumor xenografts (Figure 43A). Importantly, combination therapies involving anti-ABCB5 mAb plus carboplatin or anti-ABCB5 mAb plus etoposide resulted in significantly greater inhibition of tumor growth compared to treatment with either chemotherapeutic alone (P<0.05, respectively) (Figure 43A). Immunohistochemical analysis of serial sections of resected MKL-1 and WaGa specimens revealed binding of *in vivo*-administered mAb to tumor target tissue, which coincided with regions of ABCB5 positivity, in anti-ABCB5 mAb-co-treated, but not isotype control mAb-co-treated carboplatin or etoposide treatment groups (Figure 43B). This finding suggests a direct anti-ABCB5 mAb effect on $ABCB5^+$ MCC target cells. MKL-1 and WaGa xenografts of NSG mice treated with either carboplatin or etoposide plus isotype control mAb showed only moderate apoptotic cell death compared with vehicle controls, as determined by CC3 immunostaining (Figure 43B). However, the combination therapies involving carboplatin or etoposide plus anti-ABCB5 mAb resulted in enhanced MCC apoptosis in tumor areas that also showed binding of anti-ABCB5 mAb to MCC cells (Figure 43B).

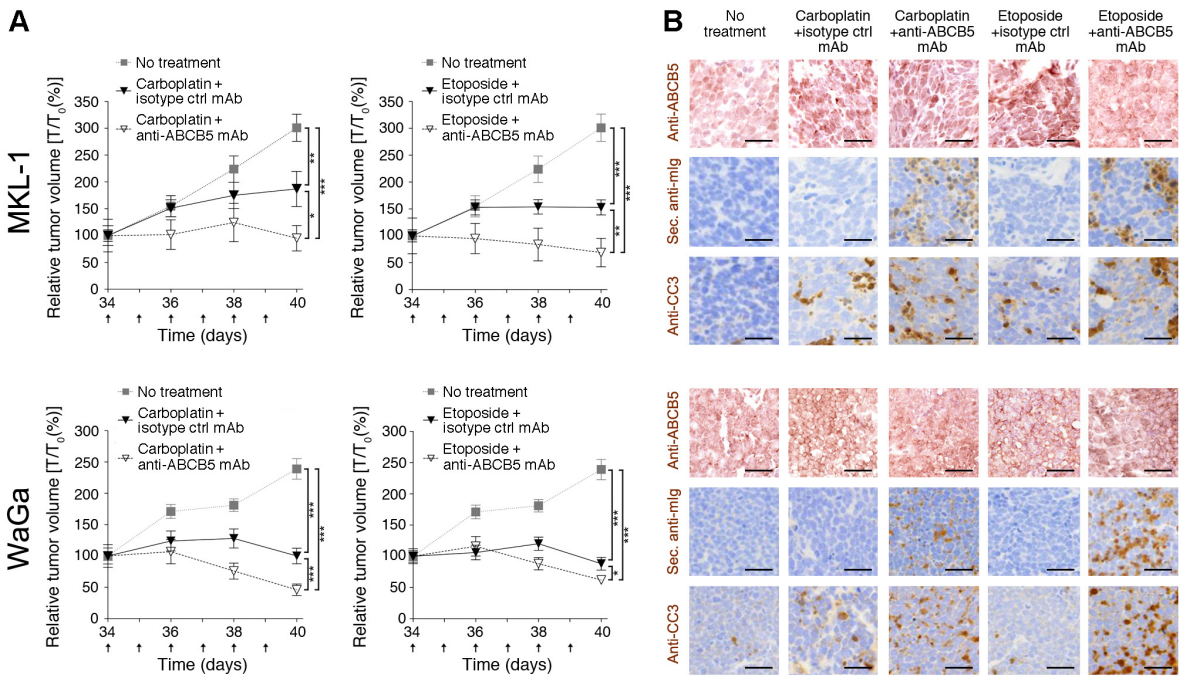

Figure 43. Effect of ABCB5 blockade on MCC tumor xenograft growth and chemotherapy-induced cytotoxicity. (A) Tumor growth kinetics (mean ± SD) and (B) ABCB5, secondary Ab (sec. anti-mIg staining, recognizing *in vivo*-administered anti-ABCB5 Ab) and CC3 IHC staining of MKL-1 (top, n = 6-8) and WaGa (bottom, n = 8-9) xenografts dissected from vehicle control-, carboplatin- (30 mg/kg/d) or etoposide-treated (5 mg/kg/d) NSG mice also treated with anti-human ABCB5- or isotype control Ab (500 µg/d), respectively. Arrows in panel (A) indicate days of carboplatin or etoposide, and isotype control or anti-ABCB5 Ab administration. Size bars, 50 µm. (* P<0.05, ** P<0.01, *** P<0.001). The data presented in this figure has been previously published (Kleffel et al., 2016).

Without concurrent administration of carboplatin or etoposide, anti-ABCB5 mAb administration to MKL-1 or WaGa tumor xenograft-bearing NSG mice at the equivalent experimental endpoint did not result in significant differences in tumor growth (Figure 44A) and did not induce apoptosis in tumor target cell death, compared with isotype control mAb treatment alone (Figure 44B).

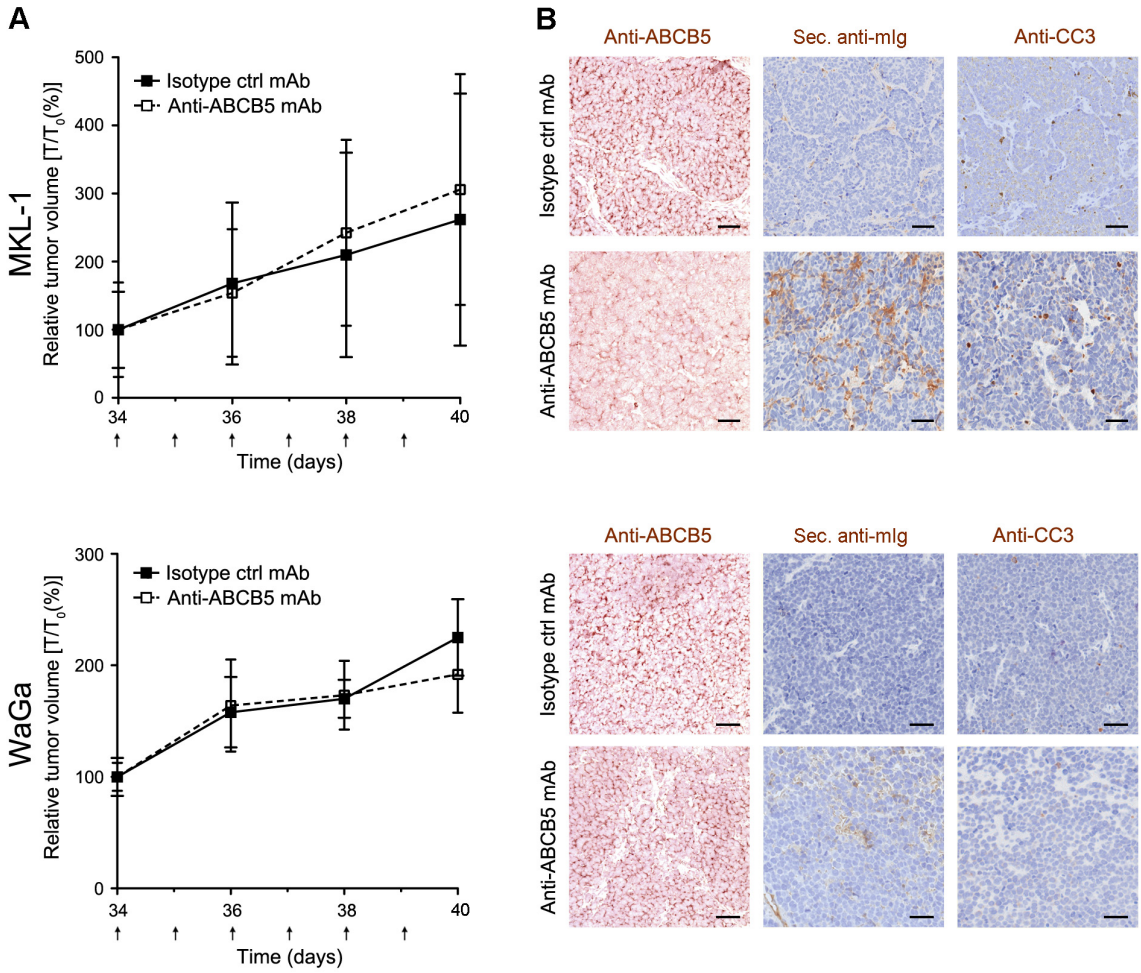

Figure 44. Effect of anti-ABCB5 blocking Ab on MCC tumor xenograft growth. (A) Tumor growth kinetics (mean ± SD) and (B) ABCB5, secondary Ab (sec. anti-mIg staining, recognizing *in vivo*-administered anti-ABCB5 Ab) and CC3 IHC staining of MKL-1 (top) and WaGa (bottom) xenografts dissected from NSG mice (n = 5, respectively) treated with isotype control Ab or anti-human ABCB5 Ab (500 µg/d) without concurrent administration of chemotherapeutic agents. Arrows in panel (A) indicate days of isotype control or anti-ABCB5 Ab administration. Size bars, 50 µm. The data presented in this figure has been previously published (Kleffel et al., 2016).

4.4.7 Discussion

Although the majority of patients with metastatic MCC initially respond to treatment with chemotherapeutic agents like carboplatin and etoposide (Poulsen, 2004), emergence of resistance is common and poses a major barrier to successful therapy. To date, the

mechanisms underlying chemotherapeutic resistance are poorly understood, and second-line treatment options for MCC patients with progressive disease do not exist (Eng et al., 2007). On the basis of previously established roles of ABCB5 as a clinically relevant chemoresistance mechanism in cutaneous melanoma (Chartrain et al., 2012, Frank et al., 2005, Wilson et al., 2014) and other cancers (Cheung et al., 2011b, Wang and Teng, 2016, Wilson et al., 2011), ABCB5 was hypothesized to also mediate resistance to the standard-of-care chemotherapeutic agents, carboplatin and etoposide, in MCC.

To dissect the potential role of ABCB5 in chemotherapy-resistant MCC tumors, ABCB5 expression and function was analyzed in MCC biospecimens (n = 85) obtained from 66 patients, healthy human skin specimens from 10 individuals, and 4 established MCC cell lines. ABCB5 was highly expressed in MCC, with expression levels markedly surpassing those in healthy human skin. This is consistent with findings of ABCB5 overexpression in melanoma and hepatocellular carcinoma compared to respective non-malignant tissues (Frank et al., 2005, Schatton et al., 2008, Wilson et al., 2011). Importantly, $ABCB5^+$ MCC cell subsets were resistant to the standard-of-care chemotherapeutic agents carboplatin and etoposide *in vitro* and *in vivo* in tumor xenografts and clinical specimens. Additional ABC transporters, namely ABCB1 and ABCC3, were also overexpressed in carboplatin- and etoposide-resistant compared to wildtype MCC cell lines and tumor xenografts. Because it has been suggested that ABCB1 and ABCC3 can mediate multidrug resistance in solid cancers of various etiology (Frank et al., 2005, Huang et al., 2004), multiple ABC transporters, in addition to ABCB5, might be involved in MCC chemoresistance. Dedicated experiments involving RNA interference and antibody-mediate blockade of ABCB1, ABCC3 and other ABC transporters are required to determine their respective contributions to MCC chemoresistance.

ABCB5 may function as a drug efflux transporter in MCC, because antibody-mediated blockade of ABCB5 on MCC cells has been shown to mediate the retention of

the ATP transporter substrate, Rh123. However, whether ABCB5 directly effluxes carboplatin and etoposide as a mechanism of resistance, or if alternative, efflux-independent ABCB5 functions might be primarily responsible for MCC chemoresistance requires further investigation. For example, ABCB5 has been previously shown to regulate the maintenance of slow-cycling chemoresistant melanoma subpopulations (Wilson et al., 2014) and limbal stem cells (Ksander et al., 2014). Thus, the possibility that ABCB5-dependent cellular quiescence might be more pronounced in chemorefractory MCC cells and therefore contributed to the occurrence of chemoresistance in this study cannot be excluded.

The finding that ABCB5 serves as a chemoresistance mediator in MCC is of potentially high clinical significance, because the emergence of resistance to first-line chemotherapy is a major impediment to successful MCC treatment (Azuma et al., 2008, Tai et al., 2000). Indeed, the addition of an ABCB5 blocking mAb to carboplatin or etoposide treatment resulted in enhanced tumor cell apoptosis and significant inhibition of tumor xenograft growth. This establishes initial proof-of-principle that ABCB5 can be targeted in MCC to attenuate resistance to clinically relevant chemotherapeutic agents.

Because ABCB5 marks therapy-refractory cancer subpopulations in both melanoma and MCC, and is preferentially expressed by melanoma-initiating cells (Schatton et al., 2008), ABCB5 may also mark tumorigenic MCC subpopulations. Determining whether $ABCB5^+$ MCC cell subsets are able to initiate and maintain MCC tumors via their capacity to self-renew and differentiate into $ABCB5^-$ tumor bulk populations requires additional dedicated experiments, using spheroid cell cultures and serial human MCC-to-mouse xenotransplantation assays. In aggregate, the data presented in this chapter provide a clear rationale to translate ABCB5-targeted chemoresistance reversal strategies to the clinic, in order to enhance the efficacy of currently available MCC therapies. The key findings of this chapter are summarized in Figure 45.

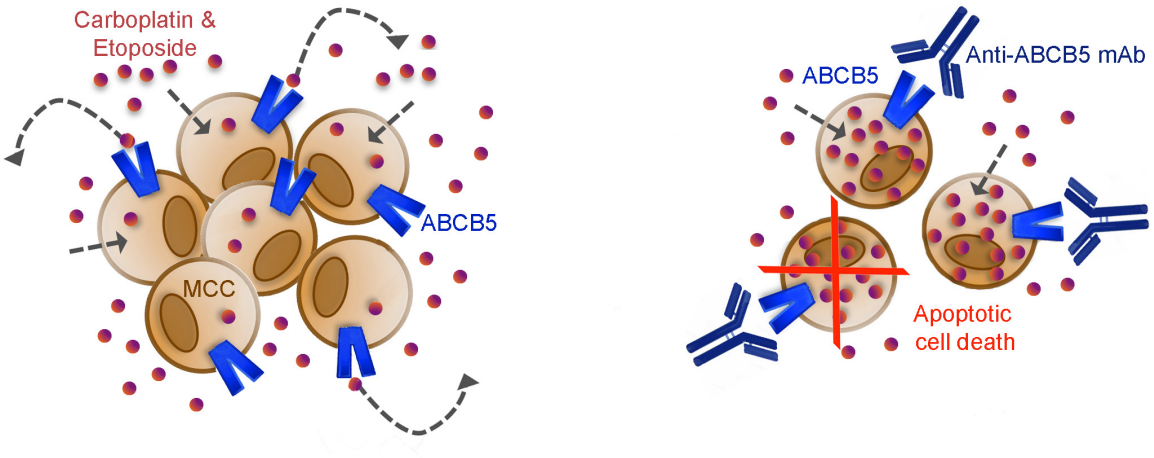

Figure 45. ABCB5 confers resistance to standard-of-care chemotherapeutic agents in MCC. The ATP-dependent drug efflux pump ABCB5 is expressed by a subpopulation of MCC cells. ABCB5$^+$ MCC cells preferentially survive chemotherapy-induced cytotoxicity. Antibody-mediated blockade of the ABCB5 transporter can sensitize MCC cells to carboplatin- and etoposide-mediated apoptotic cell death in *in vitro* and *in vivo* MCC xenograft models.

4.5 Tumor-intrinsic PD-1 signaling promotes Merkel cell carcinoma growth

4.5.1 Introduction

MCC, like melanoma, is a highly immunogenic cancer (Paulson et al., 2013). In immunocompetent individuals, who account for the vast majority of MCC patients (Heath et al., 2008), lymphocytic infiltration of the TME, particularly by CD8$^+$ T cells, has been correlated with improved survival (Paulson et al., 2011). Robust humoral and cellular immune responses against cancer-specific viral T antigens and neoantigens are frequently detected in MCC patients (Goh et al., 2015, Iyer et al., 2011, Paulson et al., 2010). However, clinical data suggest that MCC tumors exploit various immune checkpoints to

evade antitumor immune response in order to progress (Thakuria et al., 2014). For example, the expression of the immunosuppressive ligand, PD-L1, by cancer cells, DCs, and macrophages in the TME can be detected in up to 50% of MCC tumor biopsies (Afanasiev et al., 2013, Dowlatshahi et al., 2013, Lipson et al., 2013). In addition, tumor-infiltrating $CD8^+$ T cells express high levels of the PD-1 receptor, particularly in progressive lesions (Afanasiev et al., 2013, Dowlatshahi et al., 2013). Conversely, frequencies of PD-1 positive TILs were significantly decreased in MCC tumors that spontaneously regressed after biopsy compared to MCC lesions that did not (Afanasiev et al., 2013, Dowlatshahi et al., 2013, Fujimoto et al., 2015). Together, these findings suggest that the PD-1 pathway plays a critical role in maintaining an immunosuppressive TME and regulate MCC pathogenesis. Moreover, this provides a rationale for treating MCC patients with agents aimed at re-activating tumor-specific immunity. Immunotherapies, including high-dose recombinant IL-2 and Abs targeting CTLA-4, have previously failed to mediate durable responses in MCC patients (Drs. Manisha Thakuria and Tobias Schatton, personal communication). Interestingly, in phase 2 clinical trials, Ab-mediated PD-1 blockade yielded objective response rates in 56% of patients with advanced MCC (Nghiem et al., 2016), and PD-L1 inhibitors in 32% of MCC patients (Kaufman et al., 2016). Moreover, clinical trials of PD-1 pathway interference demonstrated encouraging safety profiles and durable responses (Kaufman et al., 2016, Mantripragada and Birnbaum, 2015, Nghiem et al., 2016, Patnaik et al., 2015). The superior clinical efficacy of PD-1 targeted therapies compared to other immunotherapies in MCC raises the possibility that, in addition to re-activating MCC-specific immune responses, PD-1 blockade might also inhibit immune-independent, MCC-intrinsic growth-promoting mechanisms, consistent with the herein described protumorigenic effects of melanoma-expressed PD-1.

Previous studies revealed that ABCB5 marks chemotherapy-refractory cell subsets in melanoma (Frank et al., 2005) and MCC (discussed in chapter 4.4). Tumorigenic $ABCB5^+$

melanoma-initiating cells (Schatton et al., 2008) and subpopulations of normal ABCB5$^+$ skin cells preferentially co-express the PD-1 receptor (demonstrated in chapter 4.1 and previously published (Schatton et al., 2010, Schatton et al., 2015)). Activation of the melanoma-expressed PD-1 receptor by PD-L1 induces the mTOR signaling pathway and promotes tumor growth independent of immunity (demonstrated in chapter 4.3). Aberrant activation of the mTOR pathway can frequently be detected in MCC tumors, and its role in MCC survival and growth is well established (Bhatia et al., 2011, Lin et al., 2014). It was therefore hypothesized that ABCB5$^+$ MCC cells might also co-express the PD-1 receptor, and that MCC cell-intrinsic PD-1 receptor functions may serve as a protumorigenic mechanism via activation of the mTOR pathway. PD-1 expression by established MCC cell lines, experimental tumor xenografts, and MCC biopsies, and the potential role of cancer-expressed PD-1 in tumorigenesis, were characterized next.

4.5.2 PD-1 is expressed by Merkel cell carcinoma cells

PD-1 expression was first characterized in established human MCC cell lines, MCC tumor xenografts and MCC patient samples, to expand upon previous demonstrations of functional PD-1 expression by healthy human skin and melanoma cells (demonstrated in chapter 4.1 and previously published (Schatton et al., 2010, Schatton et al., 2015). RT-PCR amplification and sequencing of the full CDS of the human PD-1 (*PDCD1*) gene revealed *PDCD1* mRNA expression (Figure 46A), and immunoblot analysis demonstrated PD-1 protein expression by established human MKL-1, MKL-2, MS-1, and WaGa MCC cells (Figure 46B). Flow cytometric analysis demonstrated PD-1 surface protein expression by all MCC cell lines tested, with PD-1$^+$ tumor cell frequencies ranging from 21.2% ± 2.9 to 42.6% ± 4.1% (mean ± SEM, Figure 46C), compared to 11.3% ± 1.2% to 29.5% ± 3.7% (mean ± SEM) in melanoma cell lines (Figure 3C). Established MKL-1, MKL-2, MS-1

and WaGa cell lines did not express either PD-1 ligand, PD-L1 or PD-L2, as determined by flow cytometry (Figure 46D).

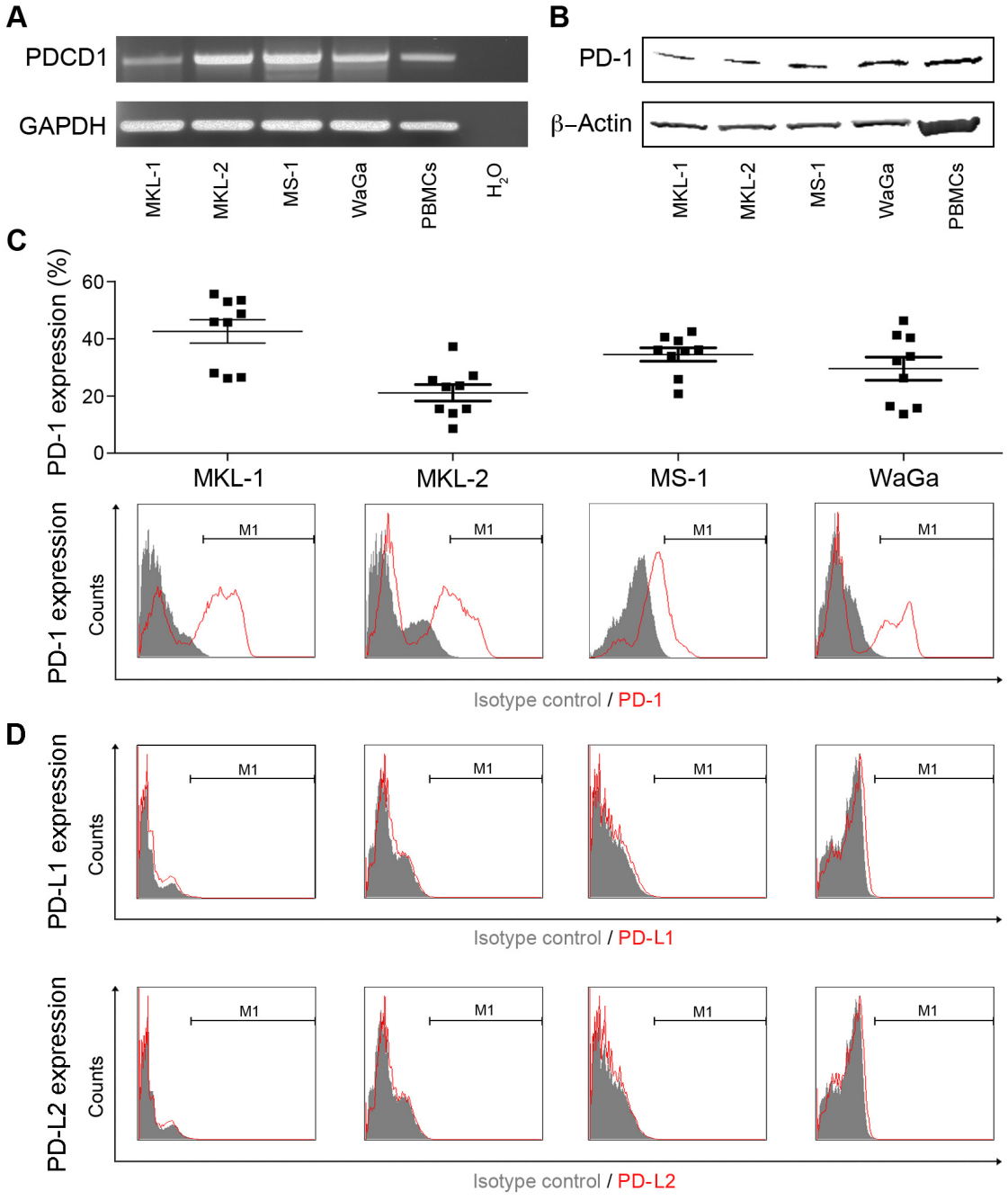

Figure 46. PD-1 expression by established MCC cells. (A) RT-PCR expression analysis of full-length PD-1 (*PDCD1*) mRNA and (B) immunoblot of PD-1 protein expression by established MCC cell lines and PBMCs. (C) Percentages (mean ± SEM, top) and representative flow cytometry (bottom) of PD-1 surface protein expression by MCC cell lines. (D) Representative histogram plots of PD-L1 (top) and PD-L2 (bottom) surface

protein expression by MCC cells as determined by single-color flow cytometry. This figure shows previously unpublished data.

Notably, flow cytometric analysis determined preferential expression of the PD-1 receptor by ABCB5$^+$ MCC subpopulations in 4/4 cell lines examined (Figure 47).

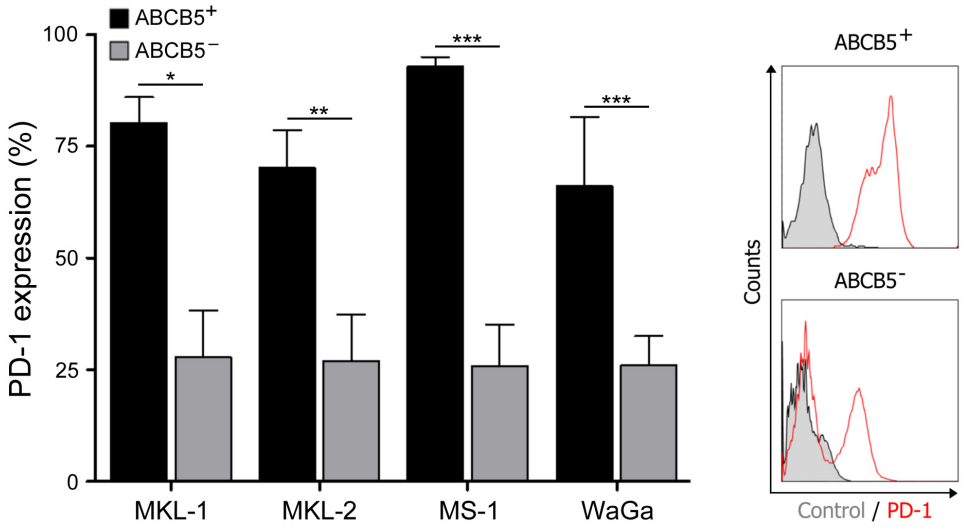

Figure 47. PD-1 is preferentially expressed by ABCB5$^+$ MCC cell subsets. Percentages of PD-1 protein expression (mean ± SEM) by ABCB5$^+$ versus ABCB5$^-$ MCC cells, as determined by flow cytometry (left). Representative histogram plots of PD-1 protein expression by ABCB5$^+$ versus ABCB5$^-$ cells are shown on the right. (*P<0.05, **P<0.01, ***P<0.001). This figure shows previously unpublished data.

To determine the potential clinical significance of PD-1$^+$ MCC cells, PD-1 expression was assessed in human tumor xenografts grown in immunocompromised NSG mice (Figure 40A) and in human MCC biopsies. Immunofluorescence double labeling for PD-1 and the MCC marker, CK20, confirmed PD-1 protein expression by subpopulations of CK20$^+$ MCC cells in of MKL-1 and WaGa tumor xenografts (Figure 48A), and in biopsies obtained from MCC patients (Figure 48B).

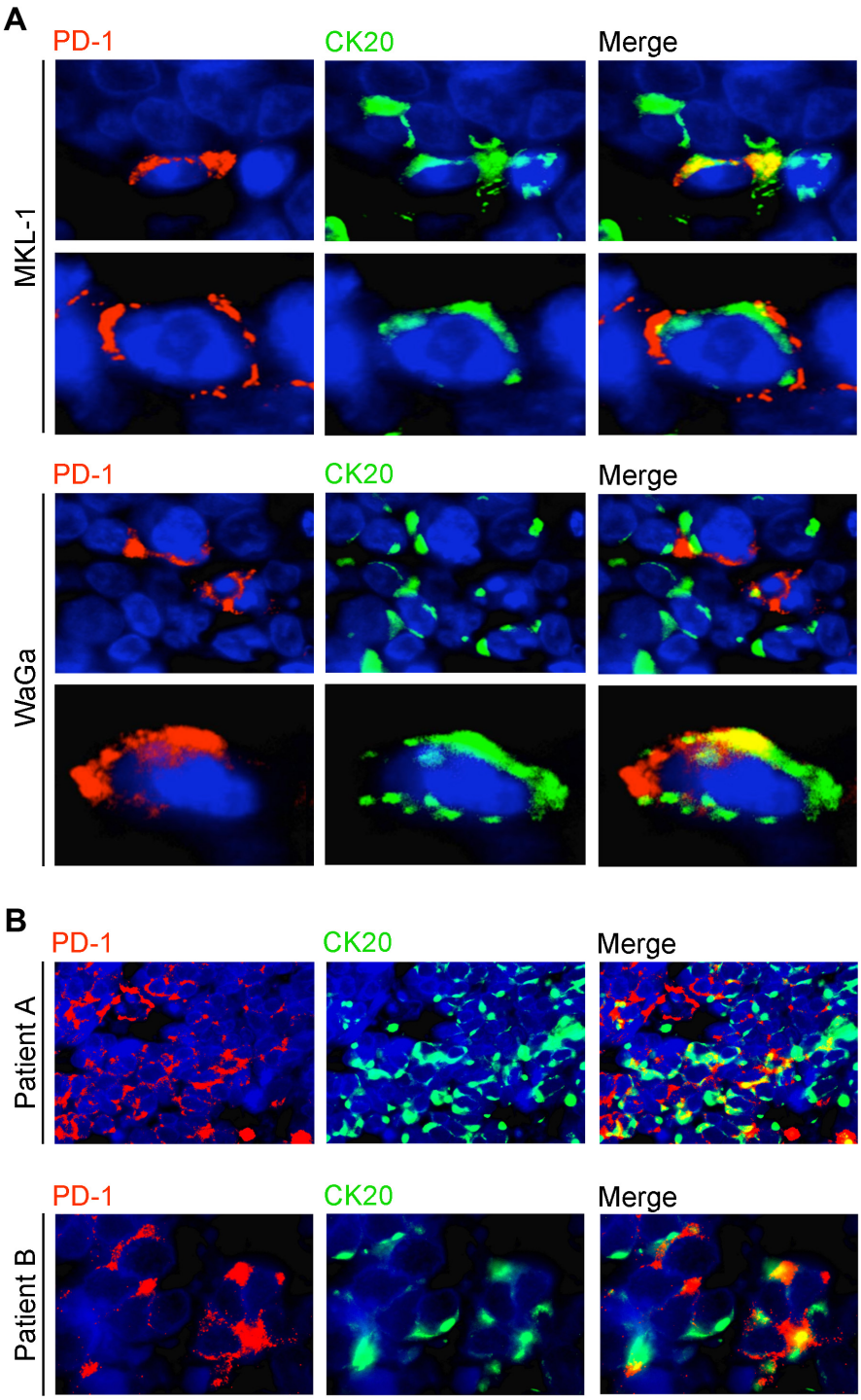

Figure 48. PD-1 expression by tumor xenografts and clinical MCC specimens. (A) Representative immunofluorescence double stainings for co-expression of PD-1 (red) and CK20 (green) on serial tissue sections of MKL-1 and WaGa tumor xenografts grown in NSG mice, and (B) two representative clinical MCC biopsies. Nuclei were counterstained with DAPI (blue). This figure shows previously unpublished data.

4.5.3 MCC-expressed PD-1 promotes tumor growth and activates cancer cell-intrinsic mTOR signaling

To mechanistically dissect the role of MCC-expressed PD-1 in experimental tumor growth, PD-1-dependent activation of MCC-intrinsic protumorigenic pathways was assessed next. Addition of either recombinant PD-1 ligand, PD-L1 Ig or PD-L2 Ig, to *in vitro* MCC cultures significantly enhanced proliferation of MS-1 and WaGa, but not MKL-1 cells compared to control Ig treatment (Figure 49A). No significant differences in cell death, as determined by Annexin V/7-AAD positivity, were measured in MCC cultures treated with PD-L1 Ig or PD-L2 Ig versus control Ig (Figure 49B). In T cells, PD-1 receptor signaling regulates several pathways downstream of the TCR, including MAPK, PI3K/AKT and mTOR (Riley, 2009), that also play important roles in MCC pathogenesis (Bhatia et al., 2011). Addition of PD-L1 Ig or PD-L2 Ig to MCC *in vitro* cultures increased the phosphorylation of signaling mediators of the mTOR pathway, including mTOR, ribosomal protein S6 kinase beta-1 (S6K1), and the eukaryotic translation initiation factor 4B (EIF-4B) compared to control Ig treatment (Figure 49C). Together, these findings suggest that activation of MCC-expressed PD-1 by PD-L1 and PD-L2 promote proliferation and cancer-cell intrinsic activation of the protumorigenic mTOR signaling pathway *in vitro*.

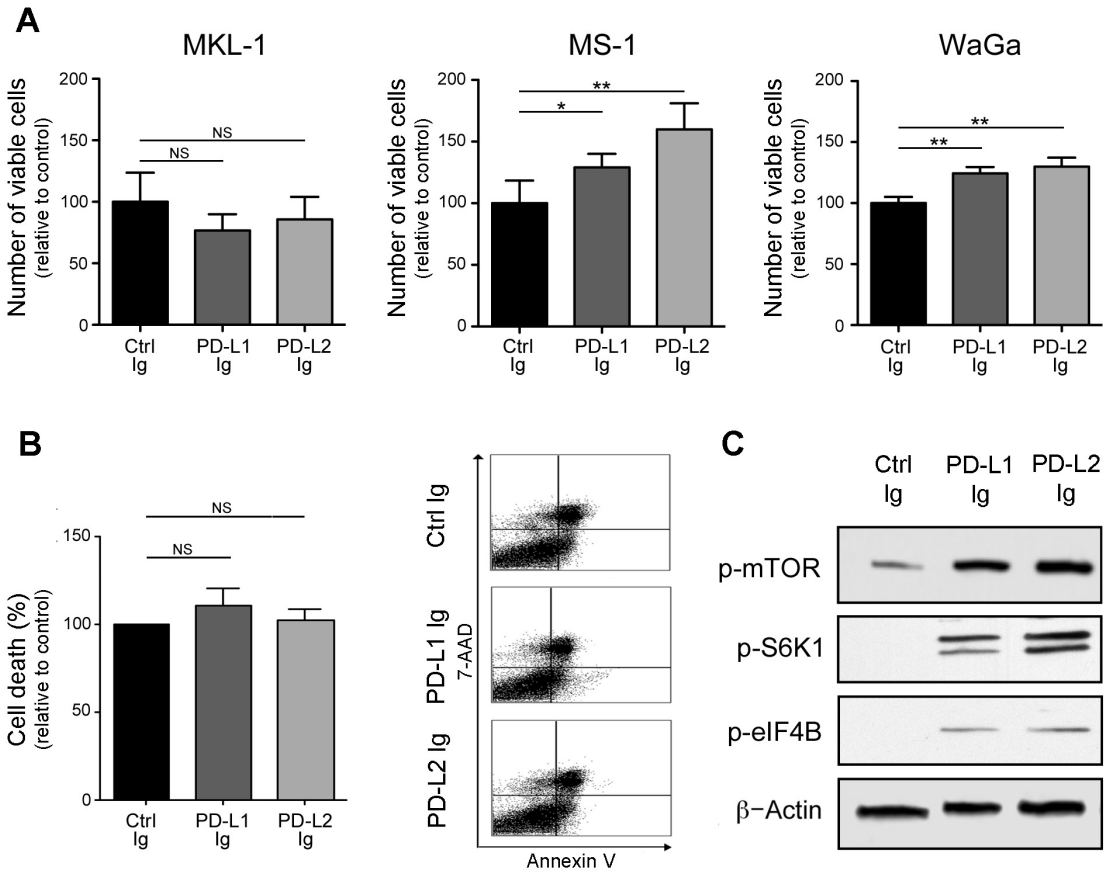

Figure 49. Recombinant PD-L1 and PD-L2 activates the protumorigenic mTOR pathway in MCC cells. (A) Cell viability ± SEM of PD-L1 Ig or PD-L2 Ig - versus control Ig-treated MCC cultures. (B) Flow cytometric assessment of cell death (percent $AnnexinV^+/7AAD^+$ cells, mean ± SEM) (left) and representative flow cytometry plots (right) of PD-L1 Ig, PD-L2 Ig or control Ig-treated WaGa cultures. (C) Immunoblot analysis of phosphorylated (p) mTOR, S6K1, and eIF4B in WaGa cultures concurrently treated with PD-L1 Ig or PD-L2 Ig versus control Ig. β-Actin was used as an input control. (NS: not significant, **P*<0.05, ***P*<0.01). This figure shows previously unpublished data.

4.5.4 Antibody-mediated blockade of MCC-expressed PD-1 inhibits tumor xenograft growth and downstream mTOR signaling.

Based on the demonstration of MCC cell-intrinsic, protumorigenic PD-1 receptor functions *in vitro,* in the complete absence of immune cells, antibody-mediated blockade of MMC-expressed PD-1 was hypothesized to inhibit tumor xenograft growth in mice lacking

adaptive immunity. Anti-PD-1 or isotype control mAbs were administered to B and T cell deficient NSG recipient mice every other day, starting one day before inoculation with MKL-1 or WaGa cells. Antibody-mediated blockade of PD-1 moderately inhibited MKL-1 tumor xenograft growth in NSG mice, particularly between days 9 and 11 post inoculation ($P<0.01$), but did not result in significant tumor growth inhibition compared to isotype control Ab-treatment at later time points (Figure 50A). However, anti-PD-1 treatment significantly ($P<0.001$) inhibited WaGa tumor xenograft growth for the entire duration of the experiment (Figure 50B). IHC analysis of MCC grafts that were harvested at the experimental endpoint revealed binding of the *in vivo*-administered anti-PD-1 Ab, but not the isotype control Ab, to MCC target tissue in NSG hosts (Figure 50B). Compared to isotype control mAb treatment, antibody-mediated inhibition of PD-1 function *in vivo* resulted in significantly decreased phosphorylation of the mTOR protein in MCC tumor xenografts (Figure 50C). This finding is consistent with the herein demonstrated activation of the mTOR signaling pathway in MCC cells upon addition of recombinant PD-1 ligands to MCC cultures *in vitro* (Figure 49C). In summary, the observed inhibition of tumor xenograft growth and oncogenic mTOR signaling in immunocompromised, T and B cell-deficient NSG mice suggest that Ab-mediated PD-1 blockade directly on MCC cells may inhibit tumor cell-intrinsic, protumorigenic PD-1 functions independent of adaptive immunity.

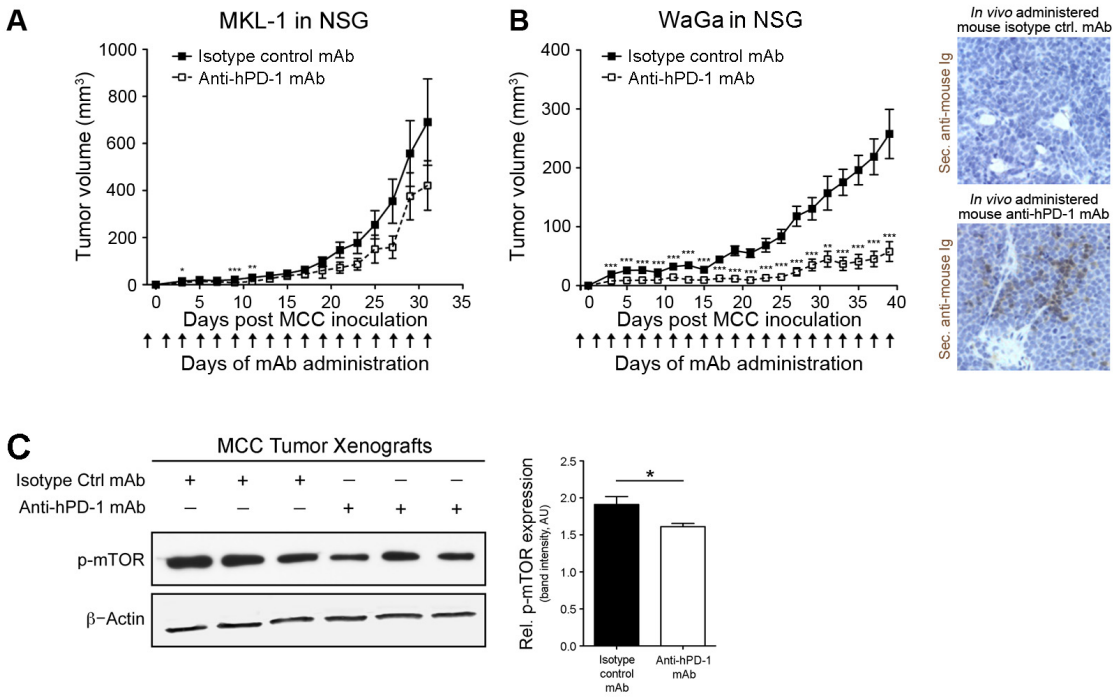

Figure 50. Antibody-mediated PD-1 blockade inhibits protumorigenic effects of MCC-expressed PD-1. (A) Kinetics (mean ± SD) of MKL-1 and (B) WaGa xenograft growth in NSG mice treated with anti-human PD-1 or isotype control Ab (*n*=10 each) (left). Arrows indicate days of Ab administration. Representative IHC images of WaGa xenografts (right) illustrate binding of *in vivo*-administered mouse anti-human PD-1 blocking, but not isotype control Ab, to the respective MCC grafts. (C) Immunoblot analysis of phosphorylated (p) mTOR protein in MCC xenografts resected from NSG mice treated with anti-human PD-1 or isotype control Ab as in (A). (* P<0.05, ** P<0.01, *** P<0.001). This figure shows previously unpublished data.

4.5.5 Discussion

MCC and melanoma are both highly aggressive neuroendocrine skin cancers, that contain ABCB5$^+$ cell subsets which are resistant to standard-of-care chemotherepeutic agents. In melanoma, PD-1 is preferentially expressed by ABCB5$^+$ tumor cells. Chapter 4.3 provides a comprehensive analysis of previously unrecognized immune-independent, tumor-growth promoting functions of melanoma-expressed PD-1. Therefore, ABCB5$^+$ MCC

subpopulations where hypothesized to similarly express PD-1, which may also serve as a protumorigenic mechanism in MCC.

Indeed, RT-PCR, immunoblot and flow cytometric analysis determined that subpopulations of MCC cells express the PD-1 receptor in 4/4 cell lines tested. Moreover, immunofluorescence stainings revealed PD-1 expression by subpopulations of $CK20^+$ cancer cells in MCC tumor xenografts and clinical MCC biopsies. The frequencies of $PD\text{-}1^+$ MCC cells markedly exceeded those observed in melanoma. PD-1 was preferentially expressed by $ABCB5^+$ MCC cells, and frequencies of $ABCB5^+$ cancer cells were also higher in MCC compared to melanoma (discussed in chapter 4.4).

Unlike melanoma cells, cultured MKL-1, MKL-2, MS-1 and WaGa cells did not express either PD-1 ligand, PD-L1 or PD-L2, in this study. Addition of recombinant PD-L1 Ig or PD-L2 Ig to MCC cultures enhanced proliferation of MS-1 and WaGa, but not MKL-1 cells, despite all three cell lines being $MCPyV^+$ and expressing similar PD-1 levels *in vitro*. Consistently, Ab-mediated PD-1 blockade significantly suppressed experimental WaGa xenograft growth, however, MKL-1 tumor xenograft growth was only modestly inhibited in immunocompromised NSG mice.

Engagement of melanoma-expressed PD-1 by host- or tumor cell-expressed PD-L1 activates cancer cell-intrinsic mTOR signaling mediators. The mTOR pathway is a well-established driver of MCC pathogenesis. In preclinical studies, mTOR inhibition significantly attenuated MCC tumor xenograft growth, and clinical trials testing the therapeutic efficacy in MCC patients are currently ongoing (Kannan et al., 2015). Addition of recombinant PD-L1 Ig or PD-L2 Ig to MCC *in vitro* cultures induced downstream effectors of the mTOR pathway. Conversely, Ab-mediated PD-1 blockade inhibited tumor cell-intrinsic mTOR activity in MCC xenografts, paralleling findings in melanoma. The herein described PD-1-dependent mTOR activation in MCC cultures and xenografts is consistent with the growth promoting effects observed in some MCC cell lines.

Whether the divergent effects of PD-1 pathway functions in MKL-1 versus WaGa cells are the result of cell-intrinsic variations in mTOR activity, differences in genomic MCPyV integration or viral Ag activation, or whether the PD-1 receptor signals via alternative adaptor molecules or downstream oncogenic pathways in MKL-1 versus WaGa cells requires additional dedicated studies. In activated T cells, for example, the PD-1 receptor also controls MAPK/ERK and PI3K/AKT pathways downstream of the TCR complex (Patsoukis et al., 2012, Patsoukis et al., 2013, Sheppard et al., 2004). Thus, MCC-expressed PD-1 might also regulate these or additional oncogenic pathways. Their potential involvement in mediating protumorigenic PD-1 receptor functions in different MCC cell lines and clinical specimens requires additional dedicated studies.

In summary, increased frequencies of PD-1^+ cancer cells in established MCC versus melanoma cell lines, and the greater importance of mTOR signaling in MCC versus melanoma pathogenesis, are entirely consistent with the superior clinical activity of PD-1 pathway blockade observed in patients with advanced MCC compared to melanoma. Moreover, the mTOR pathway is abberrantly activated by the ST antigen in $MCPyV^+$ MCCs, and a recent phase 2 clinical trial for the anti-PD-1 Ab pembrolizumab reported objective response rates in 62% of patients with $MCPyV^+$ MCCs versus 44% in virus-negative patients (Nghiem et al., 2016). This also suggests that combining PD-1 blockade with mTOR inhibitors might yield synergistic effects that further improve the clinical efficacy of PD-1-targeted therapy.

The microenvironment of MCCs is frequently infiltrated by PD-1- and PD-L1-expressing tumor-reactive immune cells, and MCC tumors itself often express PD-L1 to suppress tumor-specific immune responses (Nghiem et al., 2016). Melanoma-expressed PD-1 has been shown to inhibit T effector cell functions and increase intra-tumoral frequencies of tolerogenic MDSCs (discussed in chapter 4.2). Thus, MCC-expressed PD-1 might also modulate anti-tumor immunity. The lack of good MCC animal models, the

paucity of patient-matched PBMC and MCC samples and the inherent challenges of conducting longitudinal studies in at-risk patients make it difficult to dissect the immunomodulatory effects of MCC-expressed PD-1. To overcome these limitations, genetically-induced or humanized MCC mouse models should be developed to unravel potential mechanisms of MCC-PD-1-dependent tumor immune escape.

In summary, the herein presented results identify MCC-expressed PD-1 as a previously unrecognized protumorigenic mechanism and modulator of MCC cell-intrinsic mTOR signaling. These observations suggest that direct inhibition of MCC-intrinsic, tumor growth promoting PD-1 functions might, at least in part, explain the superior clinical efficacy of anti-PD-1 treatment compared to other immunotherapies in MCC. In addition, these findings raise the possibility that MCC-intrinsic PD-1 effector molecules, for example signaling mediators of the mTOR pathway, could serve as novel clinical biomarkers to discriminate responders from non-responders and help evaluate therapeutic responses. In addition, downstream effectors of MCC-expressed PD-1 may also represent novel therapeutic targets that work synergistically to increase the clinical efficacy of PD-1 pathway blockade. The key findings of this chapter are summarized in Figure 51.

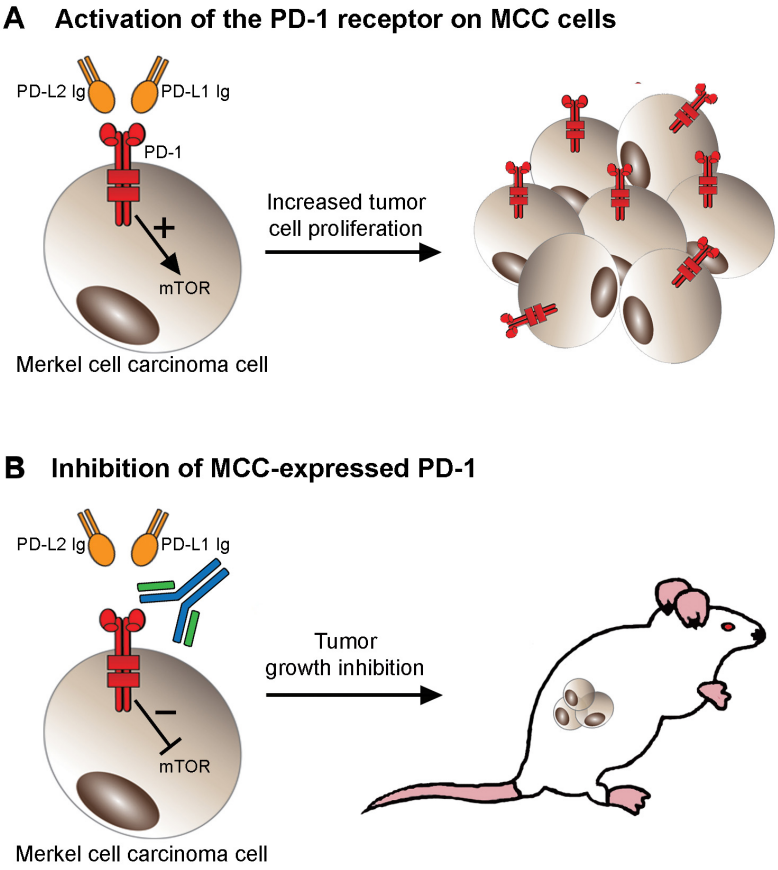

Figure 51. MCC-expressed PD-1 is a protumorigenic mechanism, even in the absence of adaptive immunity. (A) Subsets of MCC cells express PD-1, but not its ligands PD-L1 or PD-L2. Addition of recombinant PD-L1 Ig or PD-L2 Ig to MCC *in vitro* cultures promotes proliferation and activates the protumorigenic mTOR pathway. (B) Inhibition of MCC-PD-1 via PD-1-directed blocking Abs reduces tumor growth and phosphorylation of mTOR in MCC tumor xenografts, independent of adaptive immunity.

5 Discussion

Melanoma and MCC are highly aggressive, proliferative, and immunogenic cancers that are notoriously resistant to cytotoxic and immune-based therapies. Both cancers exploit numerous mechanisms to evade and downmodulate tumor-specific immunity in order to thrive (Bhatia et al., 2011, Eggermont et al., 2014, Paulson et al., 2013). This poses a significant barrier to successful cancer treatment and highlights the need for novel therapeutic regimens to cure advanced disease.

5.1 Role of melanoma-expressed PD-1 in modulating antitumor immunity

The PD-1 pathway plays a well-established role in suppressing antitumor immunity, thereby promoting cancer growth (Topalian et al., 2012a). Expression of the PD-1 receptor is commonly thought to be restricted to T lymphocytes and other immune cells (Topalian et al., 2012a). This thesis provides the first comprehensive characterization of PD-1 expression by subsets of melanoma and MCC cells in established cell lines, tumor xenografts, and surgical specimens. Consistent with findings of cancer cell-expressed PD-1, melanoma cells have previously been shown to express the alternative checkpoint receptors, CTLA-4 and TIM-3, both of which are also predominantly studied in immune cells (Contardi et al., 2005, Klijn et al., 2015, Schatton et al., 2010, Shah et al., 2008, Wiener et al., 2007). The herein reported expression of PD-1 was limited to small subpopulations of melanoma and MCC cells among heterogeneous tumor samples. Consistently, PD-L1, ABCB5, and TIM-3 expression are also restricted to melanoma cell subsets (Herbst et al., 2014, Schatton et al., 2008, Schatton et al., 2010, Topalian et al., 2012b, Wiener et al., 2007). Interestingly, the PD-1 receptor was preferentially co-

expressed with PD-L1 and ABCB5 in the present study. Transcription factors and exogenous signals that regulate PD-1 expression in this small subpopulation of cancer cells have yet to be identified, but could potentially overlap with inducers of PD-L1 and ABCB5 expression.

Binding of PD-1 ligands to T cell-expressed PD-1 impairs activation, proliferation, and effector function of T lymphocytes (Wherry, 2011). Melanoma, stromal, and tumor-infiltrating immune cells frequently express the major PD-1 ligand, PD-L1, which induces an immunosuppressive TME and attenuates tumor-specific CTL responses (Dong et al., 2002a, Topalian et al., 2012a). Similar to the immune inhibitory effects of T cell-expressed PD-1, melanoma-expressed PD-1 also suppressed T cell effector functions. For example, enforced PD-1 expression by melanoma cells resulted in decreased, and melanoma-specific PD-1 KD in increased frequencies of IFN-γ- and TNF-α-producing T effector cells in the TME. In addition, melanoma-expressed PD-1 increased intratumoral frequencies of tolerogenic MDSCs. MDSCs utilize several mechanisms to suppress T cell responses, consistent with the herein demonstrated inhibition of T effector cell functions by PD-1^{+} melanoma cells. Whether melanoma-expressed PD-1 impairs T cell responses directly or via MDSC-mediated T cell suppression requires further dedicated studies, including *in vitro* coculture systems to study T effector functions and tumorigenicity studies in MDSC-depleted mice.

The herein observed melanoma-PD-1-dependent increase in intratumoral MDSC frequency relied on host-PD-L1 expression, because no differences in MDSC frequencies where observed in PD-1-OE versus control melanomas grafted to PD-L1-deficient mice. PD-L1 has been previously suggested to also function as a receptor, allowing for bi-directional signaling interactions with PD-1 (Azuma et al., 2008, Francisco et al., 2010). A study by Pinton and colleagues showed that MDSC-expressed PD-L1 upregulates PD-1 expression by activated T effector and Treg cells, which further promotes an

immunosuppressive TME (Pinton et al., 2015). In light of the herein presented data, MDSC-expressed PD-L1 might potentially also upregulate PD-1 expression by melanoma cells, thereby creating a positive feedback loop that further inhibits tumor-specific immune responses.

Additional immune cells that frequently infiltrate the TME of melanomas and MCCs, including macrophages, DCs, and B cells, also express PD-1 ligands (Francisco et al., 2010). For example, PD-L1 signaling has been shown to suppress humoral immunity and maintain the suppressive capacity of Bregs (Khan et al., 2015). Based on these observations, melanoma-expressed PD-1 might also suppress humoral and innate antitumor immune responses. This could present additional mechanisms through which melanoma-expressed PD-1 inhibits cytotoxic T cell activity to further promote tumor immune escape. However, additional studies are needed to better understand the complex molecular and cellular mechanisms that govern melanoma-PD-1-dependent immunoregulation.

Although B16 melanomas express MAAs and harbor higher loads of neoantigens compared to inducible melanoma models, the study of melanoma-specific immune responses in the B16 model is inherently difficult due to its less pronounced immunogenicity compared to many human melanomas (Celik et al., 1983, Schatton et al., 2010). Thus, future studies aimed at dissecting the effects of melanoma-expressed PD-1 on antitumor immunity should also be conducted in model systems that elicit more potent and reproducible immune responses, such as the transgenic B16-OVA melanoma model. To study the effects of MCC-expressed PD-1 on antitumor immunity *in vivo,* humanized mouse models should be used to overcome the current lack of syngeneic MCC animal models.

Together, the herein presented findings represent a critical first step towards comprehensively dissecting the immunoregulatory functions of melanoma-expressed PD-

1. Immunosuppressive effects of PD-1 expressed by melanoma cells add another layer of complexity to the crosstalk between tumor, stromal, and immune cells that regulates tumor initiation and growth.

5.2 Significance of tumor-cell intrinsic PD-1 signaling in tumorigenesis

Current understanding holds that PD-1 promotes tumorigenesis by attenuating tumor-specific CTL responses (Topalian et al., 2012a). Consistently, it was herein demonstrated that melanoma-expressed PD-1 also suppresses T cell immunity. However, melanoma- and MCC-expressed PD-1 had protumorigenic functions, even in the absence of adaptive and humoral immmunity. Particularly, the engagement of cancer cell-expressed PD-1 by its ligands induced tumor growth and resulted in the activation of cancer cell-intrinsic mTOR signaling mediators. Mutation of the ITIM and ITSM signaling motifs within the cytoplasmic tail of melanoma-expressed PD-1 abrogated the tumor growth-promoting effects of PD-1^+ melanoma cells and attenuated phosphorylation of the mTOR signaling effector, ribosomal protein S6. This suggests that the protumorigenic effects of melanoma-expressed PD-1 may rely, at least in part, on cancer cell-intrinsic signaling downstream of the PD-1 receptor. However, whether the observed tumor growth-promoting effects of cancer cell-expressed PD-1 depend entirely on mTOR signaling requires additional dedicated studies. For example, the effects of mTOR-directed loss- and gain-of-function on tumor growth of melanoma-PD-1 variant cell lines would be insightful in this regard.

In T cells, engagement of PD-1 by its ligands, PD-L1 or PD-L2, controls several signaling networks downstream of the TCR complex, including MAPK, mTOR and PI3K/AKT (Patsoukis et al., 2012, Riley, 2009, Sheppard et al., 2004). These pathways are also critically important for melanoma and MCC initiation and growth (Flaherty et al., 2012, Thakuria et al., 2014). Thus, cancer cell-expressed PD-1 might potentially also

signal via additional pathways, including PI3K/AKT, to promote tumor growth. Future studies are required to identify alternative oncogenic pathways downstream of the PD-1 receptor in cancer cells, in addition to mTOR, and dissect their potential contribution to PD-1-dependent tumor growth.

Interestingly, the aberrant activation of mTOR, MAPK, and PI3K/AKT signaling pathways has been shown to promote PD-L1 expression by cancer cells (Jiang et al., 2013a, Lastwika et al., 2016, Parsa et al., 2007, Song et al., 2013). IFN-γ also induces the expression of PD-L1 by cancer cells, which is, at least partly, mediated via cancer cell-intrinsic mTOR activation (Chen et al., 2012, Lastwika et al., 2016, Mandai et al., 2016). This raises the possibility that the IFN-γ:mTOR:PD-L1:PD-1 axis may serve as a feed-forward loop that further enhances the growth-promoting effects of cancer cell-expressed PD-1. Additional studies aimed at comprehensively characterizing transcription factors, cytokines, growth factors, and signaling pathways that regulate the expression of both, PD-L1 and PD-1, in melanoma and MCC cells are required.

In addition to these tumor cell-intrinsic protumorigenic effects, hyperactivation of MAPK and PI3K/AKT signaling pathways increases the expression of immunosuppressive cytokines by melanoma cells and attenuates T cell proliferation, T effector functions, and migration of T cells to the TME (Khalili et al., 2012, Peng et al., 2016). If cancer cell-expressed PD-1, like T cell-expressed PD-1, also controls downstream PI3K/AKT or additional pathways, this might represent another possible mechanism through which PD-1^+ cancer cells promote an immunosuppressive TME and inhibit CTL function.

Here, Ab-mediated blockade of cancer cell-expressed PD-1 suppressed the activation of mTOR signaling and tumor growth of PD-1^+ cancer cells. Moreover, melanoma-specific PD-L1 KD and antibody-mediated PD-L1 blockade inhibited tumor growth in immunocompromised NSG mice. In a study by Chang and colleagues, cancer cell-specific PD-L1 blockade also attenuated tumor cell-intrinsic mTOR activity (Chang et al., 2015).

Consistently, Clark and colleagues showed that melanoma-specific PD-L1 KD inhibits tumor growth and mTOR signaling in immunodeficient NSG mice (Clark et al., 2016). Together, this raises the question whether activation of both, PD-1 and PD-L1, promote mTOR signaling, or whether antibody-mediated PD-L1 blockade merely inhibits the PD-L1-dependent activation of the PD-1 receptor to attenuate mTOR signaling. In support of the latter possibility, PD-L1 KD reversed the growth-promoting effects of enforced PD-1 expression in the present study. However, further studies are required to dissect the signaling cascades downstream of cancer cell-expressed PD-1 versus PD-L1.

Chang and colleagues also demonstrated decreased expression of glycolytic enzymes following tumor-specific PD-L1 blockade, which resulted in inhibition of cancer cell-intrinsic glycolysis and mTOR signaling. Consistently, in the same study, Ab-mediated PD-1 blockade re-established glucose availability in the TME (Chang et al., 2015). Moreover, a study by Lutz and colleagues suggested that ABCB5 promotes glycolysis in melanoma cells (Lutz et al., 2016), and ABCB5 and PD-1 are preferentially co-expressed by subsets of melanoma and MCC cells (discussed in chapters 4.1 and 4.5 and previously published (Schatton et al., 2010). This raises the question of whether tumor cell-expressed PD-1 can also induce glycolysis, consistent with the herein reported tumor growth promoting effects of cancer cell-expressed PD-1. Interestingly, glycolysis is critical for T cell activation, growth, Th cell differentiation, and effector function (Ho et al., 2015, Patsoukis et al., 2015). Therefore, if activation of the PD-1 pathway in tumor cells would promote glycolysis and thereby deplete glucose from the TME, cancer cell-expressed PD-1 might also indirectly induce metabolic changes in T cells, thereby inhibiting their differentiation and effector function. Experiments aimed at understanding potential effects of cancer cell-expressed PD-1 on tumor metabolism will be informative in this regard.

A study by Black and colleagues showed that antibody-mediated blockade of the PD-1 pathway on cancer cells inhibits metastatic dissemination, and reverses resistance to

doxorubicin chemotherapy (Black et al., 2016). Consistently, in the present study, PD-1$^+$ melanoma and MCC cells preferentially co-expressed ABCB5, and ABCB5 has previously been shown to identify melanoma-initiating cell subsets that foster metastatic disease (Kupas et al., 2011, Ma et al., 2010, Schatton et al., 2008) and mediate resistance to chemotherapeutic agents, including doxorubicin (Frank et al., 2005). These observations raise the possibility that cancer cell-expressed PD-1 may also promote metastatic dissemination and cancer progression. However, additional studies are required to assess the potential pro-metastatic capacity of PD-1$^+$ versus PD-1$^-$ cancer cell subsets.

Finally, the mTOR pathway and its downstream mediators, including S6K1, have been previously shown to control the G1 checkpoint, thereby regulating cell cycle progression (Fingar et al., 2004, Foster et al., 2010). Because cancer cell-expressed PD-1 was herein demonstrated to activate the mTOR signaling cascade, including its effector molecules, S6K1 and S6, cancer cell-expressed PD-1 might also promote cell cycle progression. Patsoukis and colleagues have previously shown that activation of the PD-1 receptor on T cells blocks cell cycle progression at G1 via inhibition of the MAPK pathway (Patsoukis et al., 2012). These potentially divergent effects of PD-1 signaling on cell cycle regulation in cancer cells compared to T cells would thus be consistent with the opposing, activating versus inhibitory effects of PD-1 receptor activation on mTOR signaling in the respective cell types.

In summary, engagement of cancer cell-expressed PD-1 by its ligands activates mTOR signaling and promotes tumor growth, even in the absence of adaptive immunity. Activation of the PD-L1:PD-1:mTOR axis in cancer cells could amplify protumorigenic functions through a positive feedback loop and possibly also regulate metabolism and cell cycle progression to promote tumor growth and metastasis.

5.3 Relevance of cancer cell-expressed PD-1 for therapies targeting the PD-1 pathway

Therapeutic PD-1 blockade produces greater clinical benefit and fewer immune related adverse events compared to other immunotherapies, including Abs targeting the checkpoint receptor, CTLA-4, in patients with melanoma and MCC (Hamid et al., 2013, Nghiem, 2015, Postow et al., 2015b, Robert et al., 2015b, Topalian et al., 2012b, Weber et al., 2015, Wolchok et al., 2013). Moreover, PD-1 inhibition also yields meaningful clinical responses in melanoma patients that do not benefit from anti-CTLA-4 therapy (Hamid et al., 2013, Ribas et al., 2015, Weber et al., 2013), in patients with lesser immunogenic cancers that typically do not respond to immunotherapy (Borghaei et al., 2015, Herbst et al., 2014, Topalian et al., 2012b), in patients with pre-existing autoimmune disorders, as well as those suffering from major irAE during treatment with ipilimumab (Menzies et al., 2016). Together, these observations raise the possibility that PD-1 blockade might also inhibit additional protumorigenic PD-1 receptor functions, including cancer cell-intrinsic mechanisms, secondary to the re-activation and expansion of antitumor immunity. Anti-CTLA-4 Abs, on the other hand, might inhibit cancer cell apoptosis (Contardi et al., 2005), thereby potentially counteracting its T cell-dependent effects on tumor growth inhibition. However, whether the therapeutic anti-PD-1 Abs used in the clinic also block the herein demonstrated tumor growth-promoting effects of cancer cell-expressed PD-1 requires further investigation. Notably, while the PD-1 amino acid sequences were identical between melanoma, MCC and T cell-expressed PD-1 in the present study, posttranslational modifications might vary. For example, glycan structures are different in cancer versus normal cells (Stowell et al., 2015), and variations in PD-1 glycosylation patterns could potentially result in differences in Ab recognition of immune- versus cancer cell-expressed PD-1.

Although therapeutic PD-1 inhibition shows remarkable clinical efficacy compared to other available therapies, the majority of patients with advanced disease still do not respond to PD-1 inhibitors. Thus, biomarkers that reliably predict which patients will benefit from PD-1 blockade are urgently needed to effectively guide treatment selection and further improve patient outcome. Here, intratumoral expression of the mTOR signaling mediator p-S6, a downstream effector of melanoma-expressed PD-1, correlated with response to anti-PD-1 Abs in melanoma patients with stage IV disease. This pilot study highlights the potential utility of p-S6 as a biomarker of PD-1 inhibitor sensitivity. However, independent validations in larger patient cohorts, including prospective studies, will be required to further establish p-S6 as a biomarker of clinical responses.

The present study identified additional mTOR signaling effectors as downstream targets of the PD-1 receptor on cancer cells, including mTOR, S6K1, and eIF4B. Moreover, cancer cell-expressed PD-1 might also control other oncogenic pathways, including PI3K/AKT, consistent with PD-1 receptor functions in T cells. Hence, additional signaling mediators of cancer cell-expressed PD-1 may hold the promise to be translationally relevant for guiding treatment selection.

A recent study provides initial evidence that melanoma-specific MHC-II expression correlates with responses to immunotherapies targeting the PD-1:PD-L1 axis (Johnson et al., 2016a), highlighting the potential use of MHC-II as a predictive biomarker of anti-PD-1 therapeutic efficacy. Here, PD-1^{+} melanoma and MCC cells preferentially co-expressed ABCB5. It was previously demonstrated that ABCB5^{+} melanoma cells express significantly higher levels of MHC-II compared to ABCB5^{-} melanoma cells (Schatton et al., 2010). This supports the possibility that ABCB5, PD-1, and MHC-II proteins may potentially be co-expressed by the same cancer cell subset. Because melanoma-expressed MHC-II correlates with therapeutic response to anti-PD-1 treatment, by extension, expression of PD-1 or melanoma cell-intrinsic PD-1 signaling mediators might also

correlate with improved clinical outcome. However, additional studies are required to establish the possible link between MHC-II and PD-1 expression in melanoma cells, and its potential utility for clinical biomarker development. Finally, the frequency of tumor-infiltrating immune cells, like T effector cells and MDSCs, might also serve as potential response biomarkers, based on the observation that melanoma-expressed PD-1 can modulate immune cell frequencies in the TME.

Interestingly, both elevated PD-L1 and p-S6 expression level have previously been implicated as potential biomarkers of resistance to BRAF inhibitors in melanoma patients (Corcoran et al., 2013, Jiang et al., 2013b). Consistently, hyperactivation of the MAPK pathway (e.g. resulting from resistance to BRAF-targeted therapy) and aberrant signaling via mTOR and PI3K/AKT pathways also promote PD-L1 expression by cancer cells (Jiang et al., 2013a, Lastwika et al., 2016, Parsa et al., 2007, Song et al., 2013). In addition, the present study demonstrated that PD-L1-mediated activation of cancer cell-expressed PD-1 promotes oncogenic mTOR signaling. Thus, combining PD-1 targeted therapies with mTOR, MAPK and/or PI3K/AKT inhibitors might work synergistically to improve clinical efficacy, not only because they re-activate tumor-specific immunity while concurrently blocking oncogenic pathways, but also because PD-1/PD-L1 blockade might additionally suppress mTOR-associated protumorigenic signals.

Melanoma-expressed PD-1 might also be relevant for other forms of cancer treatment, including chemotherapy. For example, activation of tumor cell-expressed PD-L1 by PD-1 confers resistance to chemotherapeutic drugs, at least partly, via activation of the mTOR signaling pathway (Black et al., 2016). Conversely, cancer cell-specific inhibition of the PD-1:PD-L1 signaling axis reversed chemotherapeutic-refractoriness (Black et al., 2016). Here, PD-1^{+} melanoma and MCC cells preferentially co-expressed the transmembrane transporter ABCB5, which is a well-established mediator of resistance to standard-of-care chemotherapeutic drugs in melanoma (Frank et al., 2005) and, as

demonstrated in this thesis, MCC. Thus, in light of the findings by Black and colleagues, ligation of tumor-expressed PD-1 by PD-L1 might serve as an additional chemoresistance mechanism. Accordingly, the combination of chemotherapeutic agents with PD-1 pathway inhibitors may work synergistically to enhance treatment efficacy in patients with metastatic disease. However, the precise mechanisms through which PD-1:PD-L1 interactions promote chemotherapy resistance require further elucidation.

Taken together, the combination of p-S6 with additional, yet to be identified biomarkers downstream of cancer cell-expressed PD-1 could be beneficial in more accurately stratifying patient outcome. Moreover, based on the possible link between the PD-1 pathway and resistance to both chemotherapy and BRAF inhibitors, combining PD-1 blockade with standard-of-care chemotherapeutic drugs or targeted therapies might further improve clinical benefit based on the herein presented findings of protumorigenic melanoma-PD-1 receptor functions.

5.4 Role of ABCB5 in the pathogenesis of Merkel cell carcinoma

Resistance to chemotherapy poses a major obstacle to successful treatment of advanced MCC. The present study identified the energy-dependent drug efflux transporter ABCB5 as a marker of chemotherapy-refractory cell populations in human MCC, consistent with its previously established role as a chemoresistance mediator in melanoma (Chartrain et al., 2012, Frank et al., 2005, Wilson et al., 2014) and other solid cancers (Cheung et al., 2011b, Wang and Teng, 2016, Wilson et al., 2011). This suggests that $ABCB5^+$ MCC cell subsets might be a potential cause for disease relapse following treatment with chemotherapeutic drugs. Here, Ab-mediated blockade of the ABCB5 transporter sensitized $ABCB5^+$ MCC cells to chemotherapy-induced apoptosis and inhibited experimental tumor xenograft growth, paralleling previous findings in melanoma (Frank et al., 2005). This

provides proof-of-principle that resistance to chemotherapy can be reversed by inhibiting MCC-expressed ABCB5, and offers a rationale for targeting $ABCB5^+$ MCC subpopulations to enhance the clinical efficacy of currently available therapies. The present study identified additional ABC transporters, namely ABCB1 and ABCC3, that were overexpressed in chemotherapy-resistant MCCs. In previous studies, both ABCB1 and ABCC3 mediated multidrug resistance in solid cancers of various etiology (Frank et al., 2005, Huang et al., 2004). However, whether multiple ABC transporters, in addition to ABCB5, may contribute to MCC chemoresistance requires dedicated experiments involving RNA interference and Ab-mediate blockade of ABCB1, ABCC3 and other ABC transporters.

In melanoma, ABCB5 is expressed by virulent MMICs and serves as a molecular determinant of neoplastic progression (Kupas et al., 2011, Ma et al., 2010, Schatton et al., 2008). According to epidemiologic studies, MCC is more lethal than melanoma on a per case basis (Lemos et al., 2010). Consistent with the increased aggressiveness of MCC versus melanoma, the present study identified higher frequencies of $ABCB5^+$ cell subsets in MCC compared to melanoma. This raises the possibility that ABCB5 could potentially also serve as a marker for tumorigenic MCC cells capable of initiating and maintaining MCC growth and progression. However, to test whether ABCB5 expression also defines TIC subsets in MCC, serial xenotransplantation at limiting dilution of $ABCB5^+$ MCC subpopulations into immunocompromised NSG mice is required (Schatton et al., 2009). In addition, the potential utility of MCC-expressed ABCB5 as a clinically relevant marker to predict therapeutic resistance and disease aggressiveness requires independent validation in larger patient cohorts, including in prospective studies.

In summary, the present study indentifies ABCB5 as a novel chemoresistance mechanisms in MCC. In addition, it provides a rationale for translating ABCB5-targeted

chemoresistance reversal strategies to the clinic, in order to improve currently available therapies for advanced MCC.

6 Conclusions

The results presented in this thesis expand upon the current understanding of PD-1 pathway functions in cancer in several ways. Firstly, using a syngeneic tumor model, melanoma-expressed PD-1 was identified as a previously unrecognized immunosuppressive mechanism that promotes tumor immune escape. Understanding the molecular and cellular mechanisms underlying melanoma-PD-1-driven tumor immune evasion might identify additional immunomodulatory pathways, immunosuppressive factors, and tolerogenic cell populations, that could be targeted in combination with anti-PD-1 treatment to further improve clinical benefit. Secondly, cancer cell-expressed PD-1 was identified as a novel tumor cell-intrinsic growth-promoting mechanism, including in the absence of immunity. For example, enforced expression of PD-1 by melanoma cells and engagement of cancer cell-expressed PD-1 by its ligand, PD-L1, promoted, while PD-1 KD, inhibition of intracellular PD-1 signaling motifs, and antibody-mediated PD-1 blockade inhibited tumor cell growth *in vitro*, in the absence of immune cells, as well as *in vivo* in immunocompromised, T and B cell deficient mice. Thus, Ab-mediated inhibition of these complementary protumorigenic PD-1 functions might explain the superior therapeutic efficacy of PD-1 Abs, compared to immunotherapies targeting the alternative immune checkpoint CTLA-4. The possible link between cancer cell-expressed PD-1 and hyperactivation of oncogenic pathways, including PI3K/AKT/mTOR, PD-L1 expression, cancer cell metabolism, cell cycle progression, metastasis, and therapeutic resistance could critically enhance the basic understanding of cancer initiation and growth. Combining anti-PD-1 Abs with therapies that target oncogenic pathways downstream of cancer cell-

expressed PD-1 might work synergistically to further improve the clinical efficacy of PD-1 inhibition.

Thirdly, ABCB5 mediates resistance to standard-of-care chemotherapeutic agents in melanoma and MCC. Because $ABCB5^{+}$ cancer cells preferentially co-express the PD-1 receptor, the PD-1 pathway could potentially also confer chemotherapy resistance in melanoma and MCC. Strategies to target ABCB5 in combination with chemotherapy and PD-1 pathway inhibitors might thus enhance clinical efficacy of currently available melanoma and MCC therapies.

7 Future directions

As discussed, antibody-based therapeutics targeting the PD-1 pathway have demonstrated unprecedented response rates and encouraging toxicity profiles in patients with advanced-stage cancers of various etiology (Borghaei et al., 2015, Brahmer et al., 2015, Hamid et al., 2013, Motzer et al., 2015, Nghiem et al., 2016, Postow et al., 2015a, Topalian et al., 2012b, Wolchok et al., 2013). This has led to the FDA approval of anti-PD-1 Abs for the treatment of metastatic melanoma, NSCLC, RCC, head and neck squamous cell carcinoma, and Hodgkin's lymphoma. In light of the herein presented cancer cell-intrinsic protumorigenic PD-1 functions in melanoma and MCC, and given the fact that lesser immunogenic cancers, including NSCLC, respond to PD-1 therapy, PD-1 might also serve as an immune-independent tumor growth-promoting mechanism in other cancers, including NSCLC, RCC, head and neck squamous cell carcinoma, and Hodgkin's lymphoma. Indeed, in early proof-of-concept studies, the Ph.D. candidate identified PD-1-expressing cancer cell subsets in established human NSCLC and RCC cell lines. Whether PD-1 ecpression by NSCLC and RCC is clinically relevant, and whether the PD-1 receptor also modulates tumor cell-intrinsic oncogenic pathways, including mTOR activity, requires

further investigation. To this end, the Ph.D. candidate has already generated stable *PDCD1*-KD and *PDCD1*-OE cell line variants that will enable the study of PD-1 receptor functions in NSCLC and RCC, similar to the experimental setup for melanoma and MCC. In addition, cancer cell-specific PD-1 signaling studies might identify putative biomarkers for predicting response to therapeutic PD-1 blockade in patients with NSCLC and RCC, among other cancers that contain PD-1^+ subpopulations.

Additional studies should also aim towards determining tissue-specific factors that regulate PD-1 expression by cancer cells. Here, PD-1 was expressed by a small subset of melanoma and MCC cells. Interestingly, the frequency of PD-1^+ melanoma cells is increased in three-dimensional spheroid cultures and *in vivo,* in tumor xenografts, as compared to standard two-dimensional cultures. In addition, *in vitro* culture of FACS-sorted PD-1^+ versus PD-1^- melanoma cells subsets re-established the original cancer cell heterogeneity, suggesting cancer cell plasticity with respect to PD-1 expression. In a preliminary study, frequency of PD-1^+ cancer cells was not affected by hypoxia. In T cells, transcription factors, such as NFATc1 and AP-1 induce, while Tbet represses PD-1 expression (Bally et al., 2016). Paracrine stimulation by its ligand, PD-L1, also upregulates PD-1 expression by T cells (Pinton et al., 2015). Whether the same transcription factors, paracrine PD-L1 stimulation and/or environmental cues regulate PD-1 expression by cancer cells requires additional experiments, including quantitative RT-PCR analysis and gain- or loss-of function experiments of various transcription factors in native PD-1-sorted cells, 2D versus 3D cultures, and genetically engineered melanoma cell line variants.

Future experiments should also be geared towards identifying tissue-specific differences in adaptor molecules, including SHP-2, that mediate PD-1 downstream signaling in T cells versus cancer cells. The present study demonstrates that cancer cell-expressed PD-1 promotes tumor growth and activates cancer cell-intrinsic mTOR signaling, both of which are abrogated upon mutation of the PD-1 signaling motifs, ITIM

and ITSM, in cancer cells. In T cells, PD-1 ligation recruits phosphatases SHP-1 and SHP-2 to its ITIM and ITSM cytosolic loci, which mediates suppression of MAPK, PI3K/AKT and mTOR pathways downstream of the TCR signaling complex (Riley, 2009, Yokosuka et al., 2012). SHP-2 is also expressed by tumorigenic cancer cell subsets (Aceto et al., 2012, Liu et al., 2011), and SHP-2-dependent signaling promotes the activation of protumorigenic pathways, including mTOR, in cancer cells (Liu et al., 2011, Ostman et al., 2006). The divergent effects of PD-1 ligation on mTOR signaling in cancer cells versus T cells are thus entirely consistent with the opposing, protumorigenic versus growth-inhibitory roles of SHP-2 in the respective cell types. However, whether tissue-specific differences in PD-1 function are mediated by SHP-2, and/or other adaptor molecules or enzymes that are associated with the TCR complex in T cells and absent in melanoma cells requires future dedicated studies. To this end, the effects of PD-1 activation on mTOR signaling in SHP-2 KD or SHP-2 loss of function melanoma cell lines are being investigated. Moreover, whether tumor cell-intrinsic activation of the mTOR pathway is required for the observed protumorigenic effect of cancer-expressed PD-1, or whether additional pathways, including PI3K/AKT might also be regulated by PD-1 to promote tumor growth will need to be addressed. This may also help identify new targets downstream of cancer cell-expressed PD-1, which could possibly also serve as biomarkers of response or targets for therapeutic intervention.

In addition, future studies to further dissect the role of PD-1 in MCC tumorigenesis are required. While Ab-mediated PD-1 blockade significantly inhibited experimental tumor growth in mice grafted with all established melanoma cell lines and melanoma biopsies tested, it failed to consistently inhibit experimental MCC growth *in vivo,* in the present study. Anti-PD-1 Abs attenuated WaGa, but not MKL-1 tumor xenograft growth, although both cell lines are $MCPyV^{+}$ and express PD-1 at similar levels. In MCC tumors, the mTOR pathway is aberrantly activated, which, at least in part, results from viral ST

antigen-mediated activation. Moreover, mTOR signaling plays an important role in MCC tumorigenesis. Whether differences in baseline ST antigen expression and/or activation of the mTOR pathway could account for variations in response to PD-1 inhibition, or whether additional oncogenic pathways account for these differences also requires dedicated studies.

Lastly, the effects of cancer cell-expressed PD-1 on cell cycle regulation should be addressed experimentally. In the present study, cancer cell-expressed PD-1 activates mTOR signaling effectors, including S6K1 and S6. Consistently, activation of the mTOR pathway and its downstream signaling mediators, including S6K1, have been previously shown to control the G1 checkpoint and regulate cell cycle progression (Fingar et al., 2004, Foster et al., 2010). In T cells, activation of the PD-1 receptor by its ligands blocks cell cycle progression at G1 by controlling multiple cell cycle regulators, including cyclin-dependent kinases (CDKs) (Patsoukis et al., 2012). Interestingly, a tissue microarray analysis of the herein used genetically engineered melanoma-PD-1 variant cell lines showed differential expression of several genes associated with cell cycle regulation, including CDKs. Preliminary studies showed no differences in β-galactosidase activity at pH 6 - a known characteristic of senescent cells - in PD-1-OE versus PD-1-KD compared to control cultures, suggesting that melanoma-expressed PD-1 may not modulate cellular senescence. However, whether cancer cell-expressed PD-1 regulates cell cycle progression, for example via activation of CDKs, requires future dedicated studies.

While these studies are beyond the scope of this thesis, dedicated experiments aimed at further dissecting molecular and cellular mechanism underlying the protumorigenic functions of cancer cell-expressed PD-1 are critical to further understand melanoma and MCC initiation, growth and progression, and to improve the therapeutic benefits of current treatment regimens for patients with disseminated disease.

Table 1. Melanoma patient biopsies analyzed for melanoma-PD-1 expression.

Patient number	Gender	Age	Tumor site	Melanoma-PD-1 expression[a]
1	F	68	Cutaneous primary	++
2	F	31	Cutaneous primary	n.d.
3	F	91	Cutaneous metastasis	++
4	F	79	Cutaneous primary	+
5a	M	35	Cutaneous metastasis	n.d.
5b			Brain metastasis	n.d.
6a	M	55	Subcutaneous metastasis	+
6b			Cutaneous metastasis	n.d.
7	M	77	Cutaneous metastasis	n.d.
8	F	67	Cutaneous metastasis	+
9	M	49	Cutaneous metastasis	+
10a	M	47	Lymph node metastasis	n.d.
10b			Lymph node metastasis	+
11	M	71	Brain metastasis	+
12a	M	56	Cutaneous metastasis	n.d.
12b			Lymph node metastasis	n.d.
13	F	59	Cutaneous metastasis	n.d.
14	M	74	Pulmonary metastasis	n.d.
15	F	52	Subcutaneous metastasis	+
16	M	68	Cutaneous metastasis	+++
17	F	54	Lymph node metastasis	+
18	M	57	Subcutaneous metastasis	+
19a	M	59	Cutaneous metastasis	+
19b			Cutaneous metastasis	n.d.
20	F	52	Subcutaneous metastasis	+
21a	M	82	Cutaneous metastasis	+
21b			Cutaneous metastasis	n.d.
22	F	75	Cutaneous metastasis	+
23	F	78	Cutaneous metastasis	n.d.
24	M	42	Subcutaneous metastasis	n.d.
25a	M	77	Subcutaneous metastasis	n.d.
25b			Lymph node metastasis	n.d.
26	M	65	Abdominal metastasis	+
27a	F	75	Subcutaneous metastasis	n.d.
27b			Subcutaneous metastasis	+
28	M	88	Subcutaneous metastasis	+
29a	M	55	Subcutaneous metastasis	n.d.
29b			Subcutaneous metastasis	n.d.
29c			Subcutaneous metastasis	n.d.
30	F	56	Subcutaneous metastasis	+++
31	M	49	Subcutaneous metastasis	n.d.
32a	M	72	Subcutaneous metastasis	n.d.
32b			Subcutaneous metastasis	+
33	M	51	Lymph node metastasis	n.d.
34a	F	40	Subcutaneous metastasis	n.d.
34b			Subcutaneous metastasis	n.d.
35	F	36	Subcutaneous metastasis	n.d.
36a	F	69	Subcutaneous metastasis	n.d.
36b			Subcutaneous metastasis	++
36c			Adrenal metastasis	n.d.

[a]Melanoma-PD-1 expression was determined by immunofluorescence double labeling and defined as PD-1(+)CD45(-) and/or PD-1(+)MART-1(+); (+, 1-10%; ++, 10-25%; +++, >25%; n.d., not detected). This table has been previously published (Kleffel et al., 2015).

Table 2. Correlation of progression-free and overall survival with p-S6 expression in tumor biospecimens obtained from melanoma patients before initiation of anti-PD-1 Ab therapy.

	Group	Cases	Events[a]	Mean time to progression or death [months (95% CI[b])]	Log-rank test statistic	Log-rank test *P*-value
Time to progression (PFS)[c]	p-S6 <25%	14	13	4.5 (2-7)	10.74, df[e]=1	0.00105
	p-S6 >25%	20	11	17.0 (11-23)		
Time to death (OS)[d]	p-S6 <25%	14	8	13.0 (8-18)	3.99, df=1	0.04586
	p-S6 >25%	20	5	25.1 (20-30)		

[a]Disease progression or death; [b]confidence interval; [c]progression-free survival; [d]overall survival; [e]degree of freedom. This table has been previously published (Kleffel et al., 2015).

Table 3. Characteristics of clinical MCC tumor biospecimens.

Patient #	Gender	Age*	Tumor type	Chemo	Chemo regimen	Stage*
1	F	90	Primary cancer	N		IIIA
2	M	74	Local recurrence	Y	Carboplatin, Etoposide	IIIB
3	M	54	Visceral met	Y	Carboplatin, Etoposide	IIIA
			Visceral met	Y	Carboplatin, Etoposide	IIIA
4	M	75	Primary cancer	N		IIIA
5	M	80	Primary cancer	N		IIIB
			Local recurrence	N		IIIB
6	F	60	Primary cancer	N		IIIA
			Local recurrence	N		IIIA
			Local recurrence	N		IIIA
			Local recurrence	Y	Carboplatin, Etoposide	IIIA
7	F	78	Primary cancer	N		IIB
8	F	78	Lymph node met	N		IIIB
9	M	77	Local recurrence	Y	Carboplatin, Etoposide	IIIA
10	M	47	Primary cancer	N		IIIA
11	F	52	Primary cancer	N		IA
12	M	81	Primary cancer	N		IIIA
			Lymph node met	N		IIIA
13	F	49	Primary cancer	N		IIIA
14	M	80	Primary cancer	N		IIIA
15	M	58	Primary cancer	N		IA
16	M	74	Primary cancer	N		IIIA
			Primary cancer	N		IIIA
17	F	51	Primary cancer	Y	Carboplatin, Etoposide	IIIB
18	F	78	Primary cancer	N		IIA
			Lymph node met	N		IIA
19	M	63	Lymph node met	Y	Carboplatin, Etoposide	IIIB
20	F	81	Primary cancer	N		IIIA
21	M	60	Lymph node met	N		IIIB
22	M	65	Primary cancer	N		IA
			Primary cancer	N		IA
23	M	83	Primary cancer	N		IB
24	M	82	Primary cancer	Y	Carboplatin, Etoposide	IIIB
25	M	50	Primary cancer	N		IIIA
			Lymph node met	N		IIIA
26	M	81	Primary cancer	N		IIIA
27	F	77	Primary cancer	N		IV
28	F	70	Primary cancer	Y	Carboplatin, Etoposide	IIIB
29	F	84	Primary cancer	N		IIIB
30	M	79	Lymph node met	N		IIIB
31	F	74	Primary cancer	N		IIIA
32	M	85	Primary cancer	N		IIIA
33	M	72	Primary cancer	N		IA
34	F	84	Primary cancer	N		IIIA

35	M	81	Primary cancer	N		IIIA
36	M	45	Lymph node met	Y	Carboplatin, Etoposide	IIIB
37	M	73	Primary cancer	N		IIIB
			Local recurrence	Y	Carboplatin, Etoposide	IIIB
38	F	76	Lymph node met	Y	Carboplatin, Etoposide	IIIB
39	F	77	Lymph node met	N		IIIB
40	M	51	Visceral met	Y	Carboplatin, Etoposide	IIIA
41	F	86	Local recurrence	Y	Carboplatin, Etoposide	IIB
42	F	58	Primary cancer	Y	Carboplatin, Etoposide	IIA
43	F	51	Visceral met	Y	Cisplatin, 5-FU, Irinotecan	IV
44	F	54	Primary cancer	N		IA
45	F	67	Primary cancer	Y	Carboplatin, Etoposide	IIIA
46	M	59	Primary cancer	Y	Cisplatin, Etoposide	IA
47	M	54	Primary cancer	Y	BB10901 (huN901-DM1)	IIIB
			Primary cancer	Y	BB10901 (huN901-DM1)	IIIB
48	M	50	Primary cancer	N		IIIA
49	F	80	Primary cancer	N		IA
50	F	65	Primary cancer	N		IB
			Primary cancer	N		IB
51	M	56	Local recurrence	Y	Cisplatin, Etoposide	IIIA
52	M	70	Primary cancer	Y	Carboplatin, Etoposide	IA
			Primary cancer	Y	Carboplatin, Etoposide	IA
			Local recurrence	Y	Carboplatin, Etoposide	IA
			Local recurrence	Y	Carboplatin, Etoposide	IA
			Local recurrence	Y	Carboplatin, Etoposide	IA
53	M	79	Primary cancer	Y	Carboplatin, Etoposide	IIIA
			Local recurrence	Y	Carboplatin, Etoposide	IIIA
54	M	71	Local recurrence	N		IIIA
55	M	83	Lymph node met	N		IIIA
56	M	75	Primary cancer	N		IIIA
57	F	69	Local recurrence	Y	Carboplatin, Etoposide	IA
58	F	80	Primary cancer	N		IIIA
59	M	85	Primary cancer	N		IIIA
60	M	47	Local recurrence	Y	Cisplatin	IA
61	F	80	Local recurrence	Y	Carboplatin, Etoposide	IB
62	F	80	Primary cancer	N		IIIA
63	M	51	Local recurrence	N		IA

64	F	75	Lymph node met	Y	Carboplatin, Etoposide	IIIB
65	M	76	Primary cancer	N		IIIA
			Local recurrence	Y	Carboplatin, Etoposide	IIIA
66	M	56	Primary cancer	Y	Carboplatin, Etoposide	IIIA

*At time of initial presentation.). This table has been previously published (Kleffel et al., 2016).

8 Acknowledgements

I would like to acknowledge many of the remarkable individuals who made this thesis possible. First and foremost, I would like to thank my mentor and PhD advisor, Professor Dr. Tobias Schatton for your support and guidance during the past 5 years. You enabled me to work on scientifically fascinating and clinically relevant projects and I will always be grateful. I truly appreciate your time, insight, and constant encouragements that made my Ph.D. experience both productive and stimulating, and resulted in the publication of 9 manuscripts. You were a great cheerleader, and your energy and constant enthusiasm for the research was contagious and motivational, especially during difficult times. It has been an honor to be the first member of the Schatton lab and your first Ph.D. student. You have helped me become the scientist and person I am today.

I would also like to thank the members of my Ph.D. committee, Professor Dr. Ana-Maria Waaga-Gasser, Professor Dr. Manfred Schartl and Professor Dr. Markus Frank, for your time and continuous support. Your insightful questions and discussions helped to shape my research. I am professionally and personally grateful for everything you have done. Thank you for being on my committee.

I am also grateful to have worked alongside and collaborated with wonderful scientists and physicians from the Departments of Dermatology and Pathology at Brigham and Women's Hospital. Specifically, I would like to thank Professor Dr. Thomas Kupper,

who provided invaluable feedback on my research during weekly lab meetings, and financial support. I would also like to thank Professor Dr. Robert Fuhlbrigge - your office door was always open for me. You made sure that I focused on becoming a better scientist, and provided a great framework for personal growth and invaluable career advice. Your work in the department has been inspirational in many ways. I would also like to thank my collaborator and dear friend, Dr. Steven Barthel. I appreciate the time you took to teach me how to engineer melanoma cell line variants, writing poems about adding antibiotics to my transduced cells instead of handing me the protocol and using “hockey sticks” to spread bacteria. I would have not successfully done this work without your help. You are one of the nicest, most helpful people that I have ever met, and I truly value our friendship.

Many thanks to Professor Dr. George Murphy, who was instrumental for the analysis and interpretion of the pathology slides. Your enthusiasm for research and love for teaching is contagious. You are a great expert in the field, and it has been a great honor to work and learn from you. Many thanks to Dr. Christopher Elco, Dr. Qian Zhan, Dr. Cecilia Lezcano and Professor Dr. Christine Lian. The pathology studies discussed in this thesis would have not been possible without you, and I appreciate all of your time, support and helpful discussions. Many thanks also to Dr. Chung-Wei Lee, who taught me the melanoma spheroid culture technique. I would also like to thank our collaborator, Professor Dr. Arlene Sharpe, a leading expert in PD-1 biology, whose expertise and support were instrumental to the success of this project, and her graduate student, Vikram Juneja, who taught me how to analyze tumor-infiltrating lymphocytes. I was also fortunate to pursue my graduate studies in a laboratory that collaborated with many wonderful clinicians, including Dr. Christoph Schlapbach, Dr. Emmanuella Guenova, Dr. Wolfram Hoetzenecker, Dr. Antonio Cozzio, Dr. Reinhard Dummer, Dr. Keith Flaherty, Dr. Linda Wang and Dr. Manisha Thakuria. This enabled access to rare patient samples, expanding the impact and relevance of our studies. I am grateful to the past and present members of

the Schatton and Frank laboratories, particularly Dr. Christian Posch, Dr. Hansgeorg Müller, Dr. Nayoung Lee, Dr. Brian Wilson and Dr. Karim Saab. You have taught, supported and inspired me so much, and made my daily work in the lab more fun. Many thanks also go to the summer students that have rotated through the lab, who helped me develop my mentoring skills. Thank you for all your help - particularly with dissecting the mice. Your questions have helped me become a better scientist and teacher, and I appreciate the joy and constant enthusiasm you shared with me.

A good support system is key to survive and stay sane during graduate school. I was lucky to be a part of a department that contributed to my personal and professional development. I am especially grateful for Dr. Sherrie Divito, Nicholas Giovannone, Jenna Geddes and Russel Griffith, who stuck with me. You have been a great source of inspiration, advice, collaboration and invaluable friendship. Thank you for your enthusiasm, support, and unfiltered feedback. Thank you for making me laugh, no matter how draining and frustrating my day had been. Thank you for all the fun lunches, the walk'n talks around the block, for not judging my Starbucks consumption, and for obsessing slightly more about new protocols than me. Special thanks to Sherrie for providing feedback on my thesis, for pushing me and keeping me company during the late nights and weekends in the lab. I am grateful to have you as my friend, and I truly admire your work ethic and your ability to smile despite sliding down the mountain.

Finally, I would like to thank my parents Achim and Renate Kleffel for their love, support and constant encouragement. You raised me to be dedicated and hard-working, instilled a love of science in me, and always supported me. Most of all, I would like to thank my loving, understanding, encouraging, and patient husband Michael LaFleur, whose faithful support during this Ph.D. is greatly appreciated.

Thank you.

9 Credits

Dr. Christian Posch, during his time as a fellow in the laboratory of Prof. Dr. Tobias Schatton at the Department of Dermatology at Brigham and Women's Hospital and Harvard Medical School performed and analysed the immunoblot data shown in Figures 16B, 19A and B, 20E, 24C and D, 25F, 29C, 31C, 46B, 49C, and 50C.

Dr. Steven Barthel, member of the Department of Dermatology at Brigham and Women's Hospital and Harvard Medical School performed the immunoblot analyses shown in Figures 3B and 4B.

Dr. Hansgeorg Müller, during his time as a fellow in the laboratory of Prof. Dr. Tobias Schatton at the Department of Dermatology at Brigham and Women's Hospital and Harvard Medical School helped with the quantitative RT-PCR analyses in Figures 7D and E, 14B and C, and 22B and C, and performed the image analyses shown in Figures 34D and 41C.

Dr. Christoph Schlapbach, member of the Department of Dermatology at the University of Bern contributed to the FACS stainings of patient samples shown in Figure 2A and performed and analyzed the immunohistochemical stainings in Figure 22B and C.

Dr. Brian Wilson, fellow in the laboratory of Prof. Dr. Markus Frank at the Boston Children's Hospital and Harvard Medical School performed and analyzed the data shown in Figure 39C and D.

Prof. Dr. George F. Murphy, along with the members of his laboratory Dr. Qian Zhan, Dr. Christopher P. Elco, and Dr. C. Lezcano and Prof. Dr. C. Lian from the Department of Pathology at Brigham and Women's Hospital and Harvard Medical School performed and analysed the immunohistochemical and immunofluorescence stainings in Figures 2C, 4D, 34A and D, 35B, 40B, 41C, 43B, 44B, and 48A and B.

Dr. Emmanuella Guenova, Dr.Wolfram Hoetzenecker, Dr. Antonio Cozzi, and Prof. Dr. Reinhard Dummer performed the IHC stainings and analyzed the data shown in Figure 32.

Dr. Nayoung Lee, during her time as a medical student in the Schatton laboratory at the Department of Dermatology at Brigham and Women's Hospital and Harvard Medical School performed and analysed the flow cytometry experiments in Figures 35C, 37B and 39B and helped with the immunophenotyping analyses in Figures 9, 10 and 11.

Dr. Kristine Sobolewski, during her time as a student in the laboratory of Prof. Dr. Schatton at the Department of Dermatology at Brigham and Women's Hospital and Harvard Medical School performed and analysed the MTT assays in Figure 39A and helped maintain the drug-resistant MCC cell lines used in this study.

Margot Joubert, during her time as a student in the laboratory of Prof. Dr. Schatton at the Department of Dermatology at Brigham and Women's Hospital and Harvard Medical School performed and analysed the flow cytometry experiments in Figure 47.

Prof. Dr. Tobias Schatton, Dr. Hansgeorg Müller, Dr. Christian Posch, Dr. Nayoung Lee and summer students of the Schatton laboratory contributed significantly to the *in vivo* tumorigenicity studies presented in this thesis.

The Pathology Core Facility at Brigham and Women's Hospital and Harvard Medical School performed the immunohistochemical stainings shown in Figures 4D, 7D, 14B and C, 26, 28B, 30C and D, and 50B.

Sorting of melanoma cells was performed at the cell sorting facility at the Center for Neurologic Disease at Brigham and Women's Hospital and Harvard Medical School.

10 References

Aceto, N., Sausgruber, N., Brinkhaus, H., Gaidatzis, D., Martiny-Baron, G., Mazzarol, G., Confalonieri, S., Quarto, M., Hu, G., Balwierz, P. J., Pachkov, M., Elledge, S. J., van Nimwegen, E., Stadler, M. B. & Bentires-Alj, M. 2012. Tyrosine phosphatase SHP2 promotes breast cancer progression and maintains tumor-initiating cells via activation of key transcription factors and a positive feedback signaling loop. *Nat Med,* 18**,** 529-37.

Afanasiev, O. K., Yelistratova, L., Miller, N., Nagase, K., Paulson, K., Iyer, J. G., Ibrani, D., Koelle, D. M. & Nghiem, P. 2013. Merkel polyomavirus-specific T cells fluctuate with merkel cell carcinoma burden and express therapeutically targetable PD-1 and Tim-3 exhaustion markers. *Clin Cancer Res,* 19**,** 5351-60

.

Agelli, M. & Clegg, L. X. 2003. Epidemiology of primary Merkel cell carcinoma in the United States. *J Am Acad Dermatol,* 49**,** 832-41.

Ahmadzadeh, M., Johnson, L. A., Heemskerk, B., Wunderlich, J. R., Dudley, M. E., White, D. E. & Rosenberg, S. A. 2009. Tumor antigen-specific CD8 T cells infiltrating the tumor express high levels of PD-1 and are functionally impaired. *Blood,* 114**,** 1537-44.

Ahmadzadeh, M. & Rosenberg, S. A. 2006. IL-2 administration increases CD4+ CD25(hi) Foxp3+ regulatory T cells in cancer patients. *Blood,* 107**,** 2409-14.

Amarnath, S., Mangus, C. W., Wang, J. C., Wei, F., He, A., Kapoor, V., Foley, J. E., Massey, P. R., Felizardo, T. C., Riley, J. L., Levine, B. L., June, C. H., Medin, J. A. & Fowler, D. H. 2011. The PDL1-PD1 axis converts human TH1 cells into regulatory T cells. *Sci Transl Med,* 3**,** 111ra20.

Andtbacka, R. H., Kaufman, H. L., Collichio, F., Amatruda, T., Senzer, N., Chesney, J., Delman, K. A., Spitler, L. E., Puzanov, I., Agarwala, S. S., Milhem, M., Cranmer, L., Curti, B., Lewis, K., Ross, M., Guthrie, T., Linette, G. P., Daniels, G. A., Harrington, K., Middleton, M. R., Miller, W. H., Jr., Zager, J. S., Ye, Y., Yao, B., Li, A., Doleman, S., VanderWalde, A., Gansert, J. & Coffin, R. S. 2015. Talimogene Laherparepvec Improves Durable Response Rate in Patients With Advanced Melanoma. *J Clin Oncol,* 33**,** 2780-8.

Ansell, S. M., Lesokhin, A. M., Borrello, I., Halwani, A., Scott, E. C., Gutierrez, M., Schuster, S. J., Millenson, M. M., Cattry, D., Freeman, G. J., Rodig, S. J., Chapuy, B., Ligon, A. H., Zhu, L., Grosso, J. F., Kim, S. Y., Timmerman, J. M., Shipp, M. A. & Armand, P. 2015. PD-1 blockade with nivolumab in relapsed or refractory Hodgkin's lymphoma. *N Engl J Med,* 372**,** 311-9.

Atkins, M. B., Lotze, M. T., Dutcher, J. P., Fisher, R. I., Weiss, G., Margolin, K., Abrams, J., Sznol, M., Parkinson, D., Hawkins, M., Paradise, C., Kunkel, L. & Rosenberg, S. A. 1999. High-dose recombinant interleukin 2 therapy for patients with metastatic melanoma: analysis of 270 patients treated between 1985 and 1993. *J Clin Oncol,* 17**,** 2105-16.

Azimi, F., Scolyer, R. A., Rumcheva, P., Moncrieff, M., Murali, R., McCarthy, S. W., Saw, R. P. & Thompson, J. F. 2012. Tumor-infiltrating lymphocyte grade is an independent predictor of sentinel lymph node status and survival in patients with cutaneous melanoma. *J Clin Oncol,* 30**,** 2678-83.

Azuma, T., Yao, S., Zhu, G., Flies, A. S., Flies, S. J. & Chen, L. 2008. B7-H1 is a ubiquitous antiapoptotic receptor on cancer cells. *Blood,* 111**,** 3635-43.

Baitsch, L., Baumgaertner, P., Devevre, E., Raghav, S. K., Legat, A., Barba, L., Wieckowski, S., Bouzourene, H., Deplancke, B., Romero, P., Rufer, N. & Speiser, D. E. 2011a. Exhaustion of tumor-specific CD8(+) T cells in metastases from melanoma patients. *J Clin Invest,* 121**,** 2350-60.

Baitsch, L., Baumgaertner, P., Devevre, E., Raghav, S. K., Legat, A., Barba, L., Wieckowski, S., Bouzourene, H., Deplancke, B., Romero, P., Rufer, N. & Speiser, D. E. 2011b. Exhaustion of tumor-specific CD8(+) T cells in metastases from melanoma patients. *J Clin Invest,* 121**,** 2350-60.

Balkwill, F. & Mantovani, A. 2001. Inflammation and cancer: back to Virchow? *Lancet,* 357**,** 539-45.

Bally, A. P., Austin, J. W. & Boss, J. M. 2016. Genetic and Epigenetic Regulation of PD-1 Expression. *J Immunol,* 196**,** 2431-7.

Barker, N., Ridgway, R. A., van Es, J. H., van de Wetering, M., Begthel, H., van den Born, M., Danenberg, E., Clarke, A. R., Sansom, O. J. & Clevers, H. 2009. Crypt stem cells as the cells-of-origin of intestinal cancer. *Nature,* 457**,** 608-11.

Baumeister, S. H., Freeman, G. J., Dranoff, G. & Sharpe, A. H. 2016. Coinhibitory Pathways in Immunotherapy for Cancer. *Annu Rev Immunol*.

Becker, J. C. 2010. Merkel cell carcinoma. *Ann Oncol,* 21 Suppl 7**,** vii81-5.

Becker, J. C., Houben, R., Schrama, D., Voigt, H., Ugurel, S. & Reisfeld, R. A. 2010. Mouse models for melanoma: a personal perspective. *Exp Dermatol,* 19**,** 157-64.

Beddingfield, F. C., 3rd 2003. The melanoma epidemic: res ipsa loquitur. *Oncologist,* 8**,** 459-65.

Belikov, A. V., Schraven, B. & Simeoni, L. 2015. T cells and reactive oxygen species. *J Biomed Sci,* 22**,** 85.

Benson, D. M., Jr., Bakan, C. E., Mishra, A., Hofmeister, C. C., Efebera, Y., Becknell, B., Baiocchi, R. A., Zhang, J., Yu, J., Smith, M. K., Greenfield, C. N., Porcu, P., Devine, S. M., Rotem-Yehudar, R., Lozanski, G., Byrd, J. C. & Caligiuri, M. A. 2010. The PD-1/PD-

L1 axis modulates the natural killer cell versus multiple myeloma effect: a therapeutic target for CT-011, a novel monoclonal anti-PD-1 antibody. *Blood,* 116**,** 2286-94.

Bhatia, S., Afanasiev, O. & Nghiem, P. 2011. Immunobiology of Merkel cell carcinoma: implications for immunotherapy of a polyomavirus-associated cancer. *Curr Oncol Rep,* 13**,** 488-97.

Black, M., Barsoum, I. B., Truesdell, P., Cotechini, T., Macdonald-Goodfellow, S. K., Petroff, M., Siemens, D. R., Koti, M., Craig, A. W. & Graham, C. H. 2016. Activation of the PD-1/PD-L1 immune checkpoint confers tumor cell chemoresistance associated with increased metastasis. *Oncotarget*.

Boiko, A. D., Razorenova, O. V., van de Rijn, M., Swetter, S. M., Johnson, D. L., Ly, D. P., Butler, P. D., Yang, G. P., Joshua, B., Kaplan, M. J., Longaker, M. T. & Weissman, I. L. 2010. Human melanoma-initiating cells express neural crest nerve growth factor receptor CD271. *Nature,* 466**,** 133-7.

Boon, T., Coulie, P. G., Van den Eynde, B. J. & van der Bruggen, P. 2006. Human T cell responses against melanoma. *Annu Rev Immunol,* 24**,** 175-208.

Borghaei, H., Paz-Ares, L., Horn, L., Spigel, D. R., Steins, M., Ready, N. E., Chow, L. Q., Vokes, E. E., Felip, E., Holgado, E., Barlesi, F., Kohlhaufl, M., Arrieta, O., Burgio, M. A., Fayette, J., Lena, H., Poddubskaya, E., Gerber, D. E., Gettinger, S. N., Rudin, C. M., Rizvi, N., Crino, L., Blumenschein, G. R., Jr., Antonia, S. J., Dorange, C., Harbison, C. T., Graf Finckenstein, F. & Brahmer, J. R. 2015. Nivolumab versus Docetaxel in Advanced Nonsquamous Non-Small-Cell Lung Cancer. *N Engl J Med,* 373**,** 1627-39.

Boyman, O. & Sprent, J. 2012. The role of interleukin-2 during homeostasis and activation of the immune system. *Nat Rev Immunol,* 12**,** 180-90.

Bradbury, P. A. & Middleton, M. R. 2004. DNA repair pathways in drug resistance in melanoma. *Anticancer Drugs,* 15**,** 421-6.

Brahmer, J., Reckamp, K. L., Baas, P., Crino, L., Eberhardt, W. E., Poddubskaya, E., Antonia, S., Pluzanski, A., Vokes, E. E., Holgado, E., Waterhouse, D., Ready, N., Gainor, J., Aren Frontera, O., Havel, L., Steins, M., Garassino, M. C., Aerts, J. G., Domine, M., Paz-Ares, L., Reck, M., Baudelet, C., Harbison, C. T., Lestini, B. & Spigel, D. R. 2015. Nivolumab versus Docetaxel in Advanced Squamous-Cell Non-Small-Cell Lung Cancer. *N Engl J Med,* 373**,** 123-35.

Brahmer, J. R., Tykodi, S. S., Chow, L. Q., Hwu, W. J., Topalian, S. L., Hwu, P., Drake, C. G., Camacho, L. H., Kauh, J., Odunsi, K., Pitot, H. C., Hamid, O., Bhatia, S., Martins, R., Eaton, K., Chen, S., Salay, T. M., Alaparthy, S., Grosso, J. F., Korman, A. J., Parker, S. M., Agrawal, S., Goldberg, S. M., Pardoll, D. M., Gupta, A. & Wigginton, J. M. 2012.

Safety and activity of anti-PD-L1 antibody in patients with advanced cancer. *N Engl J Med,* 366**,** 2455-65.

Braumuller, H., Wieder, T., Brenner, E., Assmann, S., Hahn, M., Alkhaled, M., Schilbach, K., Essmann, F., Kneilling, M., Griessinger, C., Ranta, F., Ullrich, S., Mocikat, R., Braungart, K., Mehra, T., Fehrenbacher, B., Berdel, J., Niessner, H., Meier, F., van den Broek, M., Haring, H. U., Handgretinger, R., Quintanilla-Martinez, L., Fend, F., Pesic, M., Bauer, J., Zender, L., Schaller, M., Schulze-Osthoff, K. & Rocken, M. 2013. T-helper-1-cell cytokines drive cancer into senescence. *Nature,* 494**,** 361-5.

Bruce, W. R. & Van Der Gaag, H. 1963. A Quantitative Assay for the Number of Murine Lymphoma Cells Capable of Proliferation in Vivo. *Nature,* 199**,** 79-80.

Burnet, M. 1957. Cancer; a biological approach. I. The processes of control. *Br Med J,* 1**,** 779-86.

Busch, D. H., Frassle, S. P., Sommermeyer, D., Buchholz, V. R. & Riddell, S. R. 2016. Role of memory T cell subsets for adoptive immunotherapy. *Semin Immunol*.

Celik, C., Lewis, D. A. & Goldrosen, M. H. 1983. Demonstration of immunogenicity with the poorly immunogenic B16 melanoma. *Cancer Res,* 43**,** 3507-10.

Chaffer, C. L., Brueckmann, I., Scheel, C., Kaestli, A. J., Wiggins, P. A., Rodrigues, L. O., Brooks, M., Reinhardt, F., Su, Y., Polyak, K., Arendt, L. M., Kuperwasser, C., Bierie, B. & Weinberg, R. A. 2011. Normal and neoplastic nonstem cells can spontaneously convert to a stem-like state. *Proc Natl Acad Sci U S A,* 108**,** 7950-5.

Chang, C. H., Qiu, J., O'Sullivan, D., Buck, M. D., Noguchi, T., Curtis, J. D., Chen, Q., Gindin, M., Gubin, M. M., van der Windt, G. J., Tonc, E., Schreiber, R. D., Pearce, E. J. & Pearce, E. L. 2015. Metabolic Competition in the Tumor Microenvironment Is a Driver of Cancer Progression. *Cell,* 162**,** 1229-41.

Chartrain, M., Riond, J., Stennevin, A., Vandenberghe, I., Gomes, B., Lamant, L., Meyer, N., Gairin, J. E., Guilbaud, N. & Annereau, J. P. 2012. Melanoma chemotherapy leads to the selection of ABCB5-expressing cells. *PLoS One,* 7**,** e36762.

Cheever, M. A., Allison, J. P., Ferris, A. S., Finn, O. J., Hastings, B. M., Hecht, T. T., Mellman, I., Prindiville, S. A., Viner, J. L., Weiner, L. M. & Matrisian, L. M. 2009. The prioritization of cancer antigens: a national cancer institute pilot project for the acceleration of translational research. *Clin Cancer Res,* 15**,** 5323-37.

Chemnitz, J. M., Parry, R. V., Nichols, K. E., June, C. H. & Riley, J. L. 2004. SHP-1 and SHP-2 associate with immunoreceptor tyrosine-based switch motif of programmed death 1 upon primary human T cell stimulation, but only receptor ligation prevents T cell activation. *J Immunol,* 173**,** 945-54.

Chen, J., Feng, Y., Lu, L., Wang, H., Dai, L., Li, Y. & Zhang, P. 2012. Interferon-gamma-induced PD-L1 surface expression on human oral squamous carcinoma via PKD2 signal pathway. *Immunobiology,* 217**,** 385-93.

Chen, L. & Flies, D. B. 2013. Molecular mechanisms of T cell co-stimulation and co-inhibition. *Nat Rev Immunol,* 13**,** 227-42.

Cheng, J., Rozenblatt-Rosen, O., Paulson, K. G., Nghiem, P. & DeCaprio, J. A. 2013. Merkel cell polyomavirus large T antigen has growth-promoting and inhibitory activities. *J Virol,* 87**,** 6118-26.

Cheung, P. F., Cheng, C. K., Wong, N. C., Ho, J. C., Yip, C. W., Lui, V. C., Cheung, A. N., Fan, S. T. & Cheung, S. T. 2011a. Granulin-epithelin precursor is an oncofetal protein defining hepatic cancer stem cells. *PLoS One,* 6**,** e28246.

Cheung, S. T., Cheung, P. F., Cheng, C. K., Wong, N. C. & Fan, S. T. 2011b. Granulin-epithelin precursor and ATP-dependent binding cassette (ABC)B5 regulate liver cancer cell chemoresistance. *Gastroenterology,* 140**,** 344-55.

Civenni, G., Walter, A., Kobert, N., Mihic-Probst, D., Zipser, M., Belloni, B., Seifert, B., Moch, H., Dummer, R., van den Broek, M. & Sommer, L. 2011. Human CD271-positive melanoma stem cells associated with metastasis establish tumor heterogeneity and long-term growth. *Cancer Res,* 71**,** 3098-109.

Clark, C. A., Gupta, H. B., Sareddy, G., Pandeswara, S., Lao, S., Yuan, B., Drerup, J. M., Padron, A., Conejo-Garcia, J., Murthy, K., Liu, Y., Turk, M. J., Thedieck, K., Hurez, V., Li, R., Vadlamudi, R. & Curiel, T. J. 2016. Tumor-Intrinsic PD-L1 Signals Regulate Cell Growth, Pathogenesis, and Autophagy in Ovarian Cancer and Melanoma. *Cancer Res,* 76**,** 6964-74.

Clark, W. H., Jr., Elder, D. E., Guerry, D. t., Braitman, L. E., Trock, B. J., Schultz, D., Synnestvedt, M. & Halpern, A. C. 1989. Model predicting survival in stage I melanoma based on tumor progression. *J Natl Cancer Inst,* 81**,** 1893-904.

Clarke, M. F., Dick, J. E., Dirks, P. B., Eaves, C. J., Jamieson, C. H., Jones, D. L., Visvader, J., Weissman, I. L. & Wahl, G. M. 2006. Cancer stem cells--perspectives on current status and future directions: AACR Workshop on cancer stem cells. *Cancer Res,* 66**,** 9339-44.

Clemente, C. G., Mihm, M. C., Jr., Bufalino, R., Zurrida, S., Collini, P. & Cascinelli, N. 1996. Prognostic value of tumor infiltrating lymphocytes in the vertical growth phase of primary cutaneous melanoma. *Cancer,* 77**,** 1303-10.

Condamine, T., Ramachandran, I., Youn, J. I. & Gabrilovich, D. I. 2015. Regulation of tumor metastasis by myeloid-derived suppressor cells. *Annu Rev Med,* 66**,** 97-110.

Contardi, E., Palmisano, G. L., Tazzari, P. L., Martelli, A. M., Fala, F., Fabbi, M., Kato, T., Lucarelli, E., Donati, D., Polito, L., Bolognesi, A., Ricci, F., Salvi, S., Gargaglione, V., Mantero, S., Alberghini, M., Ferrara, G. B. & Pistillo, M. P. 2005. CTLA-4 is constitutively expressed on tumor cells and can trigger apoptosis upon ligand interaction. *Int J Cancer,* 117**,** 538-50.

Cooper, Z. A., Juneja, V. R., Sage, P. T., Frederick, D. T., Piris, A., Mitra, D., Lo, J. A., Hodi, F. S., Freeman, G. J., Bosenberg, M. W., McMahon, M., Flaherty, K. T., Fisher, D. E., Sharpe, A. H. & Wargo, J. A. 2014. Response to BRAF inhibition in melanoma is enhanced when combined with immune checkpoint blockade. *Cancer Immunol Res,* 2**,** 643-54.

Corcoran, R. B., Rothenberg, S. M., Hata, A. N., Faber, A. C., Piris, A., Nazarian, R. M., Brown, R. D., Godfrey, J. T., Winokur, D., Walsh, J., Mino-Kenudson, M., Maheswaran, S., Settleman, J., Wargo, J. A., Flaherty, K. T., Haber, D. A. & Engelman, J. A. 2013. TORC1 suppression predicts responsiveness to RAF and MEK inhibition in BRAF-mutant melanoma. *Sci Transl Med,* 5**,** 196ra98.

Dahlke, E., Murray, C. A., Kitchen, J. & Chan, A. W. 2014. Systematic review of melanoma incidence and prognosis in solid organ transplant recipients. *Transplant Res,* 3**,** 10.

Day, C. L., Jr., Sober, A. J., Kopf, A. W., Lew, R. A., Mihm, M. C., Jr., Hennessey, P., Golomb, F. M., Harris, M. N., Gumport, S. L., Raker, J. W., Malt, R. A., Cosimi, A. B., Wood, W. C., Roses, D. F., Gorstein, F., Postel, A., Grier, W. R., Mintzis, M. N. & Fitzpatrick, T. B. 1981. A prognostic model for clinical stage I melanoma of the upper extremity. The importance of anatomic subsites in predicting recurrent disease. *Ann Surg,* 193**,** 436-40.

de Visser, K. E., Eichten, A. & Coussens, L. M. 2006. Paradoxical roles of the immune system during cancer development. *Nat Rev Cancer,* 6**,** 24-37.

Dean, M., Rzhetsky, A. & Allikmets, R. 2001. The human ATP-binding cassette (ABC) transporter superfamily. *Genome Res,* 11**,** 1156-66.

Dillon, P., Thomas, N., Sharpless, N. & Collichio, F. 2010. Regression of advanced melanoma upon withdrawal of immunosuppression: case series and literature review. *Med Oncol,* 27**,** 1127-32.

Dirks, P. 2010. Cancer stem cells: Invitation to a second round. *Nature,* 466**,** 40-1.

Dong, H., Strome, S. E., Salomao, D. R., Tamura, H., Hirano, F., Flies, D. B., Roche, P. C., Lu, J., Zhu, G., Tamada, K., Lennon, V. A., Celis, E. & Chen, L. 2002a. Tumor-associated B7-H1 promotes T-cell apoptosis: a potential mechanism of immune evasion. *Nat Med,* 8**,** 793-800.

Dong, H., Strome, S. E., Salomao, D. R., Tamura, H., Hirano, F., Flies, D. B., Roche, P. C., Lu, J., Zhu, G., Tamada, K., Lennon, V. A., Celis, E. & Chen, L. 2002b. Tumor-associated B7-H1 promotes T-cell apoptosis: a potential mechanism of immune evasion. *Nat Med,* 8**,** 793-800.

Dowlatshahi, M., Huang, V., Gehad, A. E., Jiang, Y., Calarese, A., Teague, J. E., Dorosario, A. A., Cheng, J., Nghiem, P., Schanbacher, C. F., Thakuria, M., Schmults, C. D., Wang, L. C. & Clark, R. A. 2013. Tumor-specific T cells in human Merkel cell carcinomas: a possible role for Tregs and T-cell exhaustion in reducing T-cell responses. *J Invest Dermatol,* 133**,** 1879-89.

Dudley, M. E., Wunderlich, J. R., Robbins, P. F., Yang, J. C., Hwu, P., Schwartzentruber, D. J., Topalian, S. L., Sherry, R., Restifo, N. P., Hubicki, A. M., Robinson, M. R., Raffeld, M., Duray, P., Seipp, C. A., Rogers-Freezer, L., Morton, K. E., Mavroukakis, S. A., White, D. E. & Rosenberg, S. A. 2002. Cancer regression and autoimmunity in patients after clonal repopulation with antitumor lymphocytes. *Science,* 298**,** 850-4.

Eggermont, A. M., Spatz, A. & Robert, C. 2014. Cutaneous melanoma. *Lancet,* 383**,** 816-27.

Elliott, A. M. & Al-Hajj, M. A. 2009. ABCB8 mediates doxorubicin resistance in melanoma cells by protecting the mitochondrial genome. *Mol Cancer Res,* 7**,** 79-87.

Eng, T. Y., Boersma, M. G., Fuller, C. D., Goytia, V., Jones, W. E., 3rd, Joyner, M. & Nguyen, D. D. 2007. A comprehensive review of the treatment of Merkel cell carcinoma. *American journal of clinical oncology,* 30**,** 624-36.

Engelstein, R., Merims, S., Eisenberg, G., Cohen, J., Frank, S., Hamburger, T., Frankenburg, S., Ron, I., Isacson, R., Grenader, T., Steinberg, H., Cohen, C. J., Peretz, T. & Lotem, M. 2016. Immune Monitoring of Patients Treated With a Whole-Cell Melanoma Vaccine Engineered to Express 4-1BBL. *J Immunother,* 39**,** 321-8.

Eriksson, E., Wenthe, J., Irenaeus, S., Loskog, A. & Ullenhag, G. 2016. Gemcitabine reduces MDSCs, tregs and TGFbeta-1 while restoring the teff/treg ratio in patients with pancreatic cancer. *J Transl Med,* 14**,** 282.

Feng, H., Shuda, M., Chang, Y. & Moore, P. S. 2008. Clonal integration of a polyomavirus in human Merkel cell carcinoma. *Science,* 319**,** 1096-100.

Fichtner, I., Rolff, J., Soong, R., Hoffmann, J., Hammer, S., Sommer, A., Becker, M. & Merk, J. 2008. Establishment of patient-derived non-small cell lung cancer xenografts as models for the identification of predictive biomarkers. *Clin Cancer Res,* 14**,** 6456-68.

Fidler, I. J. & Nicolson, G. L. 1976. Organ selectivity for implantation survival and growth of B16 melanoma variant tumor lines. *J Natl Cancer Inst,* 57**,** 1199-202.

Fingar, D. C., Richardson, C. J., Tee, A. R., Cheatham, L., Tsou, C. & Blenis, J. 2004. mTOR controls cell cycle progression through its cell growth effectors S6K1 and 4E-BP1/eukaryotic translation initiation factor 4E. *Mol Cell Biol,* 24**,** 200-16.

Fitzgerald, T. L., Dennis, S., Kachare, S. D., Vohra, N. A., Wong, J. H. & Zervos, E. E. 2015. Dramatic Increase in the Incidence and Mortality from Merkel Cell Carcinoma in the United States. *Am Surg,* 81**,** 802-6.

Flaherty, K. T. & Fisher, D. E. 2011. New strategies in metastatic melanoma: oncogene-defined taxonomy leads to therapeutic advances. *Clin Cancer Res,* 17**,** 4922-8.

Flaherty, K. T., Hodi, F. S. & Fisher, D. E. 2012. From genes to drugs: targeted strategies for melanoma. *Nat Rev Cancer,* 12**,** 349-61.

Folkman, J. 2002. Role of angiogenesis in tumor growth and metastasis. *Semin Oncol,* 29**,** 15-8.

Foster, D. A., Yellen, P., Xu, L. & Saqcena, M. 2010. Regulation of G1 Cell Cycle Progression: Distinguishing the Restriction Point from a Nutrient-Sensing Cell Growth Checkpoint(s). *Genes Cancer,* 1**,** 1124-31.

Francisco, L. M., Sage, P. T. & Sharpe, A. H. 2010. The PD-1 pathway in tolerance and autoimmunity. *Immunological reviews,* 236**,** 219-42.

Francisco, L. M., Salinas, V. H., Brown, K. E., Vanguri, V. K., Freeman, G. J., Kuchroo, V. K. & Sharpe, A. H. 2009. PD-L1 regulates the development, maintenance, and function of induced regulatory T cells. *J Exp Med,* 206**,** 3015-29.

Frank, N. Y., Margaryan, A., Huang, Y., Schatton, T., Waaga-Gasser, A. M., Gasser, M., Sayegh, M. H., Sadee, W. & Frank, M. H. 2005. ABCB5-mediated doxorubicin transport and chemoresistance in human malignant melanoma. *Cancer Res,* 65**,** 4320-33.

Frank, N. Y., Pendse, S. S., Lapchak, P. H., Margaryan, A., Shlain, D., Doeing, C., Sayegh, M. H. & Frank, M. H. 2003. Regulation of progenitor cell fusion by ABCB5 P-glycoprotein, a novel human ATP-binding cassette transporter. *J Biol Chem,* 278**,** 47156-65.

Frank, N. Y., Schatton, T., Kim, S., Zhan, Q., Wilson, B. J., Ma, J., Saab, K. R., Osherov, V., Widlund, H. R., Gasser, M., Waaga-Gasser, A. M., Kupper, T. S., Murphy, G. F. & Frank, M. H. 2011. VEGFR-1 expressed by malignant melanoma-initiating cells is required for tumor growth. *Cancer Res,* 71**,** 1474-85.

Fraser, C. C., Chen, B. P., Webb, S., van Rooijen, N. & Kraal, G. 1995. Circulation of human hematopoietic cells in severe combined immunodeficient mice after Cl2MDP-liposome-mediated macrophage depletion. *Blood,* 86**,** 183-92.

Frederick, D. T., Piris, A., Cogdill, A. P., Cooper, Z. A., Lezcano, C., Ferrone, C. R., Mitra, D., Boni, A., Newton, L. P., Liu, C., Peng, W., Sullivan, R. J., Lawrence, D. P., Hodi, F. S., Overwijk, W. W., Lizee, G., Murphy, G. F., Hwu, P., Flaherty, K. T., Fisher, D. E. & Wargo, J. A. 2013. BRAF inhibition is associated with enhanced melanoma antigen expression and a more favorable tumor microenvironment in patients with metastatic melanoma. *Clin Cancer Res,* 19**,** 1225-31.

Freeman, G. J., Long, A. J., Iwai, Y., Bourque, K., Chernova, T., Nishimura, H., Fitz, L. J., Malenkovich, N., Okazaki, T., Byrne, M. C., Horton, H. F., Fouser, L., Carter, L., Ling, V., Bowman, M. R., Carreno, B. M., Collins, M., Wood, C. R. & Honjo, T. 2000. Engagement of the PD-1 immunoinhibitory receptor by a novel B7 family member leads to negative regulation of lymphocyte activation. *J Exp Med,* 192**,** 1027-34.
F
rese, K. K. & Tuveson, D. A. 2007. Maximizing mouse cancer models. *Nat Rev Cancer,* 7**,** 645-58.

Fujimoto, N., Nakanishi, G., Kabuto, M., Nakano, T., Eto, H., Nakajima, H., Sano, S. & Tanaka, T. 2015. Merkel cell carcinoma showing regression after biopsy: Evaluation of programmed cell death 1-positive cells. *J Dermatol,* 42**,** 496-9.

Fusi, A., Festino, L., Botti, G., Masucci, G., Melero, I., Lorigan, P. & Ascierto, P. A. 2015. PD-L1 expression as a potential predictive biomarker. *Lancet Oncol,* 16**,** 1285-7.

Gabrilovich, D. I., Ostrand-Rosenberg, S. & Bronte, V. 2012. Coordinated regulation of myeloid cells by tumours. *Nat Rev Immunol,* 12**,** 253-68.

Gambichler, T., Petig, A. L., Stockfleth, E. & Stucker, M. 2016. Expression of SOX10, ABCB5 and CD271 in melanocytic lesions and correlation with survival data of patients with melanoma. *Clin Exp Dermatol,* 41**,** 709-16.

Gandini, S., Sera, F., Cattaruzza, M. S., Pasquini, P., Abeni, D., Boyle, P. & Melchi, C. F. 2005a. Meta-analysis of risk factors for cutaneous melanoma: I. Common and atypical naevi. *Eur J Cancer,* 41**,** 28-44.

Gandini, S., Sera, F., Cattaruzza, M. S., Pasquini, P., Picconi, O., Boyle, P. & Melchi, C. F. 2005b. Meta-analysis of risk factors for cutaneous melanoma: II. Sun exposure. *Eur J Cancer,* 41**,** 45-60.

Gandini, S., Sera, F., Cattaruzza, M. S., Pasquini, P., Zanetti, R., Masini, C., Boyle, P. & Melchi, C. F. 2005c. Meta-analysis of risk factors for cutaneous melanoma: III. Family history, actinic damage and phenotypic factors. *Eur J Cancer,* 41**,** 2040-59.

Garon, E. B., Rizvi, N. A., Hui, R., Leighl, N., Balmanoukian, A. S., Eder, J. P., Patnaik, A., Aggarwal, C., Gubens, M., Horn, L., Carcereny, E., Ahn, M. J., Felip, E., Lee, J. S., Hellmann, M. D., Hamid, O., Goldman, J. W., Soria, J. C., Dolled-Filhart, M., Rutledge,

R. Z., Zhang, J., Lunceford, J. K., Rangwala, R., Lubiniecki, G. M., Roach, C., Emancipator, K., Gandhi, L. & Investigators, K.-. 2015. Pembrolizumab for the treatment of non-small-cell lung cancer. *N Engl J Med,* 372**,** 2018-28.

Gazzaniga, P., Cigna, E., Panasiti, V., Devirgiliis, V., Bottoni, U., Vincenzi, B., Nicolazzo, C., Petracca, A. & Gradilone, A. 2010. CD133 and ABCB5 as stem cell markers on sentinel lymph node from melanoma patients. *European journal of surgical oncology : the journal of the European Society of Surgical Oncology and the British Association of Surgical Oncology,* 36**,** 1211-4.

Goh, G., Walradt, T., Markarov, V., Blom, A., Riaz, N., Doumani, R., Stafstrom, K., Moshiri, A., Yelistratova, L., Levinsohn, J., Chan, T. A., Nghiem, P., Lifton, R. P. & Choi, J. 2015. Mutational landscape of MCPyV-positive and MCPyV-negative merkel cell carcinomas with implications for immunotherapy. *Oncotarget*.

Gottesman, M. M., Fojo, T. & Bates, S. E. 2002. Multidrug resistance in cancer: role of ATP-dependent transporters. *Nat Rev Cancer,* 2**,** 48-58.

Gottesman, M. M., Lavi, O., Hall, M. D. & Gillet, J. P. 2016. Toward a Better Understanding of the Complexity of Cancer Drug Resistance. *Annu Rev Pharmacol Toxicol,* 56**,** 85-102.

Green, K. A., Cook, W. J. & Green, W. R. 2013. Myeloid-derived suppressor cells in murine retrovirus-induced AIDS inhibit T- and B-cell responses in vitro that are used to define the immunodeficiency. *J Virol,* 87**,** 2058-71.

Greenwald, R. J., Freeman, G. J. & Sharpe, A. H. 2005. The B7 family revisited. *Annu Rev Immunol,* 23**,** 515-48.

Grulich, A. E., van Leeuwen, M. T., Falster, M. O. & Vajdic, C. M. 2007. Incidence of cancers in people with HIV/AIDS compared with immunosuppressed transplant recipients: a meta-analysis. *Lancet,* 370**,** 59-67.

Guastafierro, A., Feng, H., Thant, M., Kirkwood, J. M., Chang, Y., Moore, P. S. & Shuda, M. 2013. Characterization of an early passage Merkel cell polyomavirus-positive Merkel cell carcinoma cell line, MS-1, and its growth in NOD scid gamma mice. *Journal of virological methods,* 187**,** 6-14.

Gubin, M. M., Zhang, X., Schuster, H., Caron, E., Ward, J. P., Noguchi, T., Ivanova, Y., Hundal, J., Arthur, C. D., Krebber, W. J., Mulder, G. E., Toebes, M., Vesely, M. D., Lam, S. S., Korman, A. J., Allison, J. P., Freeman, G. J., Sharpe, A. H., Pearce, E. L., Schumacher, T. N., Aebersold, R., Rammensee, H. G., Melief, C. J., Mardis, E. R., Gillanders, W. E., Artyomov, M. N. & Schreiber, R. D. 2014. Checkpoint blockade cancer immunotherapy targets tumour-specific mutant antigens. *Nature,* 515**,** 577-81.

Gupta, P. B., Chaffer, C. L. & Weinberg, R. A. 2009. Cancer stem cells: mirage or reality? *Nat Med,* 15**,** 1010-2.

Habicht, A., Dada, S., Jurewicz, M., Fife, B. T., Yagita, H., Azuma, M., Sayegh, M. H. & Guleria, I. 2007. A link between PDL1 and T regulatory cells in fetomaternal tolerance. *J Immunol,* 179**,** 5211-9.

Hamburger, A. W. & Salmon, S. E. 1977. Primary bioassay of human tumor stem cells. *Science,* 197**,** 461-3.

Hamid, O., Robert, C., Daud, A., Hodi, F. S., Hwu, W. J., Kefford, R., Wolchok, J. D., Hersey, P., Joseph, R. W., Weber, J. S., Dronca, R., Gangadhar, T. C., Patnaik, A., Zarour, H., Joshua, A. M., Gergich, K., Elassaiss-Schaap, J., Algazi, A., Mateus, C., Boasberg, P., Tumeh, P. C., Chmielowski, B., Ebbinghaus, S. W., Li, X. N., Kang, S. P. & Ribas, A. 2013. Safety and tumor responses with lambrolizumab (anti-PD-1) in melanoma. *N Engl J Med,* 369**,** 134-44.

Hanahan, D. & Weinberg, R. A. 2011. Hallmarks of cancer: the next generation. *Cell,* 144**,** 646-74.

Harms, P. W., Vats, P., Verhaegen, M. E., Robinson, D. R., Wu, Y. M., Dhanasekaran, S. M., Palanisamy, N., Siddiqui, J., Cao, X., Su, F., Wang, R., Xiao, H., Kunju, L. P., Mehra, R., Tomlins, S. A., Fullen, D. R., Bichakjian, C. K., Johnson, T. M., Dlugosz, A. A. & Chinnaiyan, A. M. 2015. The Distinctive Mutational Spectra of Polyomavirus-Negative Merkel Cell Carcinoma. *Cancer Res,* 75**,** 3720-7.

Heath, M., Jaimes, N., Lemos, B., Mostaghimi, A., Wang, L. C., Penas, P. F. & Nghiem, P. 2008. Clinical characteristics of Merkel cell carcinoma at diagnosis in 195 patients: the AEIOU features. *J Am Acad Dermatol,* 58**,** 375-81.

Helmbach, H., Sinha, P. & Schadendorf, D. 2003. Human melanoma: drug resistance. *Recent Results Cancer Res,* 161**,** 93-110.

Herbst, R. S., Soria, J. C., Kowanetz, M., Fine, G. D., Hamid, O., Gordon, M. S., Sosman, J. A., McDermott, D. F., Powderly, J. D., Gettinger, S. N., Kohrt, H. E., Horn, L., Lawrence, D. P., Rost, S., Leabman, M., Xiao, Y., Mokatrin, A., Koeppen, H., Hegde, P. S., Mellman, I., Chen, D. S. & Hodi, F. S. 2014. Predictive correlates of response to the anti-PD-L1 antibody MPDL3280A in cancer patients. *Nature,* 515**,** 563-7.

Hidalgo, M., Amant, F., Biankin, A. V., Budinska, E., Byrne, A. T., Caldas, C., Clarke, R. B., de Jong, S., Jonkers, J., Maelandsmo, G. M., Roman-Roman, S., Seoane, J., Trusolino, L. & Villanueva, A. 2014. Patient-derived xenograft models: an emerging platform for translational cancer research. *Cancer Discov,* 4**,** 998-1013.

Highfill, S. L., Cui, Y., Giles, A. J., Smith, J. P., Zhang, H., Morse, E., Kaplan, R. N. & Mackall, C. L. 2014. Disruption of CXCR2-mediated MDSC tumor trafficking enhances anti-PD1 efficacy. *Sci Transl Med,* 6**,** 237ra67.

Hildeman, D. A., Mitchell, T., Kappler, J. & Marrack, P. 2003. T cell apoptosis and reactive oxygen species. *J Clin Invest,* 111**,** 575-81.

Hillen, F., Baeten, C. I., van de Winkel, A., Creytens, D., van der Schaft, D. W., Winnepenninckx, V. & Griffioen, A. W. 2008. Leukocyte infiltration and tumor cell plasticity are parameters of aggressiveness in primary cutaneous melanoma. *Cancer Immunol Immunother,* 57**,** 97-106.

Ho, P. C., Bihuniak, J. D., Macintyre, A. N., Staron, M., Liu, X., Amezquita, R., Tsui, Y. C., Cui, G., Micevic, G., Perales, J. C., Kleinstein, S. H., Abel, E. D., Insogna, K. L., Feske, S., Locasale, J. W., Bosenberg, M. W., Rathmell, J. C. & Kaech, S. M. 2015. Phosphoenolpyruvate Is a Metabolic Checkpoint of Anti-tumor T Cell Responses. *Cell,* 162**,** 1217-28.

Hodgson, N. C. 2005. Merkel cell carcinoma: changing incidence trends. *J Surg Oncol,* 89**,** 1-4.

Hodi, F. S., Butler, M., Oble, D. A., Seiden, M. V., Haluska, F. G., Kruse, A., Macrae, S., Nelson, M., Canning, C., Lowy, I., Korman, A., Lautz, D., Russell, S., Jaklitsch, M. T., Ramaiya, N., Chen, T. C., Neuberg, D., Allison, J. P., Mihm, M. C. & Dranoff, G. 2008. Immunologic and clinical effects of antibody blockade of cytotoxic T lymphocyte-associated antigen 4 in previously vaccinated cancer patients. *Proc Natl Acad Sci U S A,* 105**,** 3005-10.

Hodi, F. S., O'Day, S. J., McDermott, D. F., Weber, R. W., Sosman, J. A., Haanen, J. B., Gonzalez, R., Robert, C., Schadendorf, D., Hassel, J. C., Akerley, W., van den Eertwegh, A. J., Lutzky, J., Lorigan, P., Vaubel, J. M., Linette, G. P., Hogg, D., Ottensmeier, C. H., Lebbe, C., Peschel, C., Quirt, I., Clark, J. I., Wolchok, J. D., Weber, J. S., Tian, J., Yellin, M. J., Nichol, G. M., Hoos, A. & Urba, W. J. 2010. Improved survival with ipilimumab in patients with metastatic melanoma. *N Engl J Med,* 363**,** 711-23.

Hogquist, K. A., Jameson, S. C., Heath, W. R., Howard, J. L., Bevan, M. J. & Carbone, F. R. 1994. T cell receptor antagonist peptides induce positive selection. *Cell,* 76**,** 17-27.

Houben, R., Shuda, M., Weinkam, R., Schrama, D., Feng, H., Chang, Y., Moore, P. S. & Becker, J. C. 2010. Merkel cell polyomavirus-infected Merkel cell carcinoma cells require expression of viral T antigens. *J Virol,* 84**,** 7064-72.

Housman, G., Byler, S., Heerboth, S., Lapinska, K., Longacre, M., Snyder, N. & Sarkar, S. 2014. Drug resistance in cancer: an overview. *Cancers (Basel),* 6**,** 1769-92.

Howlader, N. N., A.M.; Krapcho, M.; Miller, D.; Bishop, K.; Altekruse, S.F.; Kosary, C.L.; Yu, M.; Ruhl, J.; Tatalovich, Z.; Mariotto, A.; Lewis, D.R.; Chen, H.S.; Feuer, E.J.; Cronin, K.A. 2016. SEER Cancer Statistics Review, 1975-2013.

Huang, S. K., Okamoto, T., Morton, D. L. & Hoon, D. S. 1998. Antibody responses to melanoma/melanocyte autoantigens in melanoma patients. *J Invest Dermatol,* 111**,** 662-7.

Huang, X., Venet, F., Wang, Y. L., Lepape, A., Yuan, Z., Chen, Y., Swan, R., Kherouf, H., Monneret, G., Chung, C. S. & Ayala, A. 2009. PD-1 expression by macrophages plays a pathologic role in altering microbial clearance and the innate inflammatory response to sepsis. *Proc Natl Acad Sci U S A,* 106**,** 6303-8.

Huang, Y., Anderle, P., Bussey, K. J., Barbacioru, C., Shankavaram, U., Dai, Z., Reinhold, W. C., Papp, A., Weinstein, J. N. & Sadee, W. 2004. Membrane transporters and channels: role of the transportome in cancer chemosensitivity and chemoresistance. *Cancer Res,* 64**,** 4294-301.

Hugo, W., Zaretsky, J. M., Sun, L., Song, C., Moreno, B. H., Hu-Lieskovan, S., Berent-Maoz, B., Pang, J., Chmielowski, B., Cherry, G., Seja, E., Lomeli, S., Kong, X., Kelley, M. C., Sosman, J. A., Johnson, D. B., Ribas, A. & Lo, R. S. 2016. Genomic and Transcriptomic Features of Response to Anti-PD-1 Therapy in Metastatic Melanoma. *Cell,* 165**,** 35-44.

Ibrani, D. I., JG.;Vendeven,N.;Miller,N.;Afanasiev,O.;Koelle,D.;Nghiem,P.; 2015. Identifying Merkel polyomavirus-specific CD4+ and CD8+ T-cells in Merkel cell carcinoma patients' tumor-infiltrating lymphocytes. *J Invest Dermatol*.

Iyer, J. G., Afanasiev, O. K., McClurkan, C., Paulson, K., Nagase, K., Jing, L., Marshak, J. O., Dong, L., Carter, J., Lai, I., Farrar, E., Byrd, D., Galloway, D., Yee, C., Koelle, D. M. & Nghiem, P. 2011. Merkel cell polyomavirus-specific CD8(+) and CD4(+) T-cell responses identified in Merkel cell carcinomas and blood. *Clin Cancer Res,* 17**,** 6671-80.

Jacobs, J. F., Nierkens, S., Figdor, C. G., de Vries, I. J. & Adema, G. J. 2012. Regulatory T cells in melanoma: the final hurdle towards effective immunotherapy? *Lancet Oncol,* 13**,** e32-42.

Jaeger, B. N., Donadieu, J., Cognet, C., Bernat, C., Ordonez-Rueda, D., Barlogis, V., Mahlaoui, N., Fenis, A., Narni-Mancinelli, E., Beaupain, B., Bellanne-Chantelot, C., Bajenoff, M., Malissen, B., Malissen, M., Vivier, E. & Ugolini, S. 2012. Neutrophil depletion impairs natural killer cell maturation, function, and homeostasis. *J Exp Med,* 209**,** 565-80.

Jamieson, C. H., Ailles, L. E., Dylla, S. J., Muijtjens, M., Jones, C., Zehnder, J. L., Gotlib, J., Li, K., Manz, M. G., Keating, A., Sawyers, C. L. & Weissman, I. L. 2004. Granulocyte-

macrophage progenitors as candidate leukemic stem cells in blast-crisis CML. *N Engl J Med,* 351**,** 657-67.

Jandus, C., Bioley, G., Speiser, D. E. & Romero, P. 2008. Selective accumulation of differentiated FOXP3(+) CD4 (+) T cells in metastatic tumor lesions from melanoma patients compared to peripheral blood. *Cancer Immunol Immunother,* 57**,** 1795-805.

Jiang, X., Zhou, J., Giobbie-Hurder, A., Wargo, J. & Hodi, F. S. 2013a. The activation of MAPK in melanoma cells resistant to BRAF inhibition promotes PD-L1 expression that is reversible by MEK and PI3K inhibition. *Clin Cancer Res,* 19**,** 598-609.

Jiang, X., Zhou, J., Giobbie-Hurder, A., Wargo, J. & Hodi, F. S. 2013b. The activation of MAPK in melanoma cells resistant to BRAF inhibition promotes PD-L1 expression that is reversible by MEK and PI3K inhibition. *Clin Cancer Res,* 19**,** 598-609.

Johnson, D. B., Estrada, M. V., Salgado, R., Sanchez, V., Doxie, D. B., Opalenik, S. R., Vilgelm, A. E., Feld, E., Johnson, A. S., Greenplate, A. R., Sanders, M. E., Lovly, C. M., Frederick, D. T., Kelley, M. C., Richmond, A., Irish, J. M., Shyr, Y., Sullivan, R. J., Puzanov, I., Sosman, J. A. & Balko, J. M. 2016a. Melanoma-specific MHC-II expression represents a tumour-autonomous phenotype and predicts response to anti-PD-1/PD-L1 therapy. *Nat Commun,* 7**,** 10582.

Johnson, D. B., Frampton, G. M., Rioth, M. J., Yusko, E., Xu, Y., Guo, X., Ennis, R. C., Fabrizio, D., Chalmers, Z. R., Greenbowe, J., Ali, S. M., Balasubramanian, S., Sun, J. X., He, Y., Frederick, D. T., Puzanov, I., Balko, J. M., Cates, J. M., Ross, J. S., Sanders, C., Robins, H., Shyr, Y., Miller, V., Stephens, P. J., Sullivan, R. J., Sosman, J. A. & Lovly, C. M. 2016b. Targeted next generation sequencing identifies markers of response to PD-1 blockade. *Cancer Immunol Res*.

Jordan, C. T. 2009. Cancer stem cells: controversial or just misunderstood? *Cell Stem Cell,* 4**,** 203-5.

Jordan, K. R., Amaria, R. N., Ramirez, O., Callihan, E. B., Gao, D., Borakove, M., Manthey, E., Borges, V. F. & McCarter, M. D. 2013. Myeloid-derived suppressor cells are associated with disease progression and decreased overall survival in advanced-stage melanoma patients. *Cancer Immunol Immunother,* 62**,** 1711-22.

Kabbarah, O. & Chin, L. 2006. Advances in malignant melanoma: genetic insights from mouse and man. *Front Biosci,* 11**,** 928-42.

Kakavand, H., Vilain, R. E., Wilmott, J. S., Burke, H., Yearley, J. H., Thompson, J. F., Hersey, P., Long, G. V. & Scolyer, R. A. 2015. Tumor PD-L1 expression, immune cell correlates and PD-1+ lymphocytes in sentinel lymph node melanoma metastases. *Mod Pathol,* 28**,** 1535-44.

Kalialis, L. V., Drzewiecki, K. T. & Klyver, H. 2009. Spontaneous regression of metastases from melanoma: review of the literature. *Melanoma Res,* 19**,** 275-82.

Kannan, A., Lin, Z., Shao, Q., Zhao, S., Fang, B., Moreno, M. A., Vural, E., Stack, B. C., Jr., Suen, J. Y., Kannan, K. & Gao, L. 2015. Dual mTOR inhibitor MLN0128 suppresses Merkel cell carcinoma (MCC) xenograft tumor growth. *Oncotarget*.

Karyampudi, L., Lamichhane, P., Krempski, J., Kalli, K. R., Behrens, M. D., Vargas, D. M., Hartmann, L. C., Janco, J. M., Dong, H., Hedin, K. E., Dietz, A. B., Goode, E. L. & Knutson, K. L. 2016. PD-1 Blunts the Function of Ovarian Tumor-Infiltrating Dendritic Cells by Inactivating NF-kappaB. *Cancer Res,* 76**,** 239-50.

Kaufman, H. L., Russell, J., Hamid, O., Bhatia, S., Terheyden, P., D'Angelo, S. P., Shih, K. C., Lebbe, C., Linette, G. P., Milella, M., Brownell, I., Lewis, K. D., Lorch, J. H., Chin, K., Mahnke, L., von Heydebreck, A., Cuillerot, J. M. & Nghiem, P. 2016. Avelumab in patients with chemotherapy-refractory metastatic Merkel cell carcinoma: a multicentre, single-group, open-label, phase 2 trial. *Lancet Oncol*.

Kawakami, Y., Robbins, P. F. & Rosenberg, S. A. 1996. Human melanoma antigens recognized by T lymphocytes. *Keio J Med,* 45**,** 100-8.

Keir, M. E., Butte, M. J., Freeman, G. J. & Sharpe, A. H. 2008. PD-1 and its ligands in tolerance and immunity. *Annu Rev Immunol,* 26**,** 677-704.

Keir, M. E., Liang, S. C., Guleria, I., Latchman, Y. E., Qipo, A., Albacker, L. A., Koulmanda, M., Freeman, G. J., Sayegh, M. H. & Sharpe, A. H. 2006. Tissue expression of PD-L1 mediates peripheral T cell tolerance. *J Exp Med,* 203**,** 883-95.

Kerbel, R. S. 2008. Tumor angiogenesis. *N Engl J Med,* 358**,** 2039-49.

Kershaw, M. H., Westwood, J. A. & Darcy, P. K. 2013. Gene-engineered T cells for cancer therapy. *Nat Rev Cancer,* 13**,** 525-41.

Khalili, J. S., Liu, S., Rodriguez-Cruz, T. G., Whittington, M., Wardell, S., Liu, C., Zhang, M., Cooper, Z. A., Frederick, D. T., Li, Y., Zhang, M., Joseph, R. W., Bernatchez, C., Ekmekcioglu, S., Grimm, E., Radvanyi, L. G., Davis, R. E., Davies, M. A., Wargo, J. A., Hwu, P. & Lizee, G. 2012. Oncogenic BRAF(V600E) promotes stromal cell-mediated immunosuppression via induction of interleukin-1 in melanoma. *Clin Cancer Res,* 18**,** 5329-40.

Khan, A. R., Hams, E., Floudas, A., Sparwasser, T., Weaver, C. T. & Fallon, P. G. 2015. PD-L1hi B cells are critical regulators of humoral immunity. *Nat Commun,* 6**,** 5997.

Khavari, P. A. 2006. Modelling cancer in human skin tissue. *Nat Rev Cancer,* 6**,** 270-80.

Khong, H. T., Wang, Q. J. & Rosenberg, S. A. 2004. Identification of multiple antigens recognized by tumor-infiltrating lymphocytes from a single patient: tumor escape by antigen loss and loss of MHC expression. *J Immunother,* 27**,** 184-90.

Kitano, S., Tsuji, T., Liu, C., Hirschhorn-Cymerman, D., Kyi, C., Mu, Z., Allison, J. P., Gnjatic, S., Yuan, J. D. & Wolchok, J. D. 2013. Enhancement of tumor-reactive cytotoxic CD4+ T cell responses after ipilimumab treatment in four advanced melanoma patients. *Cancer Immunol Res,* 1**,** 235-44.

Kleffel, S., Lee, N., Lezcano, C., Wilson, B. J., Sobolewski, K., Saab, K. R., Mueller, H., Zhan, Q., Posch, C., Elco, C. P., DoRosario, A., Garcia, S. S., Thakuria, M., Wang, Y. E., Wang, L. C., Murphy, G. F., Frank, M. H. & Schatton, T. 2016. ABCB5-targeted chemoresistance reversal inhibits Merkel cell carcinoma growth. *J Invest Dermatol*.

Kleffel, S., Posch, C., Barthel, S. R., Mueller, H., Schlapbach, C., Guenova, E., Elco, C. P., Lee, N., Juneja, V. R., Zhan, Q., Lian, C. G., Thomi, R., Hoetzenecker, W., Cozzio, A., Dummer, R., Mihm, M. C., Jr., Flaherty, K. T., Frank, M. H., Murphy, G. F., Sharpe, A. H., Kupper, T. S. & Schatton, T. 2015. Melanoma Cell-Intrinsic PD-1 Receptor Functions Promote Tumor Growth. *Cell,* 162**,** 1242-56.

Klijn, C., Durinck, S., Stawiski, E. W., Haverty, P. M., Jiang, Z., Liu, H., Degenhardt, J., Mayba, O., Gnad, F., Liu, J., Pau, G., Reeder, J., Cao, Y., Mukhyala, K., Selvaraj, S. K., Yu, M., Zynda, G. J., Brauer, M. J., Wu, T. D., Gentleman, R. C., Manning, G., Yauch, R. L., Bourgon, R., Stokoe, D., Modrusan, Z., Neve, R. M., de Sauvage, F. J., Settleman, J., Seshagiri, S. & Zhang, Z. 2015. A comprehensive transcriptional portrait of human cancer cell lines. *Nat Biotechnol,* 33**,** 306-12.

Krempski, J., Karyampudi, L., Behrens, M. D., Erskine, C. L., Hartmann, L., Dong, H., Goode, E. L., Kalli, K. R. & Knutson, K. L. 2011. Tumor-infiltrating programmed death receptor-1+ dendritic cells mediate immune suppression in ovarian cancer. *J Immunol,* 186**,** 6905-13.

Krivtsov, A. V., Twomey, D., Feng, Z., Stubbs, M. C., Wang, Y., Faber, J., Levine, J. E., Wang, J., Hahn, W. C., Gilliland, D. G., Golub, T. R. & Armstrong, S. A. 2006. Transformation from committed progenitor to leukaemia stem cell initiated by MLL-AF9. *Nature,* 442**,** 818-22.

Kruper, L. L., Spitz, F. R., Czerniecki, B. J., Fraker, D. L., Blackwood-Chirchir, A., Ming, M. E., Elder, D. E., Elenitsas, R., Guerry, D. & Gimotty, P. A. 2006. Predicting sentinel node status in AJCC stage I/II primary cutaneous melanoma. *Cancer,* 107**,** 2436-45.

Krupnick, A. S., Gelman, A. E., Barchet, W., Richardson, S., Kreisel, F. H., Turka, L. A., Colonna, M., Patterson, G. A. & Kreisel, D. 2005. Murine vascular endothelium activates and induces the generation of allogeneic CD4+25+Foxp3+ regulatory T cells. *J Immunol,* 175**,** 6265-70.

Ksander, B. R., Kolovou, P. E., Wilson, B. J., Saab, K. R., Guo, Q., Ma, J., McGuire, S. P., Gregory, M. S., Vincent, W. J., Perez, V. L., Cruz-Guilloty, F., Kao, W. W., Call, M. K., Tucker, B. A., Zhan, Q., Murphy, G. F., Lathrop, K. L., Alt, C., Mortensen, L. J., Lin, C. P., Zieske, J. D., Frank, M. H. & Frank, N. Y. 2014. ABCB5 is a limbal stem cell gene required for corneal development and repair. *Nature,* 511**,** 353-7.

Kumar, R., Angelini, S. & Hemminki, K. 2003. Activating BRAF and N-Ras mutations in sporadic primary melanomas: an inverse association with allelic loss on chromosome 9. *Oncogene,* 22**,** 9217-24.

Kumar, V., Patel, S., Tcyganov, E. & Gabrilovich, D. I. 2016. The Nature of Myeloid-Derived Suppressor Cells in the Tumor Microenvironment. *Trends Immunol,* 37**,** 208-20.

Kupas, V., Weishaupt, C., Siepmann, D., Kaserer, M. L., Eickelmann, M., Metze, D., Luger, T. A., Beissert, S. & Loser, K. 2011. RANK is expressed in metastatic melanoma and highly upregulated on melanoma-initiating cells. *J Invest Dermatol,* 131**,** 944-55.

Ladanyi, A., Somlai, B., Gilde, K., Fejos, Z., Gaudi, I. & Timar, J. 2004. T-cell activation marker expression on tumor-infiltrating lymphocytes as prognostic factor in cutaneous malignant melanoma. *Clin Cancer Res,* 10**,** 521-30.

Larkin, J., Chiarion-Sileni, V., Gonzalez, R., Grob, J. J., Cowey, C. L., Lao, C. D., Schadendorf, D., Dummer, R., Smylie, M., Rutkowski, P., Ferrucci, P. F., Hill, A., Wagstaff, J., Carlino, M. S., Haanen, J. B., Maio, M., Marquez-Rodas, I., McArthur, G. A., Ascierto, P. A., Long, G. V., Callahan, M. K., Postow, M. A., Grossmann, K., Sznol, M., Dreno, B., Bastholt, L., Yang, A., Rollin, L. M., Horak, C., Hodi, F. S. & Wolchok, J. D. 2015. Combined Nivolumab and Ipilimumab or Monotherapy in Untreated Melanoma. *N Engl J Med,* 373**,** 23-34.

Larsen, T. E. & Grude, T. H. 1978. A retrospective histological study of 669 cases of primary cutaneous malignant melanoma in clinical stage I. I. Histological classification, sex and age of the patients, localization of tumour and prognosis. *Acta Pathol Microbiol Scand A,* 86A**,** 437-50.

Lastwika, K. J., Wilson, W., 3rd, Li, Q. K., Norris, J., Xu, H., Ghazarian, S. R., Kitagawa, H., Kawabata, S., Taube, J. M., Yao, S., Liu, L. N., Gills, J. J. & Dennis, P. A. 2016. Control of PD-L1 Expression by Oncogenic Activation of the AKT-mTOR Pathway in Non-Small Cell Lung Cancer. *Cancer Res,* 76**,** 227-38.

Latchman, Y., Wood, C. R., Chernova, T., Chaudhary, D., Borde, M., Chernova, I., Iwai, Y., Long, A. J., Brown, J. A., Nunes, R., Greenfield, E. A., Bourque, K., Boussiotis, V. A., Carter, L. L., Carreno, B. M., Malenkovich, N., Nishimura, H., Okazaki, T., Honjo, T., Sharpe, A. H. & Freeman, G. J. 2001. PD-L2 is a second ligand for PD-1 and inhibits T cell activation. *Nat Immunol,* 2**,** 261-8.

Latchman, Y. E., Liang, S. C., Wu, Y., Chernova, T., Sobel, R. A., Klemm, M., Kuchroo, V. K., Freeman, G. J. & Sharpe, A. H. 2004. PD-L1-deficient mice show that PD-L1 on T cells, antigen-presenting cells, and host tissues negatively regulates T cells. *Proc Natl Acad Sci U S A,* 101**,** 10691-6.

Lathia, J. D., Gallagher, J., Myers, J. T., Li, M., Vasanji, A., McLendon, R. E., Hjelmeland, A. B., Huang, A. Y. & Rich, J. N. 2011. Direct in vivo evidence for tumor propagation by glioblastoma cancer stem cells. *PLoS One,* 6**,** e24807.

Le Magnen, C., Dutta, A. & Abate-Shen, C. 2016. Optimizing mouse models for precision cancer prevention. *Nat Rev Cancer,* 16**,** 187-96.

Lee, J. R., Bechstein, D. J., Ooi, C. C., Patel, A., Gaster, R. S., Ng, E., Gonzalez, L. C. & Wang, S. X. 2016a. Magneto-nanosensor platform for probing low-affinity protein-protein interactions and identification of a low-affinity PD-L1/PD-L2 interaction. *Nat Commun,* 7**,** 12220.

Lee, N., Zakka, L. R., Mihm, M. C., Jr. & Schatton, T. 2016b. Tumour-infiltrating lymphocytes in melanoma prognosis and cancer immunotherapy. *Pathology,* 48**,** 177-87.
Lei, G. S., Zhang, C. & Lee, C. H. 2015. Myeloid-derived suppressor cells impair alveolar macrophages through PD-1 receptor ligation during Pneumocystis pneumonia. *Infect Immun,* 83**,** 572-82.

Lemos, B. D., Storer, B. E., Iyer, J. G., Phillips, J. L., Bichakjian, C. K., Fang, L. C., Johnson, T. M., Liegeois-Kwon, N. J., Otley, C. C., Paulson, K. G., Ross, M. I., Yu, S. S., Zeitouni, N. C., Byrd, D. R., Sondak, V. K., Gershenwald, J. E., Sober, A. J. & Nghiem, P. 2010. Pathologic nodal evaluation improves prognostic accuracy in Merkel cell carcinoma: analysis of 5823 cases as the basis of the first consensus staging system. *J Am Acad Dermatol,* 63**,** 751-61.

Lezcano, C., Kleffel, S., Lee, N., Larson, A. R., Zhan, Q., DoRosario, A., Wang, L. C., Schatton, T. & Murphy, G. F. 2014. Merkel cell carcinoma expresses vasculogenic mimicry: demonstration in patients and experimental manipulation in xenografts. *Lab Invest*.

Li, C. W., Lim, S. O., Xia, W., Lee, H. H., Chan, L. C., Kuo, C. W., Khoo, K. H., Chang, S. S., Cha, J. H., Kim, T., Hsu, J. L., Wu, Y., Hsu, J. M., Yamaguchi, H., Ding, Q., Wang, Y., Yao, J., Lee, C. C., Wu, H. J., Sahin, A. A., Allison, J. P., Yu, D., Hortobagyi, G. N. & Hung, M. C. 2016. Glycosylation and stabilization of programmed death ligand-1 suppresses T-cell activity. *Nat Commun,* 7**,** 12632.

Lin, J. Y., Zhang, M., Schatton, T., Wilson, B. J., Alloo, A., Ma, J., Qureshi, A. A., Frank, N. Y., Han, J. & Frank, M. H. 2013. Genetically determined ABCB5 functionality correlates with pigmentation phenotype and melanoma risk. *Biochem Biophys Res Commun*.

Lin, Z., McDermott, A., Shao, L., Kannan, A., Morgan, M., Stack, B. C., Jr., Moreno, M., Davis, D. A., Cornelius, L. A. & Gao, L. 2014. Chronic mTOR activation promotes cell survival in Merkel cell carcinoma. *Cancer Lett,* 344**,** 272-81.

Lipson, E. J., Vincent, J. G., Loyo, M., Kagohara, L. T., Luber, B. S., Wang, H., Xu, H., Nayar, S. K., Wang, T. S., Sidransky, D., Anders, R. A., Topalian, S. L. & Taube, J. M. 2013. PD-L1 expression in the Merkel cell carcinoma microenvironment: association with inflammation, Merkel cell polyomavirus and overall survival. *Cancer Immunol Res,* 1**,** 54-63.

Liu, K. W., Feng, H., Bachoo, R., Kazlauskas, A., Smith, E. M., Symes, K., Hamilton, R. L., Nagane, M., Nishikawa, R., Hu, B. & Cheng, S. Y. 2011. SHP-2/PTPN11 mediates gliomagenesis driven by PDGFRA and INK4A/ARF aberrations in mice and humans. *J Clin Invest,* 121**,** 905-17.

Lorvik, K. B., Hammarstrom, C., Fauskanger, M., Haabeth, O. A., Zangani, M., Haraldsen, G., Bogen, B. & Corthay, A. 2016. Adoptive transfer of tumor-specific Th2 cells eradicates tumors by triggering an in situ inflammatory immune response. *Cancer Res*.

Lutz, N. W., Banerjee, P., Wilson, B. J., Ma, J., Cozzone, P. J. & Frank, M. H. 2016. Expression of Cell-Surface Marker ABCB5 Causes Characteristic Modifications of Glucose, Amino Acid and Phospholipid Metabolism in the G3361 Melanoma-Initiating Cell Line. *PLoS One,* 11**,** e0161803.

Ma, J., Lin, J. Y., Alloo, A., Wilson, B. J., Schatton, T., Zhan, Q., Murphy, G. F., Waaga-Gasser, A. M., Gasser, M., Stephen Hodi, F., Frank, N. Y. & Frank, M. H. 2010. Isolation of tumorigenic circulating melanoma cells. *Biochem Biophys Res Commun,* 402**,** 711-7.

MacKie, R. M., Reid, R. & Junor, B. 2003. Fatal melanoma transferred in a donated kidney 16 years after melanoma surgery. *N Engl J Med,* 348**,** 567-8.

Maeurer, M. J., Gollin, S. M., Martin, D., Swaney, W., Bryant, J., Castelli, C., Robbins, P., Parmiani, G., Storkus, W. J. & Lotze, M. T. 1996. Tumor escape from immune recognition: lethal recurrent melanoma in a patient associated with downregulation of the peptide transporter protein TAP-1 and loss of expression of the immunodominant MART-1/Melan-A antigen. *J Clin Invest,* 98**,** 1633-41.

Mahoney, K. M., Rennert, P. D. & Freeman, G. J. 2015. Combination cancer immunotherapy and new immunomodulatory targets. *Nat Rev Drug Discov,* 14**,** 561-84.

Malhotra, V. & Perry, M. C. 2003. Classical chemotherapy: mechanisms, toxicities and the therapeutic window. *Cancer Biol Ther,* 2**,** S2-4.

Mandai, M., Hamanishi, J., Abiko, K., Matsumura, N., Baba, T. & Konishi, I. 2016. Dual faces of IFN-gamma in cancer progression: a role of PD-L1 induction in the determination of pro- and anti-tumor immunity. *Clin Cancer Res*.

Mantripragada, K. & Birnbaum, A. 2015. Response to Anti-PD-1 Therapy in Metastatic Merkel Cell Carcinoma Metastatic to the Heart and Pancreas. *Cureus,* 7**,** e403.

Massi, D., Brusa, D., Merelli, B., Ciano, M., Audrito, V., Serra, S., Buonincontri, R., Baroni, G., Nassini, R., Minocci, D., Cattaneo, L., Tamborini, E., Carobbio, A., Rulli, E., Deaglio, S. & Mandala, M. 2014. PD-L1 marks a subset of melanomas with a shorter overall survival and distinct genetic and morphological characteristics. *Ann Oncol,* 25**,** 2433-42.

Melnikova, V. O., Bolshakov, S. V., Walker, C. & Ananthaswamy, H. N. 2004. Genomic alterations in spontaneous and carcinogen-induced murine melanoma cell lines. *Oncogene,* 23**,** 2347-56.

Menzies, A. M., Johnson, D. B., Ramanujam, S., Atkinson, V. G., Wong, A. N., Park, J. J., McQuade, J. L., Shoushtari, A. N., Tsai, K. K., Eroglu, Z., Klein, O., Hassel, J. C., Sosman, J. A., Guminski, A., Sullivan, R. J., Ribas, A., Carlino, M. S., Davies, M. A., Sandhu, S. K. & Long, G. V. 2016. Anti-PD-1 therapy in patients with advanced melanoma and preexisting autoimmune disorders or major toxicity with ipilimumab. *Ann Oncol*.

Michor, F., Iwasa, Y. & Nowak, M. A. 2004. Dynamics of cancer progression. *Nat Rev Cancer,* 4**,** 197-205.

Mihm, M. C., Jr., Clemente, C. G. & Cascinelli, N. 1996. Tumor infiltrating lymphocytes in lymph node melanoma metastases: a histopathologic prognostic indicator and an expression of local immune response. *Lab Invest,* 74**,** 43-7.

Mittal, D., Gubin, M. M., Schreiber, R. D. & Smyth, M. J. 2014. New insights into cancer immunoediting and its three component phases--elimination, equilibrium and escape. *Curr Opin Immunol,* 27**,** 16-25.

Mogha, A., Fautrel, A., Mouchet, N., Guo, N., Corre, S., Adamski, H., Watier, E., Misery, L. & Galibert, M. D. 2010. Merkel cell polyomavirus small T antigen mRNA level is increased following in vivo UV-radiation. *PLoS One,* 5**,** e11423.

Morrison, K. M., Miesegaes, G. R., Lumpkin, E. A. & Maricich, S. M. 2009. Mammalian Merkel cells are descended from the epidermal lineage. *Dev Biol,* 336**,** 76-83.

Morrison, S. J. & Kimble, J. 2006. Asymmetric and symmetric stem-cell divisions in development and cancer. *Nature,* 441**,** 1068-74.

Moshiri, A. S. & Nghiem, P. 2014. Milestones in the staging, classification, and biology of Merkel cell carcinoma. *J Natl Compr Canc Netw,* 12**,** 1255-62.

Motzer, R. J., Escudier, B., McDermott, D. F., George, S., Hammers, H. J., Srinivas, S., Tykodi, S. S., Sosman, J. A., Procopio, G., Plimack, E. R., Castellano, D., Choueiri, T. K., Gurney, H., Donskov, F., Bono, P., Wagstaff, J., Gauler, T. C., Ueda, T., Tomita, Y., Schutz, F. A., Kollmannsberger, C., Larkin, J., Ravaud, A., Simon, J. S., Xu, L. A., Waxman, I. M., Sharma, P. & CheckMate, I. 2015. Nivolumab versus Everolimus in Advanced Renal-Cell Carcinoma. *N Engl J Med,* 373**,** 1803-13.

Mueller, M. M. & Fusenig, N. E. 2004. Friends or foes - bipolar effects of the tumour stroma in cancer. *Nat Rev Cancer,* 4**,** 839-49.

Nagaraj, S., Youn, J. I. & Gabrilovich, D. I. 2013. Reciprocal relationship between myeloid-derived suppressor cells and T cells. *J Immunol,* 191**,** 17-23.

Nardi, V., Song, Y., Santamaria-Barria, J. A., Cosper, A. K., Lam, Q., Faber, A. C., Boland, G. M., Yeap, B. Y., Bergethon, K., Scialabba, V. L., Tsao, H., Settleman, J., Ryan, D. P., Borger, D. R., Bhan, A. K., Hoang, M. P., Iafrate, A. J., Cusack, J. C., Engelman, J. A. & Dias-Santagata, D. 2012. Activation of PI3K signaling in Merkel cell carcinoma. *Clin Cancer Res,* 18**,** 1227-36.

Nghiem, P. B., S.; Daud,A.; Friedlander, P.; Kluger,H.; Kohrt,H.; Kudchadkar, R.; Lipson,E.; Lundgren,L.; Margolin,K.; Reddy,S.; Shantha, E.; Sharfman, W.; Sharon,E.; Thompson, J.; Topalian, S; Cheever,M. 2015. Activity of PD-1 blockade with pembrolizumab as first systemic therapy in patients with advanced Merkel cell carcinoma.

Nghiem, P. T., Bhatia, S., Lipson, E. J., Kudchadkar, R. R., Miller, N. J., Annamalai, L., Berry, S., Chartash, E. K., Daud, A., Fling, S. P., Friedlander, P. A., Kluger, H. M., Kohrt, H. E., Lundgren, L., Margolin, K., Mitchell, A., Olencki, T., Pardoll, D. M., Reddy, S. A., Shantha, E. M., Sharfman, W. H., Sharon, E., Shemanski, L. R., Shinohara, M. M., Sunshine, J. C., Taube, J. M., Thompson, J. A., Townson, S. M., Yearley, J. H., Topalian, S. L. & Cheever, M. A. 2016. PD-1 Blockade with Pembrolizumab in Advanced Merkel-Cell Carcinoma. *N Engl J Med,* 374**,** 2542-52.

Nishikawa, H. & Sakaguchi, S. 2010. Regulatory T cells in tumor immunity. *Int J Cancer,* 127**,** 759-67.

Nishikawa, H. & Sakaguchi, S. 2014. Regulatory T cells in cancer immunotherapy. *Curr Opin Immunol,* 27**,** 1-7.

Noman, M. Z., Desantis, G., Janji, B., Hasmim, M., Karray, S., Dessen, P., Bronte, V. & Chouaib, S. 2014. PD-L1 is a novel direct target of HIF-1alpha, and its blockade under hypoxia enhanced MDSC-mediated T cell activation. *J Exp Med,* 211**,** 781-90.

Nowell, P. C. 1976. The clonal evolution of tumor cell populations. *Science,* 194**,** 23-8.

Okazaki, T., Chikuma, S., Iwai, Y., Fagarasan, S. & Honjo, T. 2013. A rheostat for immune responses: the unique properties of PD-1 and their advantages for clinical application. *Nat Immunol,* 14**,** 1212-8.

Ostman, A., Hellberg, C. & Bohmer, F. D. 2006. Protein-tyrosine phosphatases and cancer. *Nat Rev Cancer,* 6**,** 307-20.

Ott, P. A., Hodi, F. S. & Robert, C. 2013. CTLA-4 and PD-1/PD-L1 blockade: new immunotherapeutic modalities with durable clinical benefit in melanoma patients. *Clin Cancer Res,* 19**,** 5300-9.

Pai, S. I., Zandberg, D. P. & Strome, S. E. 2016. The role of antagonists of the PD-1:PD-L1/PD-L2 axis in head and neck cancer treatment. *Oral Oncol,* 61**,** 152-8.

Pang, C., Sharma, D. & Sankar, T. 2015. Spontaneous regression of Merkel cell carcinoma: A case report and review of the literature. *Int J Surg Case Rep,* 7C**,** 104-8.

Pardoll, D. M. 2012. The blockade of immune checkpoints in cancer immunotherapy. *Nat Rev Cancer,* 12**,** 252-64.

Park, S. J., Namkoong, H., Doh, J., Choi, J. C., Yang, B. G., Park, Y. & Chul Sung, Y. 2014. Negative role of inducible PD-1 on survival of activated dendritic cells. *J Leukoc Biol,* 95**,** 621-9.

Parsa, A. T., Waldron, J. S., Panner, A., Crane, C. A., Parney, I. F., Barry, J. J., Cachola, K. E., Murray, J. C., Tihan, T., Jensen, M. C., Mischel, P. S., Stokoe, D. & Pieper, R. O. 2007. Loss of tumor suppressor PTEN function increases B7-H1 expression and immunoresistance in glioma. *Nat Med,* 13**,** 84-8.

Patnaik, A., Kang, S. P., Rasco, D., Papadopoulos, K. P., Elassaiss-Schaap, J., Beeram, M., Drengler, R., Chen, C., Smith, L., Espino, G., Gergich, K., Delgado, L., Daud, A., Lindia, J. A., Li, X. N., Pierce, R. H., Yearley, J. H., Wu, D., Laterza, O., Lehnert, M., Iannone, R. & Tolcher, A. W. 2015. Phase I Study of Pembrolizumab (MK-3475; Anti-PD-1 Monoclonal Antibody) in Patients with Advanced Solid Tumors. *Clin Cancer Res,* 21**,** 4286-93.

Patsoukis, N., Bardhan, K., Chatterjee, P., Sari, D., Liu, B., Bell, L. N., Karoly, E. D., Freeman, G. J., Petkova, V., Seth, P., Li, L. & Boussiotis, V. A. 2015. PD-1 alters T-cell metabolic reprogramming by inhibiting glycolysis and promoting lipolysis and fatty acid oxidation. *Nat Commun,* 6**,** 6692.

Patsoukis, N., Brown, J., Petkova, V., Liu, F., Li, L. & Boussiotis, V. A. 2012. Selective effects of PD-1 on Akt and Ras pathways regulate molecular components of the cell cycle and inhibit T cell proliferation. *Science signaling,* 5**,** ra46.

Patsoukis, N., Li, L., Sari, D., Petkova, V. & Boussiotis, V. A. 2013. PD-1 increases PTEN phosphatase activity while decreasing PTEN protein stability by inhibiting casein kinase 2. *Mol Cell Biol,* 33**,** 3091-8.

Paulson, K. G., Carter, J. J., Johnson, L. G., Cahill, K. W., Iyer, J. G., Schrama, D., Becker, J. C., Madeleine, M. M., Nghiem, P. & Galloway, D. A. 2010. Antibodies to merkel cell polyomavirus T antigen oncoproteins reflect tumor burden in merkel cell carcinoma patients. *Cancer Res,* 70**,** 8388-97.

Paulson, K. G., Iyer, J. G., Blom, A., Warton, E. M., Sokil, M., Yelistratova, L., Schuman, L., Nagase, K., Bhatia, S., Asgari, M. M. & Nghiem, P. 2013. Systemic immune suppression predicts diminished Merkel cell carcinoma-specific survival independent of stage. *J Invest Dermatol,* 133**,** 642-6.

Paulson, K. G., Iyer, J. G., Tegeder, A. R., Thibodeau, R., Schelter, J., Koba, S., Schrama, D., Simonson, W. T., Lemos, B. D., Byrd, D. R., Koelle, D. M., Galloway, D. A., Leonard, J. H., Madeleine, M. M., Argenyi, Z. B., Disis, M. L., Becker, J. C., Cleary, M. A. & Nghiem, P. 2011. Transcriptome-wide studies of merkel cell carcinoma and validation of intratumoral CD8+ lymphocyte invasion as an independent predictor of survival. *J Clin Oncol,* 29**,** 1539-46.

Paulson, K. G., Tegeder, A., Willmes, C., Iyer, J. G., Afanasiev, O. K., Schrama, D., Koba, S., Thibodeau, R., Nagase, K., Simonson, W. T., Seo, A., Koelle, D. M., Madeleine, M., Bhatia, S., Nakajima, H., Sano, S., Hardwick, J. S., Disis, M. L., Cleary, M. A., Becker, J. C. & Nghiem, P. 2014. Downregulation of MHC-I expression is prevalent but reversible in Merkel cell carcinoma. *Cancer Immunol Res,* 2**,** 1071-9.

Peggs, K. S., Quezada, S. A., Chambers, C. A., Korman, A. J. & Allison, J. P. 2009. Blockade of CTLA-4 on both effector and regulatory T cell compartments contributes to the antitumor activity of anti-CTLA-4 antibodies. *J Exp Med,* 206**,** 1717-25.

Peng, W., Chen, J. Q., Liu, C., Malu, S., Creasy, C., Tetzlaff, M. T., Xu, C., McKenzie, J. A., Zhang, C., Liang, X., Williams, L. J., Deng, W., Chen, G., Mbofung, R., Lazar, A. J., Torres-Cabala, C. A., Cooper, Z. A., Chen, P. L., Tieu, T. N., Spranger, S., Yu, X., Bernatchez, C., Forget, M. A., Haymaker, C., Amaria, R., McQuade, J. L., Glitza, I. C., Cascone, T., Li, H. S., Kwong, L. N., Heffernan, T. P., Hu, J., Bassett, R. L., Jr., Bosenberg, M. W., Woodman, S. E., Overwijk, W. W., Lizee, G., Roszik, J., Gajewski, T. F., Wargo, J. A., Gershenwald, J. E., Radvanyi, L., Davies, M. A. & Hwu, P. 2016. Loss of PTEN Promotes Resistance to T Cell-Mediated Immunotherapy. *Cancer Discov,* 6**,** 202-16.

Peng, W., Liu, C., Xu, C., Lou, Y., Chen, J., Yang, Y., Yagita, H., Overwijk, W. W., Lizee, G., Radvanyi, L. & Hwu, P. 2012. PD-1 blockade enhances T-cell migration to tumors by elevating IFN-gamma inducible chemokines. *Cancer Res,* 72**,** 5209-18.

Pinton, L., Solito, S., Damuzzo, V., Francescato, S., Pozzuoli, A., Berizzi, A., Mocellin, S., Rossi, C. R., Bronte, V. & Mandruzzato, S. 2015. Activated T cells sustain myeloid-derived suppressor cell-mediated immune suppression. *Oncotarget*.

Pommier, Y., Sordet, O., Antony, S., Hayward, R. L. & Kohn, K. W. 2004. Apoptosis defects and chemotherapy resistance: molecular interaction maps and networks. *Oncogene,* 23**,** 2934-49.

Posch, C., Moslehi, H., Feeney, L., Green, G. A., Ebaee, A., Feichtenschlager, V., Chong, K., Peng, L., Dimon, M. T., Phillips, T., Daud, A. I., McCalmont, T. H., LeBoit, P. E. & Ortiz-Urda, S. 2013. Combined targeting of MEK and PI3K/mTOR effector pathways is necessary to effectively inhibit NRAS mutant melanoma in vitro and in vivo. *Proc Natl Acad Sci U S A,* 110**,** 4015-20.

Postow, M. A., Callahan, M. K. & Wolchok, J. D. 2015a. Immune Checkpoint Blockade in Cancer Therapy. *J Clin Oncol*.

Postow, M. A., Chesney, J., Pavlick, A. C., Robert, C., Grossmann, K., McDermott, D., Linette, G. P., Meyer, N., Giguere, J. K., Agarwala, S. S., Shaheen, M., Ernstoff, M. S., Minor, D., Salama, A. K., Taylor, M., Ott, P. A., Rollin, L. M., Horak, C., Gagnier, P., Wolchok, J. D. & Hodi, F. S. 2015b. Nivolumab and ipilimumab versus ipilimumab in untreated melanoma. *N Engl J Med,* 372**,** 2006-17.

Poulsen, M. 2004. Merkel-cell carcinoma of the skin. *The lancet oncology,* 5**,** 593-9.

Quintana, E., Shackleton, M., Foster, H. R., Fullen, D. R., Sabel, M. S., Johnson, T. M. & Morrison, S. J. 2010. Phenotypic heterogeneity among tumorigenic melanoma cells from patients that is reversible and not hierarchically organized. *Cancer Cell,* 18**,** 510-23.

Quintana, E., Shackleton, M., Sabel, M. S., Fullen, D. R., Johnson, T. M. & Morrison, S. J. 2008. Efficient tumour formation by single human melanoma cells. *Nature,* 456**,** 593-8.

Redman, J. M., Gibney, G. T. & Atkins, M. B. 2016. Advances in immunotherapy for melanoma. *BMC Med,* 14**,** 20.

Reya, T., Morrison, S. J., Clarke, M. F. & Weissman, I. L. 2001. Stem cells, cancer, and cancer stem cells. *Nature,* 414**,** 105-11.

Ribas, A., Butterfield, L. H., Glaspy, J. A. & Economou, J. S. 2003. Current developments in cancer vaccines and cellular immunotherapy. *J Clin Oncol,* 21**,** 2415-32.

Ribas, A., Puzanov, I., Dummer, R., Schadendorf, D., Hamid, O., Robert, C., Hodi, F. S., Schachter, J., Pavlick, A. C., Lewis, K. D., Cranmer, L. D., Blank, C. U., O'Day, S. J., Ascierto, P. A., Salama, A. K., Margolin, K. A., Loquai, C., Eigentler, T. K., Gangadhar, T. C., Carlino, M. S., Agarwala, S. S., Moschos, S. J., Sosman, J. A., Goldinger, S. M., Shapira-Frommer, R., Gonzalez, R., Kirkwood, J. M., Wolchok, J. D., Eggermont, A., Li, X. N., Zhou, W., Zernhelt, A. M., Lis, J., Ebbinghaus, S., Kang, S. P. & Daud, A. 2015. Pembrolizumab versus investigator-choice chemotherapy for ipilimumab-refractory melanoma (KEYNOTE-002): a randomised, controlled, phase 2 trial. *Lancet Oncol,* 16**,** 908-18.

Ridgway, D. 2003. The first 1000 dendritic cell vaccinees. *Cancer Invest,* 21**,** 873-86.

Riley, J. L. 2009. PD-1 signaling in primary T cells. *Immunological reviews,* 229**,** 114-25.

Rizvi, N. A., Hellmann, M. D., Snyder, A., Kvistborg, P., Makarov, V., Havel, J. J., Lee, W., Yuan, J., Wong, P., Ho, T. S., Miller, M. L., Rekhtman, N., Moreira, A. L., Ibrahim, F., Bruggeman, C., Gasmi, B., Zappasodi, R., Maeda, Y., Sander, C., Garon, E. B., Merghoub, T., Wolchok, J. D., Schumacher, T. N. & Chan, T. A. 2015. Mutational landscape determines sensitivity to PD-1 blockade in non-small cell lung cancer. *Science*.

Robert, C., Long, G. V., Brady, B., Dutriaux, C., Maio, M., Mortier, L., Hassel, J. C., Rutkowski, P., McNeil, C., Kalinka-Warzocha, E., Savage, K. J., Hernberg, M. M., Lebbe, C., Charles, J., Mihalcioiu, C., Chiarion-Sileni, V., Mauch, C., Cognetti, F., Arance, A., Schmidt, H., Schadendorf, D., Gogas, H., Lundgren-Eriksson, L., Horak, C., Sharkey, B., Waxman, I. M., Atkinson, V. & Ascierto, P. A. 2015a. Nivolumab in previously untreated melanoma without BRAF mutation. *N Engl J Med,* 372**,** 320-30.

Robert, C., Schachter, J., Long, G. V., Arance, A., Grob, J. J., Mortier, L., Daud, A., Carlino, M. S., McNeil, C., Lotem, M., Larkin, J., Lorigan, P., Neyns, B., Blank, C. U., Hamid, O., Mateus, C., Shapira-Frommer, R., Kosh, M., Zhou, H., Ibrahim, N., Ebbinghaus, S., Ribas, A. & investigators, K.-. 2015b. Pembrolizumab versus Ipilimumab in Advanced Melanoma. *N Engl J Med,* 372**,** 2521-32.

Robert, C., Thomas, L., Bondarenko, I., O'Day, S., Weber, J., Garbe, C., Lebbe, C., Baurain, J. F., Testori, A., Grob, J. J., Davidson, N., Richards, J., Maio, M., Hauschild, A., Miller, W. H., Jr., Gascon, P., Lotem, M., Harmankaya, K., Ibrahim, R., Francis, S., Chen, T. T., Humphrey, R., Hoos, A. & Wolchok, J. D. 2011. Ipilimumab plus dacarbazine for previously untreated metastatic melanoma. *N Engl J Med,* 364**,** 2517-26.

Rodig, S. J., Cheng, J., Wardzala, J., DoRosario, A., Scanlon, J. J., Laga, A. C., Martinez-Fernandez, A., Barletta, J. A., Bellizzi, A. M., Sadasivam, S., Holloway, D. T., Cooper, D. J., Kupper, T. S., Wang, L. C. & DeCaprio, J. A. 2012a. Improved detection suggests all Merkel cell carcinomas harbor Merkel polyomavirus. *J Clin Invest,* 122**,** 4645-53.

Rodig, S. J., Cheng, J., Wardzala, J., DoRosario, A., Scanlon, J. J., Laga, A. C., Martinez-Fernandez, A., Barletta, J. A., Bellizzi, A. M., Sadasivam, S., Holloway, D. T., Cooper, D. J., Kupper, T. S., Wang, L. C. & DeCaprio, J. A. 2012b. Improved detection suggests all Merkel cell carcinomas harbor Merkel polyomavirus. *J Clin Invest,* 122**,** 4645-53.

Rongvaux, A., Willinger, T., Martinek, J., Strowig, T., Gearty, S. V., Teichmann, L. L., Saito, Y., Marches, F., Halene, S., Palucka, A. K., Manz, M. G. & Flavell, R. A. 2014. Development and function of human innate immune cells in a humanized mouse model. *Nat Biotechnol,* 32**,** 364-72.

Rosen, S. T., Gould, V. E., Salwen, H. R., Herst, C. V., Le Beau, M. M., Lee, I., Bauer, K., Marder, R. J., Andersen, R., Kies, M. S. & et al. 1987. Establishment and characterization of a neuroendocrine skin carcinoma cell line. *Lab Invest,* 56**,** 302-12.

Rosenberg, J. E., Hoffman-Censits, J., Powles, T., van der Heijden, M. S., Balar, A. V., Necchi, A., Dawson, N., O'Donnell, P. H., Balmanoukian, A., Loriot, Y., Srinivas, S., Retz, M. M., Grivas, P., Joseph, R. W., Galsky, M. D., Fleming, M. T., Petrylak, D. P., Perez-Gracia, J. L., Burris, H. A., Castellano, D., Canil, C., Bellmunt, J., Bajorin, D., Nickles, D., Bourgon, R., Frampton, G. M., Cui, N., Mariathasan, S., Abidoye, O., Fine, G. D. & Dreicer, R. 2016. Atezolizumab in patients with locally advanced and metastatic urothelial carcinoma who have progressed following treatment with platinum-based chemotherapy: a single-arm, multicentre, phase 2 trial. *Lancet,* 387**,** 1909-20.

Rosenberg, S. A., Yang, J. C. & Restifo, N. P. 2004. Cancer immunotherapy: moving beyond current vaccines. *Nat Med,* 10**,** 909-15.

Rosenberg, S. A., Yang, J. C., Sherry, R. M., Kammula, U. S., Hughes, M. S., Phan, G. Q., Citrin, D. E., Restifo, N. P., Robbins, P. F., Wunderlich, J. R., Morton, K. E., Laurencot, C. M., Steinberg, S. M., White, D. E. & Dudley, M. E. 2011. Durable complete responses in heavily pretreated patients with metastatic melanoma using T-cell transfer immunotherapy. *Clin Cancer Res,* 17**,** 4550-7.

Rosenberg, S. A., Yang, J. C., White, D. E. & Steinberg, S. M. 1998. Durability of complete responses in patients with metastatic cancer treated with high-dose interleukin-2: identification of the antigens mediating response. *Ann Surg,* 228**,** 307-19.

Rubin, J. T., Elwood, L. J., Rosenberg, S. A. & Lotze, M. T. 1989. Immunohistochemical correlates of response to recombinant interleukin-2-based immunotherapy in humans. *Cancer Res,* 49**,** 7086-92.

Said, E. A., Dupuy, F. P., Trautmann, L., Zhang, Y., Shi, Y., El-Far, M., Hill, B. J., Noto, A., Ancuta, P., Peretz, Y., Fonseca, S. G., Van Grevenynghe, J., Boulassel, M. R., Bruneau, J., Shoukry, N. H., Routy, J. P., Douek, D. C., Haddad, E. K. & Sekaly, R. P. 2010. Programmed death-1-induced interleukin-10 production by monocytes impairs CD4+ T cell activation during HIV infection. *Nat Med,* 16**,** 452-9.

Sakuishi, K., Apetoh, L., Sullivan, J. M., Blazar, B. R., Kuchroo, V. K. & Anderson, A. C. 2010. Targeting Tim-3 and PD-1 pathways to reverse T cell exhaustion and restore anti-tumor immunity. *J Exp Med,* 207**,** 2187-94.

Scadden, D. T. 2006. The stem-cell niche as an entity of action. *Nature,* 441**,** 1075-9.

Schadendorf, D., Hodi, F. S., Robert, C., Weber, J. S., Margolin, K., Hamid, O., Patt, D., Chen, T. T., Berman, D. M. & Wolchok, J. D. 2015. Pooled Analysis of Long-Term Survival Data From Phase II and Phase III Trials of Ipilimumab in Unresectable or Metastatic Melanoma. *J Clin Oncol,* 33**,** 1889-94.

Schalper, K. A., Kaftan, E. & Herbst, R. S. 2016. Predictive Biomarkers for PD-1 Axis Therapies: The Hidden Treasure or a Call for Research. *Clin Cancer Res*.

Schatton, T. & Frank, M. H. 2009. Antitumor immunity and cancer stem cells. *Ann N Y Acad Sci,* 1176**,** 154-69.

Schatton, T., Frank, N. Y. & Frank, M. H. 2009. Identification and targeting of cancer stem cells. *Bioessays,* 31**,** 1038-49.

Schatton, T., Murphy, G. F., Frank, N. Y., Yamaura, K., Waaga-Gasser, A. M., Gasser, M., Zhan, Q., Jordan, S., Duncan, L. M., Weishaupt, C., Fuhlbrigge, R. C., Kupper, T. S., Sayegh, M. H. & Frank, M. H. 2008. Identification of cells initiating human melanomas. *Nature,* 451**,** 345-9.

Schatton, T., Schutte, U., Frank, N. Y., Zhan, Q., Hoerning, A., Robles, S. C., Zhou, J., Hodi, F. S., Spagnoli, G. C., Murphy, G. F. & Frank, M. H. 2010. Modulation of T-cell activation by malignant melanoma initiating cells. *Cancer Res,* 70**,** 697-708.

Schatton, T., Yang, J., Kleffel, S., Uehara, M., Barthel, S. R., Schlapbach, C., Zhan, Q., Dudeney, S., Mueller, H., Lee, N., de Vries, J. C., Meier, B., Vander Beken, S., Kluth, M. A., Ganss, C., Sharpe, A. H., Waaga-Gasser, A. M., Sayegh, M. H., Abdi, R., Scharffetter-Kochanek, K., Murphy, G. F., Kupper, T. S., Frank, N. Y. & Frank, M. H. 2015. ABCB5 Identifies Immunoregulatory Dermal Cells. *Cell Rep,* 12**,** 1564-74.

Schreiber, R. D., Old, L. J. & Smyth, M. J. 2011. Cancer immunoediting: integrating immunity's roles in cancer suppression and promotion. *Science,* 331**,** 1565-70.

Schumacher, T. N. & Schreiber, R. D. 2015. Neoantigens in cancer immunotherapy. *Science,* 348**,** 69-74.

Schwartz, R. H. 2003. T cell anergy. *Annu Rev Immunol,* 21**,** 305-34.

Serrone, L. & Hersey, P. 1999. The chemoresistance of human malignant melanoma: an update. *Melanoma Res,* 9**,** 51-8.

Setia, N., Abbas, O., Sousa, Y., Garb, J. L. & Mahalingam, M. 2012. Profiling of ABC transporters ABCB5, ABCF2 and nestin-positive stem cells in nevi, in situ and invasive melanoma. *Mod Pathol,* 25**,** 1169-75.

Shackleton, M., Quintana, E., Fearon, E. R. & Morrison, S. J. 2009. Heterogeneity in cancer: cancer stem cells versus clonal evolution. *Cell,* 138**,** 822-9.

Shah, K. V., Chien, A. J., Yee, C. & Moon, R. T. 2008. CTLA-4 is a direct target of Wnt/beta-catenin signaling and is expressed in human melanoma tumors. *J Invest Dermatol,* 128**,** 2870-9.

Shankaran, V., Ikeda, H., Bruce, A. T., White, J. M., Swanson, P. E., Old, L. J. & Schreiber, R. D. 2001. IFNgamma and lymphocytes prevent primary tumour development and shape tumour immunogenicity. *Nature,* 410**,** 1107-11.

Sharma, B. K., Manglik, V. & Elias, E. G. 2010. Immuno-expression of human melanoma stem cell markers in tissues at different stages of the disease. *The Journal of surgical research,* 163**,** e11-5.

Sheppard, K. A., Fitz, L. J., Lee, J. M., Benander, C., George, J. A., Wooters, J., Qiu, Y., Jussif, J. M., Carter, L. L., Wood, C. R. & Chaudhary, D. 2004. PD-1 inhibits T-cell receptor induced phosphorylation of the ZAP70/CD3zeta signalosome and downstream signaling to PKCtheta. *FEBS Lett,* 574**,** 37-41.

Shtivelman, E., Davies, M. Q., Hwu, P., Yang, J., Lotem, M., Oren, M., Flaherty, K. T. & Fisher, D. E. 2014. Pathways and therapeutic targets in melanoma. *Oncotarget,* 5**,** 1701-52.
Shuda, M., Feng, H., Kwun, H. J., Rosen, S. T., Gjoerup, O., Moore, P. S. & Chang, Y. 2008. T antigen mutations are a human tumor-specific signature for Merkel cell polyomavirus. *Proc Natl Acad Sci U S A,* 105**,** 16272-7.

Shuda, M., Kwun, H. J., Feng, H., Chang, Y. & Moore, P. S. 2011. Human Merkel cell polyomavirus small T antigen is an oncoprotein targeting the 4E-BP1 translation regulator. *J Clin Invest,* 121**,** 3623-34.

Simons, B. D. & Clevers, H. 2011. Strategies for homeostatic stem cell self-renewal in adult tissues. *Cell,* 145**,** 851-62.

Slominski, A., Wortsman, J., Carlson, A. J., Matsuoka, L. Y., Balch, C. M. & Mihm, M. C. 2001. Malignant melanoma. *Arch Pathol Lab Med,* 125**,** 1295-306.

Snyder, A., Makarov, V., Merghoub, T., Yuan, J., Zaretsky, J. M., Desrichard, A., Walsh, L. A., Postow, M. A., Wong, P., Ho, T. S., Hollmann, T. J., Bruggeman, C., Kannan, K., Li, Y., Elipenahli, C., Liu, C., Harbison, C. T., Wang, L., Ribas, A., Wolchok, J. D. & Chan, T. A. 2014a. Genetic basis for clinical response to CTLA-4 blockade in melanoma. *N Engl J Med,* 371**,** 2189-99.

Snyder, A., Makarov, V., Merghoub, T., Yuan, J., Zaretsky, J. M., Desrichard, A., Walsh, L. A., Postow, M. A., Wong, P., Ho, T. S., Hollmann, T. J., Bruggeman, C., Kannan, K., Li, Y., Elipenahli, C., Liu, C., Harbison, C. T., Wang, L., Ribas, A., Wolchok, J. D. & Chan, T. A. 2014b. Genetic basis for clinical response to CTLA-4 blockade in melanoma. *N Engl J Med,* 371**,** 2189-99.

Soengas, M. S. & Lowe, S. W. 2003. Apoptosis and melanoma chemoresistance. *Oncogene,* 22**,** 3138-51.

Song, M., Chen, D., Lu, B., Wang, C., Zhang, J., Huang, L., Wang, X., Timmons, C. L., Hu, J., Liu, B., Wu, X., Wang, L., Wang, J. & Liu, H. 2013. PTEN loss increases PD-L1 protein expression and affects the correlation between PD-L1 expression and clinical parameters in colorectal cancer. *PLoS One,* 8**,** e65821.

Spranger, S., Spaapen, R. M., Zha, Y., Williams, J., Meng, Y., Ha, T. T. & Gajewski, T. F. 2013. Up-regulation of PD-L1, IDO, and T(regs) in the melanoma tumor microenvironment is driven by CD8(+) T cells. *Sci Transl Med,* 5**,** 200ra116.

Stowell, S. R., Ju, T. & Cummings, R. D. 2015. Protein glycosylation in cancer. *Annu Rev Pathol,* 10**,** 473-510.

Sun, B., Chen, M., Hawks, C. L., Pereira-Smith, O. M. & Hornsby, P. J. 2005. The minimal set of genetic alterations required for conversion of primary human fibroblasts to cancer cells in the subrenal capsule assay. *Neoplasia,* 7**,** 585-93.

Tai, P. T., Yu, E., Winquist, E., Hammond, A., Stitt, L., Tonita, J. & Gilchrist, J. 2000. Chemotherapy in neuroendocrine/Merkel cell carcinoma of the skin: case series and review of 204 cases. *J Clin Oncol,* 18**,** 2493-9.

Tas, F., Keskin, S., Karadeniz, A., Dagoglu, N., Sen, F., Kilic, L. & Yildiz, I. 2011. Noncutaneous melanoma have distinct features from each other and cutaneous melanoma. *Oncology,* 81**,** 353-8.

Taube, J. M., Anders, R. A., Young, G. D., Xu, H., Sharma, R., McMiller, T. L., Chen, S., Klein, A. P., Pardoll, D. M., Topalian, S. L. & Chen, L. 2012. Colocalization of inflammatory response with B7-h1 expression in human melanocytic lesions supports an adaptive resistance mechanism of immune escape. *Sci Transl Med,* 4**,** 127ra37.

Taube, J. M., Klein, A., Brahmer, J. R., Xu, H., Pan, X., Kim, J. H., Chen, L., Pardoll, D. M., Topalian, S. L. & Anders, R. A. 2014. Association of PD-1, PD-1 ligands, and other features of the tumor immune microenvironment with response to anti-PD-1 therapy. *Clin Cancer Res,* 20**,** 5064-74.

Taylor, R. C., Patel, A., Panageas, K. S., Busam, K. J. & Brady, M. S. 2007. Tumor-infiltrating lymphocytes predict sentinel lymph node positivity in patients with cutaneous melanoma. *J Clin Oncol,* 25**,** 869-75.

Thakuria, M., LeBoeuf, N. R. & Rabinowits, G. 2014. Update on the biology and clinical management of Merkel cell carcinoma. *Am Soc Clin Oncol Educ Book***,** e405-10.

Thompson, J. F., Scolyer, R. A. & Kefford, R. F. 2005. Cutaneous melanoma. *Lancet,* 365**,** 687-701.

Topalian, S. L., Drake, C. G. & Pardoll, D. M. 2012a. Targeting the PD-1/B7-H1(PD-L1) pathway to activate anti-tumor immunity. *Curr Opin Immunol,* 24**,** 207-12.

Topalian, S. L., Hodi, F. S., Brahmer, J. R., Gettinger, S. N., Smith, D. C., McDermott, D. F., Powderly, J. D., Carvajal, R. D., Sosman, J. A., Atkins, M. B., Leming, P. D., Spigel, D. R., Antonia, S. J., Horn, L., Drake, C. G., Pardoll, D. M., Chen, L., Sharfman, W. H., Anders, R. A., Taube, J. M., McMiller, T. L., Xu, H., Korman, A. J., Jure-Kunkel, M., Agrawal, S., McDonald, D., Kollia, G. D., Gupta, A., Wigginton, J. M. & Sznol, M. 2012b. Safety, activity, and immune correlates of anti-PD-1 antibody in cancer. *N Engl J Med,* 366**,** 2443-54.

Topalian, S. L., Sznol, M., McDermott, D. F., Kluger, H. M., Carvajal, R. D., Sharfman, W. H., Brahmer, J. R., Lawrence, D. P., Atkins, M. B., Powderly, J. D., Leming, P. D., Lipson, E. J., Puzanov, I., Smith, D. C., Taube, J. M., Wigginton, J. M., Kollia, G. D., Gupta, A., Pardoll, D. M., Sosman, J. A. & Hodi, F. S. 2014. Survival, durable tumor remission, and long-term safety in patients with advanced melanoma receiving nivolumab. *J Clin Oncol,* 32**,** 1020-30.

Tothill, R., Estall, V. & Rischin, D. 2015. Merkel cell carcinoma: emerging biology, current approaches, and future directions. *Am Soc Clin Oncol Educ Book***,** e519-26.

Touze, A., Le Bidre, E., Laude, H., Fleury, M. J., Cazal, R., Arnold, F., Carlotti, A., Maubec, E., Aubin, F., Avril, M. F., Rozenberg, F., Tognon, M., Maruani, A., Guyetant, S., Lorette, G. & Coursaget, P. 2011. High levels of antibodies against merkel cell polyomavirus identify a subset of patients with merkel cell carcinoma with better clinical outcome. *J Clin Oncol,* 29**,** 1612-9.

Tsao, H., Chin, L., Garraway, L. A. & Fisher, D. E. 2012. Melanoma: from mutations to medicine. *Genes Dev,* 26**,** 1131-55.

Tumeh, P. C., Harview, C. L., Yearley, J. H., Shintaku, I. P., Taylor, E. J., Robert, L., Chmielowski, B., Spasic, M., Henry, G., Ciobanu, V., West, A. N., Carmona, M., Kivork, C., Seja, E., Cherry, G., Gutierrez, A. J., Grogan, T. R., Mateus, C., Tomasic, G., Glaspy, J. A., Emerson, R. O., Robins, H., Pierce, R. H., Elashoff, D. A., Robert, C. & Ribas, A.

2014. PD-1 blockade induces responses by inhibiting adaptive immune resistance. *Nature,* 515**,** 568-71.

Untergasser, A., Cutcutache, I., Koressaar, T., Ye, J., Faircloth, B. C., Remm, M. & Rozen, S. G. 2012. Primer3--new capabilities and interfaces. *Nucleic Acids Res,* 40**,** e115.

Van Allen, E. M., Miao, D., Schilling, B., Shukla, S. A., Blank, C., Zimmer, L., Sucker, A., Hillen, U., Foppen, M. H., Goldinger, S. M., Utikal, J., Hassel, J. C., Weide, B., Kaehler, K. C., Loquai, C., Mohr, P., Gutzmer, R., Dummer, R., Gabriel, S., Wu, C. J., Schadendorf, D. & Garraway, L. A. 2015. Genomic correlates of response to CTLA-4 blockade in metastatic melanoma. *Science,* 350**,** 207-11.

van Houdt, I. S., Sluijter, B. J., Moesbergen, L. M., Vos, W. M., de Gruijl, T. D., Molenkamp, B. G., van den Eertwegh, A. J., Hooijberg, E., van Leeuwen, P. A., Meijer, C. J. & Oudejans, J. J. 2008. Favorable outcome in clinically stage II melanoma patients is associated with the presence of activated tumor infiltrating T-lymphocytes and preserved MHC class I antigen expression. *Int J Cancer,* 123**,** 609-15.

Vence, L., Palucka, A. K., Fay, J. W., Ito, T., Liu, Y. J., Banchereau, J. & Ueno, H. 2007. Circulating tumor antigen-specific regulatory T cells in patients with metastatic melanoma. *Proc Natl Acad Sci U S A,* 104**,** 20884-9.

Vesely, M. D., Kershaw, M. H., Schreiber, R. D. & Smyth, M. J. 2011. Natural innate and adaptive immunity to cancer. *Annu Rev Immunol,* 29**,** 235-71.

Vignali, D. A., Collison, L. W. & Workman, C. J. 2008. How regulatory T cells work. *Nat Rev Immunol,* 8**,** 523-32.

Vlashi, E., Kim, K., Lagadec, C., Donna, L. D., McDonald, J. T., Eghbali, M., Sayre, J. W., Stefani, E., McBride, W. & Pajonk, F. 2009. In vivo imaging, tracking, and targeting of cancer stem cells. *J Natl Cancer Inst,* 101**,** 350-9.

von Boehmer, L., Mattle, M., Bode, P., Landshammer, A., Schafer, C., Nuber, N., Ritter, G., Old, L., Moch, H., Schafer, N., Jager, E., Knuth, A. & van den Broek, M. 2013. NY-ESO-1-specific immunological pressure and escape in a patient with metastatic melanoma. *Cancer Immun,* 13**,** 12.

Wang, W., Yu, D., Sarnaik, A. A., Yu, B., Hall, M., Morelli, D., Zhang, Y., Zhao, X. & Weber, J. S. 2012. Biomarkers on melanoma patient T cells associated with ipilimumab treatment. *J Transl Med,* 10**,** 146.

Wang, Y. & Teng, J. S. 2016. Increased multi-drug resistance and reduced apoptosis in osteosarcoma side population cells are crucial factors for tumor recurrence. *Exp Ther Med,* 12**,** 81-86.

Weber, J. S., D'Angelo, S. P., Minor, D., Hodi, F. S., Gutzmer, R., Neyns, B., Hoeller, C., Khushalani, N. I., Miller, W. H., Jr., Lao, C. D., Linette, G. P., Thomas, L., Lorigan, P., Grossmann, K. F., Hassel, J. C., Maio, M., Sznol, M., Ascierto, P. A., Mohr, P., Chmielowski, B., Bryce, A., Svane, I. M., Grob, J. J., Krackhardt, A. M., Horak, C., Lambert, A., Yang, A. S. & Larkin, J. 2015. Nivolumab versus chemotherapy in patients with advanced melanoma who progressed after anti-CTLA-4 treatment (CheckMate 037): a randomised, controlled, open-label, phase 3 trial. *Lancet Oncol*.

Weber, J. S., Hamid, O., Chasalow, S. D., Wu, D. Y., Parker, S. M., Galbraith, S., Gnjatic, S. & Berman, D. 2012. Ipilimumab increases activated T cells and enhances humoral immunity in patients with advanced melanoma. *J Immunother,* 35**,** 89-97.

Weber, J. S., Kudchadkar, R. R., Yu, B., Gallenstein, D., Horak, C. E., Inzunza, H. D., Zhao, X., Martinez, A. J., Wang, W., Gibney, G., Kroeger, J., Eysmans, C., Sarnaik, A. A. & Chen, Y. A. 2013. Safety, efficacy, and biomarkers of nivolumab with vaccine in ipilimumab-refractory or -naive melanoma. *J Clin Oncol,* 31**,** 4311-8.

Weide, B., Martens, A., Zelba, H., Stutz, C., Derhovanessian, E., Di Giacomo, A. M., Maio, M., Sucker, A., Schilling, B., Schadendorf, D., Buttner, P., Garbe, C. & Pawelec, G. 2014. Myeloid-derived suppressor cells predict survival of patients with advanced melanoma: comparison with regulatory T cells and NY-ESO-1- or melan-A-specific T cells. *Clin Cancer Res,* 20**,** 1601-9.

Wherry, E. J. 2011. T cell exhaustion. *Nat Immunol,* 12**,** 492-9.

Wiener, Z., Kohalmi, B., Pocza, P., Jeager, J., Tolgyesi, G., Toth, S., Gorbe, E., Papp, Z. & Falus, A. 2007. TIM-3 is expressed in melanoma cells and is upregulated in TGF-beta stimulated mast cells. *J Invest Dermatol,* 127**,** 906-14.

Wilson, B. J., Saab, K. R., Ma, J., Schatton, T., Putz, P., Zhan, Q., Murphy, G. F., Gasser, M., Waaga-Gasser, A. M., Frank, N. Y. & Frank, M. H. 2014. ABCB5 Maintains Melanoma-Initiating Cells through a Proinflammatory Cytokine Signaling Circuit. *Cancer Res,* 74**,** 4196-207.

Wilson, B. J., Schatton, T., Zhan, Q., Gasser, M., Ma, J., Saab, K. R., Schanche, R., Waaga-Gasser, A. M., Gold, J. S., Huang, Q., Murphy, G. F., Frank, M. H. & Frank, N. Y. 2011. ABCB5 identifies a therapy-refractory tumor cell population in colorectal cancer patients. *Cancer Res,* 71**,** 5307-16.

Win-Piazza, H., Schneeberger, V. E., Chen, L., Pernazza, D., Lawrence, H. R., Sebti, S. M., Lawrence, N. J. & Wu, J. 2012. Enhanced anti-melanoma efficacy of interferon alfa-2b via inhibition of Shp2. *Cancer Lett,* 320**,** 81-5.

Wolchok, J. D., Kluger, H., Callahan, M. K., Postow, M. A., Rizvi, N. A., Lesokhin, A. M., Segal, N. H., Ariyan, C. E., Gordon, R. A., Reed, K., Burke, M. M., Caldwell, A.,

Kronenberg, S. A., Agunwamba, B. U., Zhang, X., Lowy, I., Inzunza, H. D., Feely, W., Horak, C. E., Hong, Q., Korman, A. J., Wigginton, J. M., Gupta, A. & Sznol, M. 2013. Nivolumab plus ipilimumab in advanced melanoma. *N Engl J Med,* 369**,** 122-33.

Wong, S. Q., Waldeck, K., Vergara, I. A., Schroder, J., Madore, J., Wilmott, J. S., Colebatch, A. J., De Paoli-Iseppi, R., Li, J., Lupat, R., Semple, T., Arnau, G. M., Fellowes, A., Leonard, J. H., Hruby, G., Mann, G. J., Thompson, J. F., Cullinane, C., Johnston, M., Shackleton, M., Sandhu, S., Bowtell, D. D., Johnstone, R. W., Fox, S. B., McArthur, G. A., Papenfuss, A. T., Scolyer, R. A., Gill, A. J., Hicks, R. J. & Tothill, R. W. 2015. UV-Associated Mutations Underlie the Etiology of MCV-Negative Merkel Cell Carcinomas. *Cancer Res,* 75**,** 5228-34.

Woo, S. R., Turnis, M. E., Goldberg, M. V., Bankoti, J., Selby, M., Nirschl, C. J., Bettini, M. L., Gravano, D. M., Vogel, P., Liu, C. L., Tangsombatvisit, S., Grosso, J. F., Netto, G., Smeltzer, M. P., Chaux, A., Utz, P. J., Workman, C. J., Pardoll, D. M., Korman, A. J., Drake, C. G. & Vignali, D. A. 2012. Immune inhibitory molecules LAG-3 and PD-1 synergistically regulate T-cell function to promote tumoral immune escape. *Cancer Res,* 72**,** 917-27.

Wu, X., Peng, M., Huang, B., Zhang, H., Wang, H., Huang, B., Xue, Z., Zhang, L., Da, Y., Yang, D., Yao, Z. & Zhang, R. 2013. Immune microenvironment profiles of tumor immune equilibrium and immune escape states of mouse sarcoma. *Cancer Lett,* 340**,** 124-33.

Yadav, M., Jhunjhunwala, S., Phung, Q. T., Lupardus, P., Tanguay, J., Bumbaca, S., Franci, C., Cheung, T. K., Fritsche, J., Weinschenk, T., Modrusan, Z., Mellman, I., Lill, J. R. & Delamarre, L. 2014. Predicting immunogenic tumour mutations by combining mass spectrometry and exome sequencing. *Nature,* 515**,** 572-6.

Yokosuka, T., Takamatsu, M., Kobayashi-Imanishi, W., Hashimoto-Tane, A., Azuma, M. & Saito, T. 2012. Programmed cell death 1 forms negative costimulatory microclusters that directly inhibit T cell receptor signaling by recruiting phosphatase SHP2. *J Exp Med,* 209**,** 1201-17.

Zhang, T., Dutton-Regester, K., Brown, K. M. & Hayward, N. K. 2016a. The genomic landscape of cutaneous melanoma. *Pigment Cell Melanoma Res*.

Zhang, X., Cheng, X., Lai, Y., Zhou, Y., Cao, W. & Hua, Z. C. 2016b. Salmonella VNP20009-mediated RNA interference of ABCB5 moderated chemoresistance of melanoma stem cell and suppressed tumor growth more potently. *Oncotarget*.

Zhang, Y., Ma, C. J., Ni, L., Zhang, C. L., Wu, X. Y., Kumaraguru, U., Li, C. F., Moorman, J. P. & Yao, Z. Q. 2011. Cross-talk between programmed death-1 and suppressor of cytokine signaling-1 in inhibition of IL-12 production by monocytes/macrophages in hepatitis C virus infection. *J Immunol,* 186**,** 3093-103.

Zhu, L., Gibson, P., Currle, D. S., Tong, Y., Richardson, R. J., Bayazitov, I. T., Poppleton, H., Zakharenko, S., Ellison, D. W. & Gilbertson, R. J. 2009. Prominin 1 marks intestinal stem cells that are susceptible to neoplastic transformation. *Nature,* 457**,** 603-7.

Zou, W. 2005. Immunosuppressive networks in the tumour environment and their therapeutic relevance. *Nat Rev Cancer,* 5**,** 263-74.

11 Curriculum Vitae - Sonja B. Kleffel

Bibliography

Kleffel S, Lee N, Lezcano C, Wilson BJ, Sobolewski K, Saab KR, Mueller H, Zhan Q, Posch C, Elco CP, DoRosario A, Garcia SS, Thakuria M, Wang YE, Wang LC, Murphy GF, Frank MH, Schatton T. ABCB5-targeted chemoresistance reversal inhibits Merkel cell carcinoma growth. **J Invest Dermatol**. 2016 Apr;136(4):838-46.

Kleffel S, Posch C, Barthel SR, Mueller H, Schlapbach C, Guenova E, Elco CP, Lee N, Juneja VR, Zhan Q, Lian CG, Thomi R, Hoetzenecker W, Cozzio A, Dummer R, Mihm MC Jr, Flaherty KT, Frank MH, Murphy GF, Sharpe AH, Kupper TS, Schatton T. Melanoma Cell-Intrinsic PD-1 Receptor Functions Promote Tumor Growth. **Cell** 2015 Sep; 162(6):1242-56.

Schatton T, Yang J, **Kleffel S**, Uehara M, Barthel SR, Schlapbach C, Zhan Q, Dudeney S, Mueller H, Lee N, de Vries JC, Meier B, Vander Beken S, Kluth MA, Ganss C, Sharpe AH, Waaga-Gasser AM, Sayegh MH, Abdi R, Scharffetter-Kochanek K, Murphy GF, Kupper TS, Frank NY, Frank MH. ABCB5 Identifies Immunoregulatory Dermal Cells. **Cell Rep**. 2015 Sep;12(10):1564-74.

Posch C, Cholewa BD, Vujic I, Sanlorenzo M, Ma J, Kim ST, **Kleffel S**, Schatton T, Rappersberger K, Gutteridge R, Ahmad N, Ortiz-Urda S. Combined Inhibition of MEK and Plk1 Has Synergistic Antitumor Activity in NRAS Mutant Melanoma. **J Invest Dermatol**. 2015 Oct;135(10):2475-83.

Lee CW, Zhan Q, Lezcano C, Frank MH, Huang J, Larson AR, Lin JY, Wan MT, Lin PI, Ma J, **Kleffel S**, Schatton T, Lian CG, Murphy GF. Nestin depletion induces melanoma matrix metalloproteinases and invasion. **Lab Invest**. 2014 Dec; 94(12):1382-95.

Kleffel S, Vergani A, Tezza S, Ben Nasr M, Niewczas MA, Wong S, Bassi R, D'Addio F, Schatton T, Abdi R, Atkinson M, Sayegh MH, Wen L, Wasserfall CH, O'Connor KC, Fiorina P. Interleukin-10+ Regulatory B cells arise within antigen-experienced CD40+ B cells to maintain tolerance to islet autoantigens. **Diabetes** 2015 Jan;64(1):158-71.

Lezcano C, **Kleffel S**, Lee N, Larson AR, Zhan Q, DoRosario A, Wang LC, Schatton T, Murphy GF. Merkel cell carcinoma expresses vasculogenic mimicry: demonstration in patients and experimental manipulation in xenografts. **Lab Invest**. 2014 Oct;94(10):1092-102.

Vergani A, Tezza S, D'Addio F, Fotino C, Liu K, Molano RD, **Kleffel S**, Bassi R, Petrelli A, Soleti A, Ammirati E, Frigerio M, Visner G, Grassi F, Ferrero ME, Corradi D, Abdi R, Ricordi C, Sayegh MH, Pileggi A, Fiorina P. Long-term heart transplant survival by targeting the ionotropic purinergic receptor P2X7. **Circulation** 2013 Jan 29;127(4):463-75.

Lian CG, Xu Y, Ceol C, Wu F, Larson A, Dresser K, Xu W, Tan L, Hu Y, Zhan Q, Lee CW, Hu D, Lian BQ, **Kleffel S**, Yang Y, Neiswender J, Khorasani AJ, Fang R, Lezcano C, Duncan LM, Scolyer RA, Thompson JF, Kakavand H, Houvras Y, Zon LI, Mihm MC Jr, Kaiser UB, Schatton T, Woda BA, Murphy GF, Shi YG. Loss of 5-hydroxymethylcytosine is an epigenetic hallmark of melanoma. **Cell** 2012; 150(6):1135-46.

Denecke C, Ge X, Jurisch A, **Kleffel S**, Kim IK, Padera RF, Weiland A, Fiorina P, Pratschke J, Tullius SG. Modified CD4(+) T-cell responses in recipients of old cardiac allografts. **Transpl Int**. 2012; 25(3):328-36.

Petrelli A, Carvello M, Vergani A, Lee KM, Tezza S, Du M, **Kleffel S**, Chengwen L, Mfarrej BG, Hwu P, Secchi A, Leonard WJ, Young D, Sayegh MH, Markmann JF, Zajac AJ, Fiorina P. IL-21 is an antitolerigenic cytokine of the late-phase alloimmune response. **Diabetes** 2011; 60(12):3223-34.

Petrelli A, Maestroni A, Fadini GP, Belloni D, Venturini M, Albiero M, **Kleffel S**, Mfarrej BG, Maschio AD, Maffi P, Avogaro A, Ferrero E, Zerbini G, Secchi A, Fiorina P. Improved function of circulating angiogenic cells is evident in Type 1 Diabetic- islet transplanted patients. **Am J Transplant** 2010 Dec; 10(12):2690-700.

Book Chapter
Kleffel S, Schatton T. Tumor dormancy and cancer stem cells: two sides of the same coin? In Heiko Enderling (ed.), Systems Biology of Tumor Dormancy. Springer. 2013.

Provisional patent
Treatment selection and assessment of therapeutic response to programmed cell death 1 (PD-1) inhibitor therapy for patients with PD-1-expressing cancers. Schatton T, **Kleffel S**, Posch C/

Teaching

Frontiers in Stem Cells in Cancer (FRISC^2), NIH-sponsored advanced training course, Ponce Medical School Puerto Rico, February 2015.

A week-long advanced training course designed for young independent scientist, physicians and established investigators from predominantly underrepresented communities, with the purpose of providing sophisticated training in state-of-the-art methods to advance cancer stem cell research. Taught isolation of cancer stem cells from human melanoma cultures using MACS cell sorting.

Boston, January 14th 2017 _____